Mass Spectrometry to Determine Intracellular Concentrations of Antiretroviral Drugs

From chemistry to clinical application

ISBN: 978-90-8559-573-1

Layout and printing: Optima Grafische Communicatie, Rotterdam, The Netherlands

Mass Spectrometry to Determine Intracellular Concentrations of Antiretroviral Drugs

From chemistry to clinical application

Intracellulaire concentraties van antiretrovirale geneesmiddelen bepaald met massaspectrometrie

PROEFSCHRIFT

Ter verkrijging van de graad doctor aan de
Erasmus Universiteit Rotterdam
op gezag van de rector magnificus
prof.dr. H.G. Schmidt
en volgens besluit van het College voor Promoties.
De openbare verdediging zal plaatsvinden op
woensdag 21 oktober 2009 om 15:30 uur

door

Jeroen Jacob Alexander van Kampen

geboren te Gouda

ERASMUS UNIVERSITEIT ROTTERDAM

Promotiecommissie

Promotoren:	Prof.dr. P.A.E. Sillevis Smitt
	Prof.dr. R. de Groot
Copromotor:	Dr. T.M. Luider
Overige Leden:	Prof.dr. R.M.A. Heeren
	Prof.dr. J. Lindemans
	Prof.dr. A.D.M.E. Osterhaus

voor Hee Jin

Contents

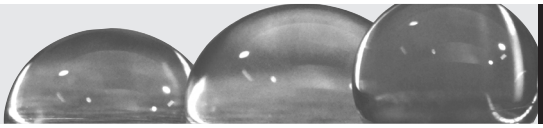

Chapter 1

Introduction

Introduction

Around 1995 – 1996, treatment options for patients infected with the human immunodefiency virus (HIV), the causative agent of acquired immunodeficiency syndrome (AIDS) [1,2], improved dramatically. Therapy with a combination of several classes of antiretroviral drugs resulted in a sustained suppression of HIV replication, and changed HIV infection from a fatal disease to a chronic disease. This cocktail of drugs, which is still widely used today, normally includes one non-nucleoside reverse transcriptase inhibitor (NNRTI) or one HIV protease inhibitor with two nucleoside reverse transcriptase inhibitors (NRTIs). This therapy, however, does not cure HIV infection and life-long treatment is needed to suppress the virus. Although this therapy resulted in a significant decrease in HIV-related morbidity and mortality [3-5], drug-toxicity and emerge of drug-resistant HIV strains were and remain significant problems associated with antiretroviral therapy.

For NNRTIs and protease inhibitors, relationships have been found between plasma exposure and drug efficacy as well as drug toxicity [6-9]. Therapeutic drug monitoring (TDM) has been explored as a mean to optimize pharmacotherapy of HIV infected patients [3,5,10,11]. Some studies have shown that this approach improves outcome in HIV infected adults, but there is still debate whether this approach should be applied as standard of care to all patients or only to a selected group of patients such as children [11-16]. HIV infected children represent a group of patients that may particularly benefit from therapeutic drug monitoring because the pharmacokinetics of antiretroviral drugs change significantly during development and maturation of the child [3,5,11].

Although the plasma levels of protease inhibitors and NNRTIs are used for therapeutic drug monitoring, it is thought that NRTIs, NNRTIs, and protease inhibitors exert their action inside cells that are susceptible for infection with HIV. Therefore, studies have been performed to investigate the intracellular pharmacokinetics of antiretroviral drugs and its relation to the plasma pharmacokinetics [16-27]. The data currently present on the intracellular concentrations of antiretroviral drugs have almost exclusively been obtained using peripheral blood mononuclear cells (PBMCs) of patients, because these cells can be relatively easy obtained from patients, and because part of the PBMCs, i.e. $CD4^+$ T-cells and monocytes, are cellular targets for HIV. Interestingly, plasma concentrations correlate poorly to the intracellular concentrations of HIV protease inhibitors and NNRTIs in HIV infected adults. Studies in HIV infected children have not been performed yet, which is probably in part due to the large volumes of blood needed for intracellular measurements.

NRTIs are prodrugs and are phosphorylated inside cells to their active triphosphate form. In general the intracellular half-life of the active NRTI-triphosphate is much longer than that of the NRTI prodrug in plasma, and correlations between plasma concentrations of NRTIs and intracellular concentrations of NRTI-triphosphates is absent or poor.

For these reasons, therapeutic drug monitoring of NRTIs using the plasma levels of the prodrug is normally not performed.

Aim of this thesis

The aim of the thesis was to develop assays for quantitative analysis of drugs in cells, and to apply these assays to determine the intracellular concentrations of antiretroviral drugs in HIV-1 infected children.

Criteria set for the assays

One of the criteria that we set for our assays was that the measurements could be applied to HIV-1 infected children. A volume of maximal two milliliter of peripheral blood was found to be acceptable to conduct pharmacokinetic studies, considering that blood samples are also obtained from these patients to determine e.g. $CD4^+$ T-cell count and viral load. Roughly one million PBMCs can be obtained from a sample of one - two milliliter of peripheral blood. We therefore chose to develop assays that could determine clinically relevant intracellular concentrations of antiretroviral drugs using one million PBMCs.

We used the report of the FDA for bioanalytical method validation [28] as guideline to develop our assays. The two most important parameters described in this report are precision and accuracy. Precision is a parameter which described the variation in instrument response when replicates of the same sample are measured. Precision can be calculated in the following way: (mean instrument response / standard deviation in the instrument response) x 100%. The precisions are in this case expressed as % coefficient of variation (CV), which is also know as % relative standard deviation (RSD). According to the FDA criteria, precisions should be ≤ 15 %CV for the quality control samples tested except for the lower limit of quantification which should have a precision of ≤ 20 %CV. Accuracy is a parameter to determine whether the measured concentration corresponds to the actual concentration in a sample. Accuracy can be calculated in the following way: ((measured concentration – spiked concentration) / spiked concentration) x 100%. The accuracies are in this case expressed as % deviation from the spiked concentration. According to the FDA criteria, accuracies should be ≤ 15% for the quality control samples tested except for the lower limit of quantification which should have an accuracy of ≤ 20%. For our assays, we used these so-called ± 20/15% criteria for precision and accuracy.

To allow measurements of a relatively large number of samples, it is highly desirable that the assays developed allow for high throughput analysis. We therefore set that measurements should be performed within a few minutes and, preferably, by automation.

Techniques used & rationale

The volume of plasma that can be obtained from a patient's blood sample is far greater than the volume represented by the amount of PBMCs that can be obtained from that same blood sample. From a volume of two mL peripheral blood, approximately 1,000 µL of plasma can be obtained and one million PBMCs which represent an intracellular volume of only 0.4 µL. To determine the intracellular concentrations of antiretroviral drugs using 1 x 10^6 PBMC, an assay is needed which has a high absolute sensitivity. Therefore, we explored the use of electrospray ionization (ESI) mass spectrometry and matrix-assisted laser desorption/ionization (MALDI) mass spectrometry for this purpose.

ESI mass spectrometry is the most widely used mass spectrometric technique for quantitative analysis of non-volatile and labile small molecules, i.e. molecules with molecular masses below 1,000 Dalton, which encompass most of the pharmaceutical compounds currently used. Normally, for quantitative analysis of small molecule drugs, high performance liquid chromatography (HPLC) is coupled to an ESI mass spectrometry equipped with a triple quadrupole mass analyzer. The various compounds in a sample are first separated by HPLC, then ionized using ESI, and finally analyzed in the triple quadrupole mass analyzer. In most of the studies presented in this thesis, however, we explored the use of MALDI. For MALDI mass spectrometry, separation of compounds by HPLC is not obligatory, because this technique suffers less from signal suppression when complex samples are measured compared to ESI mass spectrometry. This results in much faster analyses, because the HPLC step is omitted, which is advantageous when relatively large numbers of samples need to be measured. Yet, poor precisions are frequently reported when MALDI mass spectrometry is used. When protocols are developed specifically for quantitative analysis using MALDI mass spectrometry, the precisions can be improved to values that fall within the criterion set, i.e. CVs of 15% and less. Furthermore, interfering signals derived from the matrix itself complicate small molecule analysis by MALDI mass spectrometry. Again, protocols developed specifically for small molecule analysis using MALDI mass spectrometry can alleviate this problem. The common denominator in this thesis is the development of protocols specifically designed for quantitative analysis of antiretroviral drugs in biological samples by MALDI mass spectrometry.

Outline of the thesis

In **Chapter 2**, we describe an assay for analysis of triphosphate forms of NRTIs and endogenous (deoxy)nucleosides using MALDI-TOF mass spectrometry. In **Chapter 3**, we show the analysis of (deoxy)nucleosides, NRTIs, and mono-, di-, and triphosphorylated forms thereof by ion-pair LC-MS/MS. In **Chapter 4**, we used MALDI-TOF mass spectrometry for qualitative and quantitative analysis of pharmaceutical compounds including NRTIs, NNRTIs, and HIV protease inhibitors. The high molecular weight matrix meso-tetrakis(pentafluorophenyl)porphyrin was used to eliminate matrix-derived interfering

signals in the low *m/z* range, and lithium iodide was added to the matrix solution to induce strong signals for lithiated drugs. In **Chapter 5**, we explore the mechanism of cationization by porphyrin matrices in MALDI-MS and why lithium produces such strong signals for analytes compared to other alkali metals. In **Chapter 6**, we show the validation of a mass spectrometry compatible protocol for simultaneous inactivation of infectious HIV-1 and extraction of antiretroviral drugs from cells. In **Chapter 7**, we used MALDI mass spectrometry to image antiretroviral drugs present in cytocentrifuged cells in an effort to simplify sample preparation and measurements. In **Chapter 8**, we used MALDI-FTICR mass spectrometry for quantitative analysis of HIV protease inhibitors in lysates of 1 x 10^6 PBMCs. In **Chapter 9,** we used MALDI-triple quadrupole mass spectrometry for quantitative analysis of antiretroviral drugs in lysates of 1 x 10^6 PBMCs. DHB was used as matrix. In addition, we report on the novel matrix 7-hydroxy-4-(trifluoromethyl)coumarin and on the use of target plates coated with a strongly hydrophobic fluoropolymer to improve sensitivity, precisions, and accuracies. In **Chapter 10**, we show the validation of a MALDI-triple quadrupole MS assay for quantitative analysis of five HIV protease inhibitors in plasma and two HIV protease inhibitors in lysates of 1 x 10^6 PBMCs. For quantification in plasma, we show a cross-validation with HPLC-UV. We used the assay to determine the intracellular concentrations of lopinavir and ritonavir in 1 x 10^6 PBMC obtained from HIV-1 infected children treated with Kaletra. In **Chapter 11**, we review the current literature on analysis of small molecules by MALDI-MS, and present our thoughts on the use of MALDI-MS for qualitative and quantitative analysis of small molecules in biomedical research. The results of our studies are summarized and discussed in **Chapter 12**.

References

1. Barre-Sinoussi F, Chermann JC, Rey F, et al. Isolation of a T-lymphotropic retrovirus from a patient at risk for acquired immune deficiency syndrome (AIDS). Science 1983;220(4599):868-71.
2. Gallo RC, Sarin PS, Gelmann EP, et al. Isolation of human T-cell leukemia virus in acquired immune deficiency syndrome (AIDS). Science 1983;220(4599):865-7.
3. Fraaij PLA, van Kampen JJA, Burger DM, de Groot R. Pharmacokinetics of antiretroviral therapy in HIV-1 infected children. Clin Pharmacokinet 2005;44(9):935-56.
4. Palella FJ, Jr., Delaney KM, Moorman AC, et al. Declining morbidity and mortality among patients with advanced human immunodeficiency virus infection. HIV Outpatient Study Investigators. N Engl J Med 1998;338(13):853-60.
5. van Rossum AM, Fraaij PL, de Groot R. Efficacy of highly active antiretroviral therapy in HIV-1 infected children. Lancet Infect Dis 2002;2(2):93-102.
6. Bergshoeff AS, Fraaij PL, Ndagijimana J, et al. Increased dose of lopinavir/ritonavir compensates for efavirenz-induced drug-drug interaction in HIV-1-infected children. J Acquir Immune Defic Syndr 2005;39(1):63-8.
7. Dieleman JP, Gyssens IC, van der Ende ME, de Marie S, Burger DM. Urological complaints in relation to indinavir plasma concentrations in HIV-infected patients. Aids 1999;13(4):473-8.
8. Fraaij PL, Verweel G, van Rossum AM, Hartwig NG, Burger DM, de Groot R. Indinavir/low-dose ritonavir containing HAART in HIV-1 infected children has potent antiretroviral activity, but is associated with side effects and frequent discontinuation of treatment. Infection 2007;35(3):186-9.
9. Veldkamp AI, Weverling GJ, Lange JM, et al. High exposure to nevirapine in plasma is associated with an improved virological response in HIV-1-infected individuals. Aids 2001;15(9):1089-95.
10. Aarnoutse RE, Schapiro JM, Boucher CA, Hekster YA, Burger DM. Therapeutic drug monitoring: an aid to optimising response to antiretroviral drugs? Drugs 2003;63(8):741-53.
11. Fraaij PL, Rakhmanina N, Burger DM, de Groot R. Therapeutic drug monitoring in children with HIV/AIDS. Ther Drug Monit 2004;26(2):122-6.
12. Best BM, Goicoechea M, Witt MD, et al. A randomized controlled trial of therapeutic drug monitoring in treatment-naive and -experienced HIV-1-infected patients. J Acquir Immune Defic Syndr 2007;46(4):433-42.
13. Burger D, Hugen P, Reiss P, et al. Therapeutic drug monitoring of nelfinavir and indinavir in treatment-naive HIV-1-infected individuals. Aids 2003;17(8):1157-65.
14. Crommentuyn KM, Huitema AD, Brinkman K, van der Ende ME, de Wolf F, Beijnen JH. Therapeutic drug monitoring of nevirapine reduces pharmacokinetic variability but does not affect toxicity or virologic success in the ATHENA study. J Acquir Immune Defic Syndr 2005;39(2):249-50.
15. Demeter LM, Jiang H, Mukherjee AL, et al. A randomized trial of therapeutic drug monitoring of protease inhibitors in antiretroviral-experienced, HIV-1-infected patients. Aids 2009;23(3):357-68.
16. Ford J, Boffito M, Maitland D, et al. Influence of atazanavir 200 mg on the intracellular and plasma pharmacokinetics of saquinavir and ritonavir 1600/100 mg administered once daily in HIV-infected patients. J Antimicrob Chemother 2006;58(5):1009-16.
17. Almond LM, Edirisinghe D, Dalton M, Bonington A, Back DJ, Khoo SH. Intracellular and plasma pharmacokinetics of nevirapine in human immunodeficiency virus-infected individuals. Clin Pharmacol Ther 2005;78(2):132-42.
18. Almond LM, Hoggard PG, Edirisinghe D, Khoo SH, Back DJ. Intracellular and plasma pharmacokinetics of efavirenz in HIV-infected individuals. J Antimicrob Chemother 2005;56(4):738-44.

19. Breilh D, Pellegrin I, Rouzes A, et al. Virological, intracellular and plasma pharmacological parameters predicting response to lopinavir/ritonavir (KALEPHAR study). Aids 2004;18(9):1305-10.
20. Colombo S, Telenti A, Buclin T, et al. Are plasma levels valid surrogates for cellular concentrations of antiretroviral drugs in HIV-infected patients? Ther Drug Monit 2006;28(3):332-8.
21. Crommentuyn KM, Mulder JW, Mairuhu AT, et al. The plasma and intracellular steady-state pharmacokinetics of lopinavir/ritonavir in HIV-1-infected patients. Antivir Ther 2004;9(5):779-85.
22. Durand-Gasselin L, Pruvost A, Dehee A, et al. High levels of zidovudine (AZT) and its intracellular phosphate metabolites in AZT- and AZT-lamivudine-treated newborns of human immunodeficiency virus-infected mothers. Antimicrob Agents Chemother 2008;52(7):2555-63.
23. Ford J, Boffito M, Wildfire A, et al. Intracellular and plasma pharmacokinetics of saquinavir-ritonavir, administered at 1,600/100 milligrams once daily in human immunodeficiency virus-infected patients. Antimicrob Agents Chemother 2004;48(7):2388-93.
24. Hennessy M, Clarke S, Spiers JP, et al. Intracellular accumulation of nelfinavir and its relationship to P-glycoprotein expression and function in HIV-infected patients. Antivir Ther 2004;9(1):115-22.
25. Hennessy M, Clarke S, Spiers JP, et al. Intracellular indinavir pharmacokinetics in HIV-infected patients: comparison with plasma pharmacokinetics. Antivir Ther 2003;8(3):191-8.
26. Hoggard PG, Lloyd J, Khoo SH, et al. Zidovudine phosphorylation determined sequentially over 12 months in human immunodeficiency virus-infected patients with or without previous exposure to antiretroviral agents. Antimicrob Agents Chemother 2001;45(3):976-80.
27. Moore JD, Acosta EP, Johnson VA, et al. Intracellular nucleoside triphosphate concentrations in HIV-infected patients on dual nucleoside reverse transcriptase inhibitor therapy. Antivir Ther 2007;12(6):981-6.
28. US Food and Drug Administration, Center for Drug Evaluation and Research, Guidance for Industry: Bioanalytical Method Validation 2001. Available: www.fda.gov/cder/guidance/4252fnl.htm.

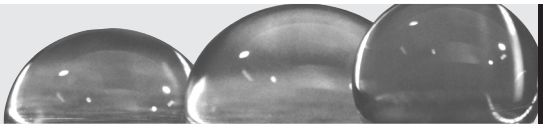

Chapter 2

A new method for analysis of AZT-triphosphate and nucleotide-triphosphates

Jeroen J.A. van Kampen, Pieter L.A. Fraaij, Vishal Hira,
Annemarie M.C. van Rossum, Nico G. Hartwig, Ronald de Groot, Theo M. Luider

Biochemical and Biophysical Research Communications 2004, 315, 151–159
Erratum in: 2004, 316, 967

Abstract

We have developed a new method based on matrix-assisted laser desorption/ionization time-of-flight (MALDI-TOF) mass spectrometry (MS) for analysis of zidovudine-triphosphate and (deoxy)nucleotide-triphosphates, which ultimately can be used for nucleoside reverse transcriptase inhibitor (NRTI) treatment monitoring in HIV-1 infected children and adults. Four different matrices were compared for sensitivity and reproducibility of zidovudine-triphosphate detection and anthranilic acid mixed with nicotinic acid (AA/NA) was selected as most suitable matrix. Solutions of zidovudine-triphosphate, ATP, and dGTP were detected up to 0.5 fmol per sample. Furthermore, intracellular zidovudine-triphosphate, ATP, and dGTP were detected in peripheral blood mononuclear cells (PBMCs). Zidovudine-triphosphate, ATP, and dGTP yield identical mass spectra, however MALDI-TOF post source decay analysis can be used for discrimination between these compounds. We conclude that this method based on MALDI-TOF MS can be used for analysis of intracellular zidovudine-triphosphate and (deoxy)nucleotide-triphosphates in PBMCs.

Introduction

Institution of optimal treatment of HIV-1 infected patients poses a major challenge. Treatment normally consists of a combination of three classes of antiretroviral drugs: the protease inhibitors (PIs), the non-nucleoside reverse transcriptase inhibitors (NNRTIs), and the nucleoside reverse transcriptase inhibitors (NRTIs). A major feature of these three drug classes is that large inter-individual and intra-individual differences are observed in their pharmacokinetics [1-5]. This is even more important when one considers the relation between viral suppression and plasma concentration of PIs and NNRTIs [1,2,6-9]. Therefore, we routinely perform pharmacokinetic analyses of PIs and NNRTIs in HIV-1 infected children and adjust the dose of PIs and NNRTIs to maintain optimal plasma concentrations. This approach has resulted in favorable results with 69% viral response after 2 years of treatment [10].

However, such an approach is not possible for NRTIs. NRTI plasma concentrations correlate poorly with HIV-1 activity, since NRTIs are prodrugs that are intracellularly converted to active NRTI-triphosphates (NRTI-TPs) using the kinases from the host cell [11]. Intracellularly, the NRTI-TP competes with its corresponding endogenous deoxynucleotide-triphosphate (dNTP) for incorporation into viral DNA by HIV reverse transcriptase. Incorporation of NRTI-TP terminates elongation of viral DNA, thus preventing viral replication. *In vitro* studies with peripheral blood mononuclear cells (PBMCs) show that HIV-1 activity of NRTIs correlates more closely to the ratio of the intracellular NRTI-TP concentration and the corresponding intracellular dNTP concentration than to the intracellular NRTI-TP concentration alone [12-14]. In addition, a clinical study with HIV-1 infected adults shows that the intracellular NRTI-TP concentration alone correlates to HIV-1 activity [15].

Current methods for quantification of NRTI-TPs, such as radio immunoassays, require large blood samples and do not allow high throughput analysis [16,17]. This complicates patient related studies, which require analysis of multiple blood samples of a large group of HIV-1 infected patients. Methods have been developed, such as HPLC coupled to electrospray ionization (ESI) MS, which allow for high throughput analysis of NRTI-TPs [18-22]. These methods still require at least 7 mL of blood to obtain sufficient material for analysis. This amount of blood allows for patient related studies in HIV-1 infected adults, but still complicates NRTI-TP studies in HIV-1 infected children, since such studies require multiple blood samples from one individual on a single day.

We aimed to develop a relatively easy method for analysis of intracellular NRTI-TPs, which ultimately can be used for studies in HIV-1 infected children and adults. We studied the usability of matrix-assisted laser desorption/ionization time-of-flight (MALDI-TOF) mass spectrometry (MS) for this method, since: (1) MALDI-TOF MS methods have been developed for quantification of drugs, such as antibiotics and intracellular tetraphenylphosphonium [23-25]. (2) MALDI-TOF MS is able to detect compounds at very

low concentrations, which allows for analysis when only small amounts of material can be obtained [26]. (3) MALDI-TOF MS is more tolerant to salts and other contaminants compared to other forms of MS [26]. This allows for reduction in sample preparation steps, which reduces sample loss and sample preparation time. (4) MALDI-TOF MS allows for rapid and fully automated analysis of large amounts of samples, which allows for high throughput use [27,28].

We studied the use of MALDI-TOF MS for analysis of the triphosphate form of the most widely used NRTI zidovudine (AZT-TP). We also examined if MALDI-TOF MS is capable of detecting dNTPs (dGTP), since *in vitro* studies show that HIV-1 activity correlates better to the ratio of intracellular NRTI-TP and dNTP concentration than to the intracellular NRTI-TP concentration alone [12-14]. In addition, we studied the analysis of NTPs (ATP, CTP, GTP, and UTP) by MALDI-TOF MS, since these compounds share many features (e.g., size, triphosphate group) with dNTPs and NRTI-TPs and could cause interferences. To our knowledge, this is the first time MALDI-TOF MS is used for analysis of NRTI-TP and endogenous (d)NTPs. Therefore, no suitable matrices are known for MALDI-TOF analysis of these compounds. We studied the usability of four different matrices, which are currently used in MALDI-TOF analysis of related compounds such as oligonucleotides. Subsequently, the most suitable matrix was used for analysis of intracellular AZT-TP in PBMCs. Finally, we studied the use of MALDI-TOF post-source decay (MALDI-PSD) analysis for discrimination of AZT-TP from ATP and dGTP, since these three compounds have the same molecular weight, which can cause interferences when using a method based on mass spectrometry.

Experimental Section

Standard nucleotide solutions

ATP (molecular weight 507.2 Da), CTP (483.1 Da), GTP (523.3 Da), dGTP (507.2 Da), UTP (484.1 Da) (Amersham, Sweden), and AZT-TP (507.2 Da) (Calbiochem, Germany) were diluted with HPLC-grade water and stored at - 80°C until analysis.

Preparation of matrix solutions

Solution I: 45 mM anthranilic acid (AA) (Fluka, Switzerland) was mixed with 45 mM nicotinic acid (NA) (Fluka, Switzerland) and 55 mM diammoniumhydrogencitrate (DAHC) (Fluka, Switzerland) in 45% acetonitrile (Aldrich, Germany). Solution II: 3-hydroxypicolinic acid (3-HPA) (Aldrich, Germany) was mixed with DAHC and HPLC-grade water, until the solution had a concentration of 3 mg/mL 3-HPA and 9 mg/mL DAHC. Solution III: 5-methoxysalicylic acid (5-MSA) was saturated in one part acetonitrile and one part DAHC mixed with HPLC-grade water (50 mM). Subsequently, saturated 5-MSA solution

was 10 times diluted with DAHC mixed with HPLC-grade water (50 mM). Solution IV: 2,5-dihydroxybenzoic acid (2,5-DHB) was mixed with DAHC and HPLC-grade water, until the solution had a concentration of 3 mg/mL 2,5-DHB and 9 mg/mL DAHC. Fresh matrix solutions were prepared in Teflon tubes on the day of analysis.

Comparison of matrix solutions

Matrix solutions I–IV were compared for reproducibility and limit of detection of AZT-TP analysis in standard solution.

Relation between AZT-TP concentration and signal-to-noise ratio

Different AZT-TP dilutions were analyzed to assess the effect of the AZT-TP concentration on the signal-to-noise ratio. The signal-to-noise ratio (S/N) was calculated by dividing the maximal signal height to the local noise level. Samples were only measured if sample crystallization was observed by light microscopy (needle crystallization).

PBMC isolation

Venous blood from healthy volunteers was collected in Vacutainer CPT tubes (Becton–Dickinson). PBMCs were separated by centrifugation at 2,000 rpm for 20 min and washed twice with PBS (1,500 rpm for 10 min and 1,200 rpm for 15 min, respectively). PBS was discarded and 3 mL growth media (RPMI supplemented with 10% heat-inactivated fetal calf serum, 10,000 IU/mL penicillin, 10,000 IU/mL streptomycin, and 20% DMSO) were added.

PBMC incubation with AZT

Growth media were added until a final concentration of 1 x 10^6 PBMCs/mL was reached. One microliter AZT solution (Fluka, Switzerland) was added to reach a final concentration of 10 µM. An equal amount of deionized water was added for the creation of "negative control" samples. Cultures were incubated at 37°C for 3 h. After incubation, cells were centrifuged at 3,800 rpm for 5 min and washed with PBS (3,800 rpm for 5 min). "Positive controls" were created by adding 200 fmol AZT-TP to the PBMC pellet just before extraction.

Nucleotide extraction from PBMCs

To the PBMC pellet 500 µL cold MeOH (60%) was added and nucleotides were extracted at 4°C overnight. After extraction, samples were centrifuged (10,000 rpm for 5min), supernatants were collected and lyophilized with a SpeedVac (Savant, USA) for 45 min. Residues were stored at -80°C until analysis. Per sample 0.85 x 10^6 PBMCs were used for intracellular AZT-TP analysis.

MALDI-TOF analysis

Matrix solution (0.5 µL) was pipetted onto an Anchor Chip target plate (Bruker Daltonics, Germany) and dried at room temperature. Subsequently 0.5 µL sample was pipetted onto the crystallized matrix and dried at room temperature. Analysis was performed by a BIFLEX III MALDI-TOF mass spectrometer (Bruker Daltonics, Germany) using the negative reflectron mode. Laser attenuation was set at 40 (UNIX operating system). Hundred shots were used for each mass spectrum. Post-source decay (PSD) analysis was performed on PBMC samples and on standard solutions of AZT-TP, ATP, and dGTP by the BIFLEX III MALDI-TOF mass spectrometer in the negative mode.

Prediction of fragmentation pattern of AZT-TP, ATP, and dGTP

MS Fragmenter software from ACD/Labs was used for prediction of the fragmentation pattern of AZT-TP, ATP, and dGTP.

Results and Discussion

Comparison of different matrices for AZT-TP analysis

We tested four different matrices on their sensitivity and reproducibility of AZT-TP detection. Both the AA/NA (solution I) and 3-HPA (solution II) matrices were able to detect the expected mass signal of AZT-TP up to 0.5 fmol per sample (Figs. 1 and 2). The reproducibility of the mass spectra, however, is much better when AA/NA is used compared to the use of 3-HPA. The expected mass signal of AZT-TP was not detected

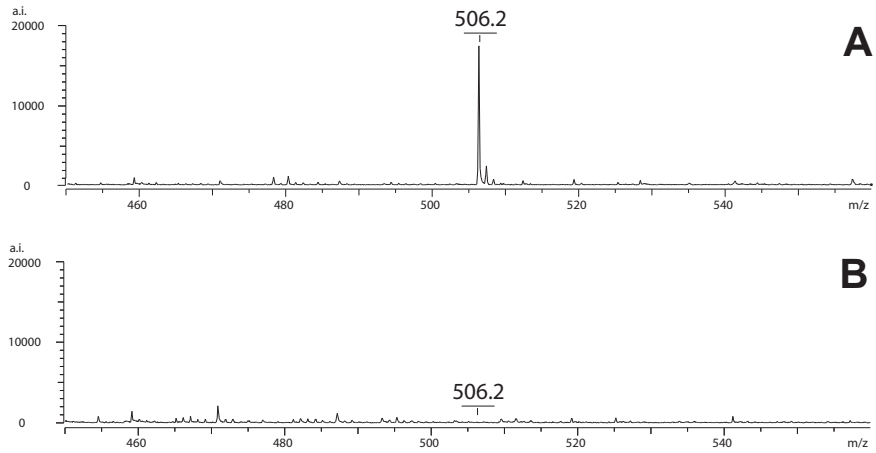

Figure 1. Measurement of 500 fmol AZT-TP (A). An expected signal was found at *m/z* 506.2. The negative control sample (B) yielded no signal at *m/z* 506.2. AA/NA was used as matrix. a.i., absolute intensity. *m/z*, mass-to-charge ratio.

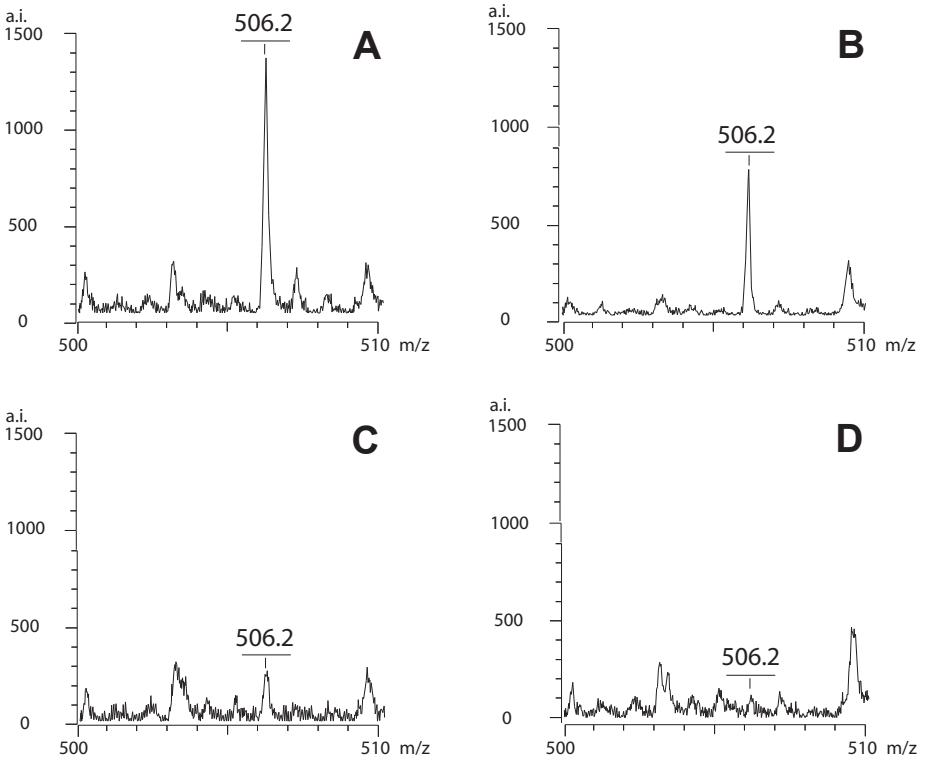

Figure 2. Measurement of 5.0 fmol (A), 2.5 fmol (B), and 0.5 fmol (C) AZT-TP. An expected signal was found at *m/z* 506.2 when AZT-TP was diluted up to 0.5 fmol per sample. The negative control sample (D) yielded no signal at *m/z* 506.2. AA/NA was used for matrix.

when 25 fmol AZT-TP was analyzed with the 5-MSA matrix (solution III). The 2,5-DHB matrix (solution IV) itself yielded a signal at *m/z* of 505.3, which can interfere with the detection of AZT-TP. AA/NA is therefore the most suitable matrix for analysis of AZT-TP.

The effect of the AZT-TP concentration on the signal-to-noise ratio

Known quantities of AZT-TP were measured to analyze the relation with the signal-to-noise ratio. Fig. 3 shows a clear linear relation between the signal-to-noise ratio and AZT-TP concentration. This allows for rough estimation of the AZT-TP concentration. However, more exact values of the intracellular AZT-TP concentration are required for patient related research, which cannot be obtained by estimation based on the AZT-TP concentration versus signal-to-noise ratio curve. There are more accurate ways for quantification by MALDI-TOF MS. By adding a known concentration of a compound (internal standard) to the sample, one can compare signal-to-noise ratio of the analyte of interest with the signal-to-noise ratio of the internal standard. This method has resulted in an accurate quantification of different compounds, as published earlier [18,23,25].

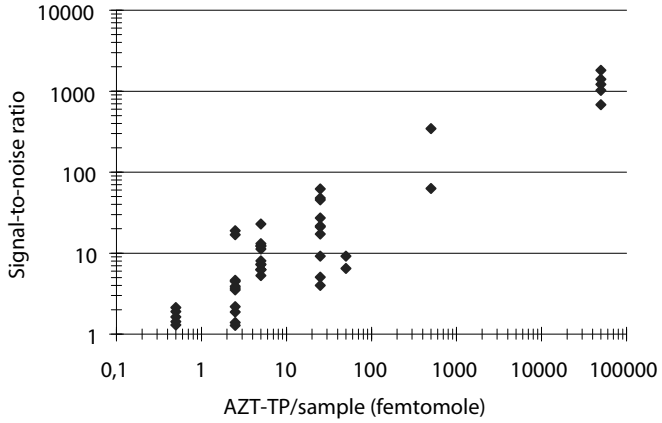

Figure 3. A linear relation was found between AZT-TP concentration and signal-to-noise ratio. AA/NA was used as matrix.

Detection of (d)NTPs in standard solution

dGTP was used for exploring the usability of MALDI-TOF MS for dNTP analysis. The expected mass signal of dGTP (*m/z* 506.2) was detected up to a dilution of 0.5 fmol per sample when using the AA/NA matrix. This shows that MALDI-TOF MS is able to detect dNTPs, which is necessary for exploring its ability of measuring the ratio of intracellular NRTI-TP and corresponding dNTP in PBMCs. It is likely that other dNTPs, such as dTTP, can be detected by MALDI-TOF MS, since related compounds (NTPs, dGTP, and AZT-TP) can be detected up to 0.5 fmol per sample. ATP, CTP, GTP, and UTP were used for exploring the usability of MALDI-TOF MS for NTP analysis. The expected mass signal of ATP (*m/z* 506.2) was detected up to a dilution of 0.5 fmol per sample when using the AA/NA matrix. Samples of 500 and 50 pmol of ATP, CTP, GTP, and UTP were analyzed using the 3-HPA matrix. All mass signals were detected at the expected mass-to-charge ratios (*m/z* 506.2, *m/z* 482.1, *m/z* 522.3, and *m/z* 483.1, respectively). This shows that MALDI-TOF MS is able to detect NTP, which is necessary for predicting possible interference of such compounds when analyzing AZT-TP. ATP, dGTP, and AZT-TP yield a mass signal at the same mass-to-charge ratio (*m/z* 506.2) in standard nucleotide solutions. This complicates future experiments for AZT-TP quantification. Therefore, we studied if ATP and dGTP also interfered with the detection of AZT-TP in PBMCs.

Intracellular AZT-TP in PBMCs

The analysis of the extract of PBMCs incubated with AZT revealed a mass signal at the expected *m/z* of 506.2 (Fig. 4). This expected mass signal was again detected when 200 fmol AZT-TP was added to the pellet of PBMCs not incubated with AZT (positive control). The extract of PBMCs not incubated with AZT (negative control) also yielded a mass

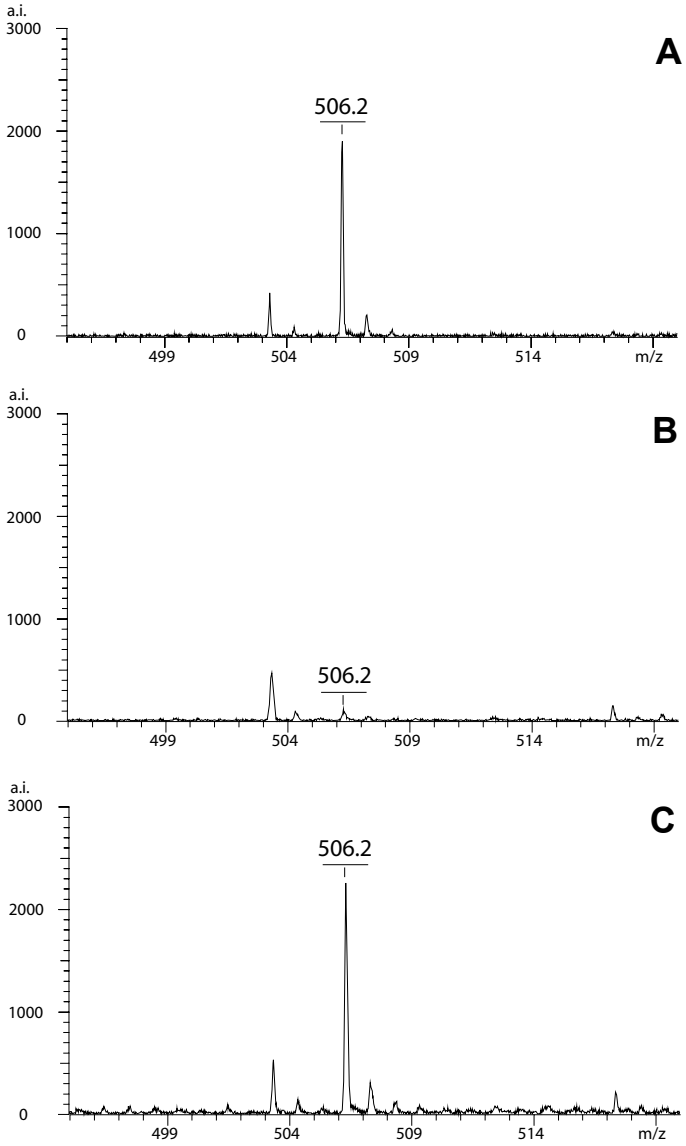

Figure 4. Mass signals of intracellular ATP, dGTP, and AZT-TP were detected at the expected *m/z* 506.2 in PBMCs incubated with AZT (A). Mass signals of intracellular ATP and dGTP were detected at the expected *m/z* 506.2 in PBMCs not incubated with AZT (negative control) (B). Mass signals of intracellular ATP, dGTP, and AZT-TP are found at the expected *m/z* 506.2 in PBMCs not incubated with AZT and spiked with 200 fmol AZT-TP (positive control) (C). Per sample 0.85 x 10^6 PBMCs were used. AA/NA was used for matrix.

signal at *m/z* of 506.2. This shows that AZT-TP, ATP, and dGTP can be detected in PBMCs by MALDI-TOF. However, ATP and dGTP interfere with AZT-TP detection in PBMCs. It is not possible to estimate the AZT-TP concentration by comparing signal-to-noise ratio of the mass signal at *m/z* 506.2 in negative controls and in PBMCs incubated with AZT. AZT

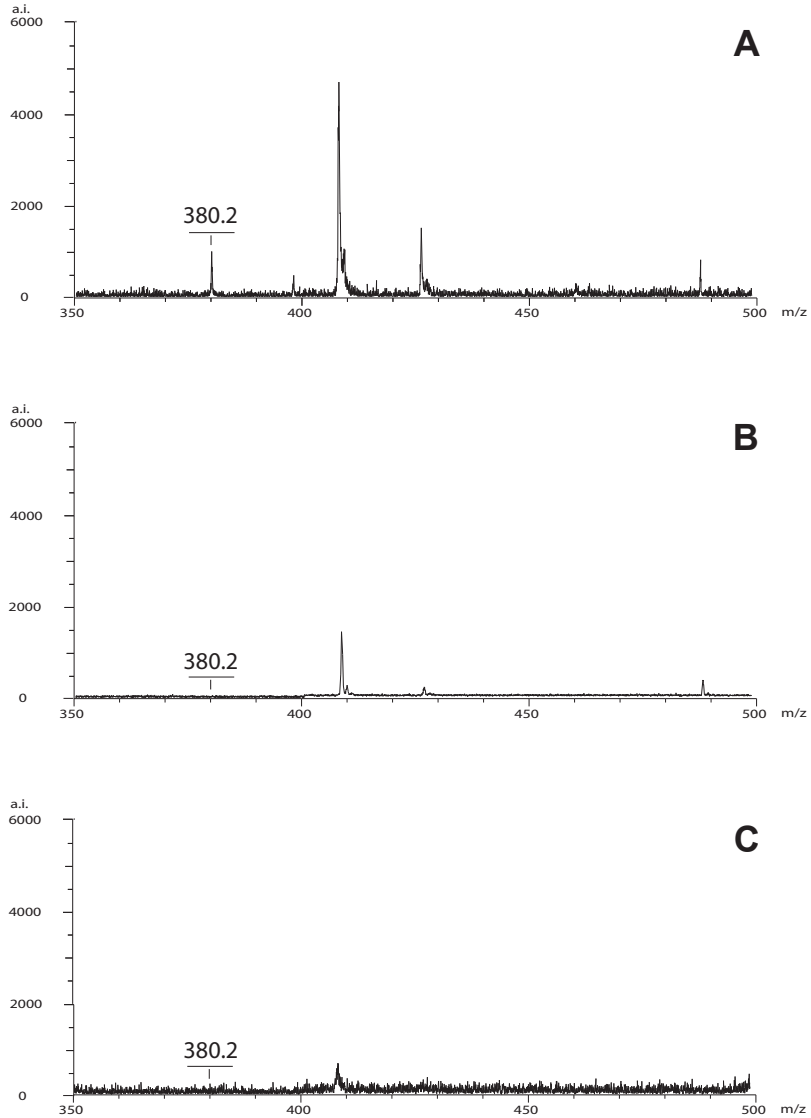

Figure 5. MALDI-PSD analysis of 0.5 nmol AZT-TP revealed a unique mass signal at m/z 380.2 (A). This mass signal was not found by MALDI-PSD analysis of 5.0 nmol ATP (B) and dGTP (C). AA/NA was used for matrix.

affects the nucleotide pool size, thus we cannot assume that ATP and dGTP are present in the same concentrations in negative controls and in PBMCs incubated with AZT [29]. Therefore, we have searched for a method to discriminate AZT-TP from ATP and dGTP.

Software prediction of AZT-TP, ATP, and dGTP fragmentation

Molecules can be fragmented and the mass of these fragments can be measured by MALDI-PSD analysis. The software prediction of the fragmentation pattern of AZT-TP, ATP, and dGTP revealed a unique fragment for AZT-TP. This fragment has a *m/z* of 382 (381 Da + 1 Da), when measuring in the positive mode. Since we measure in the negative mode, a proton is lost and the fragment should be detected at *m/z* 380 (381 Da - 1 Da).

Fragmentation of AZT-TP, ATP, and dGTP in standard nucleotide solutions

MALDI-PSD analysis was used for detection of the unique AZT-TP fragment. As predicted by software, the MALDI-PSD analysis of AZT-TP, ATP, and dGTP in standard solution revealed a unique mass signal for AZT-TP at *m/z* 380.2 (Fig. 5). This signal was not observed when analyzing ATP and dGTP by MALDI-PSD. Subsequently, we explored the ability of MALDI-PSD analysis for detecting the AZT-TP fragment in PBMCs.

Fragmentation of AZT-TP present in PBMCs

Fig. 6 depicts the detection of the mass signal at the expected *m/z* 380.2 in PBMCs incubated with AZT. This signal was not observed in the analysis of PBMCs not incubated with AZT. Thus, MALDI-PSD analysis is able to discriminate AZT-TP from ATP and dGTP in standard nucleotide solutions and in PBMCs.

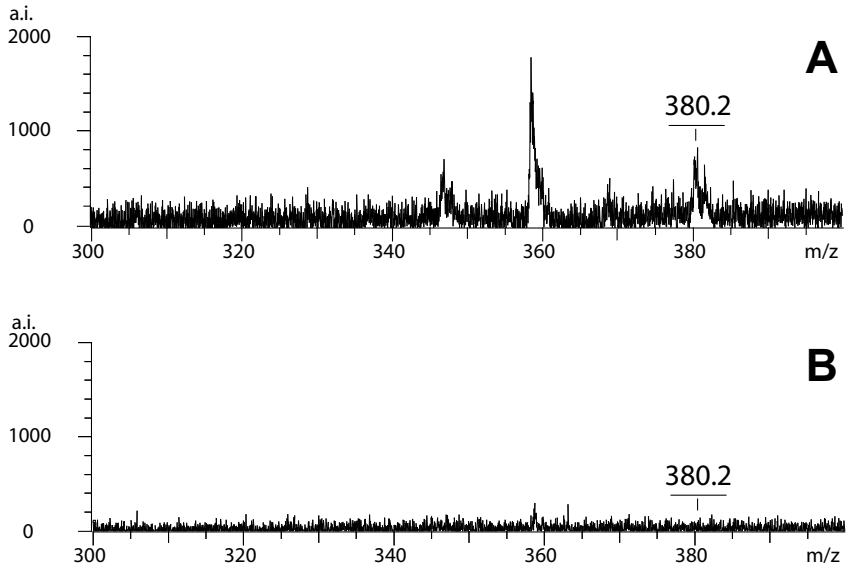

Figure 6. The MALDI-PSD analysis of PBMCs incubated with AZT (A) revealed the expected signal of the unique fragment of AZT-TP at *m/z* 380.2. This signal was not detected in the MALDI-PSD analysis of PBMCs not incubated with AZT (B).

The development of a method for quantification of NRTI-TPs in HIV-1 infected children requires that the analysis can be performed on small amounts of PBMCs. Approximately one million PBMCs can be derived from one mL blood, which is an acceptable blood sample size for studies in HIV-1 infected children. Font et al. [20] showed that the intracellular AZT-TP concentration ranges from 38 to 193 fmol per million PBMCs in HIV-1 infected adults. The signal-to-noise ratio of AZT-TP detection in standard solution obtained by our method is larger than 10 in this range of measurement. However, the limit of detection of the unique AZT-TP fragment in PBMCs is probably higher than the limit of detection of AZT-TP in standard solutions. Furthermore, we have to explore if MALDI-PSD analysis can be used for accurate quantification of AZT-TP by using an internal standard.

We conclude that: (1) AA/NA is a suitable matrix for MALDI-TOF analysis of NRTI-TPs, NTPs, and dNTPs. (2) AZT-TP, ATP, and dGTP can be detected up to 0.5 femtomole per sample by MALDI-TOF MS. (3) CTP, GTP, and UTP can be detected by MALDI-TOF MS. (4) Intracellular AZT-TP, ATP, and dGTP can be detected in PBMCs by MALDI-TOF MS. (5) Discrimination of AZT-TP from ATP and dGTP can be obtained by MALDI-PSD analysis in standard nucleotide solutions and in PBMCs. (6) Our developed method could be useful for NRTI-TP studies in HIV-1 infected children and adults.

Acknowledgements

We like to acknowledge the SKZ Foundation for financial support.

References

1. Bergshoeff AS, Fraaij PL, van Rossum AM, et al. Pharmacokinetics of nelfinavir in children: influencing factors and dose implications. Antivir Ther. 2003;8:215-222.
2. Burger DM, van Rossum AM, Hugen PW, et al. Pharmacokinetics of the protease inhibitor indinavir in human immunodeficiency virus type 1-infected children. Antimicrob Agents Chemother. 2001; 45:701-705.
3. Fraaij PL, Bergshoeff AS, van Rossum AM, Hartwig NG, Burger DM, de Groot R. Changes in indinavir exposure over time: a case study in six HIV-1-infected children. J Antimicrob Chemother. 2003; 52:727-730.
4. King JR, Kimberlin DW, Aldrovandi GM, Acosta EP. Antiretroviral pharmacokinetics in the paediatric population: a review. Clin Pharmacokinet. 2002;41:1115-1133.
5. van Rossum AM, de Groot R, Hartwig NG, Weemaes CM, Head S, Burger DM. Pharmacokinetics of indinavir and low-dose ritonavir in children with HIV-1 infection. Aids. 2000;14:2209-2210.
6. Burger DM, Hoetelmans RM, Hugen PW, et al. Low plasma concentrations of indinavir are related to virological treatment failure in HIV-1-infected patients on indinavir-containing triple therapy. Antivir Ther. 1998;3:215-220.
7. Marzolini C, Telenti A, Decosterd LA, Greub G, Biollaz J, Buclin T. Efavirenz plasma levels can predict treatment failure and central nervous system side effects in HIV-1-infected patients. Aids. 2001;15:71-75.
8. Pfister M, Labbe L, Hammer SM, et al. Population pharmacokinetics and pharmacodynamics of efavirenz, nelfinavir, and indinavir: Adult AIDS Clinical Trial Group Study 398. Antimicrob Agents Chemother. 2003;47:130-137.
9. Veldkamp AI, Weverling GJ, Lange JM, et al. High exposure to nevirapine in plasma is associated with an improved virological response in HIV-1-infected individuals. Aids. 2001;15:1089-1095.
10. van Rossum AM, Geelen SP, Hartwig NG, et al. Results of 2 years of treatment with protease-inhibitor--containing antiretroviral therapy in dutch children infected with human immunodeficiency virus type 1. Clin Infect Dis. 2002;34:1008-1016.
11. Sale M, Sheiner LB, Volberding P, Blaschke TF. Zidovudine response relationships in early human immunodeficiency virus infection. Clin Pharmacol Ther. 1993;54:556-566.
12. Arner ES, Eriksson S. Deoxycytidine and 2′,3′-dideoxycytidine metabolism in human monocyte-derived macrophages. A study of both anabolic and catabolic pathways. Biochem Biophys Res Commun. 1993;197:1499-1504.
13. Gao WY, Shirasaka T, Johns DG, Broder S, Mitsuya H. Differential phosphorylation of azidothymidine, dideoxycytidine, and dideoxyinosine in resting and activated peripheral blood mononuclear cells. J Clin Invest. 1993;91:2326-2333.
14. Perno CF, Yarchoan R, Cooney DA, et al. Inhibition of human immunodeficiency virus (HIV-1/HTLV-IIIBa-L) replication in fresh and cultured human peripheral blood monocytes/macrophages by azidothymidine and related 2′,3′-dideoxynucleosides. J Exp Med. 1988;168:1111-1125.
15. Fletcher CV, Acosta EP, Henry K, et al. Concentration-controlled zidovudine therapy. Clin Pharmacol Ther. 1998;64:331-338.
16. Kuster H, Vogt M, Joos B, Nadai V, Luthy R. A method for the quantification of intracellular zidovudine nucleotides. J Infect Dis. 1991;164:773-776.
17. Robbins BL, Waibel BH, Fridland A. Quantitation of intracellular zidovudine phosphates by use of combined cartridge-radioimmunoassay methodology. Antimicrob Agents Chemother. 1996;40: 2651-2654.

18. Becher F, Pruvost A, Gale J, et al. A strategy for liquid chromatography/tandem mass spectrometric assays of intracellular drugs: application to the validation of the triphosphorylated anabolite of antiretrovirals in peripheral blood mononuclear cells. J Mass Spectrom. 2003;38:879-890.
19. Becher F, Schlemmer D, Pruvost A, et al. Development of a direct assay for measuring intracellular AZT triphosphate in humans peripheral blood mononuclear cells. Anal Chem. 2002;74:4220-4227.
20. Font E, Rosario O, Santana J, Garcia H, Sommadossi JP, Rodriguez JF. Determination of zidovudine triphosphate intracellular concentrations in peripheral blood mononuclear cells from human immunodeficiency virus-infected individuals by tandem mass spectrometry. Antimicrob Agents Chemother. 1999;43:2964-2968.
21. Kewn S, Hoggard PG, Sales SD, et al. Development of enzymatic assays for quantification of intracellular lamivudine and carbovir triphosphate levels in peripheral blood mononuclear cells from human immunodeficiency virus-infected patients. Antimicrob Agents Chemother. 2002;46: 135-143.
22. Moore JD, Valette G, Darque A, Zhou XJ, Sommadossi JP. Simultaneous quantitation of the 5'-triphosphate metabolites of zidovudine, lamivudine, and stavudine in peripheral mononuclear blood cells of HIV infected patients by high-performance liquid chromatography tandem mass spectrometry. J Am Soc Mass Spectrom. 2000;11:1134-1143.
23. Harvey DJ. Quantitative aspects of the matrix-assisted laser desorption mass spectrometry of complex oligosaccharides. Rapid Commun Mass Spectrom. 1993;7:614-619.
24. Ling YC, Lin L, Chen YT. Quantitative analysis of antibiotics by matrix-assisted laser desorption/ionization time-of-flight mass spectrometry. Rapid Commun Mass Spectrom. 1998;12:317-327.
25. Rideout D, Bustamante A, Siuzdak G. Cationic drug analysis using matrix-assisted laser desorption/ionization mass spectrometry: application to influx kinetics, multidrug resistance, and intracellular chemical change. Proc Natl Acad Sci U S A. 1993;90:10226-10229.
26. Siuzdak G. Mass Spectrometry for Biotechnology. (ed 1st): Academic Press; 1996.
27. Leushner J, Chiu NH. Automated mass spectrometry: a revolutionary technology for clinical diagnostics. Mol Diagn. 2000;5:341-348.
28. Van Ausdall DA, Marshall WS. Automated high-throughput mass spectrometric analysis of synthetic oligonucleotides. Anal Biochem. 1998;256:220-228.
29. Fridland A, Connelly MC, Ashmun R. Relationship of deoxynucleotide changes to inhibition of DNA synthesis induced by the antiretroviral agent 3'-azido-3'-deoxythymidine and release of its monophosphate by human lymphoid cells (CCRF-CEM). Mol Pharmacol. 1990;37:665-670.

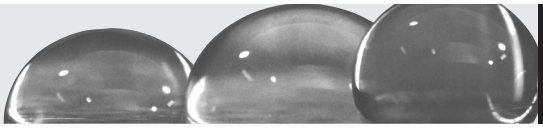

Chapter 3

Simultaneous determination of endogenous deoxynucleotides and phosphorylated nucleoside reverse transcriptase inhibitors in peripheral blood mononuclear cells using ion-pair liquid chromatography coupled to mass spectrometry

Leon Coulier, Jeroen J.A. van Kampen, Ronald de Groot, Henk W. Gerritsen, Richard C. Bas, William D. van Dongen, Lars P. Brüll, Theo M. Luider

Proteomics Clinical Applications 2008, 2, 1557–1562

Abstract

Nucleoside reverse transcriptase inhibitors (NRTIs) are activated intracellularly to their triphosphate (TP) form, which compete with endogenous deoxynucleotide-triphosphates (dNTP) as substrate for HIV reverse transcriptase. The activity of NRTIs is thus described by the NRTI-TP-to-dNTP ratio in relevant cell types. Therefore, we developed an ion-pair (IP) LC-MS method for the simultaneous analysis of the mono-, di-, and TP forms of NRTIs and endogenous deoxynucleosides in peripheral blood mononuclear cells (PBMCs). The IP-LC method was applied on an ion trap mass spectrometer using the MS-mode as well as on a triple quadrupole mass spectrometer using the MS/MS mode. The MS/MS approach on the triple quadrupole mass spectrometer demonstrated the best clinical applicability due to its higher sensitivity. The LODs (minimum amount on column) were 25 fmol for the TP forms of zidovudine, lamivudine, and stavudine, as well as for their endogenous dNTP counterparts. The linearity (r^2) of the calibration curves were > 0.99. The obtained LODs readily allow for clinical applications using just one million PBMCs obtained from HIV-infected patients under therapy.

Introduction

HIV infection is currently treated with a combination of antiretroviral drugs. Notably, two nucleoside reverse transcriptase inhibitors (NRTIs) are combined with one non-NRTI (NNRTI) or one protease inhibitor. These antiretroviral drugs must penetrate into HIV susceptible cells to exert its action. In many cases, the plasma pharmacokinetics correlates poorly to the intracellular pharmacokinetics [1-3]. Furthermore, in contrast to NNRTIs and protease inhibitors, NRTIs are prodrugs and need cellular enzymes for activation to its triphosphate (TP) form. These NRTI-TPs compete with endogenous deoxynucleotide-triphosphates (dNTPs) for incorporation into the viral DNA by HIV reverse transcriptase. The reverse transcriptase process ends prematurely after incorporation of an NRTI-TP, because NRTIs lack the 3'-hydroxyl group necessary for further elongation of the viral DNA. The efficacy of the NRTIs thus depends on the intracellular concentration of NRTI-TPs as well as on the intracellular dNTP concentration [4]. On the other hand, NRTI-TPs can inhibit the replication of human mitochondrial DNA, which causes drug toxicity [5]. Furthermore, there is considerable overlap in the cellular enzymes used for phosphorylation of various NRTIs and endogenous nucleosides, and combination therapy with two or more NRTIs can result in intracellular interactions. For example, the combination of the NRTIs stavudine (d4T) and zidovudine (AZT) leads to a reduced concentration of d4T-TP while the AZT-TP concentration remains unaffected [6]. Above considerations show that knowledge of the intracellular pharmacology of NRTIs is needed to understand how efficient suppression of HIV replication can be achieved and maintained, and how drug toxicity can be avoided.

However, understanding of the intracellular pharmacology of NRTIs *in vivo* is hampered by difficulties in detecting the phosphorylated forms of NRTIs and endogenous nucleosides at clinical relevant levels. Ideally, a single analytical method should be able to simultaneously determine the intracellular concentrations of NRTIs, endogenous deoxynucleosides, and all phosphorylated forms thereof. In this study, we investigated the use of an ion-pair (IP) LC-MS approach for quantitative analysis of endogenous deoxynucleotides and phosphorylated NRTIs in peripheral blood mononuclear cells (PBMCs).

Experimental Section

Materials

Reference standards of phosphorylated NRTIs were obtained from Moravek (Brea, CA, USA) or Jena Bioscience (Jena, Germany). Reference standards of the various endogenous nucleotides, N^6-(6-aminohexyl)-ADP (internal standard), hexylamine, ammonium acetate, ammonia, were obtained from Sigma–Aldrich (Zwijndrecht, The Netherlands).

The internal standards GMP (^{13}C10, ^{15}N5) and GTP (^{13}C10, ^{15}N5) were obtained from Cambridge Isotope Laboratories (Andover, MA, USA). Acetic acid and ammonia were obtained from Merck (Amsterdam, The Netherlands). Heparin was obtained from Leo Pharma BV (Weesp, The Netherlands), and Lymphoprep from Axis-Shield PoC AS (Oslo, Norway).

Apparatus

Experiments were carried out on two different LC-MS systems: A) Thermo Finnigan LTQ linear IT system consisting of a Surveyor AS autosampler, Surveyor MS pump, LTQ LT-10000 mass detector with an Opton ESI probe (Thermo Electron, San Jose, CA, USA). All system control, data acquisition and MSD data evaluation were performed using XCalibur software version 1.4. B) Applied Biosystems Sciex API4000 triple quadrupole mass spectrometer equipped with a Turbo Ionspray interface (PE Sciex, Toronto, Canada), a Shimadzu LC-10AD LC pump (Shimadzu, Manchester, UK), a Shimadzu SIL-HTC autosampler, and a Shimadzu CTO-10AS column oven.

LC parameters

An Inertsil 5 µm ODS-3 cartridge column (100 x 3 mm) was used in combination with an Inertsil 5 µm ODS-3 guard column (Chrompack, Middelburg, The Netherlands). A mobile phase gradient was used with a flow rate of 0.4 mL/min in which mobile phase A consisted of 5 mM hexylamine in nanopure water adjusted to pH 6.3 with acetic acid and mobile phase B consisted of 90% methanol/10% 10 mM ammoniumacetate adjusted to pH 8.5 with ammonia. A step gradient was used consisting of 80% A in 4 min, 69% A in 11 min, 40% A in 19 min, and 100% B for 5 min. The flow was reduced to 100 µL/min prior to MS detection using a T-split and a restriction column. The column temperature was maintained at 30°C and the injection volume was 10 µL. LC-MS/MS provided better selectivity, and allowed optimization of the gradient in order to increase the sample throughput. A linear gradient was used starting from 100% A to 50% A in 12 min, followed by a linear gradient from 50% A to 0% A in 3 min. The injection volume was 25 µL.

MS parameters

Both mass spectrometers were operated in the negative ionization mode. The following settings were used for the IT mass spectrometer: ESI spray voltage 3-4 kV, heated capillary 250°C, sheath gas 20, auxiliary gas 0, scan range *m/z* 150-1,200, number of microscans 3, maximum injection time 300 ms. The IT mass spectrometer was operated in the full scan mode. For the triple quadrupole mass spectrometer, nebulizer, turbo, and curtain gas used nitrogen delivered at settings of 50, 50, and 40 psi, respectively. The Turbo Ion spray temperature was maintained at 450°C. The nebuliser potential was set at

-4500 V. The triple quadrupole mass spectrometer was operated in the selected reaction monitoring (SRM) mode.

Preparation of PBMC extracts

Hundred milliliter of PBS supplemented with 0.1% heparin was added to 50 mL buffy coat (Sanquin, Rotterdam, The Netherlands), and the solution was subsequently divided into six 50 mL tubes (25 mL per tube). Fourteen milliliter Lymphoprep was gently pipetted under the buffy coat solution, and the tubes were centrifuged at 823 x *g* for 30 min. The layers containing the PBMCs were carefully collected in six 50 mL tubes, and subsequently a wash solution of PBS + 0.1% heparin was added until the total volume was 50 mL per tube. PBMC suspensions were centrifuged at 420 x *g* for 10 min, the supernatants were discarded, and the PBMC pellets were subsequently washed twice with PBS (316 x *g* for 10 min). Next, the PBMC pellets were suspended in PBS, and were directly aliquoted in 1.5 mL reaction vials at a density of 1.0 x 10^6 cells per vial. PBMCs were spun down, and the supernatants were discarded. Subsequently, 100 µL methanol/water (7:3 v/v) were added to each vial, and the PBMCs were extracted overnight at 5°C. Finally, cell debris was spun down, analytes were added to the PBMC lysates, and were analyzed using LC-MS.

Results and Discussion

Conventional RP chromatography is normally used for the separation of nonphosphorylated NRTIs and nucleosides [7]. However, irreversible adsorption and peak tailing are frequently observed when this type of chromatography is used for separation of phosphorylated nucleotides due to the strong polarity of the phosphate groups. IP reagents, which act as counter-ions for the acidic nucleotides, facilitate the elution of the nucleotides from the column and improve the peak shape [8-11]. Recently, an IP LC-ESI-IT-MS method was developed and validated for the analysis of a variety of polar metabolites in microbial extracts such as nucleotides, coenzyme A (CoA) esters, and sugar nucleotides [12]. Best chromatographic separation and peak shapes were observed when a solvent gradient was used that compromised both an IP gradient from 5 to 0 mM hexylamine as well as a pH gradient from pH 6.3 to 8.5. The combination of these two gradients leads to separation of very polar and acidic metabolites like nucleotides via an IP mechanism while less polar compounds like CoA esters are separated via a RP mechanism.

In this study, we investigated the IP LC-MS approach for quantitative analysis of various NRTIs, endogenous deoxynucleosides, as well as their mono-, di-, and triphosphates forms in lysates of human-derived PBMCs. Figure 1 demonstrates that, based on *m/z* of

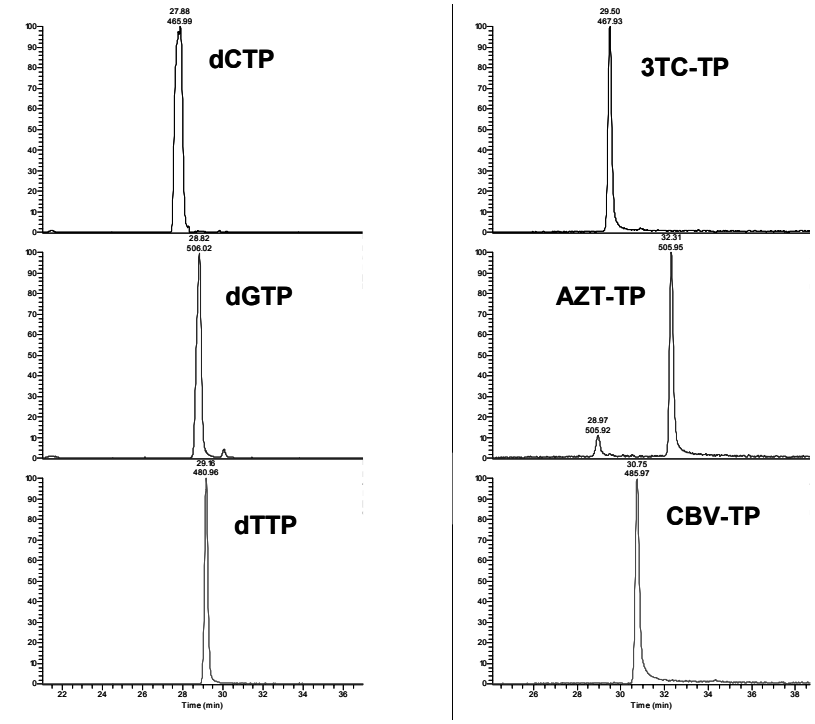

Figure 1. Extracted ion chromatograms of standard solutions of phosphorylated NRTIs and their endogenous counterparts (~ 1 mg/mL) using the IP LC approach in combination with ESI-IT-MS in the full scan MS mode.

the molecular ions and retention times, the phosphorylated NRTIs lamivudine-triphosphate (3TC-TP), zidovudine-triphosphate (AZT-TP), and carbovir-triphosphate (CBV-TP; the active metabolite of abacavir (ABC)) could be distinguished from each other as well as from their endogenous counterparts dCTP, dTTP, and dGTP, respectively.

The mass spectra of these compounds using the negative ionization mode were dominated by *m/z* values corresponding to $[M - H]^-$, and no significant adduct formation was observed. We were also able to detect the nonphosphorylated nucleosides and NRTIs using this IP LC-MS method. However, better sensitivity is obtained when these nonphosphorylated compounds are analyzed using conventional RP methods [7]. Repeated analysis of PBMC lysates (total analysis time ~24 h) showed an RSD in the peak areas of AMP, ADP, and ATP of 3% and an SD in the retention time of ~3 s. This is in agreement with the previously reported rugged analytical performance of the IP LC-MS method when used for the analysis of nucleotides in microbial extracts. In conclusion, the IP LC-MS method is capable of separating various endogenous deoxynucleotides and phosphorylated NRTIs with significant retention and good peak shapes.

To understand the intracellular pharmacology of NRTIs in HIV-infected patients, it is necessary to simultaneously determine the intracellular concentration of endogenous deoxynucleotides and phosphorylated NRTIs at clinical relevant levels [4]. The intracellular concentrations of NRTI-TPs in one million PBMCs are in the order of 10^{-15} –10^{-12} mol (one million PBMCs corresponds with a blood sample of 1–2 mL). These low intracellular concentrations hamper in particular studies in HIV-1-infected children due to the limited volume of blood that can be obtained from these patients. In addition, the intracellular concentrations of endogenous deoxynucleotides, e.g., dGTP, are significantly lower than the intracellular levels of endogenous nucleotides like GTP. Indeed, we were able to detect various endogenous nucleotides in a lysate of 1 x 10^6 PBMC using the IP LC approach on an ESI-IT mass spectrometer. However, endogenous deoxynucleotides could not be detected by this type of MS. The IP LC-MS approach was therefore further investigated using a triple quadrupole mass spectrometer that operated in the SRM mode, which should result in significantly lower LOQs and increased selectivity compared to using an IT mass spectrometer in the full scan mode. As internal standards for quantitative analysis, we used GMP (^{13}C, ^{15}N) for the analysis of the monophosphate (MP) forms of the NRTIs and deoxynucleosides, N^6-(6-aminohexyl)-ADP for the diphosphate (DP) forms, and GTP (^{13}C, ^{15}N) for the triphosphate forms. Table 1 shows that we were able to quantitatively detect in PBMC lysates the mono-, di-, and triphosphate forms of the NRTIs AZT,

Table 1. MS parameters, LOD, and linearity (r^2) obtained from calibration solutions of various endogenous deoxynucleotides and phosphorylated NTRIs in lysates of PBMCs using the SRM on a triple quadrupole mass spectrometer.

Compound	Reaction monitored (*m/z*)	Declustering potential (DP) (V)	Collision energy (CE) (V)	LOD (fmol on column)[a]	r^2 (n = 6)
dTMP	321.0 → 79.1	-30	-50	50	0.9773
dTDP	401.1 → 275.1	-70	-26	25	0.9941
dTTP	481.0 → 159.0	-90	-36	25	0.9952
AZT-MP	346.0 → 78.9	-70	-46	50	0.9869
AZT-DP	426.0 → 159.1	-85	-36	250	0.9908
AZT-TP	506.2 → 159.1	-85	-36	25	0.9956
d4T-MP	303.1 → 176.9	-60	-18	50	0.9916
d4T-DP	383.0 → 256.8	-55	-24	250	0.9746
d4T-TP	463.0 → 158.9	-90	-30	25	0.9934
dCMP	306.0 → 78.8	-60	-54	50	0.9854
dCDP	385.9 → 79.0	-55	-78	25	0.9978
dCTP	466.0 → 158.9	-90	-40	25	0.9910
3TC-MP	308.0 → 78.9	-50	-52	50	0.9835
3TC-DP	387.9 → 78.8	-50	-52	250	0.9815
3TC-TP	468.0 → 158.8	-80	-28	25	0.9919

a) Lowest point in the calibration curve (~ 1–1000 nM) with an S/N > 3.

d4T, and 3TC, as well as all phosphorylated forms of their endogenous deoxynucleoside counterparts deoxythymidine (dT) and deoxycytidine (dC). Figure 2 shows the SRM ion chromatograms of the phosphorylated forms of AZT and its endogenous counterpart dT. In general, the best sensitivity and linearity was obtained for the triphosphate forms of the NRTIs and deoxynucleosides. The LOD for the triphosphate forms of AZT, d4T, 3TC, dT, and dC were 25 fmol on column corresponding to 100 fmol per sample, and the linearity (r^2) of the calibration curves were > 0.99. Previous studies showed that the intracellular concentrations of NRTI-TPs in PBMC obtained from HIV-infected patients were 30-100 fmol/1 x 10^6 PBMCs for AZT-TP and d4T-TP and 7-50 pmol/1 x 10^6 PBMCs for 3TC-TP [13-16].

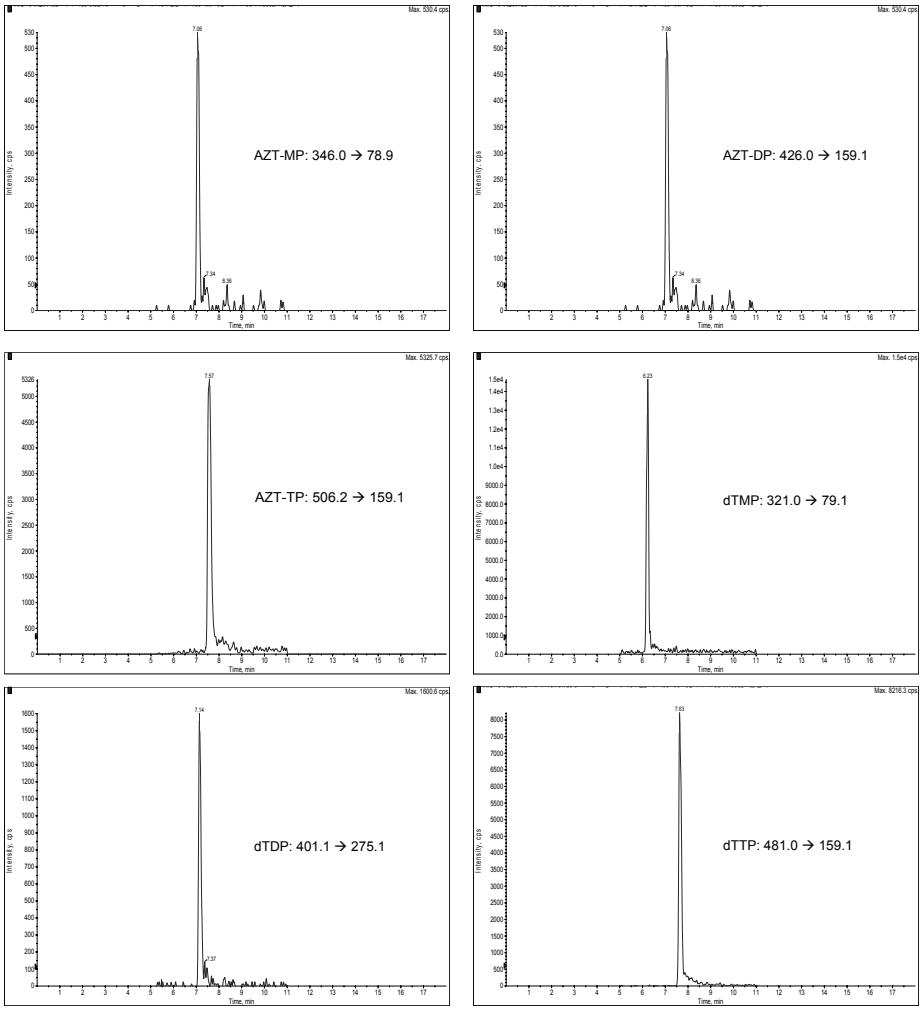

Figure 2. SRM ion chromatograms of the mono-, di-, and triphosphate forms of AZT and its endogenous counterpart dT spiked in a lysate of PBMCs using the IP LC approach on an ESI-triple quadrupole mass spectrometer.

Comparison of these values with the LOD presented in Table 1 shows that the sensitivity of the method developed in this study is sufficient for the analysis of phosphorylated NRTIs in clinical PBMC samples. Preliminary tests showed that the method is also suitable for the analysis of the endogenous deoxynucleotides dAMP, dADP, dATP en dGMP, dGDP, and dGTP and other phosphorylated NRTIs like dideoxyadenosine-triphosphate (ddATP), tenofovir, tenofovir-MP, and tenofovir-DP.

Concluding Remarks

In this study, we investigated an IP LC-MS approach for quantitative analysis of NRTIs, endogenous deoxynucleosides, and phosphorylated forms thereof. This approach is suitable for the simultaneous analysis of the mono-, di-, and triphosphate forms of NRTIs and endogenous deoxynucleosides in human PBMCs at clinical relevant levels, which shows that a single analytical method can be used to study the intracellular metabolism of NRTIs *in vivo*.

Acknowledgements

J. v. K. is supported by a grant from Aids Fonds, The Netherlands (project 2004051). The VIRGO consortium and the members of Top Institute Pharma project T4-212 (Erasmus MC (Rotterdam), TNO Quality of Life (Zeist), UMC St. Radboud (Nijmegen), and GlaxoSmithKline (Zeist)) are acknowledged for their scientific support.

References

1. Back DJ, Burger DM, Flexner CW, Gerber JG. The pharmacology of antiretroviral nucleoside and nucleotide reverse transcriptase inhibitors: implications for once-daily dosing. J Acquir Immune Defic Syndr 2005;39 Suppl 1:S1-23, quiz S4-5.
2. Djabarouti S, Breilh D, Pellegrin I, et al. Intracellular and plasma efavirenz concentrations in HIV-infected patients switching from successful protease inhibitor-based highly active antiretroviral therapy (HAART) to efavirenz-based HAART (SUSTIPHAR Study). J Antimicrob Chemother 2006; 58(5):1090-3.
3. Hennere G, Becher F, Pruvost A, Goujard C, Grassi J, Benech H. Liquid chromatography-tandem mass spectrometry assays for intracellular deoxyribonucleotide triphosphate competitors of nucleoside antiretrovirals. J Chromatogr B Analyt Technol Biomed Life Sci 2003;789(2):273-81.
4. Gao WY, Shirasaka T, Johns DG, Broder S, Mitsuya H. Differential phosphorylation of azidothymidine, dideoxycytidine, and dideoxyinosine in resting and activated peripheral blood mononuclear cells. J Clin Invest 1993;91(5):2326-33.
5. Lewis W, Day BJ, Copeland WC. Mitochondrial toxicity of NRTI antiviral drugs: an integrated cellular perspective. Nat Rev Drug Discov 2003;2(10):812-22.
6. Hoggard P, Khoo S, Barry M, Back D. Intracellular metabolism of zidovudine and stavudine in combination. J Infect Dis 1996;174(3):671-2.
7. Compain S, Schlemmer D, Levi M, et al. Development and validation of a liquid chromatographic/tandem mass spectrometric assay for the quantitation of nucleoside HIV reverse transcriptase inhibitors in biological matrices. J Mass Spectrom 2005;40(1):9-18.
8. Allinquant B, Musenger C, Schuller E. Reversed-phase high-performance liquid chromatography of nucleotides and olignucleotides. J Chromatogr 1985;326:281-91.
9. Federn H, Ristow H. Isolation of standard-, deoxy- and highly phosphorylated nucleotides fromBacillus brevis and their separation by ion-pair high-performance liquid chromatography. Chromatographia 1986;22:287-91.
10. Lopez SLB, Moal J, Serrano FSJ. Development of a method for the analysis of nucleotides from the mantle tissue of the mussel Mytilus galloprovincialis. J Chromatogr A 2000;891(1):99-107.
11. Uesugi T, Sano K, Uesawa Y, Ikegami Y, Mohri K. Ion-pair reversed-phase high-performance liquid chromatography of adenine nucleotides and nucleoside using triethylamine as a counterion. J Chromatogr B 1997;703(1-2):63-74.
12. Coulier L, Bas R, Jespersen S, Verheij E, van der Werf MJ, Hankemeier T. Simultaneous quantitative analysis of metabolites using ion-pair liquid chromatography-electrospray ionization mass spectrometry. Anal Chem 2006;78(18):6573-82.
13. Anderson PL, Kakuda TN, Kawle S, Fletcher CV. Antiviral dynamics and sex differences of zidovudine and lamivudine triphosphate concentrations in HIV-infected individuals. Aids 2003;17(15):2159-68.
14. Becher F, Landman R, Mboup S, et al. Monitoring of didanosine and stavudine intracellular trisphosphorylated anabolite concentrations in HIV-infected patients. Aids 2004;18(2):181-7.
15. Hawkins T, Veikley W, St Claire RL, 3rd, Guyer B, Clark N, Kearney BP. Intracellular pharmacokinetics of tenofovir diphosphate, carbovir triphosphate, and lamivudine triphosphate in patients receiving triple-nucleoside regimens. J Acquir Immune Defic Syndr 2005;39(4):406-11.
16. Yuen GJ, Lou Y, Bumgarner NF, et al. Equivalent steady-state pharmacokinetics of lamivudine in plasma and lamivudine triphosphate within cells following administration of lamivudine at 300 milligrams once daily and 150 milligrams twice daily. Antimicrob Agents Chemother 2004;48(1): 176-82.

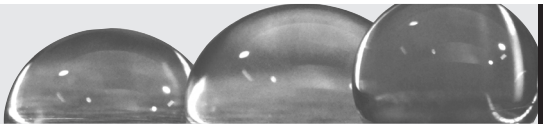

Chapter 4

Qualitative and quantitative analysis of pharmaceutical compounds by MALDI-TOF mass spectrometry

Jeroen J.A. van Kampen, Peter C. Burgers, Ronald de Groot, and Theo M. Luider

Analytical Chemistry 2006, 78, 5403-5411

Abstract

In this report, we discuss key issues for the successful application of MALDI-TOF mass spectrometry to quantify drugs. These include choice and preparation of matrix, nature of cationization agent, automation, and data analysis procedures. The high molecular weight matrix meso-tetrakis(pentafluorophenyl)porphyrin eliminates chemical noise in the low-mass range, a "brushing" spotting technique in combination with prestructured target plates enables fast preparation of homogeneous matrix crystals, and addition of Li^+ leads to intense cationized drug species. Complex biological samples were cleaned up using a 96-well solid-phase extraction plate, and the purified samples were automatically spotted by a pipetting robot. To obtain a suitable data analysis procedure for the quantitative analysis of drugs by MALDI-TOF mass spectrometry, various data processing parameters were evaluated on our two model drugs lopinavir and ritonavir. Finally, and most importantly, it is shown that the above described procedure can be successfully applied to quantify clinically relevant concentrations of lopinavir, an HIV protease inhibitor, in extracts of small numbers of peripheral blood mononuclear cells (1×10^6).

Introduction

In our pediatrics departments, we need a fast, reliable, and sensitive method to quantify antiretroviral drugs in various biological samples, such as extracts from peripheral blood mononuclear cells (PBMCs). To this end, we have initiated a study to test the suitability of matrix-assisted laser desorption/ionization time-of-flight (MALDI-TOF) mass spectrometry for such clinical applications.

MALDI and electrospray ionization (ESI) are the two most extensively used ionization techniques for the mass spectrometric analysis of biological and biomedical compounds. However, only ESI is commonly used for qualitative and quantitative analysis of low molecular weight compounds (< 1,000 Da) such as drugs. This is because, in contrast to MALDI, ESI does not require the addition of matrix molecules; such matrix molecules may undergo association reactions leading to interference peaks in the low-mass range. Nevertheless, MALDI offers some specific advantages over ESI. Perhaps the most important distinction of MALDI is that it is capable of very high sample throughput with minimum instrument maintenance. In addition, MALDI is less susceptible to ion suppression. It is for these reasons that in recent years MALDI has seen its emergence in the field of small-molecule analysis [1].

Two major phenomena hamper the application of the MALDI technique to the analysis of small molecules. As mentioned above, MALDI suffers from matrix-derived chemical interference in the low-mass range [2]. From a quantitative perspective, MALDI suffers from poor reproducibility of the signal abundance [1].

The molecular masses of conventional MALDI matrixes range from 100 to 300 Da. Due to ion/molecule reactions in the matrix plume, a large number of matrix-derived peaks are usually observed in the low-mass range [2]. For example, the often used matrix 2,5-dihydroxybenzoic acid (DHB; $C_7H_6O_4$) produces, after laser irradiation, the series of $(C_7H_5O_4Na)_nNa^+$ ions in admixture with other adducts, even in the presence of residual sodium ions [3]. These abundant matrix-related peaks seriously hamper the qualitative and quantitative analysis of small molecules. One way to avoid such interference signals is to choose a matrix whose molecular weight is in excess of that of the analyte molecule [4,5]. Meso-tetrakis(pentafluorophenyl)porphyrin (F20TPP) is such a high molecular MALDI matrix (MW 974.6 Da) and has successfully been used for the analysis of various small molecules, for example, poly(ethylene glycol)s, fatty acids, and sugars [6-8].

A variety of approaches have been reported to enhance the signal reproducibility of MALDI mass spectrometers, and they can be divided into two main groups: (1) enhancement of homogeneous matrix crystallization, enhancement of homogeneous analyte incorporation into the matrix crystals, or both. This can be achieved, for example, by preparing matrix crystals using a fast evaporation protocol or by using prestructured

target plates [9,10]. (2) averaging out variations in instrument response by employing an internal standard and by averaging out multiple spectra of one sample [11-13].

In this study, a strategy is presented to overcome the two main limitations of MALDI-TOF mass spectrometry for the qualitative and quantitative analysis of small molecules. To reduce the number of matrix-derived peaks in the low-mass range, we have used a high molecular weight matrix, viz. F20TPP. To increase reproducibility (precision), we have developed, using prestructured target plates, a fast evaporation protocol for the matrix F20TPP. To increase reproducibility further, instrument response variation was minimized by using an internal standard, by averaging out 1,000 spectra per sample, and by measuring each sample 4-fold. In addition, the effects of various data analysis procedures on the precision and accuracy of analyte abundances was investigated. Finally, we demonstrate that MALDI-TOF mass spectrometry can be successfully used for the quantitative analysis of lopinavir, an HIV protease inhibitor, in extracts of PBMCs.

Experimental Section

Pharmaceutical compounds

Lopinavir and ritonavir were kindly provided by Abbott Laboratories. Indinavir was kindly supplied by Merck Sharp & Dohme. Saquinavir was kindly provided by F. Hoffmann-La Roche. Nelfinavir was kindly provided by Pfizer Inc. Zidovudine, lamivudine, abacavir, and amprenavir were kindly provided by GlaxoSmithKline. Nevirapine and tipranavir were kindly provided by Boehringer Ingelheim. Erythromycin, omeprazole, carbamazepine, sulfamethoxazole, levofloxacin, primaquine, metoprolol, acetylsalicylic acid, amikacin, tobramycin, ampicillin, acetaminophen, trimethoprim, penicillin G, and rifampicin were purchased from Sigma-Aldrich.

Chemicals

Lithium iodide, sodium iodide, potassium iodide, rubidium iodide, cesium iodide, HPLC grade water, and 5,10,15,20-tetrakis(pentafluorophenyl)porphyrin were obtained from Sigma-Aldrich. All organic solvents were obtained from J. T. Baker. All chemicals were purchased at the highest purity grade available and were used without further purification.

Standards for qualitative analysis

Dilution series for each pharmaceutical compound were prepared in ethanol/water (1:1). Dilution series A contained pharmaceutical compounds at a concentration of 8,000, 4,000, 2,000, 1,000, and 500 fmol/µL. Dilution series B contained pharmaceutical

compounds at a concentration of 80, 40, 20, 10, and 5 fmol/µL. Samples were stored at -20°C.

Standards for quantitative analysis of pure lopinavir and ritonavir

Calibrators were prepared of pure lopinavir and ritonavir at concentrations of 1,000, 900, 800, 700, 500, 400, 300, 200, 100, 80, 40, 20, 15, 10, 5, and 1 fmol/µL. Each calibrator was spiked with 50 fmol/µL indinavir (internal standard). All calibrators were prepared in ethanol/water (1:1) and stored at - 80°C.

Standards for quantitative analysis of lopinavir in PBMC extracts

PBMCs were isolated from a buffy coat (Sanquin) using a Ficoll density gradient. Calibrators were prepared of pure lopinavir in ethanol/water (1:1) at concentrations of 4,000, 3,000, 2,000, 1,000, 400, 200, 100, 50, and 25 fmol/µL spiked with 500 fmol/µL saquinavir (internal standard). A 100-µL aliquot of each calibrator was added to a dry pellet of 1 x 10^6 PBMCs, and PBMCs were extracted overnight in these calibrator solutions at 5°C. Subsequently, cell debris was spun down and supernatants were loaded onto a 96-well solid-phase extraction plate (Oasis HLB µelution plate, Waters). The loaded samples were washed twice with 200 µL of methanol/water (1:19) and 200 µL of methanol/water (1:1), respectively. Samples were eluted from the solid-phase extraction plate using 100 µL of methanol/water (3:1). The eluted samples were dried using a SpeedVac (Savant) and were stored at -20°C. On the day of analysis, the dried samples were reconstituted in 100 µL of ethanol/water (1:1).

Matrix and matrix spotting technique

Four parts of 25 mg/mL F20TPP, dissolved in 100% acetone, were mixed with one part of 100 mM LiI, NaI, KI, RbI, or CsI. LiI, and NaI, dissolved in 100% acetone, and KI, RbI, and CsI were dissolved in 100% methanol. Thus, the final matrix solutions contained 20 mg/mL F20TPP and 20 mM alkali iodide. Matrix crystals were prepared on an AnchorChip target plate with 800-µm sized hydrophilic anchors (Bruker Daltonics) by the following "brushing" technique: A 10-µL pipette tip was filled with matrix solution. Next, the pipette was positioned such that the tip just touched the target plate above the first spot. Next, the plunger was slightly pressed and at the same time the pipette was quickly dragged downward over the target spots.

Sample spotting

All samples were spotted in 4-fold (1 µL/replicate) on top of the matrix crystals using a ClinProtRobot pipetting robot, which was controlled by ClinProtRobot Workflow, Editor version 1.0 software (Bruker Daltonics, Germany).

Sample measurement

All experiments were performed on an Ultraflex-I MALDI-TOF/TOF mass spectrometer (Bruker Daltonics) equipped with a 50-Hz nitrogen laser (337 nm). Mass spectra were recorded in the positive ion reflectron mode. FlexControl version 2.4 software was used to operate the mass spectrometer. A sample spot containing matrix only was used to manually set the laser power ~5% above the threshold for ionization. The samples containing the analytes were measured automatically using the AutoXecute part of the FlexControl software. Mass spectra were recorded by accumulating 50 shots on 20 different positions on each sample spot. No spectra were rejected (i.e., fuzzy control for spectra accumulation was not used). Four replicates of each sample were measured, and each experiment was repeated three times.

Data analysis

A FlexAnalysis script, kindly provided by Bruker Daltonics, was used to process the raw mass spectra in batch and to pick all peaks for a specified *m/z* range. Each mass spectrum was processed with and without baseline subtraction, and peak picking was performed using the "centroid" peak picking algorithm (monoisotope only) as well as the "SNAP" peak picking algorithm (all isotopes). Baseline subtraction was performed using the "median" baseline subtraction algorithm with 0.8 flatness. For the centroid peak picking algorithm, the signal-to-noise ratio (S/N) threshold was set at 3 times above the standard deviation of the noise. The S/N threshold was set at 5 for the SNAP peak picking algorithm. Subsequently, a "search for masses" macro, kindly provided by Bruker Daltonics, was used to automatically extract in batch peak parameters (peak intensity, peak S/N, and peak area) for specific masses (analyte and internal standard) from the peak lists generated by the above-described FlexAnalysis script.

Precision and accuracy calculations

Full analysis was performed when the analyte and internal standard were present at S/N > 3 or > 5 (vide supra) in at least two out of the four replicates. Of each experiment, the consecutive series of concentration calibrators that fulfilled the FDA ± 20/15% criteria for *precision* [14] was used for *accuracy* calculations, using the mean analyte-to-internal standard response ratios of the replicates of each calibrator. The consecutive series of calibrators was chosen in such way that it contained the calibrator with the lowest analyte concentration. Unweighed, 1/x weighed, and $1/x^2$ weighed linear, and quadratic curve fitting methods were applied to construct the calibration curves. Calibrators with the highest analyte concentration of a consecutive series were removed one by one until that calibrator series fulfilled the FDA ± 20/15% criteria for accuracy [14]. Outliers were not removed unless otherwise stated.

Results and Discussion

Meso-tetrakis(pentafluorophenyl)porphyrin matrix

The use of MALDI mass spectrometry for the quantitative analysis of drugs is normally hampered by interfering matrix peaks in the low-mass range and poor precision of signal abundances [1]. meso-Tetrakis(pentafluorophenyl)porphyrin (F20TPP) has a high molecular weight (MW 974.6 Da) compared to other more commonly used matrixes such as DHB (MW 154.1 Da) and α-cyano-4-hydroxycinnamic acid (MW 189.2 Da). Ayorinde et al. have shown that only a few interfering matrix peaks are observed in the low mass range of F20TPP, which is prerequisite for the analysis of small molecules [7]. To perform high-throughput quantitative analysis of drugs, we have developed a protocol for the rapid preparation of homogeneous F20TPP matrix crystals using prestructured target plates. F20TPP was dissolved in acetone and spotted on a hydrophobic target plate with hydrophilic anchors (AnchorChip) using a simple brushing. Each anchor absorbed ~0.2 µL of matrix solution, and homogeneous matrix crystals formed within 1 s. The matrix can be spotted on all 384 anchors of a single target plate within 5 min. Samples were spotted on top of the matrix crystals, and since F20TPP is not soluble in water, ethanol, or methanol, the sample solvent simply evaporates without perturbing matrix crystal homogeneity. Considering the good precision we can achieve (vide infra), we conclude that the analyte is indeed homogeneously incorporated into the matrix.

Upon laser irradiation, F20TPP forms radical cations and it also undergoes self-protonation. These protonated molecules may serve as proton donors for the analyte molecules. Our model compounds lopinavir and ritonavir contain peptide bonds, which have high proton affinities (PA) [15]. Thus, we expected that lopinavir and ritonavir would become protonated within the MALDI plume. However, no signals were observed for the protonated analytes when F20TPP was used as matrix (see Figure 1). Thus, F20TPP does not transfer a proton to the analyte, presumably because the PA of F20TPP is higher than that of lopinavir and ritonavir.

Another way to ionize molecules by MALDI is to add an alkali salt leading to alkali ion attachment. Indeed, for molecules lacking basic sites, such as sugars, cationization can be accomplished by the addition of alkali ions [3]. This is also true when using the matrix F20TPP, which is usually mixed with sodium or potassium salts to ionize the analytes of interest [6-8,16]. We investigated the effect of lithium, sodium, potassium, rubidium, and cesium iodide on the detection limits of lopinavir and ritonavir. Iodide was chosen as counter-anion, because the lower lattice energy of alkali iodides compared to other alkali halides results in more free gaseous alkali ions and, thus, higher signal abundances of the cationized analytes [17]. Considering the above argument based on lattice energies, it might reasonably be expected that for the alkali iodides the concentration of gaseous alkali ions will be in the order $Li^+ < Na^+ < K^+ < Rb^+ < Cs^+$. This is indeed observed. In Figure

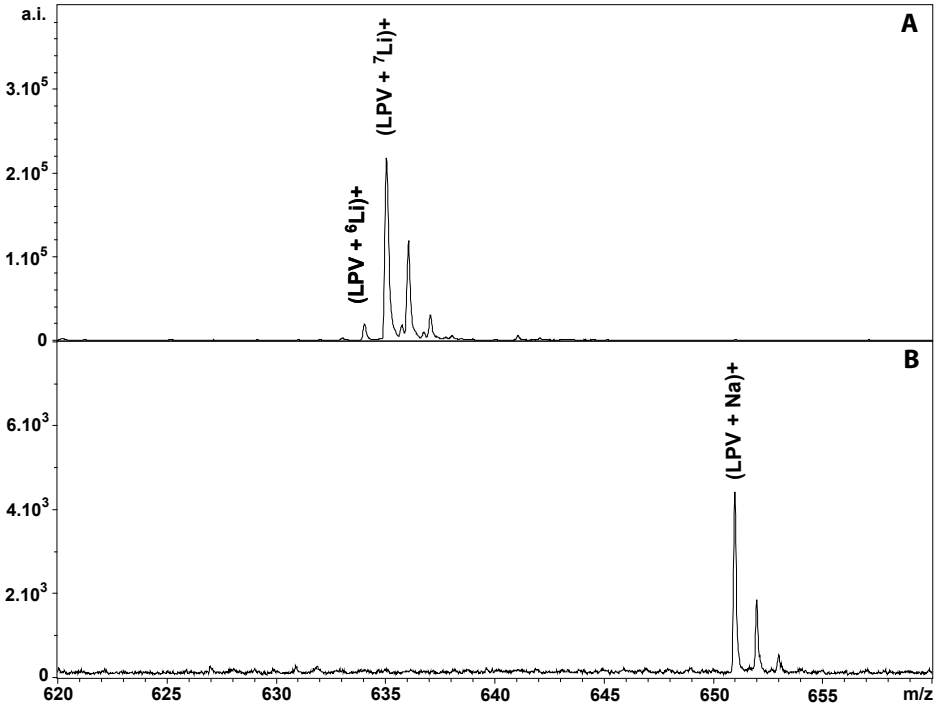

Figure 1. Analysis of lopinavir using F20TPP as matrix. a.i., absolute intensity. The molecular weight of lopinavir (LPV) is 628.8 Da. Panel A: An intense signal for lithiated lopinavir was observed when 1 pmol of lopinavir was analyzed with 20 mg/mL F20TPP + 20 mM LiI. No protonated lopinavir was observed. Panel B: A signal was observed for lopinavir cationized by residual sodium ions when 1 pmol of lopinavir was analyzed with 20 mg/mL F20TPP. No protonated lopinavir was observed.

2 are shown the MALDI-TOF mass spectra of equimolar amounts of the alkali iodides using F20TPP (Figure 2A) and DHB (Figure 2B) as matrix. As can be seen, the amount of gas-phase ions available for cationization is highest for Cs^+, whereas virtually no lithium ions are liberated. On the other hand, the alkali affinity of substrates will be in the opposite order, viz. $Li^+ > Na^+ > K^+ > Rb^+ > Cs^+$, because the smaller the ionic radius, the more stable the association of the alkali ion with the substrate will be (ion-dipole stabilization energies are inversely proportional to the *square* of the distance between the charge and substrate binding location). Thus, there are two opposing effects, to wit bare alkali ion availability and substrate alkali ion affinity. That there are indeed two opposing effects is borne out by cationization experiments using poly(ethylene glycol)s (PEGs) cationized by equimolar amounts of alkali iodides using DHB as matrix (see Figure 3B). An optimum for alkali attachment to the PEG chain was obtained for potassium in agreement with the operation of the two opposing effects discussed above. However, cationization experiments with PEGs and F20TPP showed a completely different distribution of the

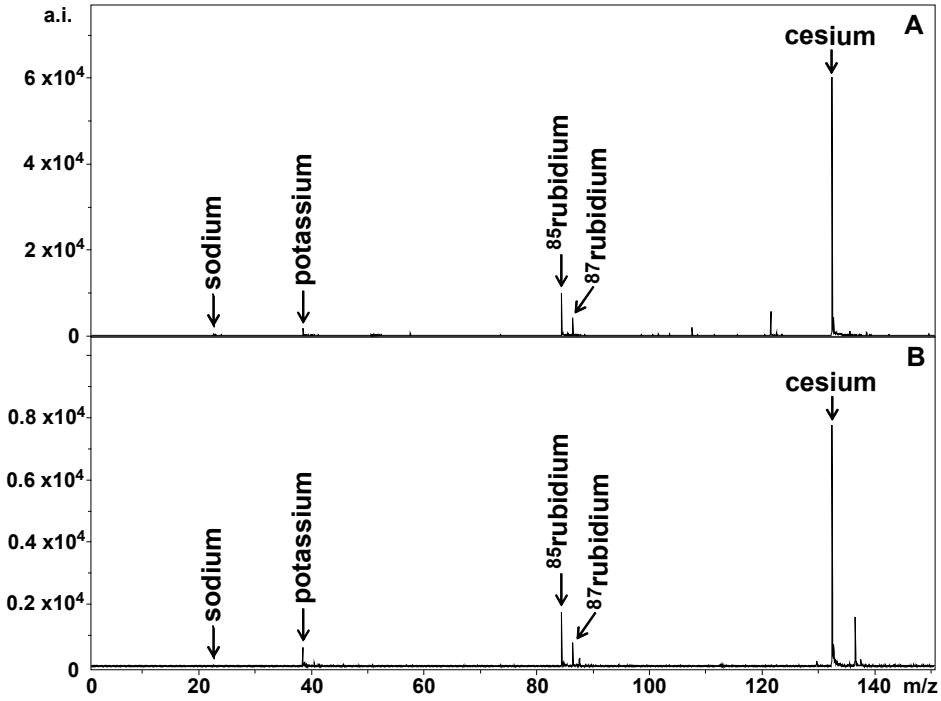

Figure 2. Abundances of free cations from equimolar alkali iodide salts. a.i., absolute intensity. Panel A: mass spectrum of 20 mg/mL F20TPP + 4 mM LiI, NaI, KI, RbI, and CsI. No free lithium ions were observed. Panel B: mass spectrum of 10 mg/mL DHB + 4 mM LiI, NaI, KI, RbI, and CsI. No free lithium ions were observed.

cationized PEG (see Figure 3A): An optimum alkali attachment to the PEG chain was obtained for lithium.

Our two model compounds lopinavir and ritonavir showed a similar cation distribution when analyzed with F20TPP (Figure 4). The highest signal abundances for cationized lopinavir and ritonavir were observed when F20TPP was mixed with lithium iodide. We therefore conclude that alkali cationization using the F20TPP matrix does not occur by attachment of free lithium ions in the gas phase. This is in sharp contrast to results obtained with low molecular weight matrixes, such as DHB, where free cation attachment is the predominant process [18]. The mechanism of alkali attachment to pharmaceutical compounds using the matrix F20TPP is currently under investigation in our laboratories. For now, we will exploit the observation that lithium attachment produces the most intense signals. The combination of F20TPP and lithium iodide was therefore used as matrix for all other experiments.

Qualitative analysis of pharmaceutical compounds

We obtained the detection limits (S/N ≥ 3) for the lithiated monoisotopic peaks of 26 drugs using the F20TPP matrix. Most of the drugs tested in this experiment are used to

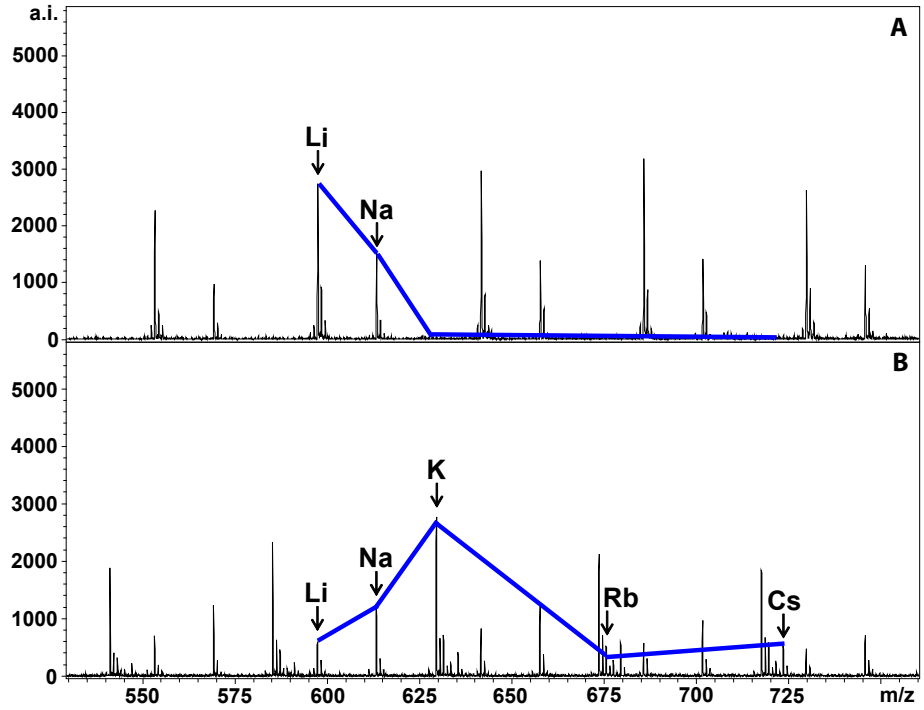

Figure 3. Distribution of cationized PEG600 using equimolar alkali iodide salts. a.i., absolute intensity. Panel A: mass spectrum of PEG600 analyzed with 20 mg/mL F20TPP + 4 mM LiI, NaI, KI, RbI, and CsI. The most abundant signals were observed for lithiated PEG600, followed by sodiated PEG600. PEG600 did not form adducts with potassium, rubidium, or cesium. Panel B: mass spectrum of PEG600 analyzed with 10 mg/mL DHB + 4 mM LiI, NaI, KI, RbI, and CsI. The abundance of cationized PEG600 signals was as follows: K > Na > Li > Rb ≈ Cs. The solid line represents the cation distribution for PEG600 with a chain length of 13 CH_2CH_2O units.

treat HIV or other infectious diseases. In addition, we tested drugs that are frequently prescribed or used to treat neurological diseases. The best detection limits were obtained for the HIV protease inhibitors lopinavir, ritonavir, saquinavir, indinavir, and nelfinavir (5 fmol). The HIV protease inhibitors amprenavir and tipranavir were detected up to 10 and 40 fmol, respectively. Erythromycin (10 fmol), omeprazole (10 fmol), carbamazepine (40 fmol), sulfamethoxazole (40 fmol), and levofloxacin (40 fmol) were detected at levels comparable to that of the HIV protease inhibitors. The detection limits for the HIV reverse transcriptase inhibitors lamivudine, nevirapine, zidovudine, and abacavir ranged from 500 to 1,000 fmol. Comparable detection limits were obtained for primaquine (500 fmol), metoprolol (500 fmol), acetylsalicylic acid (500 fmol), amikacin (1,000 fmol), and tobramycin (1,000 fmol). Ampicillin could be detected up to 4,000 fmol, and acetaminophen, trimethoprim, penicillin G, and rifampicin could not be detected using the F20TPP matrix.

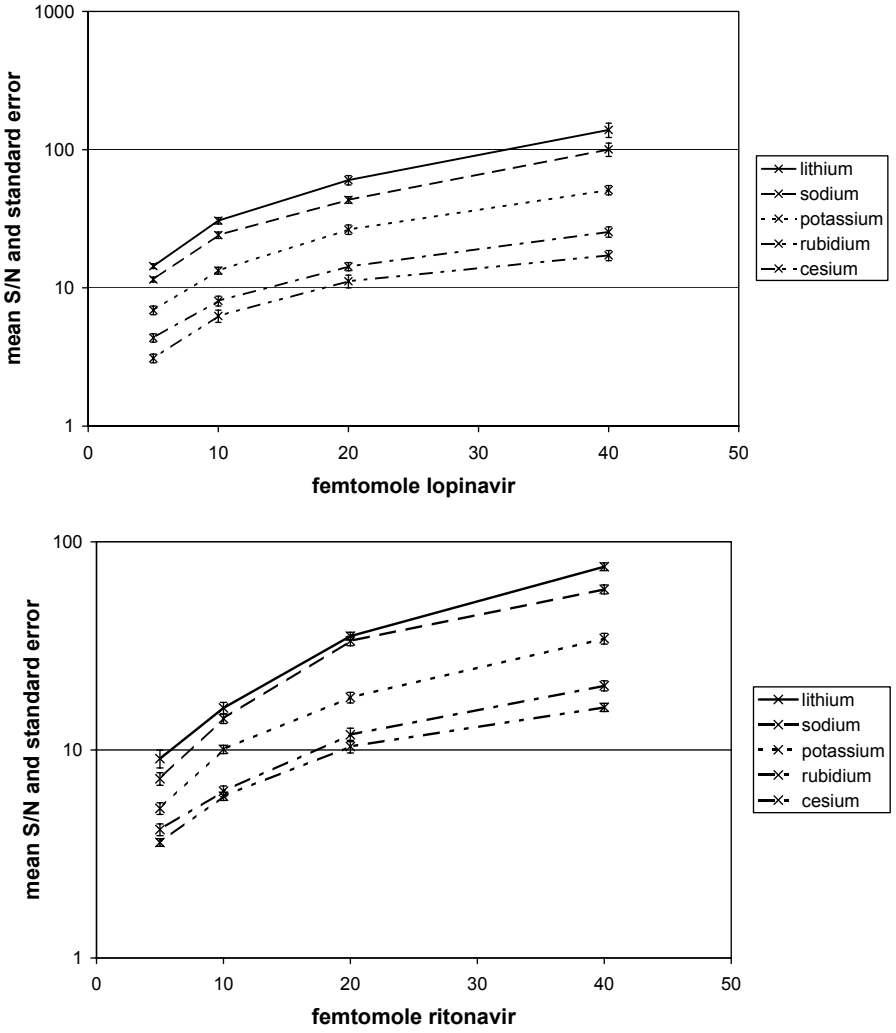

Figure 4. Effects of equimolar alkali iodide salts on the signal abundances of lopinavir and ritonavir (n = 12).

Quantitative analysis of pure lopinavir and ritonavir

In the life sciences, MALDI-TOF mass spectrometry is mostly used for qualitative analysis of compounds such as peptides and proteins. As a consequence, little is known as to how data should be treated for quantitative analysis of small molecules. Therefore, we tested the effect of baseline subtraction, choice of peak parameter (intensity, S/N, area), and choice of analyte signal (monoisotope, all isotopes) on the precision of the lopinavir and ritonavir abundances. The results are shown in Table 1. For each entry, 16 concentrations of lopinavir and ritonavir were measured in 4-fold using indinavir as internal standard, and the average precision was calculated together with the standard deviation. The above procedure was performed three times, and from these three experiments, the

Table 1. Effects of twelve data analysis procedures on the mean precisions (% CV) of all calibrators of lopinavir and ritonavir[a]

Procedures	LPV	RTV
monoisotope no intensity	11	10
monoisotope yes intensity	12	10
monoisotope no S/N	11	10
monoisotope yes S/N	12	10
monoisotope no area	8	9
monoisotope yes area	9	9
all isotopes no intensity	19	9
all isotopes yes intensity	15	9
all isotopes no S/N	19	9
all isotopes yes S/N	18	9
all isotopes no area	13	9
all isotopes yes area	11	9

[a] LPV, lopinavir. RTV, ritonavir. The left column shows which analyte signal was used (monoisotope, all isotopes), whether a baseline subtraction was used or not (yes/no), and which peak parameter was used (intensity, S/N, area).

average precision and standard deviation was extracted. Thus, the entries in Table 1 are the result of 192 measurements. The peak parameter "area" resulted in slightly better precisions of the lopinavir and ritonavir abundance compared to the peak parameter "intensity" or "S/N". Baseline subtraction did not have an effect on the precision. It can be seen that for lopinavir the precision deteriorates significantly when all isotopes are used. By contrast, for ritonavir no significant changes were observed. The poor precision of lopinavir when signal abundances of all isotopes were used may well be due to contamination of other compounds leading to interferences under the isotopic peaks of lopinavir.

Subsequently, we investigated whether drugs could be quantified by MALDI-TOF mass spectrometry according to the ± 20/15% criteria of the FDA for precision and accuracy: Precision (expressed as % relative standard deviation) and accuracy (expressed as % deviation from the theoretical concentration) should be ≤ 15% for all calibrators except for the lower limit of quantification (LLOQ), which should be ≤ 20% [14]. Table 2 shows the effects of baseline subtraction, choice of peak parameter (intensity, S/N, area), and choice of analyte signal (monoisotope, all isotopes) on the dynamic range of the lopinavir and ritonavir calibration curves that fulfilled the FDA ± 20/15% criteria for precision and accuracy. In general the best, i.e., largest, dynamic ranges were obtained by applying no baseline subtraction and by using the monoisotopic peak area. The application of baseline subtraction when the monoisotopic peak abundance of lopinavir was used resulted in a marked decrease in dynamic range. This effect was attributed to the increase in LLOQ from 1 (no baseline subtraction) to 5 fmol (baseline subtraction).

Table 2. Effects of twelve data analysis procedures on the mean dynamic range of lopinavir and ritonavir[a]

Procedures	LPV	RTV
monoisotope no intensity	86	33
monoisotope yes intensity	24	53
monoisotope no S/N	78	56
monoisotope yes S/N	21	53
monoisotope no area	186	74
monoisotope yes area	35	74
all isotopes no intensity	21	33
all isotopes yes intensity	19	32
all isotopes no S/N	19	50
all isotopes yes S/N	21	53
all isotopes no area	35	53
all isotopes yes area	10	50

[a] RTV, ritonavir. LPV, lopinavir. The left column shows which analyte signal was used (monoisotope, all isotopes), whether a baseline subtraction was used or not (yes/no), and which peak parameter was used (intensity, S/N, area). Calibrator series of lopinavir and ritonavir were analyzed in 4-fold, and experiments were repeated three times. Subsequently, data were analyzed using 12 data analysis procedures (left column of the table), and precisions were calculated for the lopinavir and ritonavir calibrators. Calibrators that fulfilled the FDA ± 20/15% criteria for precision were used to construct calibration curves in the following way: six curve fitting methods were applied and calibrators with the highest analyte concentration were removed one by one until the calibration curve fulfilled the FDA ± 20/15% criteria for accuracy. Reported here is the mean of the all dynamic ranges obtained by applying various curve fitting methods for each of the 12 data analysis procedures.

This effect was not observed for ritonavir. In general, the LLOQ increased when the signal abundances of all isotopes were used compared to the use of the monoisotopic peak abundance.

Table 3 shows the effects of the six curve fitting methods on the mean dynamic range of lopinavir and ritonavir. Quadratic curve fitting resulted in a larger dynamic range compared to linear curve fitting. Furthermore, the effect of weighing on the dynamic range, ordered from best to worst, was $1/x^2$ weighing > 1/x weighing > unweighed curve fitting. The FDA states that the simplest model that accurately describes the

Table 3. Effects of six curve fitting methods on the mean dynamic range lopinavir and ritonavir[a]

	linear			quadratic		
compound	unweighed	1/x weighed	$1/x^2$ weighed	unweighed	1/x weighed	$1/x^2$ weighed
ritonavir	25	50	54	41	69	69
lopinavir	16	41	54	30	59	76

[a] Linear unweighed, linear 1/x weighed, linear $1/x^2$ weighed, quadratic unweighed, quadratic 1/x weighed, and quadratic $1/x^2$ weighed curve fitting methods were used to construct lopinavir and ritonavir calibration curves. Here we report the mean dynamic range of all 12 data analysis procedures (see Table 2) for each curve fitting method.

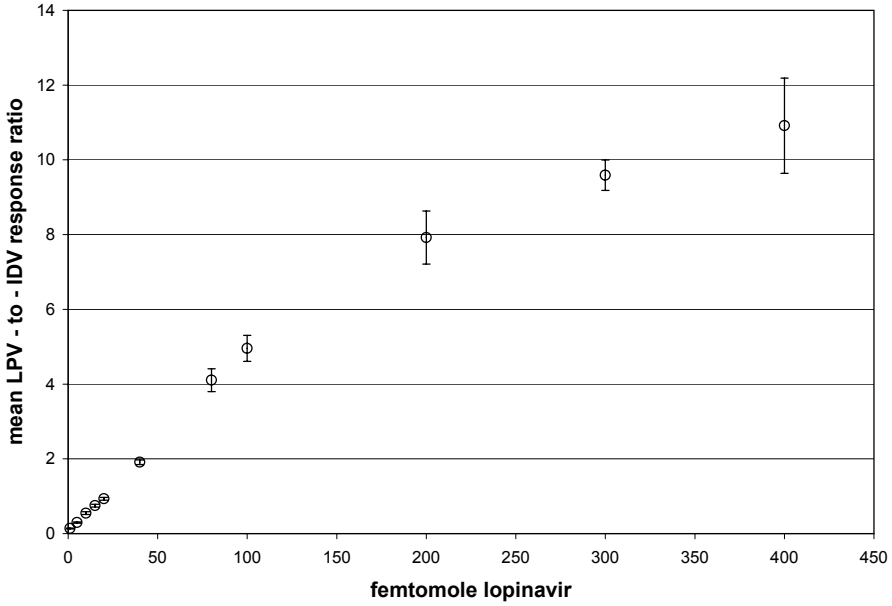

Figure 5. Concentration-response relationship of lopinavir using MALDI-TOF mass spectrometry. LPV, lopinavir; IDV, indinavir. Vertical bars represent plus and minus one standard deviation.

concentration-response relationship should be used to construct a calibration curve [19]. In addition, the selection of weighing and use of complex regression equation should be justified [19], which we do here. MALDI-TOF mass spectrometers are typically equipped with 8-bit analog-to-digital converters (ADC). These ADCs convert the intensity of the detector output into a numerical value of 0-255 [20]. Therefore, the dynamic range of MALDI-TOF mass spectrometers is generally limited to 2 orders of magnitude. Indeed, for our MALDI-TOF mass spectrometer, the concentration-response relationship was approximately linear when relative low concentrations of lopinavir were analyzed (up to 100 fmol), while the concentration-response relationship was more quadratic for higher lopinavir concentrations (see Figure 5). Furthermore, weighing functions were applied to reduce the influence of the higher concentrations on the fitted line, since the variance of the instrument response increases with the analyte concentration [19]. In conclusion, the best dynamic ranges were obtained using the following data analysis procedure: No baseline subtraction, the use of the monoisotopic peak area, and construction of a calibration curve using a $1/x^2$ weighed quadratic curve fitting method. Table 4 shows the precisions and accuracies of lopinavir and ritonavir when using this data analysis procedure.

Table 4. Quantitative analysis of pure lopinavir and ritonavir[a]

	lopinavir			ritonavir		
	exp 1	exp 2	exp 3	exp 1	exp 2	exp 3
LLOQ (fmol)	1	1	1	5	5	5
ULOQ (fmol)	200	300	500	900	500	700
mean precision	6.3 ± 2.0	6.8 ± 3.6	6.1 ± 3.9	7.0 ± 3.7	7.7 ± 3.1	7.3 ± 4.6
Mean accuracy	5.9 ± 4.2	6.7 ± 4.3	5.1 ± 3.1	4.9 ± 3.4	5.1 ± 3.5	3.7 ± 3.0

[a] LLOQ, lower limit of quantification. ULOQ, upper limit of quantification. exp, experiment. Calibrator series of pure lopinavir and ritonavir were measured in 4-fold, and experiments were repeated three times. Precisions of the mean analyte-to-internal standard response ratios for each calibrator were calculated using the monoisotopic peak areas. Calibrators that fulfilled the FDA ±20/15 criteria for precision were used to construct calibration curves in the following way: A $1/x^2$ quadratic curve fitting method was applied, and calibrators with the highest analyte concentration were removed one by one until the calibration curve fulfilled the FDA ±20/15 criteria for accuracy. The reported precisions and accuracies are the mean values for all calibrators that fulfilled the ±20/15 criteria for precision and accuracy.

Quantitative analysis of lopinavir in cell extracts

Next, we investigated whether MALDI-TOF mass spectrometry could be used to quantify clinically relevant concentrations of lopinavir in PBMC extracts according to the FDA ± 20/15% criteria for precision and accuracy. Crommentuyn et al. reported a mean intracellular lopinavir concentration in 11 HIV-1 infected adults of 6.4 pmol/1 x 10^6 PBMCs just before drug intake, and the peak concentration was 8.5 pmol/1 x 10^6 PBMCs [21]. The results of our experiments are shown in Table 5. As can be seen, our procedure allows the quantification of lopinavir down to 25 fmol in extracts of 1 x 10^6 PBMCs according to the FDA ± 20/15% criteria for precision and accuracy. This is well below the clinically relevant concentrations mentioned above. These results clearly show that MALDI-TOF mass spectrometry can be successfully used for clinical studies on the intracellular pharmacology of lopinavir. In Figure 6 are shown the mass spectra of PBMC extracts. It can be seen that after solid-phase extraction the spectra are remarkably clean. Considering

Table 5. Quantitative analysis of lopinavir in PBMC extracts[a]

	exp 1	**exp 2**	**exp 3**
LLOQ (fmol)	25	25	25
ULOQ (fmol)	4000	3000	2000
mean precision	7.4 ± 3.7	8.4 ± 4.8	6.2 ± 3.4
mean accuracy	5.5 ± 5.3	5.7 ± 4.6	4.9 ± 4.4

[a] LLOQ, lower limit of quantification. ULOQ, upper limit of quantification. exp, experiment. Processed calibrator series were measured in 4-fold, and experiments were repeated three times. The mean analyte-to-internal standard responses were calculated for each calibrator using the monoisotopic peak areas. Calibration curves were constructed using a $1/x^2$ weighed quadratic curve fitting. The reported precisions and accuracies are the mean values for all calibrators that fulfilled the FDA ±20/15 criteria for precision and accuracy. In experiment 3, one outlier was removed.

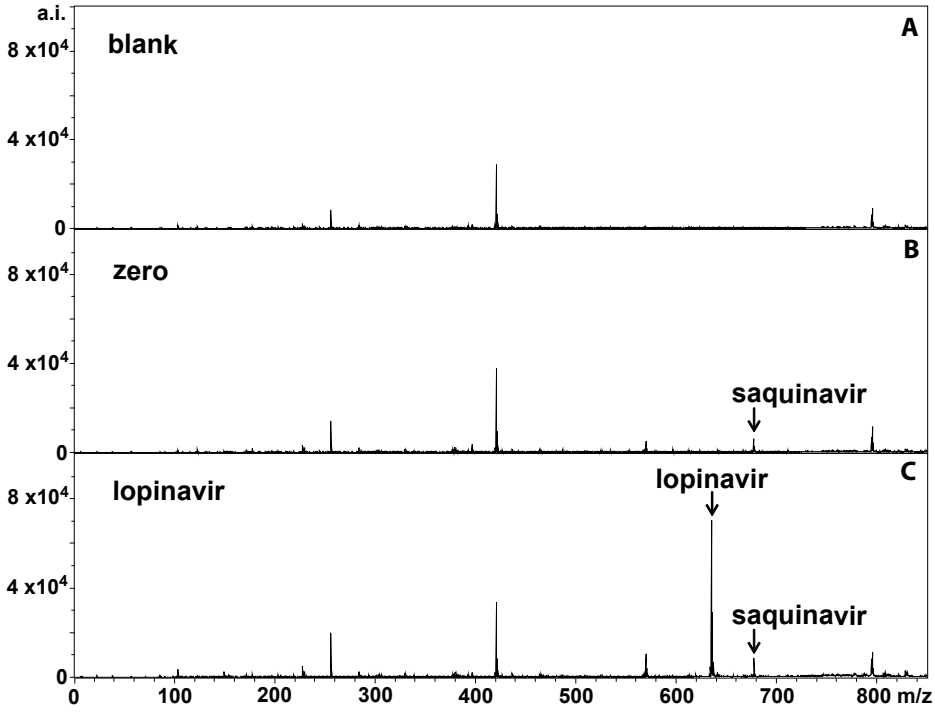

Figure 6. Mass spectra of PBMC extracts analyzed by MALDI-TOF mass spectrometry. a.i., absolute intensity. Panel A: mass spectrum of 1 x 10^6 PBMCs that were extracted using ethanol/water without adding drugs. Panel B: mass spectrum of 1 x 10^6 PBMCs that were extracted using ethanol/water spiked with internal standard only (500 fmol/µL saquinavir). Panel C: mass spectrum of 1 x 10^6 PBMCs that were extracted using ethanol/water spiked with internal standard (500 fmol/µL saquinavir) and analyte (2000 fmol/µL lopinavir).

that the mean signal-to-noise ratio (n=12) obtained at the LLOQ was 9 (sd 2.3), better quantification limits seem possible.

In clinical studies on the intracellular pharmacology of antiretroviral drugs, aqueous mixtures containing a high percentage of organic solvent are used to extract the antiretroviral drugs from the PBMCs. We therefore prepared calibrator series of lopinavir in ethanol/water (1:1), and these calibrators were used to extract 1 x 10^6 PBMCs. One million PBMCs were used for these experiments, since this amount of PBMCs can be obtained from a blood sample of 1-2 mL, a prerequisite for clinical studies in HIV-1 infected children.

A time-of-flight mass analyzer is normally not the first choice for quantitative analysis of drugs. As described above, the dynamic range is relatively small due to the use of analog-to-digital converters with an 8-bit size. Furthermore, most time-of-flight analyzers are not designed to perform tandem mass experiments (MS/MS) on small molecules in contrast to, for example, triple quadrupole mass analyzers. Tandem mass experiments are used to

increase signal-to-noise ratios and selectivity of drug measurements. Therefore, the development of new types of MALDI mass spectrometers, such as MALDI-triple quadrupole mass spectrometers, is of special interest for the quantitative analysis of drugs [12, 22-24].

Sample volumes typically used in MALDI mass spectrometry are in the order of 1 µL. The challenge for the successful application of MALDI mass spectrometry for quantitative analysis of drugs is to concentrate analytes in such a small volume in a reproducible manner. In our experiment, we reconstituted the processed calibrators in 100 µL of ethanol/water, but only 1 µL was spotted on to the target plate. Thus, a factor 100 in sensitivity was lost. Nevertheless, the obtained quantification limit of at least 25 fmol for lopinavir in cell extracts allows reliable and clinical applications of our procedure. However, loss in sensitivity of a factor 100 could complicate the quantitative analysis of other drugs that have lower intracellular concentrations than lopinavir. To circumvent this problem, smaller solvent volumes could be used to reconstitute calibrators after vacuum-drying. Another way is to elute calibrators in a smaller volume from the solid-phase extraction plate and to directly spot the eluents onto the target plate. For example, Gobey et al. eluted calibrators in volumes of 25 µL and spotted the eluents directly onto a target plate prior to quantitative analysis using a MALDI-triple quadrupole mass spectrometer [22].

One of the hallmarks of MALDI mass spectrometry is the speed of analysis. On our MALDI-TOF mass spectrometer, a typical time to analyze a sample in 4-fold in an automated way was 2 min and 20 s. Our MALDI-TOF mass spectrometer is equipped with a 50-Hz nitrogen laser, and the use of higher repetition rate lasers could further decrease analysis time to a few seconds as described by Volmer and co-workers [12]. Fast sample preparation techniques are needed to exploit the high-throughput capacity of MALDI mass spectrometers. To this end, we have used 96-well solid-phase extraction plates allowing fast sample preparation. In addition, our pipetting robot is compatible with the 96-well format, allowing fast, automated, and reproducible sample spotting. Furthermore, using the described brushing, the matrix can be spotted onto the target plate in 5 min.

Conclusions

We have constructed a protocol by which pharmaceutical drugs, especially HIV protease inhibitors, can be successfully quantified in peripheral blood mononuclear cells using MALDI-TOF mass spectrometry. We have examined various acquisition procedures and post-acquisition processing parameters. Crucial for acquiring reliable data is the use of a high molecular weight matrix, thereby virtually eliminating chemical noise, and the use of Li^+ to achieve efficient cationization of the drug. The choice of post-acquisition

data analysis procedures has a profound effect on the quantitative performance of the MALDI-TOF mass spectrometry technique. The best results were obtained using the monoisotopic peak areas of the analyte and internal standard, weighed quadratic curve fitting to construct the calibration curves, and no baseline subtraction. Using our protocol, we were able to quantify clinically relevant concentrations of lopinavir in cell extracts according to the ± 20/15% criteria of the FDA for precision and accuracy.

Acknowledgements

We gratefully acknowledge Aids Fonds, The Netherlands (project 2004051) and VIRGO for their financial support. Antiretroviral drugs were kindly provided by Abbott Laboratories, Merck Sharp & Dohme, F. Hoffmann-La Roche, Pfizer Inc., GlaxoSmithKline, and Boehringer Ingelheim. We thank Arndt Asperger (Bruker Daltonik) for showing us the how to prepare thin matrix layers on an AnchorChip target plate, and Sören-Oliver Deininger (Bruker Daltonik) for providing the FlexAnalysis scripts. Conflicts of interest: The authors have a patent pending on the use of meso-tetrakis(pentafluorophenyl) porphyrin in combination with lithium compounds for MALDI mass spectrometry.

References

1. Cohen LH, Gusev AI. Small molecule analysis by MALDI mass spectrometry. Anal Bioanal Chem 2002;373(7):571-86.
2. Krutchinsky AN, Chait BT. On the nature of the chemical noise in MALDI mass spectra. J Am Soc Mass Spectrom 2002;13(2):129-34.
3. Gouw JW, Burgers PC, Trikoupis MA, Terlouw JK. Derivatization of small oligosaccharides prior to analysis by matrix-assisted laser desorption/ionization using glycidyltrimethylammonium chloride and Girard's reagent T. Rapid Commun Mass Spectrom 2002;16(10):905-12.
4. Chen YT, Ling YC. Detection of water-soluble vitamins by matrix-assisted laser desorption/ionization time-of-flight mass spectrometry using porphyrin matrices. J Mass Spectrom 2002;37(7): 716-30.
5. Ling YC, Lin L, Chen YT. Quantitative analysis of antibiotics by matrix-assisted laser desorption/ ionization time-of-flight mass spectrometry. Rapid Commun Mass Spectrom 1998;12(6):317-27.
6. Ayorinde FO, Bezabeh DZ, Delves IG. Preliminary investigation of the simultaneous detection of sugars, ascorbic acid, citric acid, and sodium benzoate in non-alcoholic beverages by matrix-assisted laser desorption/ionization time-of-flight mass spectrometry. Rapid Commun Mass Spectrom 2003;17(15):1735-42.
7. Ayorinde FO, Hambright P, Porter TN, Keith QL, Jr. Use of meso- tetrakis(pentafluorophenyl) porphyrin as a matrix for low molecular weight alkylphenol ethoxylates in laser desorption/ ionization time-of-flight mass spectrometry. Rapid Commun Mass Spectrom 1999;13(24):2474-9.
8. Hlongwane C, Delves IG, Wan LW, Ayorinde FO. Comparative quantitative fatty acid analysis of triacylglycerols using matrix-assisted laser desorption/ionization time-of-flight mass spectrometry and gas chromatography. Rapid Commun Mass Spectrom 2001;15(21):2027-34.
9. Schuerenberg M, Luebbert C, Eickhoff H, Kalkum M, Lehrach H, Nordhoff E. Prestructured MALDI-MS sample supports. Anal Chem 2000;72(15):3436-42.
10. Vorm O, Roepstorff P, Mann M. Improved resolution and very high sensitivity in MALDI TOF of matrix surfaces made by fast evaporation. Anal Chem 1994;66(19):3281-7.
11. Duncan MW, Matanovic G, Cerpa-Poljak A. Quantitative analysis of low molecular weight compounds of biological interest by matrix-assisted laser desorption ionization. Rapid Commun Mass Spectrom 1993;7(12):1090-4.
12. Hatsis P, Brombacher S, Corr J, Kovarik P, Volmer DA. Quantitative analysis of small pharmaceutical drugs using a high repetition rate laser matrix-assisted laser/desorption ionization source. Rapid Commun Mass Spectrom 2003;17(20):2303-9.
13. Rideout D, Bustamante A, Siuzdak G. Cationic drug analysis using matrix-assisted laser desorption/ionization mass spectrometry: application to influx kinetics, multidrug resistance, and intracellular chemical change. Proc Natl Acad Sci U S A 1993;90(21):10226-9.
14. Guidance for industry: bioanalytical method validation. FDA 2001 available at http://www.fda.gov/cder/guidance/4252fnl.pdf.
15. Lias SG, Bartmess JE, Liebman JF, Holmes JL, Levin RO, Maillard WG. J Phys Chem Ref Data 1988(17).
16. Ayorinde FO, Garvin K, Saeed K. Determination of the fatty acid composition of saponified vegetable oils using matrix-assisted laser desorption/ionization time-of-flight mass spectrometry. Rapid Commun Mass Spectrom 2000;14(7):608-15.

17. Hoberg AM, Haddleton DM, Derrick PJ, Jackon AT, Scrivens JH. The effect of counter ions in matrix-assisted laser desorption/ionization of poly(methyl methacrylate). Eur Mass Spectrom 1998;4: 435-40.
18. Zhang J, Zenobi R. Matrix-dependent cationization in MALDI mass spectrometry. J Mass Spectrom 2004;39(7):808-16.
19. Garofolo F. Bioanalytical method validation. In: Chan CC, Lam H, Lee YC, Zhang XM, eds. Analytical method validation and intstrument performance verification: John Wiley & Sons; 2004:105-38.
20. Time-of-Flight Instruments. In: Gross JH, ed. Mass spectrometry: A textbook: Springer; 2004:113-30.
21. Crommentuyn KM, Mulder JW, Mairuhu AT, et al. The plasma and intracellular steady-state pharmacokinetics of lopinavir/ritonavir in HIV-1-infected patients. Antivir Ther 2004;9(5):779-85.
22. Gobey J, Cole M, Janiszewski J, et al. Characterization and performance of MALDI on a triple quadrupole mass spectrometer for analysis and quantification of small molecules. Anal Chem 2005;77(17):5643-54.
23. Sleno L, Volmer DA. Some fundamental and technical aspects of the quantitative analysis of pharmaceutical drugs by matrix-assisted laser desorption/ionization mass spectrometry. Rapid Commun Mass Spectrom 2005;19(14):1928-36.
24. Sleno L, Volmer DA. Toxin screening in phytoplankton: detection and quantitation using MALDI triple quadrupole mass spectrometry. Anal Chem 2005;77(5):1509-17.

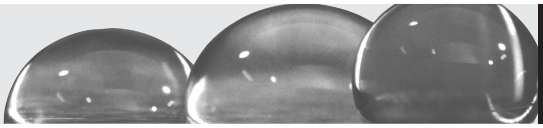

Chapter 5

Metal ion attachment to the matrix meso-tetrakis(pentafluorophenyl) porphyrin, related matrices and analytes: an experimental and theoretical study

Jeroen J.A. van Kampen, Theo M. Luider, Paul J.A. Ruttink, Peter C. Burgers

Journal of Mass Spectrometry 2009, in press

Abstract

In a previous study (van Kampen et al. Anal. Chem., 2006; 78: 5403) we found that meso-tetrakis(pentafluorophenyl)porphyrin (F20TPP), in combination with lithium salts, provides an efficient matrix to cationize small molecules by Li^+ attachment and that this combination can be successfully applied to the quantitative analysis of drugs, such as antiretroviral compounds using MALDI-TOF mass spectrometry. In the present study we further explore the mechanism of metal ion attachment to F20TPP and analytes by MALDI-FTMS(/MS). To this end, we have studied the interaction of F20TPP and analytes with various mono-, di-, and trivalent metal ions (Li^+, Na^+, K^+, Rb^+, Cs^+, Co^{2}+, Cu^{2+}, Zn^{2+}, Fe^{2+}, Fe^{3+}, Ga^{3+}). For the alkali cations, we find that F20TPP forms complexes only with Li^+ and Na^+; in addition, model analyte molecules such as poly(ethyleneglycol)s, mixed with F20TPP and the alkali cations, also only form Li^+ and Na^+ adducts. This contrasts sharply with the commonly used matrix 2,5-dihydroxybenzoic acid, where analytes are most efficiently cationized by Na^+ or K^+. Reasons for this difference are delineated. *Ab initio* calculations on porphyrin itself reveal that even the smallest alkali cation, Li^+, does not fit in the porphyrin cavity, but lies on top of it, pushing the 21H and 23H hydrogen atoms out of and below the plane with concomitant bending of the porphyrin skeleton in the opposite direction, i.e. towards the cation. Thus, the Li^+ ion is not effectively sequestered and is in fact exposed and thus accessible for donation to analyte molecules. Interaction of F20TPP with di- and trivalent metal ions leads to protoporphyrin-metal ions, where the metal ion is captured within the protoporphyrin dianion cavity. The most intense signal is obtained when F20TPP is reacted with $CuCl_2$ and then subjected to laser ablation. This method presents an easy general route to study metal containing protoporphyrin molecules, which could all acts as potential MALDI matrices.

Introduction

In a recent review Josef Chmelik wrote: "Sample preparation and protein separation are important prerequisites for successful proteomic analysis" [1]. This may be stating the obvious, but it cannot be overemphasized that any successful chemical analysis stands or falls with proper or ill-conceived sample preparation procedures. A case in point concerns our efforts to quantify antiretroviral drugs in various biological samples, such as extracts from peripheral blood mononuclear cells, by mass spectrometry based methods [2-5]. One of our approaches includes a fast, reliable and sensitive label-free method by MALDI-TOF using "look-alike" internal standards [2]. Strategies were delineated to overcome the two main limitations of MALDI-TOF for quantitative analyses, viz. matrix interference in the low mass range when employing commonly used low molecular weight (LMW) matrices, and poor reproducibility of the signal abundance. This paper deals with the first limitation.

The molecular masses of conventional MALDI matrices range from 100 to 300 Da and due to ion/molecule reactions taking place in the matrix plume, a large number of matrix-derived signals including salt adducts are observed in the low mass range [6], even in the absence of extraneous salts. Such interference signals seriously hamper the analysis of small molecules using MALDI-TOF. One way to avoid such interferences is to use a matrix whose molecular weight is in excess of that of the analyte molecules. Meso-tetrakis(pentafluorophenyl)porphyrin (F20TPP, MW = 974.6 Da) represents such a matrix and, from its introduction in 1999 [7], has been used successfully for the analysis of a variety of small molecules, including fatty acids and sugars [8, 9].

Unfortunately, F20TPP has a very large proton affinity (according to our calculations, vide infra, 245 kcal/mol) and so many analytes cannot be charged by protonation using this matrix. This is also true for the studied antiretroviral drugs, although we can not exclude prompt in-source fragmentation of the protonated compounds. In this respect, it is noteworthy that protonated forms of doping agents have been observed when using F20TPP matrix in MALDI-ion trap experiments [10]. As an alternative means for ionization we employed cationization by alkali metal ions by adding alkali iodides as is commonly done for the MALDI analysis of molecules lacking basic sites, such as sugars [8, 11]. For the alkali cations Li^+, Na^+, K^+, Rb^+ and Cs^+ and by using F20TPP, we found that the analyte molecules, as well as F20TPP itself, show a strong preference for the attachment of Li^+. This is in sharp contrast to the matrix DHB, where invariably Na^+ or K^+ give the most intense analyte signals.

To more fully understand how analytes are cationized by a mixture of F20TPP and alkali metal ions, and also how these metal ions become attached to F20TPP, we have performed a series of experiments on various mixtures of F20TPP, alkali metal ions and analyte. We have also extended our experiments to include divalent and trivalent metal

ions (Fe^{2+}, Fe^{3+}, Co^{2+}, Cu^{2+}, Zn^{2+}, Ga^{3+}) and to include compounds similar to F20TPP, such as porphyrin itself and phthalocyanine, which are expected to act as matrices too. We have also performed *ab initio* calculations on alkali-porphyrin complexes to establish the metal ions' binding sites and binding energies.

Experimental Section

Experiments

Samples were measured on an APEX IV Qe 9.4 Tesla FTICR mass spectrometer (Bruker Daltonics, USA) equipped with the first version of the vacuum Combisource, and a 20 Hz nitrogen laser with irradiation area of ~200 µm [12]. Xmass version 7.0.8 was used to operate the mass spectrometer, and DataAnalysis version 3.4 was used for data analysis (both from Bruker Daltonics). A multishot accumulation was used as recommended by O'Connor et al., Mize et al., and Moyer et al. [13-15]. Ions produced by ten laser shots were accumulated in the storage hexapole, transferred to the FTICR cell, and scanned for 0.78 seconds (TD size 512 Kb). Fifty scans were summed for each mass spectrum. The acquisition mass range was *m/z* 800 to 4,000 (fight time 2 ms) or 400 – 2,000 (flight time 1.25 ms). The mass spectra were subsequently apodized and zerofilled twice. An external mass calibration was applied using a quadratic equation.

MS/MS spectra were obtained by mass selection in the quadrupole and by setting the quadrupole to either a negative potential (for positive ions) or positive potential (for negative ions). The required collision energies are given in the legends for the Figures.

MALDI-TOF mass spectra were obtained using a Bruker Ultraflex III instrument operated in the reflectron mode. Ions were generated by a Nd:YAG laser (355 nm) and were accelerated to 25 keV. 2,000 laser shots per sample were averaged to generate the mass spectra.

All salt solutions were prepared in Milli-Q water at concentrations of 0.01 M. F20TPP and other porphyrin matrices were prepared in acetone at a concentration of 2×10^{-4} M. This concentration is lower than standard matrix concentrations (2×10^{-2} M) allowing metal ion interactions to be studied as follows. In mixing experiments equal volumes (20 µL) of a salt and the F20TPP solutions were mixed and allowed to stand for 5 min. Thus, the porphyrin : salt ratio is 1 : 50, and this ratio gives abundant signals for the metal ion adducts. Next 1 µL of this mixture was pipetted onto a stainless steel target and allowed to dry. Copper(II) phthalocyanine was dissolved to a saturated solution in chloroform.

The matrix 2,5-dihydroxybenzoic acid (DHB) was prepared at 10 mg/mL in Milli-Q water. PEGs were purchased from Polymer Laboratories Ltd, Essex Road, Church Stretton, Shropshire, UK. All other chemicals were obtaind from Sigma-Aldrich.

Theoretical methods

The calculations on the metal-porphyrin complexes were performed at the RHF/6-31G(d) [16] level of theory including ZPVE corrections scaled at 0.95 [17]. The results are given in Table 1.

Table 1. Stabilization energies of Porphyrin + M^+ ($M^+ = H^+, Li^+, Na^+, K^+$) by RHF/6-31G(d)

	HF energy (H)	ZPE/scaling (H)	Total energy (H)	Stabilization energy (H)	Stabilization energy[a] (kcal/mol)
H^+	0				
Li^+	-7.23548				
Na^+	-161.65928				
K^+	-598.97167				
Porphyrin	-983.25417	0.31918/0.95	-982.95095		
H^+ + porphyrin	-982.95095				
Li^+ + Porphyrin	-990.18643				
Na^+ + Porphyrin	-1144.61023				
K^+ + Porphyrin	-1581.92262				
Porphyrin-H^+	-983.65556	0.33153/0.95	-983.34061	0.38966	245
Porphyrin-Li^+	-990.61761	0.32272/0.95	-990.31103	0.12460	78
Porphyrin-Na^+	-1145.00418	0.32125/0.95	-1144.69990	0.08877	56
Porphyrin-K^+	-1582.28643	0.32045/0.95	-1581.98200	0.05938	37

[a] 1H = 627.5 kcal/mol

The calculations on mono- and 1,2-difluorobenzene were performed with the CBS-QB3 model chemistry [18, 19] and the results are given in Table 2. All calculations were run with the Gaussian 2003, Rev D.01 suite of programs [20]. In the CBS-QB3 model chemistry the geometries of minima are obtained from B3LYP density functional theory in combination with the 6-311G(2d,d,p) basis set (also denoted as the CBSB7 basis set). The complete set of computational results is available from the authors upon request.

Results and Discussion

Relative alkali cation affinities of PEGs using the matrix DHB

Interaction between metal ions and neutral polyethers plays a fundamental role in the selective transport of metal ions through synthetic polymer membranes [21, 22], and linear PEGs have become the standards for investigating ion-polymer interactions. From an early viscometric study [23], it appeared that inorganic salts lower the PEG crystalline melting point and it was tentatively postulated that the species which directly associates with the polymer is the anion. Subsequent NMR experiments [24] revealed that it is the

Table 2. Lithium ion affinities for benzene, mono- and 1,2-difluorobenzene[a]

	B3LYP/CBSB7	6-31G(d)
Benzene	-232.20838	-230.59546
Li^+	-7.28491	-7.23554
Benzene-Li^+	-239.55355	-237.89307
Lithium ion affinity (kcal/mol)[b]	37.8	39.0
Monofluorobenzene	-331.48103	
Monofluorobenzene-Li^+ (CS)[b]	-338.81673	
Lithium ion affinity (kcal/mol)[b]	31.9	
Monofluorobenzene-Li^+ (C1)[c]	-338.81771	
Lithium ion affinity (kcal/mol)[c]	32.5	
1,2-difluorobenzene	-430.74608	-428.30754
1,2-difluorobenzene-Li^+ (CS)[c]	-438.09510	-435.60738
Lithium ion affinity (kcal/mol)[c]	40.2	40.3
1,2-difluorobenzene-Li^+ (C1)[b]	-438.07534	-435.58572
Lithium ion affinity (kcal/mol)[b]	27.8	26.7

[a] Electronic energies in Hartrees
[b] Lithium ion affinity of the benzene ring
[c] Lithium ion affinity at fluorine

positive metal ion which interacts directly with the polymer. In the past, many different experimental techniques have been used to assess the relative affinities of alkali cations to PEGs having a wide variety of lengths. The tendency of larger PEGs to preferentially sequester larger cations is well known [25-27]. For example, solvent extraction experiments [27] revealed the order $K^+ > Cs^+ > Na^+ > Li^+$ for PEG 1,000, and conductometry measurements [26] on PEG 20,000 revealed the order $Rb^+ > Cs^+ > K^+ > Na^+ > Li^+$. However, for solution experiments, competitive solvation of the alkali cation is always a matter of concern [28]. Indeed, the efficiency for the uptake of an alkali metal ion by PEG appears to be a balance between the solvation of the ion and the capability of the PEG to displace the solvent and coordinate with the cation [29]. Dissociation of PEG 1,000, doubly cationized by different alkali metal cations using electrospray ionization, has permitted the *in situ* measurement of the relative binding strengths when a single PEG molecule coordinates to two different alkali cations [30]. From such experiments, which constitute a form of Cooks' kinetic method [31, 32], the relative intrinsic cation affinities towards PEG appear to follow the order $Na^+ > K^+ > Rb^+ > Cs^+$. In the same vein, the gas-phase affinity order of the alkali cations towards 18-crown-6 was found to be $Na^+ > K^+ > Rb^+ > Cs^+$ [16], but in solution K^+ has the highest affinity [33] and it was argued that hydration of Na^+ plays an important competitive role in solution [28, 34]. Thus for both PEG 1,000 and 18-crown-6 the intrinsic metal ion affinity appears to be determined primarily by the charge density of the cation.

In recent years, MALDI-TOF has been used to study metal ion interactions with polymers [35-41], including PEGs. For example, Rashidzadeh et al. [41] investigated the selectivity of Li^+ and Na^+ for PEG 1,450 using different matrices and concluded that the matrix itself may play an important role in the cationization of PEG polymers. For small PEG dodecyl ethers (number of ethylene oxide units, n = 1 – 8) the observed alkali ion adduct intensities ($Li^+ < Na^+ > K^+$) were subjected to a random walk model and from this analysis it was concluded [39] that despite the above observed selectivities, the binding energy between a metal ion and an oxygen atom in the ethylene glycol chain decreases in the order $Li^+ > Na^+ > K^+$, again following the charge density of the alkali cation. However, a MALDI study [40] on larger PEGs revealed the selectivity order $K^+ > Rb^+ > Cs^+ > Na^+ > Li^+$ for PEG 4,000, but this need not be the intrinsic affinity order for the following reason. Hoberg et al. [42] have shown that because of different lattice energies for different salts, different amounts of cations can be made available for gas-phase cationization and it was predicted that this could lead to severe discrimination effects in metal cation affinity studies using MALDI. Indeed, we have shown [2] that an equimolar mixture of the alkali iodides produce in MALDI, using DHB or F20TPP as matrix, alkali cations whose intensities follow the order $Li^+ < Na^+ < K^+ < Rb^+ < Cs^+$, following the decreasing lattice energies of the alkali iodides. For small PEGs, and using DHB as matrix, the alkali intensity distribution shown in Figure 1a is obtained (n = 13). Qualitatively, this distribution can be rationalized on the basis of a trade-off between two opposing effects, to wit, the gas-phase availability of the alkali cations ($Li^+ < Na^+ < K^+ < Rb^+ < Cs^+$) and the intrinsic alkali affinity of PEG ($Li^+ > Na^+ > K^+ > Rb^+ > Cs^+$), leading to an observed optimum affinity for K^+. The MALDI-FTMS distribution in Figure 1a is very similar to that obtained by MALDI-TOF [2]. Again, the intrinsic metal affinity appears to be governed primarily by the charge density of the cation.

Relative alkali cation affinities of PEGs using the matrix F20TPP

The PEG-alkali intensity distribution using F20TPP as matrix is completely different compared to the matrix DHB, see Figure 1b and the observed distribution now does follow the order of intrinsic cation affinity. Thus, the PEG + Li^+ signal is the most intense, but hardly any free Li^+ are available, vide supra, and so the PEG + Li^+ signals cannot have arisen from cationization by free Li^+ ions. In our quantitative analysis of protease inhibitors using F20TPP, we have successfully exploited this finding by doping the matrix solution with Li^+ (lithium iodide) to achieve maximum signal strength. We noticed, see Figure 1c, that F20TPP itself shows virtually the same alkali affinity order as PEG and other analytes and so the lithiated matrix ions, being present in excess, may well be the cation donator to the anayte and this prompted us to further investigate attachment of alkali and other metal ions to the matrix F20TPP.

For smaller PEG molecules the preference for Li^+ attachment using F20TPP as matrix, becomes even more extreme. This is demonstrated by the MALDI-TOF mass spectrum of

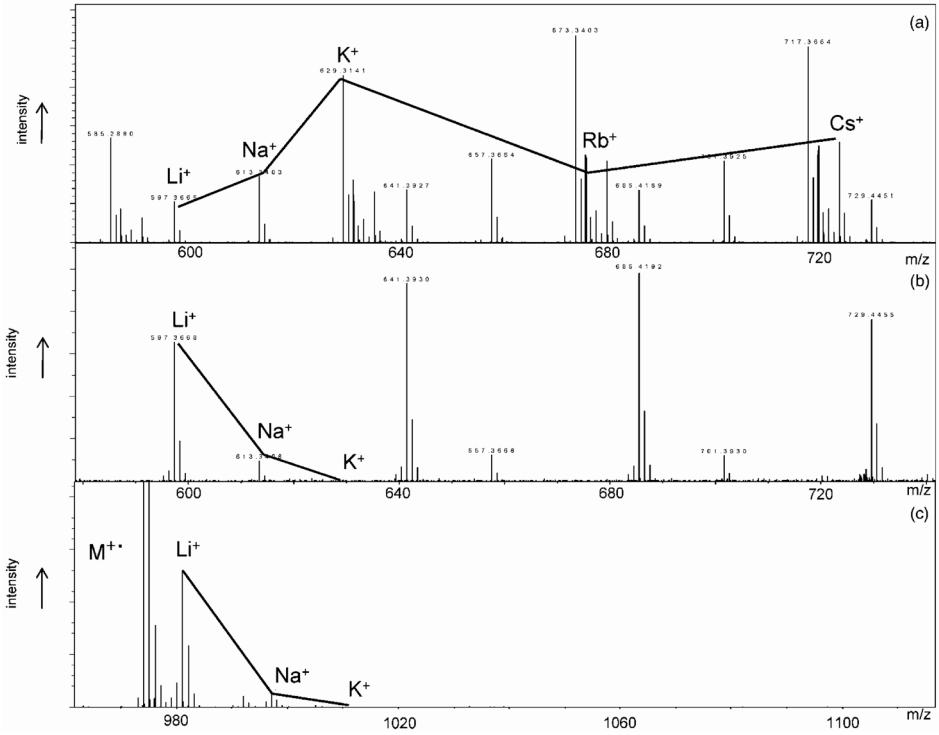

Figure 1. MALDI–FTMS mass spectra of PEG600 in the presence of an equimolar mixture of LiI, NaI, KI, RbI and CsI using matrix F20TPP (a) and DHB (b). In item (c), the mass spectrum of F20TPP in the presence of the equimolar salt mixture is shown.

an equimolar mixture of ethylene glycols (HO-(CH_2-CH_2-O)$_n$-H, n = 1 to n = 6), see Figure 2, using F20TPP as matrix. In this experiment an equimolar amount of alkali ions were added. It can be seen that, although there is an intense signal for free Cs^+, no peaks could be detected for the ethylene glycols + Cs^+ adducts. Instead, and following our results above, only Li^+ adducts are observed despite the fact that hardly any free Li^+ ions are observed. The above experiment also shows that the binding efficiency of Li^+ towards PEG molecules depends strongly on the number of sites with which the Li^+ ion can interact as has been concluded earlier [30]. Thus the signals for ethylene and diethylene glycol are very weak (two and three interaction sites), whereas the peak for hexaethylene glycol (seven interaction sites) is strongest. Studies on the matrix properties of other porphyrins such as porphyrin itself and dilithium phthalocyanine (a porphyrazin, vide infra) in combination with equimolar alkalihalides mixtures also showed that the strongest signals for the cationized matrix and model analytes are observed for the lithium adduct, followed by adduct formation with sodium, potassium, rubidium and cesium. Thus, the preference for alkali cationization with lithium may well be a general phenomenon for porphyrin matrices in MALDI.

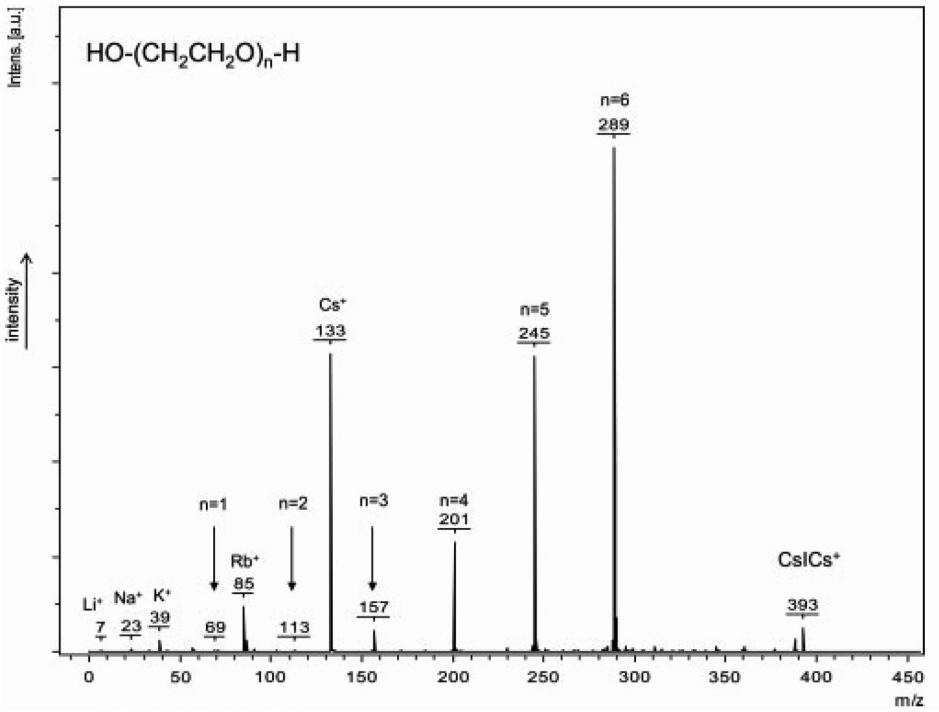

Figure 2. MALDI–TOF mass spectrum of equimolar mixture of mono-, di-, tri-, tetra-, penta- and hexaethyleneglycol in the presence of an equimolar mixture of LiI, NaI, KI, RbI and CsI.

Interaction of F20TPP with metal ions. Site of attachment of alkali cations (Li^+, Na^+)

To probe the structure of the F20TPP + Li^+ (Na^+) cations we recorded their MALDI-FTMS/MS spectra and compared these with the MS/MS spectrum of the protonated species F20TPP + H^+. The latter ions, upon collisional activation, dissociate by sequential losses of HF, see Figure 3a. By contrast, for F20TPP + Li^+ only one major fragmentation is observed, viz loss of 26.0144 Da, corresponding, surprisingly, to the loss of LiF, see Figure 3b. This could indicate either that Li^+ is bound to the cavity and that upon activation it can migrate towards one of the C_6F_5 groups where it picks up a fluorine anion, or it could be taken as evidence that the Li^+ ion is already attached to a C_6F_5 group prior to activation. To distinguish between these two possibilities we carried out appropriate *ab initio* calculations. Unfortunately, F20TPP itself is too large to allow such calculations in a realistic way and so we decomposed the calculations into: (1) Calculations on porphyrin itself to establish the affinity of Li^+ towards the cavity, see Table 1, and (2) Calculations on 1,2- difluorobenzene to obtain the affinity of Li^+ towards the C_6F_5 groups, see Table 2. The Li^+ affinity towards the cavity was found to be 78 kcal/mol (Table 1) whereas the Li^+ affinity of 1,2-difluorobenzene was found to be much smaller, 40.2 kcal/mol (for Li^+ between two F atoms; the Li^+ affinity of the benzene ring of 1,2-difluorobenzene is even

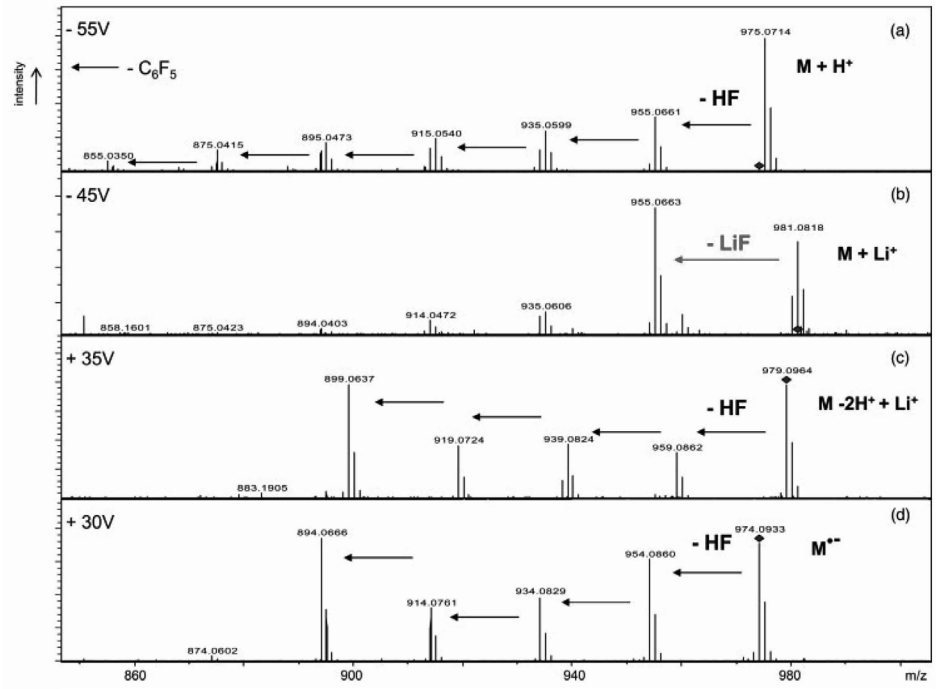

Figure 3. MALDI–FTMS/MS mass spectra of protonated F20TPP (a), of F20TPP + Li^+ (b), of the negative ion $[F20TPP - 2H^+ + Li^+]^-$ (c) and of the F20TPP radical anion (d). Collision energies are indicated.

smaller, 27.8 kcal/mol, see Table 2). Hence we conclude that in F20TPP, the Li^+ is attached to the porphyrin cavity and not to the F atoms of the C_6F_5 groups.

Structure of the F20TPP alkali cation complexes

Our *ab initio* calculations also show how the Li^+ is attached to the cavity. In Figure 4 are shown the equilibrium structures for porphyrin + Li^+ from a bird's eye view and from a side view. From the side view it can be seen that the Li^+ is situated on, but not in the porphyrin cavity and that the whole porphyrin chain becomes bent. The observation that the lithium ion is not in but outside the cavity means that the lithium ion is exposed and is therefore accessible for transfer to analyte molecules. In Figure 5 are shown the side views of porphyrin + H^+, porphyrin + Li^+, porphyrin + Na^+ and porphyrin + K^+. It can be seen that the larger the cation becomes, the more exposed the cation will be (and the lesser the porphyrin skeleton will be bent) but at the same time the cation affinities become less. This is in agreement with our experimental finding that only lithium ions produce intense signals for attachment to F20TPP, see Figure 1c and that such F20TPP + Li^+ ions can act as cation donator.

We also tried to obtain the MALDI-FTMS/MS mass spectrum of the F20TPP + Na^+ adduct, but only very weak signals were observed. However, in the MS/MS mode our FT

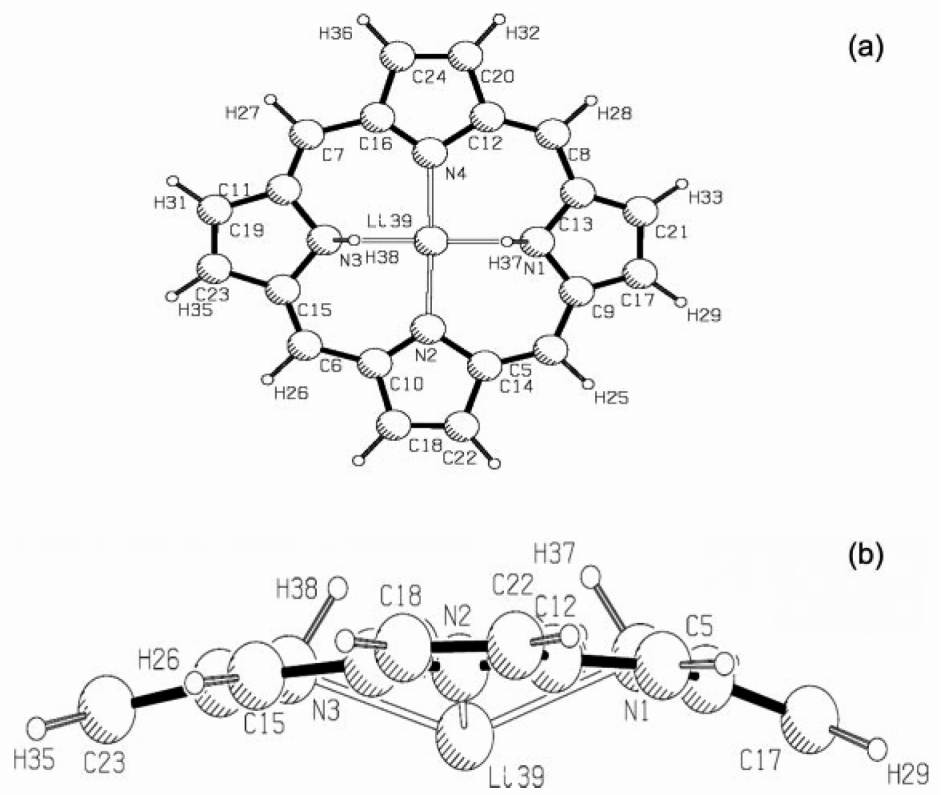

Figure 4. RHF/6-31G(d) structure of the porphyrin + Li^+ complex. (a) bird's eye view and (b) side view.

apparatus cannot detect ions having very low masses. We therefore recorded the MS/MS spectrum of the F20TPP + Li^+ and F20TPP + Na^+ on our MALDI-TOF/TOF apparatus. The TOF/TOF spectrum of F20TPP + Li^+ was found to be similar to the FTMS/MS spectrum, but the TOF/TOF spectrum of F20TPP + Na^+ is dominated by a peak at *m/z* 23, corresponding to the loss of Na^+. In addition, the corresponding peak at *m/z* 7 for Li^+ in the TOF/TOF spectrum of F20TPP + Li^+ is almost undetectable. These findings indicate that the F20TPP + Na^+ ion preferentially loses Na^+ rather than NaF, on accord of the lower stabilization energy associated with F20TPP + Na^+, 56 kcal/mol, compared to that of F20TPP + Li^+, 78 kcal/mol, see Table 1.

Interaction of F20TPP with divalent and trivalent cations

We have also briefly studied the interaction of F20TPP with other metal ions. It is well known that divalent and trivalent metal ions such as Cu^{2+}, Fe^{2+} and Fe^{3+} can be incorporated into the protoporphyrin cavity, leading to very stable inner complexes [43]. We have investigated the interaction of a variety of divalent and trivalent metal ions (Fe^{2+}, Fe^{3+}, Co^{2+}, Cu^{2+}, Zn^{2+}, Ga^{3+}) by MALDI-FTMS with F20TPP and also with porphyrin itself.

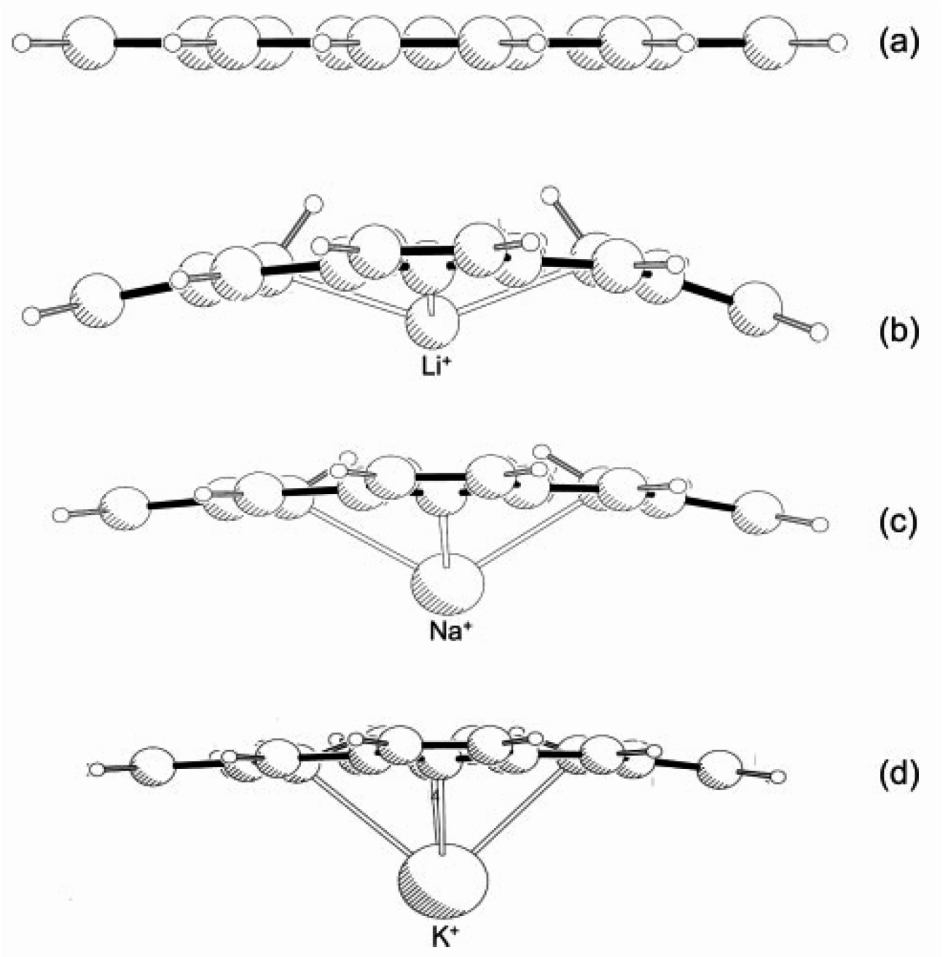

Figure 5. Side views of porphyrin + H^+ (a), porphyrin + Li^+ (b), porphyrin + Na^+ (c), and porphyrin + K^+ (d).

Incorporation of the metal ion could be achieved by mixing a water solution of the corresponding metal chloride with a solution of F20TPP in acetone, see Experimental Section. For example, mixing a solution of $CuCl_2$ with F20TPP leads to an intense peak at *m/z* 1034.9687, i.e. 60.9141 Da higher than F20TPP, see Figure 6a. This peak corresponds to displacement of two H^+ by one Cu^{2+} in F20TPP, i.e. $[F20TPP - 2H^+ + Cu^{2+}]^+$. The MS/MS spectrum of this species shows peaks for the sequential losses of HF, see Figure 6b, very similar to the behaviour observed for the radical cation of F20TPP. When $CuSO_4$ is used instead of $CuCl_2$, much weaker signals are observed for the F20TPP-copper species and in this case the copper containing ions are mostly $[F20TPP - H^+ + Cu^{2+}]$ (or $[F20TPP - H^+ + Cu^+]^+$, the charge outside the bracket indicates ionization not by oxidation of Cu^+, but by ionization of another part of the molecule) at *m/z* 1035.9784. Comparative experiments, whereby binary metal ion mixtures were allowed to interact with F20TPP revealed the

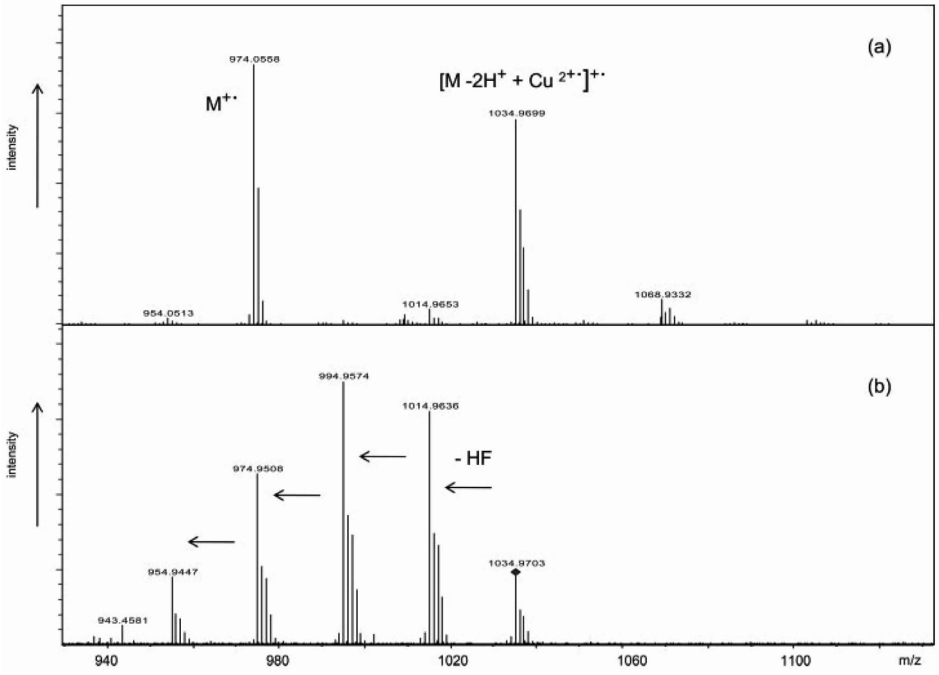

Figure 6. (a) MALDI–FTMS spectrum of F20TPP in the presence of a 50-fold excess of Cu^{2+} (from $CuCl_2$ see text). (b) MALDI–FTMS/MS spectrum of the ion $[F20TPP - 2H^+ + Cu^{2+}]^+$.

following intensity order (ionic radius in Å): Ga^{3+} (1%, 0.62) < Zn^{2+} (3%, 0.74) < Fe^{3+} (8%, 0.64) < Co^{2+} (14%, 0.72) << Cu^{2+} (100%, 0.72) and so F20TPP would appear to have the highest affinity for Cu^{2+}. Also, the ionic radius would appear not to be the sole factor governing the observed intensity ratios.

It is noteworthy that in the above experiments we could not find any evidence for the formation of F20TPP + Cu^+, although there is ample evidence from the literature that in MALDI the original Cu^{2+} ions can be reduced to Cu^+ [44-46].

The MALDI-FTMS mass spectrum of commercially available tetrakis(pentafluorophenyl) porphyrin iron(III) chloride contains an intense peak for $[F20TPP - 2H^+ + Fe^{3+}]$ whose MS/MS mass spectrum is identical to that of the $[F20TPP - 2H^+ + Fe^{3+}]$ ion generated from a mixture of $FeCl_3$ and F20TPP and this indicates that in our exchange experiments the Fe^{3+} is indeed incorporated into the porphyrin cavity.

Interaction of F20TPP with metal ions as studied by negative ion MALDI-FTMS

For the alkali cations we could, in the negative ion mode, observe incorporation only of Li^+ within F20TPP to generate the species $[F20TPP - 2H^+ + Li^+]^-$. This is not so surprising as only Li^+ has the correct ionic radius (0.68 Å) to fit in the porphyrin cavity. Indeed, according to our *ab initio* calculations, and in sharp contrast to the positive F20TPP + Li^+ ions, the lithium ion in $[F20TPP – 2H^+ + Li^+]^-$ lies within the cavity and the $[F20TPP – 2H^+$

+ $Li^+]^-$ is correspondingly planar. The MALDI-FTMS/MS spectrum of this species is shown in Figure 3c. In contrast to the ion F20TPP + Li^+, see Figure 3b, the ion [F20TPP – $2H^+$ + $Li^+]^-$ does not eliminate LiF. The observation that the [F20TPP – $2H^+$ + $Li^+]^-$ ion does not eliminate LiF indeed indicates that in the negative ions the Li^+ ion is securely sequestered. Instead four successive losses of HF are observed, very similar to the F20TPP radical anion, where the Li^+ ion is absent, see Figure 3d. This could indicate that the losses of HF occur by condensation of the phenyl rings with the porphyrin skeleton with concomitant losses of HF. We also observed that for [F20TPP – $2H^+$ + Cu^{2+}] we could not detect any signal in the negative ion mode, i.e. we could not observe [F20TPP – $2H^+$ + $Cu^{2+}]^-$. This is remarkable, because for F20TPP itself, intense signals could be observed for the radical anion, see above. Possibly this indicates that in our experiments, generation of [F20TPP – $2H^+$ + Cu^{2+}] and other metal containing porphyrin ions, occurs after laser ablation, i.e. in the MALDI plume and not during the mixing of the components in an eppendorf tube. In this case the Cu^{2+} ions cannot escape the negatively charged MALDI plate. In this respect it is of interest to note that if the copper-F20TPP reaction mixture (which contains a 50-fold excess of Cu^{2+}) is left standing at room temperature for 60 hrs instead of 5 min., no increase in the signal intensity for [F20TPP – $2H^+$ + $Cu^{2+}]^+$ relative to $F20TPP^+$ is observed. Also, when sandwich layers are prepared in which first F20TPP is allowed to dry and then a solution of $CuCl_2$ is pipetted on top (or vice versa), intense signals for of [F20TPP – $2H^+$ + $Cu^{2+}]^+$ are observed. In these cases no mixing of F20TPP and the copper ions occur prior to laser ablation. We could not find a commercial source for tetrakis(pentafluorophenyl)porphyrin copper(II), but the well known copper(II) phthalocyanine is available. In this case, we observed intense signals at *m/z* 575 in both the positive and negative ion mode at the same laser power. Clearly, [phthalocyanine - $2H^+$ + Cu^{2+}] present as crystals on the MALDI plate can produce intense signals also in the negative ion mode.

Dilithium phthalocyanine

This compound is commercially available and produces intense signals in both the positive and negative ion mode, and we found that it can serve as both matrix and (controlled) lithium donor. In the positive ion mode the most intense signal is for the protonated species and for the negative ions only [M – $Li^+]^-$ ions are seen. In the latter case the remaining Li^+ is tightly bound in the protoporphyrazin cavity, similar to the lithium ion in the protoporphyrin cavity of F20TPP, the [F20TPP – $2H^+$ + $Li^+]^-$ ion discussed above. We also observed that the two lithium ions in dilithium phthalocyanine can be easily exchanged by di- and trivalent metal ions, in the order Zn^{2+} (9%) < Co^{2+} (12%) < Fe^{3+} (15%) << Cu^{2+} similar to the ordering observed for F20TPP.

Summary

Combination of the matrix meso-tetrakis(pentafluorophenyl)porphyrin (F20TPP) and excess lithium ions is an excellent way to cationize low MW drugs, such as antiretroviral drugs prior to MALDI analysis. According to our *ab initio* calculations the Li^+ ion lies not in the porphyrin cavity, but on top of it, pushing the 21H and 23H out of the plane and bending the whole porphyrin skeleton. We propose that this structure acts as lithium donor in MALDI experiments leading to intense lithium adducts of the analytes. For both F20TPP and analyte molecules, Na^+ produces weaker adducts, whereas those for K^+, Rb^+ and Cs^+ are not detectable at all. This seems to be a more general phenomenon for porphyrin matrices in MALDI. Interaction of F20TPP with divalent and trivalent metal ions leads to protoporphyrin-metal ions, where the metal ion is situated within the protoporphyrin cavity. The most intense signal is obtained when F20TPP is reacted with $CuCl_2$ and then subjected to laser ablation. This presents an easy general route to study metal containing porphyrin molecules, which could all acts as potential MALDI matrices.

References

1. Chmelik J. Applications of field-flow fractionation in proteomics: presence and future. Proteomics 2007;7(16):2719-28.
2. van Kampen JJ, Burgers PC, de Groot R, Luider TM. Qualitative and quantitative analysis of pharmaceutical compounds by MALDI-TOF mass spectrometry. Anal Chem 2006;78(15):5403-11.
3. van Kampen JJ, Burgers PC, de Groot R, et al. Quantitative analysis of HIV-1 protease inhibitors in cell lysates using MALDI-FTICR mass spectrometry. Anal Chem 2008;80(10):3751-56.
4. Van Kampen JJ, Burgers PC, Gruters RA, et al. Rapid quantitative analysis of antiretroviral drugs in lysates of peripheral blood mononuclear cells using MALDI-triple quadrupole mass spectrometry. Anal Chem 2008;80(13):4969-75.
5. van Kampen JJ, Verschuren EJ, Burgers PC, et al. Validation of an HIV-1 inactivation protocol that is compatible with intracellular drug analysis by mass spectrometry. J Chromatogr B Analyt Technol Biomed Life Sci 2007;847(1):38-44.
6. Krutchinsky AN, Chait BT. On the nature of the chemical noise in MALDI mass spectra. J Am Soc Mass Spectrom 2002;13(2):129-34.
7. Ayorinde FO, Hambright P, Porter TN, Keith QL, Jr. Use of meso- tetrakis(pentafluorophenyl) porphyrin as a matrix for low molecular weight alkylphenol ethoxylates in laser desorption/ionization time-of-flight mass spectrometry. Rapid Commun Mass Spectrom 1999;13(24):2474-9.
8. Ayorinde FO, Bezabeh DZ, Delves IG. Preliminary investigation of the simultaneous detection of sugars, ascorbic acid, citric acid, and sodium benzoate in non-alcoholic beverages by matrix-assisted laser desorption/ionization time-of-flight mass spectrometry. Rapid Commun Mass Spectrom 2003;17(15):1735-42.
9. Hlongwane C, Delves IG, Wan LW, Ayorinde FO. Comparative quantitative fatty acid analysis of triacylglycerols using matrix-assisted laser desorption/ionization time-of-flight mass spectrometry and gas chromatography. Rapid Commun Mass Spectrom 2001;15(21):2027-34.
10. Kosanam H, Prakash PK, Yates CR, Miller DD, Ramagiri S. Rapid screening of doping agents in human urine by vacuum MALDI-linear ion trap mass spectrometry. Anal Chem 2007;79(15):6020-6.
11. Zaia J. Mass spectrometry of oligosaccharides. Mass Spectrom Rev 2004;23(3):161-227.
12. Baykut G, Jertz R, Witt M. Matrix-assisted laser desorption/ionization fourier transform ion cyclotron resonance mass spectrometry with pulsed in-source collision gas and in-source ion accumulation. Rapid Commun Mass Spectrom 2000;14(14):1238-47.
13. Mize TH, Amster IJ. Broad-band ion accumulation with an internal source MALDI-FTICR-MS. Anal Chem 2000;72(24):5886-91.
14. Moyer SC, Budnik BA, Pittman JL, Costello CE, O'Connor PB. Attomole peptide analysis by high-pressure matrix-assisted laser desorption/ionization Fourier transform mass spectrometry. Anal Chem 2003;75(23):6449-54.
15. O'Connor PB, Costello CE. Application of multishot acquisition in Fourier transform mass spectrometry. Anal Chem 2000;72(20):5125-30.
16. Hehre WJ, Radom L, Schleyer PVR, Pople JA. Ab Initio Molecular Orbital Theory: Wiley; 1986.
17. Scott AP, Radom L. Harmonic Vibrational Frequencies: An Evaluation of Hartree–Fock, Møller–Plesset, Quadratic Configuration Interaction, Density Functional Theory, and Semiempirical Scale Factors. J Phys Chem 1996;100(41):16502–13.
18. Montgomery JA, Frisch MJ, Ochterski JW, Petterson GA. A complete basis set model chemistry. VII. Use of the minimum population localization method. J Chem Phys 2000;112(15):6532.

19. Ochterski JW, Petersson GA, Montgomery JA. A complete basis set model chemistry. V. Extensions to six or more heavy atoms J Chem Phys 1996;104(7):2598-619
20. Frisch MJ. Gaussian 03 (Revision C.02). In. Wallingford CT: Gaussian Inc.; 2004.
21. MacKenzie WM, Sherrington DC. Mechanism of Solid-Liquid Phase Transfer Catalysis by Polymer-Supported Polyethers Polymer 1980.
22. Yamazahi N, Hirao A, Nakahama SJ. J Macromol Sci Chem 1999; A 13:321.
23. Lundberg RD, Bailey FE, Callard RW. Interactions of inorganic salts with poly(ethylene oxide). Journal of Polymer Science Part A-1: Polymer Chemistry 1966;4(6):1563 - 77.
24. Liu KJ. Nuclear Magnetic Resonance Studies of Polymer Solutions. IV. Polyethylene Glycols. Macromolecules 1968;1(3):213–7.
25. Chan KWS, Cook KD. Mass spectrometric study of interactions between poly(ethylene glycols) and alkali metals in solution. Macromolecules 1983;16(11):1736–40.
26. Katsumichi, Ono, Hideo, Konami, Kenkichi, Murakami. Conductometric studies of ion binding to poly(oxyethylene) in methanol. J Phys Chem 1979;83(20):2665–9.
27. Yanagida S, Takahashi K, Okahara M. Metal-ion Complexation of Noncyclic Poly(oxyethylene) Derivatives. I. Solvent Extraction of Alkali and Alkaline Earth Metal Thiocyanates and Iodides. Bulletin of the Chemical Society of Japan 1977;50(6):1386-90.
28. More MB, Ray D, Armentrout PB. Intrinsic Affinities of Alkali Cations for 15-Crown-5 and 18-Crown-6: Bond Dissociation Energies of Gas-Phase M+−Crown Ether Complexes. J Am Chem Soc 1999;121(2):417–23.
29. Gokel GW, Goli DM, Minganti C, Echegoyen L. Clarification of the hole-size cation-diameter relationship in crown ethers and a new method for determining calcium cation homogeneous equilibrium binding constants. J Am Chem Soc 1983;105(23):6786–8.
30. Bogan MJ, Agnes GR. Poly(ethylene glycol) doubly and singly cationized by different alkali metal ions: Relative cation affinities and cation-dependent resolution in a quadrupole ion trap mass spectrometer. Journal of the American Society for Mass Spectrometry 2002;13(2):177-86
31. Cooks RG, Patrick JS, Kotiaho T, McLuckey SA. Thermochemical determinations by the kinetic method. Mass spectrometry reviews 1994;13(4):287-339.
32. McLuckey SA, Cameron D, Cooks RG. Proton affinities from dissociations of proton-bound dimers. J Am Chem Soc 1981;103(6):1313–7.
33. Izatt RM, Terry RE, Haymore BL, et al. Calorimetric titration study of the interaction of several uni- and bivalent cations with 15-crown-5, 18-crown-6, and two isomers of dicyclohexo-18-crown-6 in aqueous solution at 25.degree.C and .mu. = 0.1. J Am Chem So 1976;98(24):7620–6.
34. Glendening ED, Feller D, Thompson MA. An Ab Initio Investigation of the Structure and Alkali Metal Cation Selectivity of 18-Crown-6. J Am Chem So 1994;116(23):10657–69.
35. Ackloo S, Terlouw JK, Ruttink PJ, Burgers PC. Analysis of carrageenans by matrix-assisted laser desorption/ionization and electrospray ionization mass spectrometry. I. kappa-Carrageenans. Rapid Commun Mass Spectrom 2001;15(14):1152-9.
36. Dogruel D, Nelson RW, Williams P. The Effects of Matrix pH and Cation Availability on the Matrix-assisted Laser Desorption/Ionization Mass Spectrometry of Poly(methyl methacrylate). Rapid Communications in Mass Spectrometry 1998;10(7): 801 - 4.
37. Jackson AT, T. YH, MacDonald WA, et al. Time-lag focusing and cation attachment in the analysis of synthetic polymers by matrix-assisted laser desorption/ionization-time-of-flight-mass spectrometry. Journal of the American Society for Mass Spectrometry 1997;8(2):132-9

38. Spickermann J, Martin K, Räder HJ, et al. Quantitative analysis of broad molecular weight distributions obtained by matrix-assisted laser desorption ionisation-time-of-flight mass spectrometry. European Journal of Mass Spectrometry 1996;2(3):161–5.
39. Togashi H, Kobayashi Y. Metal ion migration model for cationization of low-molecular-weight oligomers of poly(ethylene glycol) dodecyl ether in matrix-assisted laser desorption/ionization mass spectrometry. Rapid Communications in Mass Spectrometry 2002;16(16): 1531 - 7.
40. Kéki S, Szilágyi LS, Deák G, Zsuga M. Effects of different alkali metal ions on the cationization of poly(ethylene glycol)s in matrix-assisted laser desorption/ionization mass spectrometry: a new selectivity parameter. Journal of Mass Spectrometry 2002;37(10):1074 - 80.
41. Rashidzadeh H, Wang Y, Guo B. Matrix effects on selectivities of poly(ethylene glycol)s for alkali metal ion complexation in matrix-assisted laser desorption/ionization. Rapid Communications in Mass Spectrometry 2000;14(6):439 - 43.
42. Hoberg AM, Haddleton DM, Derrick PJ, Jackon AT, Scrivens JH. The effect of counter ions in matrix-assisted laser desorption/ionization of poly(methyl methacrylate). Eur Mass Spectrom 1998;4: 435-40.
43. The Porphyrin Handbook. Amsterdam: Academic Press; 1999.
44. Deery MJ, Jennings KR, Jasieczek CB, et al. A Study of Cation Attachment to Polystyrene by Means of Matrix-assisted Laser Desorption/Ionization and Electrospray Ionization-Mass Spectrometry. Rapid Communications in Mass Spectrometry 1997;11(1): 57 - 62.
45. Rashidezadeh H, Hung K, Guo B. Probing polystyrene cationization in matrix-assisted laser/desorption ionization. European Mass Spectrometry 1998.
46. Burgers PC, Terlouw JK. Monoisotopic 65Cu+ attachment to polystyrene. Rapid Commun Mass Spectrom 1998;12(12): 801 - 4.

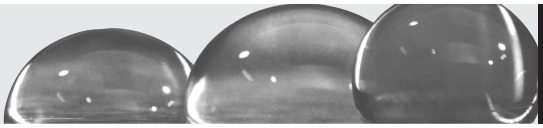

Chapter 6

Validation of an HIV-1 inactivation protocol that is compatible with intracellular drug analysis by mass spectrometry

Jeroen J.A. van Kampen, Esther J. Verschuren, Peter C. Burgers,
Theo M. Luider, Ronald de Groot, Albert D.M.E. Osterhaus, Rob A. Gruters

Journal of Chromatography B 2007, 847, 38–44

Abstract

Mass spectrometry is a powerful tool for studying the intracellular pharmacokinetics of antiretroviral drugs. However, the biohazard of HIV-1 calls for a safety protocol for such analyses. To this end, we extracted HIV-1 producing cells with methanol or ethanol at 4°C. After extraction, no viral infectivity was detected, as shown by a reduction in infectious titers of more than 6 log. In addition, this protocol is compatible with the quantitative analysis of antiretroviral drugs in cell extracts using matrix-assisted laser desorption/ ionization time-of-flight (MALDI-TOF) MS. Thus, using this protocol, infectious HIV-1 is inactivated and antiretroviral drugs are extracted from cells in a single step.

Introduction

The majority of antiretroviral drugs exert their action in target cells for HIV infection, i.e. cells that express CD4 in combination with CXCR4 and/or CCR5. The field of intracellular pharmacokinetics of antiretroviral drugs is therefore an active area of research, which is often approached through mass spectrometry [1-7]. HIV-1 represents a biohazard, so preparation of HIV-1 infected samples must be carried out in laboratories with biosafety level (BSL) 2 or 3. Since BSL 2 or 3 laboratories require specific staff training and since the necessary safety procedures involve more laborious sample preparation, it is highly desirable to minimize the sample preparation steps in such laboratories. A procedure that inactivates infectious HIV-1 in freshly isolated cells, but which does not affect drug levels, is thus warranted. Such a safety procedure should not interfere with sample analysis, which is normally performed by an HPLC system coupled online to an electrospray ionization triple quadrupole mass spectrometer. The antiretroviral drugs can be extracted from the intracellular compartment by lysing the cells with solutions containing a high percentage of organic solvents. For this purpose, methanol and ethanol are suitable candidates, which can also be used to inactivate a variety of viruses. Therefore, procedures to extract antiretroviral drugs from cells could simultaneously inactivate infectious HIV-1.

Here, we describe a dual-purpose procedure whereby antiretroviral drugs can be extracted from cells and by which infectious HIV-1 is simultaneously inactivated. To achieve this, we treated HIV-1 infected cells using phosphate buffered solution containing 40–100% methanol or ethanol. The supernatants of the extracted cells were diluted in culture medium and tested for infectious virus on susceptible cells. Finally, we show that this drug extraction/HIV-1 inactivation procedure is compatible with accurate and precise quantification of ritonavir in extracts of peripheral blood mononuclear cells (PBMCs) using a recently developed method based on matrix-assisted laser desorption/ionization time-of-flight (MALDI-TOF) mass spectrometry [6].

Experimental Section

Virus

HIV-IIIB was obtained through the NIH AIDS Research and Reference Reagent Program (Division of AIDS, NIAID, NIH) [8-10].

H9 cells

H9 cells were obtained through the NIH AIDS Research and Reference Reagent Program (Division of AIDS, NIAID, NIH) [8,9,11]. H9 cells were cultured in RPMI-1640 (Cambrex Bioscience, Belgium) supplemented with 10% heat inactivated fetal bovine serum (FBS; Hy-

Clone, USA), 100 U/mL penicillin, 100 µg/mL streptomycin, and 2 mmol/mL l-glutamine (all from Cambrex Bioscience, Belgium) (R10F). Cells were cultured at 37°C and 5% CO_2. Pellets of 4×10^6 uninfected H9 cells were resuspended in 15 mL tubes with 3 mL virus dilution, methanol/ethanol solution, or reconstituted inactivated supernatants, and were incubated for 2 h (see specific sections). Subsequently, cells were washed three times with R10F, resuspended in 5mL R10F, and cultured for 10 days for the sensitivity experiments and validation experiments, or 4 days for the methanol/ethanol titration experiments.

GHOST cells

GHOST (3) CXCR4 cells (GHOST cells) were obtained through the NIH AIDS Research and Reference Reagent Program (Division of AIDS, NIAID, NIH) [12]. GHOST cells were cultured in 24-well plates with 1mL R10F supplemented with 500 µg/mL geneticin (GIBCO, USA), 2 µg/mL puromycin (Cayla, France), and 100 µg/mL hygromycin (Cayla). GHOST cells were cultured at a density of 3.6×10^4 per well for 24 h. The next day, wells were washed with phosphate buffered saline (PBS). To each well, 500 µL virus dilution, or methanol/ethanol solution, or reconstituted inactivated supernatants was added, and cells were incubated for 4 h (see specific sections). Next, the incubation solutions were discarded, and cells were cultured with 1 mL culture medium supplemented with 4 µg/mL polybrene (Sigma–Aldrich, Germany) for 4 days. At day 4, cells were harvested with trypsin (trypsin-EDTA 1x, GIBCO, USA), and cell pellets were resuspended in an appropriate medium (see specific sections) for analysis by flow cytometry. Cells were cultured at 37°C and 5% CO_2.

Flow cytometry

Measurements were carried out on a FACSCalibur flow cytometer (Becton Dickinson, USA). For quantitative comparison of samples, running mode and measure time were kept constant from sample to sample. Flow cytometric data were analyzed using WinMDI version 2.8.

p24 ELISA

Qualitative and quantitative p24 determinations were obtained with the enzyme-linked immuno-sorbent assay (ELISA) using a Genetic Systems HIV-1 Ag EIA (Bio-Rad, France) and an HIV-1 antigen standard (Bio-Rad). All experiments were performed and interpreted according to the manufacturer's guidelines.

Sensitivity of HIV-1 detection assays

(A) Virus dilutions

The supernatant of an HIV-1 infected H9 culture (p24 concentration 200 ng/mL) was diluted 10^2 to 10^8 times (in steps of 10) in R10F supplemented with 4 µg/mL polybrene. R10F with 4 µg/mL polybrene but without supernatant was used as negative control.

(B) GHOST assay

GHOST cell pellets were resuspended in 300 µL PBS with 10% FBS and analyzed with flow cytometry. Side scatter (SSC) was plotted against the forward scatter (FSC), and debris and dead cells were gated out. Subsequently, fluorescent channel 1 (FL1) was plotted against the FSC and the percentage of green fluorescent protein (GFP)-positive cells was determined. The cut-off value for a HIV-1 positive GHOST culture was calculated as follows: mean percentage of positive cells in the negative control samples + 3 times the standard deviation. Experiments were performed in triplicate.

(C) p24 ELISA assay

After 10 days, culture media were collected and cell-free supernatants were frozen at -20°C until analysis by p24 ELISA. Three replicate inoculations were performed for each virus dilution. One p24 determination was assessed per inoculation.

(D) Statistics

The virus dilution that results in infection in 50% of the replicate inoculations, i.e. 50% tissue culture infectious dose ($TCID_{50}$), was calculated according to the Reed-Muench method [13].

Methanol/ethanol titration on H9 and GHOST cells

(A) Methanol and ethanol solutions

R10F was supplemented with 1% methanol (MeOH; Sigma–Aldrich, Germany) or 1% ethanol (EtOH; Sigma–Aldrich) and 4 µg/mL polybrene. R10F supplemented with 4 µg/mL polybrene but without methanol or ethanol was used as negative control.

(B) GHOST cells

GHOST cell pellets were resuspended in 300 µL PBS with 2% FBS, 25 nM TO-PRO-3 iodide (Molecular Probes, USA), and 2.5 mM EDTA. Cell suspensions were incubated for 20 min and subsequently analyzed with flow cytometry. FSC was plotted against the FL4 and viable cells were counted. Experiments were performed in triplicate.

(C) H9 cells

After 4 days, cell pellets were resuspended in 300 µL PBS with 2% FBS, 25 nM TO-PRO-3 iodide and 2.5 mM EDTA and incubated for 20 min. Subsequently, cell suspensions were diluted 10 times in PBS with 2% FBS, 25 nM TO-PRO-3 iodide and 2.5 mM EDTA, and analyzed with flow cytometry as described above. Experiments were performed in triplicate.

(D) Statistics

Two-tailed two-sample t-tests assuming equal variances were performed to test whether the viable cell count differed significantly between titrated and non-titrated cells. The results were considered to be significant if the p-value was ≤ 0.05.

Validation of HIV-1 inactivation protocols

(A) Virus culture

Ten pellets of 10×10^6 uninfected H9 cells were resuspended in 15 mL tubes with 300 µL virus supernatant supplemented with 4 µg/mL polybrene, and incubated for 1 h. Subsequently, cells were washed with R10F, pooled in one 162 cm^2 cell culture flask, and cultured for 6 days. At day 6, 5 mL virus culture was transferred to a 25 cm^2 cell culture flask and cultured for another day to assess whether p24 was still being actively produced. The 95 mL virus culture remaining at day 6 was washed four times with R10F, counted using trypan blue dye exclusion, and used to test the inactivation protocols.

(B) Percentage of HIV-1 infected cells

Pellets of 1×10^6 infected H9 cells and 1×10^6 uninfected H9 cells were fixed with Cytofix/Cytoperm (BD Biosciences, USA) and colored with KC57-RD1 (BD Biosciences) according to the manufacturer's protocol. Fixed cells were resuspended in 300 µL PBS with 2% FBS, and analyzed with flow cytometry. FSC was plotted against the SSC, and non-viable cells were gated out. Subsequently, FL2 was plotted against FSC and the percentage of KC57-RD1 positive cells was determined.

(C) Inactivation solutions

Solutions were made of 40, 60, 80 and 100% EtOH or MeOH in PBS. Deionized water was used as positive control.

(D) Inactivation protocols

Pellets of 1.6×10^6 infected H9 cells and 1.6×10^6 uninfected H9 cells (negative control) were resuspended in 1.5 mL tubes (Biopur; Eppendorf, Germany) with 100 µL inactivation solution, and incubated at 4°C for 1 h. Subsequently, samples were centrifuged and supernatants were collected. Experiments were performed in triplicate.

(E) p24 ELISA read-out

Supernatants (30 µL) were mixed with 2,967 µL R10F and 3 µL polybrene (4 mg/mL). Pellets of uninfected H9 cells were resuspended with reconstituted inactivated supernatants as described above. Supernatant of a virus culture on which no inactivation protocol had been performed was used as absolute positive control. At day 10, culture

media were collected and cell-free supernatants of each cell culture were stored at -20°C until analysis by p24 ELISA.

(F) GHOST assay read-out

Supernatants (5 µL) were mixed with 490 µL R10F and 5 µL polybrene (400 µg/mL). GHOST cells were incubated with the reconstituted inactivated supernatant as described above. At day 4, GHOST cells were harvested, resuspended in 300 µL PBS with 2% FBS, and analyzed with flow cytometry. SSC was plotted against the FSC and non-viable cells were gated out. Subsequently, FL1 was plotted against FSC and the percentage of GFP-positive cells was determined. Two-tailed two-sample t-tests assuming equal variances were performed to test whether the percentage of GFP-positive cells differed significantly between the negative controls and inactivated samples. The results were considered to be significant if the p-value was ≤ 0.01.

Mass spectrometry

(A) Matrix preparation and spotting

The matrix solution contained 20 mg/mL meso-Tetrakis(pentafluorophenyl)porphyrin (F20TPP; TCI Europe, Belgium) and 20 mM lithium iodide (Sigma–Aldrich, Germany) in 100% acetone. The matrix solution was spotted onto an 800 µm AnchorChip™ (Bruker Daltonics) using the brushing spotting technique, whereby a 10 µL pipette tip was filled with matrix solution, and the pipette was positioned such that the tip just touched the target plate above the first spot. Next, the plunger was slightly pressed and at the same time the pipette was quickly dragged downwards over the target spots.

(B) Sample preparation

Standards of ritonavir (kindly provided by Abbott Laboratories) were prepared in methanol/water (1:1); nelfinavir (kindly provided by Pfizer Inc.) was used as internal standard. Peripheral blood mononuclear cells were isolated from a buffy coat (Sanquin, The Netherlands) using a Ficoll density gradient. PBMCs were extracted overnight in methanol/water (1:1) (100 µL per 10^6 PBMCs) at 4°C. Subsequently, cell debris was spun down and the supernatants of 1×10^6 PBMCs (100 µL) were supplemented with 100 µL ritonavir standard, 100 µL methanol/water (1:1), and 300 µL HPLC grade water (Sigma-Aldrich, Germany). Subsequently, extracts were cleaned up using a 96-well solid phase extraction plate (Oasis HLB µelution plate, Waters, USA). The loaded samples were washed twice with 200 µL methanol/water (1:19) and once with 200 µL methanol/water (1:1). Samples were eluted from the solid phase extraction plate using 100 µL acetone. Eluents were dried using a SpeedVac (Savant, USA), and reconstituted in 25 µL ethanol/water (1:1). The reconstituted eluents were spotted in 4-fold on top of the matrix crys-

tals. The theoretical concentrations of ritonavir in the reconstituted eluents were 1,000, 500, 250, 125, 62.5, 31.25, 15.625 femtomole per µL, and the theoretical concentration of nelfinavir was 500 femtomole per µL.

(C) Sample measurement

All experiments were performed on an Ultraflex-I™ MALDI-TOF/TOF mass spectrometer (Bruker Daltonics, Germany) equipped with a 50 Hz nitrogen laser (337 nm). Mass spectra were recorded in the positive ion reflectron mode. FlexControl™ version 2.4 software (Bruker Daltonics) was used to operate the mass spectrometer. A sample spot containing matrix only was used to manually set the laser power approximately 5% above the threshold for ionization. The samples containing the analytes were measured automatically using the AutoXecute part of the FlexControl™ software. Mass spectra were recorded by accumulating 50 shots on 20 different positions on each sample spot. No spectra were rejected (i.e., fuzzy control for spectra accumulation was not used).

(D) Data analysis

The areas under the monoisotopic peaks of the lithiated ritonavir and nelfinavir were calculated using FlexAnalysis™ software (version 2.4, Bruker Daltonics). Precisions (expressed as percent relative standard deviation) of the ratio of the ritonavir-to-nelfinavir peak area (RTV/NFV) were calculated for the four replicate analyses of each calibrator. Subsequently, the mean RTV/NFV of each calibrator was plotted against the ritonavir concentrations, and accuracies (expressed as percent deviation from the theoretical concentration) were calculated using a $1/x^2$ weighed quadratic curve fitting method.

Results and Discussion

van Bueren et al. have reviewed the literature on alcohol inactivation of HIV in suspensions in addition to presenting their own data [14]. They showed that, depending on the procedure followed, reductions of infectious virus titers varied from 10^2 to 10^7. Our procedure differs in that we inactivate HIV at 4°C, whereas published protocols were executed at room temperature or at 37°C. Antiretroviral drugs are normally extracted from cells at 4°C. In addition, our inactivation protocol is compatible with intracellular drug analysis by MALDI mass spectrometry (vide infra).

To validate our HIV-1 inactivation protocol, we first tested two assays to quantify the infectious titers of HIV-1. For this, we used (1) A rapid direct assay (GHOST assay), which detects HIV replication in susceptible GHOST cells via a GFP reporter gene that is transcribed only in the presence of the HIV protein Tat. GFP-positive GHOST cells are distinguished from GFP-negative GHOST cells by flow cytometry; (2) a time-consuming

indirect assay (H9/p24 assay), which detects the viral core protein p24 by ELISA after the virus has been amplified in H9 cells.

First, we tested which of the two assays provided the best sensitivity for detecting infectious HIV-1. Supernatant of an HIV-1 infected H9 culture (p24 concentration 200 ng/mL) was diluted 10^2–10^8 times and used to inoculate non-infected GHOST cells and H9 cells. The $TCID_{50}$ was calculated for both assays according to the Reed–Muench method (see Table 1): The $TCID_{50}$ per milliliter was 7.9×10^{-7} for the H9/p24 assay and 1.6×10^{-4} for the GHOST assay. Thus, for safety reasons the H9/p24 assay is preferred to validate the HIV-1 inactivation protocol, given its superior sensitivity.

The extraction of antiretroviral drugs from the intracellular compartment is normally performed by lysing the cells in 40–100% methanol or ethanol. To test whether infectious virus was still present in the supernatant, we inoculated non-infected cells with the supernatants of such lysates (vide infra).

To avoid the cytotoxicity caused by the organic solvents, the supernatants of the lysates were diluted in culture medium to an organic solvent concentration of ≤ 1%. We verified whether 1% methanol or ethanol had affected the viability of GHOST cells or H9 cells, and found no significant difference in the total number of viable H9 or GHOST

Table 1. Calculation of $TCID_{50}$ of the H9/p24 assay and the GHOST assay.

	log virus dilution	HIV positive replicates	Cumulative HIV positive (A)	Cumulative HIV negative (B)	A/(A + B)	Percent infected replicates
p24 ELISA assay	-2	3/3	15	0	15/15	100
	-3	3/3	12	0	12/12	100
	-4	3/3	9	0	9/9	100
	-5	2/3	6	1	6/7	85.7
	-6	2/3	4	2	4/6	66.7
	-7	2/3	2	3	2/5	40
	-8	0/3	0	6	0/6	0
GHOST assay	-2	3/3	6	0	6/6	100
	-3	3/3	3	0	3/3	100
	-4	0/3	0	3	0/3	0
	-5	0/3	0	6	0/6	0
	-6	0/3	0	9	0/9	0
	-7	0/3	0	12	0/12	0
	-8	0/3	0	15	0/15	0

Proportionate distance = (% positive above 50% - 50%)/(% positive above 50% - % positive below 50%). $TCID_{50}$ = log dilution above 50% + (proportionate distance × log dilution factor). For the H9/p24 assay, the proportionate distance = 0.6, the $TCID_{50}$ = -6.6 log, the $TCID_{50}$ per mL is –6.1 log = 7.9×10^{-7}. For the GHOST assay, the proportionate distance = 0.5, the $TCID_{50}$ = -3.5 log, the $TCID_{50}$ per mL is –3.8 log = 1.6×10^{-4}.

cells between the negative controls and the cultures containing 1% methanol or ethanol (data not shown).

The percentage of HIV infected cells and the number of infectious HIV particles in *in vitro* cultures are much greater than those in clinical samples of HIV-1 infected patients. We therefore chose to validate the HIV-1 inactivation protocols on *in vitro* cultures of HIV-1 infected H9 cells. Immediately before the start of the inactivation protocols, the p24 concentration of the HIV-1 infected H9 culture was 440 ng/mL, and 12% of the cells expressed HIV-1 proteins. Part of the HIV-1 infected H9 cells were cultured for another day, in which the p24 concentration rose to 620 ng/mL, showing active viral replication on the day the inactivation protocols were tested. The inactivation solutions were prepared in phosphate buffered solution to ensure that the inactivation of infectious HIV-1 was caused only by the methanol or ethanol and not by the handling of the sample. Whereas no infectious HIV-1 was detected by either assay after HIV-1 infected H9 cells had been incubated with 40, 60, 80 or 100% methanol or ethanol at 4°C for 1 h, infectious virus was recovered after cell extraction with de-ionized water (see Table 2). This indicates that the organic solvent was indeed the inactivating factor in the protocol.

Table 2. Validation of the HIV-1 inactivation protocol.

	Loss of infectivity
No extraction procedure	-
Deionized water	-
40–100% methanol	+
40–100% ethanol	+

To eliminate spillover of p24 from the inoculum, HIV-1 infected cells were washed four times as to remove p24 that might contaminate the H9 read-out culture of the H9/p24 assay. Despite these wash steps, some p24 was still present in the positive control samples before start of the HIV-1 amplification. The OD_{450} of the positive control samples ranged between 0.067 and 0.144 after washing and before start of the HIV-1 amplification. These titers rose to ≥3.5 after the amplification in H9 cells, indicating that active virus replication was only ongoing in the positive control and in the H_2O extracted cells.

Finally, we tested whether this inactivation protocol was compatible with quantitative analysis of antiretroviral drugs by mass spectrometry. To this end, we used a recently developed method for quantitative analysis of lopinavir in PBMC extracts by MALDI-TOF mass spectrometry [6]. Normally, quantitative analysis of drugs by MALDI-TOF mass spectrometry is hampered by matrix-derived chemical interference in the low mass range and poor reproducibility of signal abundances. Our experimental method was specifically designed to enhance the precision of the MALDI-TOF response and to decrease matrix-derived chemical noise in the low mass range. The use of a high molecular

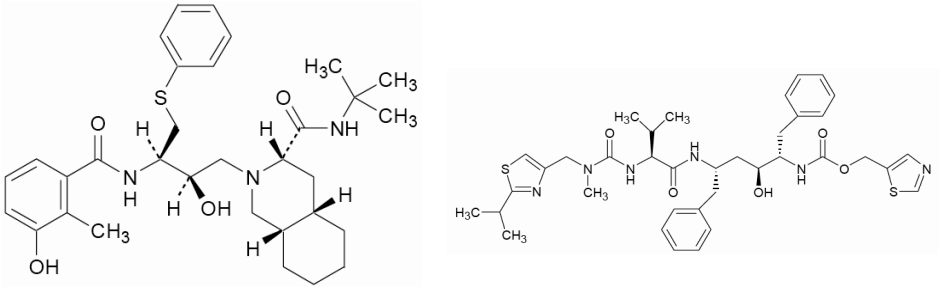

Figure 1. Structures of nelfinavir and ritonavir. The left hand shows the structure of nelfinavir (internal standard; $C_{32}H_{45}N_3O_4S$; MW 567.3). The right hand shows the structure of ritonavir ($C_{37}H_{48}N_6O_5S_2$; MW 720.3).

weight matrix, i.e. meso-Tetrakis(pentafluorophenyl)porphyrin (F20TPP), significantly decreased the matrix-derived chemical noise in the low mass range. To increase reproducibility (precision), we developed a fast evaporation protocol for the matrix F20TPP using prestructured target plates (AnchorChip™). To further increase reproducibility, instrument response variation was minimized by using an internal standard, by averaging out 1,000 spectra per sample, and by measuring each sample in 4-fold. An interesting observation for F20TPP is that this matrix is a poor proton donor and so analyte molecules do not become protonated. However, mixing the F20TPP with alkali salts, in particular with lithium salts, results in intense signals for the cationized drugs. In this study, we have extracted PBMCs in methanol/water (1:1) and spiked the supernatants with various concentrations of ritonavir and nelfinavir (see Fig. 1). The supernatants of the extracted PBMCs were cleaned up using a solid-phase extraction plate. The eluents (100 µL) were dried and subsequently reconstituted in a smaller volume of 25 µL to concentrate the sample. Acetone was used as eluents to enhance the drying speed of the samples. Fig. 2 shows the mass spectra of the F20TPP matrix, PBMC extract, and PBMC extracts spiked with nelfinavir and/or ritonavir. The mass spectrum of the F20TPP matrix shows that there are only a few matrix-derived interferences in the low mass range (see Fig. 2 panel A). The mass spectrum of the PBMC extract spiked with nelfinavir shows a peak at *m/z* 574 for nelfinavir cationized by Li^+ (see Fig. 2 panel C). In addition, there is a peak at *m/z* 467, which does not contain lithium (no $^6Li^+$ adduct is present). This peak at *m/z* 467 is not observed in the mass spectrum of the non-spiked PBMC extract. This peak was not used for the quantitative analysis of ritonavir. The concentration-response relationship showed nonetheless a good linearity with an r^2 of 0.99992 (see Fig. 3). Mean precision was 5.6% (sd 3.7) and mean accuracy was 2.4% (sd 2.2). Table 3 shows the precisions and accuracies for each ritonavir standard. All values meet the FDA ± 20/15% criteria for precision and accuracy [15].

We have previously shown that pure lopinavir, ritonavir, nelfinavir, indinavir, saquinavir, amprenavir, and tipranavir could be detected between 5 femtomole and 40 femtomole

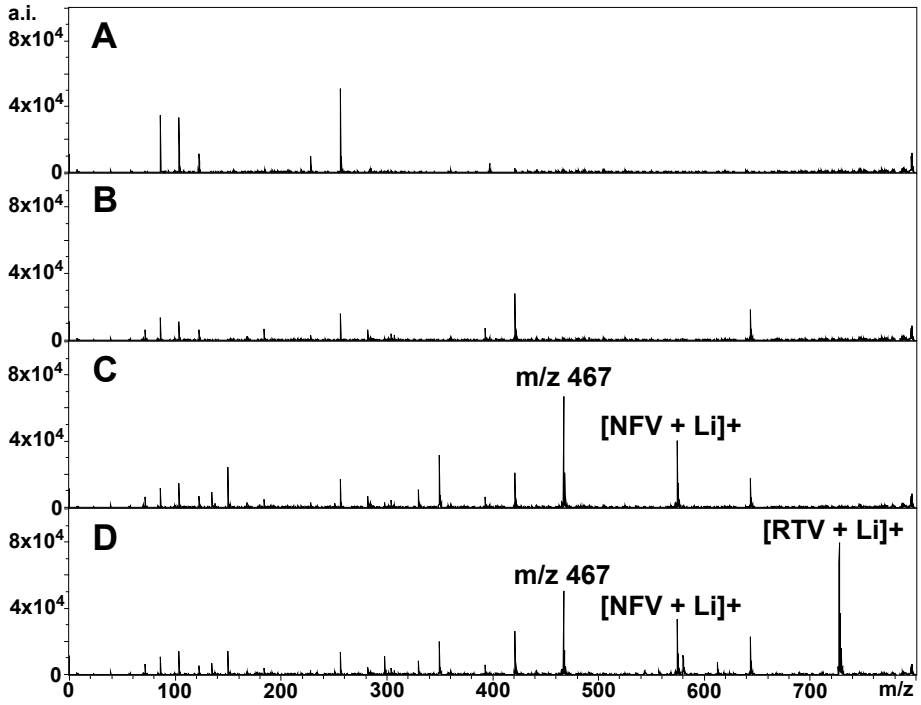

Figure 2. Mass spectra of the F20TPP matrix, PBMC extract, and PBMC extract spiked with nelfinavir and/or ritonavir. NFV= nelfinavir; RTV= ritonavir. Panel A, mass spectrum of the F20TPP matrix (20 mg/mL F20TPP + 20 mM LiI); Panel B, mass spectrum of PBMC extract cleaned with solid phase extraction; Panel C, mass spectrum of PBMC extract spiked with 500 femtomole nelfinavir; Panel D, mass spectrum of PBMC extract spiked with 500 femtomole nelfinavir and 500 femtomole ritonavir.

per µL using MALDI-TOF mass spectrometry [6]. In addition, the limit of quantification for lopinavir in PBMC extracts was 25 femtomole per µL. In the present study, we show that the limit of quantification for ritonavir in PBMC extracts is 15 femtomole per µL. Notari et al. used the tandem mass spectrometry mode (MS/MS) on a MALDI-TOF/TOF mass spectrometer for quantitative analysis of anti-HIV drugs in human plasma [5]. The limit of quantification for lopinavir and ritonavir was 2.5 femtomole per µL. These better limits of quantification can be attributed to the use of MS/MS, which leads to an increased selectivity and higher signal-to-noise ratios. Time-of-flight mass analyzers are normally not the first choice for quantitative analysis of drugs; the dynamic range is relatively small and most time-of-flight mass analyzers are not designed for tandem mass experiments. The development of new types of MALDI mass spectrometers, such as MALDI-triple quadrupole mass spectrometers, is therefore of special interest for quantitative analysis of drugs [16-20].

Consideration of MALDI for quantitative analysis of antiretroviral drugs leads to questions on how this technique performs compared to HPLC-ESI-triple quadrupole mass

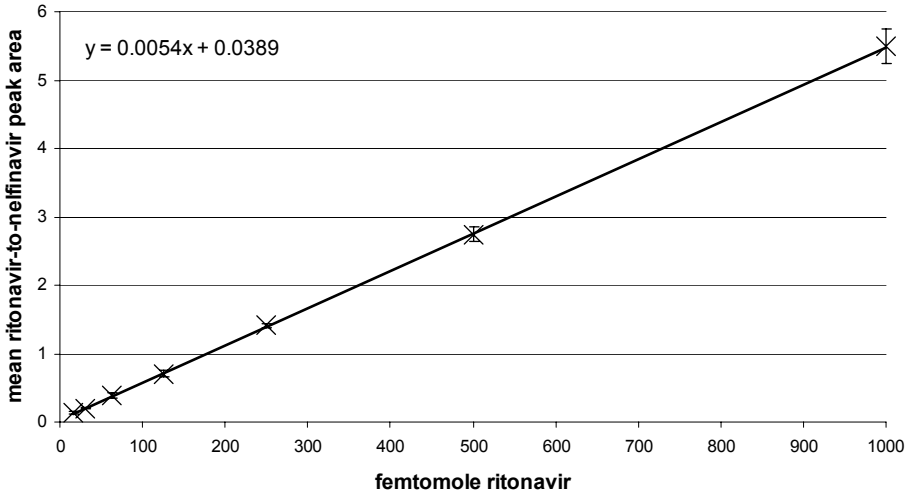

Figure 3. Concentration-response relationship for ritonavir in PBMC extracts. Concentration-response relationship for ritonavir in extracts of 1 x 10^6 PBMCs using nelfinavir as internal standard. Each ritonavir calibrator was analyzed in 4-fold. Error bars indicate the standard deviation of plus one and minus one (4 replicates per calibrator). The lower limit of quantification was 15.625 femtomole.

spectrometry (LC–MS/MS). LC–MS/MS is currently the gold standard for quantitative analysis of drugs due to its selectivity, sensitivity and robustness. To our best knowledge, three studies have been published that give an in-depth description of the development and validation of an LC–MS/MS method for quantitative analysis of protease inhibitors in PBMCs [2,21,22]. Jemal et al. developed an LC–MS/MS method for quantitative analysis of atazanavir in PBMCs [21]. The limit of quantification was 5 femtomole per 10^6 PBMCs. Rouzes et al. obtained a limit of quantification of 3 picomole per 3×10^6 PBMC for lopinavir and 1 picomole per 3×10^6 PBMC for ritonavir using an LC–MS/MS method for quantitative analysis of four protease inhibitors and one non-nucleoside reverse transcriptase inhibitor (NNRTI) [22]. Colombo et al. developed an LC–MS/MS method for quantitative analysis of seven protease inhibitors and two NNRTIs in PBMCs [2]. They obtained limits of quantification of 5 femtomole for ritonavir and 6 femtomole for lopinavir (minimum quantifiable drug on column). Our obtained limits of quantification for lopinavir and ritonavir in PBMC extracts using MALDI-TOF mass spectrometry are comparable to those obtained by LC-MS/MS. One further aspect concerns the sample analysis time, which is considerably shorter for MALDI than for LC–MS/MS. Sample analysis time of the LC–MS/MS methods discussed above range from 4 to 20 min. Time to analyze one sample in 4-fold using our MALDI-TOF method takes 2 min and 20 s. Following the development of high repetition rate lasers (1,000 Hz), sample analysis times have decreased to 15 s and less using a MALDI-triple quadrupole mass spectrometer [17,18]. More studies are needed to delineate the future role of MALDI mass spectrometry for bioanalysis of drugs. How-

Table 3. Precision and accuracy of quantitative analysis of ritonavir in PBMC extracts using MALDI-TOF mass spectrometry.

Femtomole ritonavir	Precision	Accuracy
1000	4.6	-0.7
500	4.2	0.2
250	2.1	3.0
125	7.2	-0.8
62.5	12.0	2.4
31.25	1.3	-6.8
15.625	8.0	2.7

Precision is expressed as relative standard deviations. Accuracy is expressed as the percent deviation of the measured concentration from the theoretical concentrations. The calibration curve was constructed using a $1/x^2$ quadratic curve fitting method. Each calibrator was measured in 4-fold.

ever, it already appears that the quantitative analysis of drugs is a new and promising application of MALDI mass spectrometry.

In conclusion, we have shown that extraction of HIV-1 infected cells with 40–100% methanol or ethanol for 1 h at 4 °C results in a loss of HIV infectivity of at least 6.1 log. Because this level of reduction shows that, under physiological conditions, all infectious virus particles are destroyed, it guarantees that samples can be handled safely outside special facilities. The validated HIV-1 inactivation procedure provides an opportunity to optimize the drug extraction process by adjusting extraction time and/or the percentage of methanol or ethanol without the need to re-test whether the drug extraction procedure inactivates infectious HIV-1. Furthermore, the protocol is compatible with accurate and precise quantitative analysis of ritonavir in PBMC extracts using MALDI-TOF mass spectrometry.

Acknowledgements

The following reagents were obtained through the AIDS Research and Reference Reagent Program, Division of AIDS, NIAID, NIH: GHOST (3) CXCR4 cells from Drs. Kewalramani and Littman [12], H9 and HTLV-IIIB/H9 from Dr. Robert Gallo [8,9,11]. We would like to thank Aids Fonds, The Netherlands (project numbers 2004051 JvK, 2005038 RG) and VIRGO for financial support. We would also like to thank Hetty Blaak and Carel van Baalen for their helpful discussions on the methodology. Ritonavir and nelfinavir were kindly provided by Abbott Laboratories and Pfizer Inc., respectively.

References

1. Almond LM, Edirisinghe D, Dalton M, Bonington A, Back DJ, Khoo SH. Intracellular and plasma pharmacokinetics of nevirapine in human immunodeficiency virus-infected individuals. Clin Pharmacol Ther 2005;78(2):132-42.
2. Colombo S, Beguin A, Telenti A, et al. Intracellular measurements of anti-HIV drugs indinavir, amprenavir, saquinavir, ritonavir, nelfinavir, lopinavir, atazanavir, efavirenz and nevirapine in peripheral blood mononuclear cells by liquid chromatography coupled to tandem mass spectrometry. J Chromatogr B Analyt Technol Biomed Life Sci 2005;819(2):259-76.
3. Crommentuyn KM, Mulder JW, Mairuhu AT, et al. The plasma and intracellular steady-state pharmacokinetics of lopinavir/ritonavir in HIV-1-infected patients. Antivir Ther 2004;9(5):779-85.
4. King JR, Kimberlin DW, Aldrovandi GM, Acosta EP. Antiretroviral pharmacokinetics in the paediatric population: a review. Clin Pharmacokinet 2002;41(14):1115-33.
5. Notari S, Mancone C, Tripodi M, Narciso P, Fasano M, Ascenzi P. Determination of anti-HIV drug concentration in human plasma by MALDI-TOF/TOF. J Chromatogr B Analyt Technol Biomed Life Sci 2006;833(1):109-16.
6. van Kampen JJ, Burgers PC, de Groot R, Luider TM. Qualitative and quantitative analysis of pharmaceutical compounds by MALDI-TOF mass spectrometry. Anal Chem 2006;78(15):5403-11.
7. van Kampen JJ, Fraaij PL, Hira V, et al. A new method for analysis of AZT-triphosphate and nucleotide-triphosphates. Biochem Biophys Res Commun 2004;315(1):151-9.
8. Popovic M, Read-Connole E, Gallo RC. T4 positive human neoplastic cell lines susceptible to and permissive for HTLV-III. Lancet 1984;2(8417-18):1472-3.
9. Popovic M, Sarngadharan MG, Read E, Gallo RC. Detection, isolation, and continuous production of cytopathic retroviruses (HTLV-III) from patients with AIDS and pre-AIDS. Science 1984; 224(4648):497-500.
10. Ratner L, Haseltine W, Patarca R, et al. Complete nucleotide sequence of the AIDS virus, HTLV-III. Nature 1985;313(6000):277-84.
11. Mann DL, O'Brien SJ, Gilbert DA, et al. Origin of the HIV-susceptible human CD4+ cell line H9. AIDS Res Hum Retroviruses 1989;5(3):253-5.
12. Morner A, Bjorndal A, Albert J, et al. Primary human immunodeficiency virus type 2 (HIV-2) isolates, like HIV-1 isolates, frequently use CCR5 but show promiscuity in coreceptor usage. J Virol 1999;73(3):2343-9.
13. Principles of virology. In: Knipe DM, Howley PM, eds. Fields Virology. 4th ed: Lippincott Williams & Wilkins:33 - 4.
14. van Bueren J, Larkin DP, Simpson RA. Inactivation of human immunodeficiency virus type 1 by alcohols. J Hosp Infect 1994;28(2):137-48.
15. Guidance for industry: bioanalytical method validation. FDA 2001 available at http://www.fda.gov/cder/guidance/4252fnl.pdf.
16. Corr JJ, Kovarik P, Schneider BB, Hendrikse J, Loboda A, Covey TR. Design considerations for high speed quantitative mass spectrometry with MALDI ionization. J Am Soc Mass Spectrom 2006; 17(8):1129-41.
17. Gobey J, Cole M, Janiszewski J, et al. Characterization and performance of MALDI on a triple quadrupole mass spectrometer for analysis and quantification of small molecules. Anal Chem 2005;77(17):5643-54.

18. Hatsis P, Brombacher S, Corr J, Kovarik P, Volmer DA. Quantitative analysis of small pharmaceutical drugs using a high repetition rate laser matrix-assisted laser/desorption ionization source. Rapid Commun Mass Spectrom 2003;17(20):2303-9.
19. Sleno L, Volmer DA. Some fundamental and technical aspects of the quantitative analysis of pharmaceutical drugs by matrix-assisted laser desorption/ionization mass spectrometry. Rapid Commun Mass Spectrom 2005;19(14):1928-36.
20. Sleno L, Volmer DA. Toxin screening in phytoplankton: detection and quantitation using MALDI triple quadrupole mass spectrometry. Anal Chem 2005;77(5):1509-17.
21. Jemal M, Rao S, Gatz M, Whigan D. Liquid chromatography-tandem mass spectrometric quantitative determination of the HIV protease inhibitor atazanavir (BMS-232632) in human peripheral blood mononuclear cells (PBMC): practical approaches to PBMC preparation and PBMC assay design for high-throughput analysis. J Chromatogr B Analyt Technol Biomed Life Sci 2003;795(2): 273-89.
22. Rouzes A, Berthoin K, Xuereb F, et al. Simultaneous determination of the antiretroviral agents: amprenavir, lopinavir, ritonavir, saquinavir and efavirenz in human peripheral blood mononuclear cells by high-performance liquid chromatography-mass spectrometry. J Chromatogr B Analyt Technol Biomed Life Sci 2004;813(1-2):209-16.

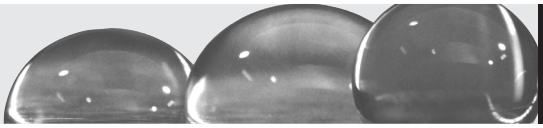

Chapter 7

A mass spectrometry based imaging method developed for the intracellular detection of HIV protease inhibitors

Lennard J.M. Dekker, Jeroen J.A. van Kampen, Mariska L. Reedijk,
Peter C. Burgers, Rob A. Gruters, Albert D.M.E. Osterhaus, Theo M. Luider

Rapid Communications in Mass Spectrometry 2009, 23, 1183 - 1188

Abstract

Mass spectrometry imaging is a promising technique for the measurement of drugs and drug metabolites in cells and tissues. Using high resolution mass spectrometry it is possible to localize and quantify in a relative way compounds of interest on a glass slide. In this manuscript we describe a method for the imaging of HIV protease inhibitors. As a model system we used Mono Mac 6 cells cultured with the HIV protease inhibitors saquinavir and nelfinavir that were deposited on glass slides using a cytocentrifuge. This model system was used to optimize and test our sample preparation and mass spectrometry imaging method. We have developed a new method for matrix deposition using an in-house-built sublimation system that is suited for imaging of HIV protease inhibitors at clinically relevant concentrations. In addition, we showed that the glass slides containing the cytocentrifuged cells could be measured and analyzed with two types of mass spectrometry; MALDI-TOF and MALDI-FTICR. The combination of the two types of mass spectrometers makes it possible to perform imaging rapidly (MALDI-TOF) and with a very high selectivity (MALDI-FTICR).

Introduction

Mass spectrometry (MS) based imaging techniques have greatly improved over recent years in terms of sensitivity, spatial resolution and speed, making them more amenable to clinical applications [1]. The unique ability of this imaging technique is that it can detect numerous different compounds at the same time in tissue without losing spatial distribution. Thus, with this technique it possible not only to detect differences in concentration of certain molecules between tissue and cell types, but also to determine the exact location (spatial resolution < 10 µm) of these differences [2]. The bottleneck of currently available MS imaging methods is that it is relatively difficult to identify the compounds observed, and that it is biased towards the detection of higher abundant compounds. The rapid progress in the use of high resolution mass spectrometry, combined with its online MS/MS capability, may alleviate this problem to a certain extent. However, identification is not required for (high resolution) mass spectrometry imaging of known drugs or drug metabolites in cells and tissues, because the masses of the compounds of interest are known [3], and can be discriminated from background noise. Thus, this technique can be used to gain a better understanding of pharmacology [4], for example by studying the distribution of antiretroviral drug in the various cell types and tissues that play a role in HIV infection.

A prerequisite for the successful quantitative imaging of drugs in various tissues or cells by matrix-assisted laser desorption/ionization (MALDI) is the preparation of a homogeneous layer of matrix crystals on top of the tissue or cells of interest without perturbing their spatial localization. As described by Hankin et al. and Yoo et al. [5,6], matrix deposition by sublimation is an ideal technique to obtain a homogeneous layer of matrix crystals. The deposition of matrix and the variation thereof has a large effect on signal intensities and background, and, for this reason, matrix deposition should be performed in an optimal way.

In this report we describe a MALDI-MS imaging technique specifically designed for the relative quantification of small molecules in cells and tissue. We used an in-house developed sublimation device for matrix deposition on top of the cells or tissues of interest. The matrix layer was subsequently recrystallized with water vapor. The combination of matrix sublimation/deposition and recrystallization resulted in maximum reproducibility and sensitivity without perturbing the spatial localization of the compounds. Imaging was performed with high resolution mass spectrometry equipment (TOF and FTICR) to obtain the best selectivity and sensitivity. For testing of our developed approach, we used a model system of Mono Mac 6 cells cultured in the presence of HIV protease inhibitors that were cytocentrifuged on glass slides.

Experimental Section

Cell culture and cytocentrifugation

Mono Mac 6 cells were cultured in a medium (RPMI with 10% FBS) and divided over a 24 well plate in order to obtain in each well 2 mL of cells in medium with a concentration of 1 x 10^6 cells/mL. We cultured these cells for 24 hours in the presence of different concentrations (0, 0.1, 1, and 10 μM) of the HIV protease inhibitors saquinavir and nelfinavir which were kindly provided by F. Hoffmann-La Roche and Pfizer, respectively. After 24 hours the cells were transferred to an Eppendorf tube, and centrifuged in a cooled centrifuge 4 ˚C for five minutes at 500 x *g*. Subsequently, the supernatant was removed and the cells were resuspended into 1 mL ice-cold PBS and centrifuged again. This wash step was repeated three times. The PBS from each wash step was stored at -20 ˚C for mass spectrometry analyses. After the last wash step the cells were counted and resuspended in PBS to obtain a final concentration of 1 x 10^6 cells/mL. Two hundred microliters of each cell suspension was cytocentrifuged onto a conductive ITO (indium tin oxide) coated glass slide (Bruker Daltonics, Bremen, Germany). In addition, one million cells of each sample were stored at -20 ˚C as a dried pellet for subsequent quantitative mass spectrometry analyses.

Sublimation

Five milliliters of a solution of 10 mg/mL 2,5-dihydroxybenzoic acid (DHB; Bruker Daltonics, Bremen, Germany) in acetone was pipetted onto the matrix table of the sublimation/deposition device which is then completely covered by the matrix solution. The temperature of the matrix table is increased to 50 ˚C to speed up evaporation without boiling. After the acetone is vaporized, small DHB crystals were observed over the complete matrix table. Next the ITO glass slides were mounted to the sample plate and the sublimation/deposition device is closed. The distance between the matrix table and sample plate was set at 5 cm, and the temperature of the sample plate is set at 4 ˚C. Vacuum was applied to the device, and, after the vacuum has reached 1 x 10^{-2} mbar, the matrix table was further heated to 120 ˚C. After approximately 10 minutes at 120 ˚C all matrix crystal were disappeared from the matrix table and a homogeneous layer of matrix can be observed on the ITO glass slides. Subsequently, the heating of the table was turned off, and the device was vented to atmospheric pressure. The ITO glass slides are removed from the device after which water vapor produced by a humidifier (Fakir, Vaihingen, Germany) was used to cover the glass slides with a film of small water droplets allowing recrystallization. The glass slides were then dried at ambient conditions and placed in a target holder (Bruker Daltonics, Bremen, Germany) compatible with the mass spectrometer.

Mass spectrometry equipment

An Ultraflex-III (Bruker Daltonics, Bremen, Germany) mass spectrometer was used for imaging of the glass slides. The mass spectrometer was controlled by FlexControl 3.0 and FlexImaging 2.0 software (Bruker Daltonics, Bremen, Germany). Selected regions of the slides are measured with a raster size varying from 500-200 µm. The results were visualized and analyzed using FlexImaging 2.0. For high resolution measurements, selected areas were measured with a MALDI-FTICR mass spectrometer (Apex IV Qe 9.4 T equipped with a combi-source, Bruker Daltonics, USA). For each scan, ions generated by 10 laser shots were accumulated in the storage hexapole. For each spectrum, 50 scans were summed to obtain one mass spectrum. MALDI-FTICR MS spectra were analyzed with the DataAnalysis software package (Bruker Daltonics, USA, version 3.4 build 184).

MALDI triple quadrupole analyses

The wash fluids and the pellets of all the samples were analyzed and measured with a MALDI-triple quadrupole mass spectrometer (FlashQuant, Applied Biosystems/MDS SCIEX, Toronto, Canada) to determine the concentration of saquinavir and nelfinavir in the samples. Sample preparation and analyses was performed as described previously [7].

Results and Discussion

The in-house built sublimation/deposition device is shown in Figure 1. A key consideration in its design was that the sublimation/deposition experiment should be performed under well-defined conditions. Thus, the temperature of the matrix table and sample plate can be precisely controlled. In addition, the pressure in the device can be monitored in such a way that the sublimation/deposition process can be started at a fixed pressure. Also, the distance between the matrix plate and sample plate can be adjusted, see Figure 2. The device can be used for matrix sublimation/deposition of complete 96-well format target plates or of up to 5 microscopic glass slides in one run.

The sublimation/deposition process was optimized with respect to temperature, amount of matrix and distance between target plate and matrix table. For DHB, the effect of temperature on the sublimation process was minimal; a minimum temperature of 110 ˚C was necessary for sublimation, and reproducible matrix deposition occurred between 120 ˚C and 150 ˚C (maximum tested temperature). The temperature of the sample plate and the distance between sample plate and matrix table had only an effect on the amount of matrix deposited on the wall and on other parts of the sublimation/deposition device, but not on the amount deposited on the sample plate. The lowest amount of a-specific sublimation/deposition (deposition to glass cylinder and other parts of the device) was observed when using a distance of 5 cm between matrix table and sample

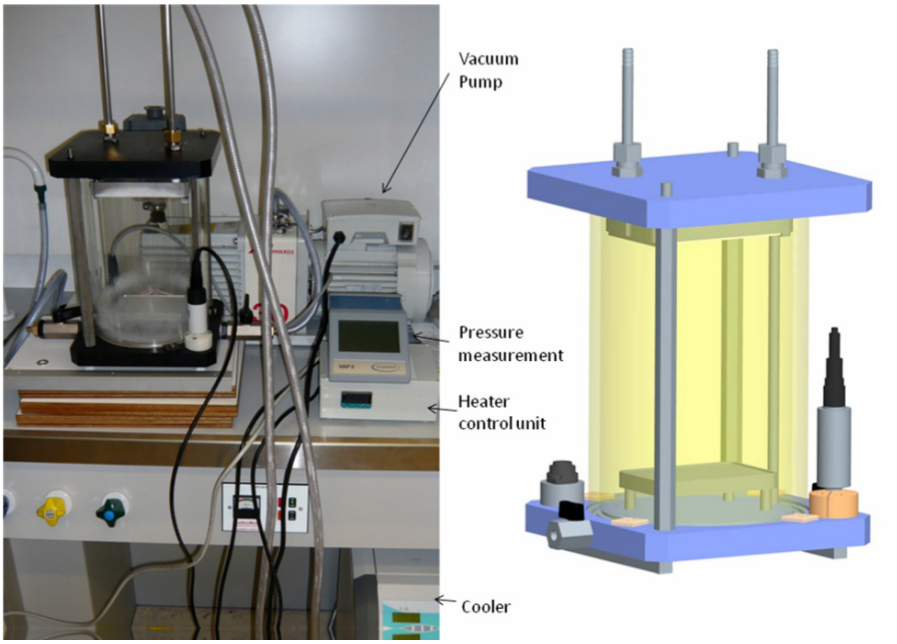

Figure 1. Photograph and schematic drawing of sublimation deposition system.

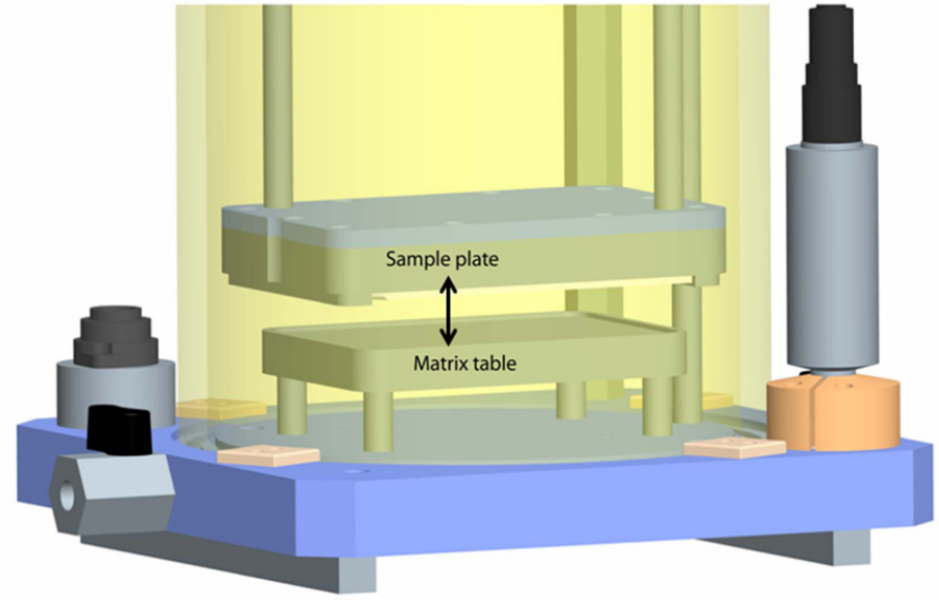

Figure 2. Close up of the sample and matrix table of the sublimation device. The distance between both plates can be varied.

plate at a temperature of the sample plate of 4 ˚C. Homogeneous application of the matrix on the matrix plate appears to be crucial to obtain a homogenous deposited layer on the glass slide; an inhomogeneous layer of matrix on the matrix table resulted in variations in the thickness of matrix layer on the glass slide. The best way to apply the matrix was to pipette a solution of the matrix in acetone on the matrix table and subsequent evaporation of the acetone at ambient or slightly increased temperatures of maximal 50 ˚C. Using MALDI-TOF MS, we found that maximum signal intensities with minimum laser power were obtained when a total amount of 10 mg DHB was deposited on the target slides. A photo of a glass slide and microscopic enlargement of the DHB crystals are shown in Figure 3.

First, we spotted 150 fmol and 500 fmol of HIV protease inhibitors saquinavir and nelfinavir onto an ITO glass slide, and matrix was subsequently deposited onto these slides using the optimized matrix sublimation/deposition protocol described above. However, this resulted in very weak signals for both protease inhibitors (not shown). The low signal intensities are probably due to poor and inhomogeneous co-crystallization of analyte and matrix. Recrystallization of the matrix resulted in the incorporation of the analyte molecule within the crystals of the matrix. Applying a droplet of water for recrystallization of the matrix on the position at the glass slide where the protease inhibitors were spotted did not compromise the homogeneity of the matrix layer. This recrystallization step resulted in increased signal intensities. However, recrystallization

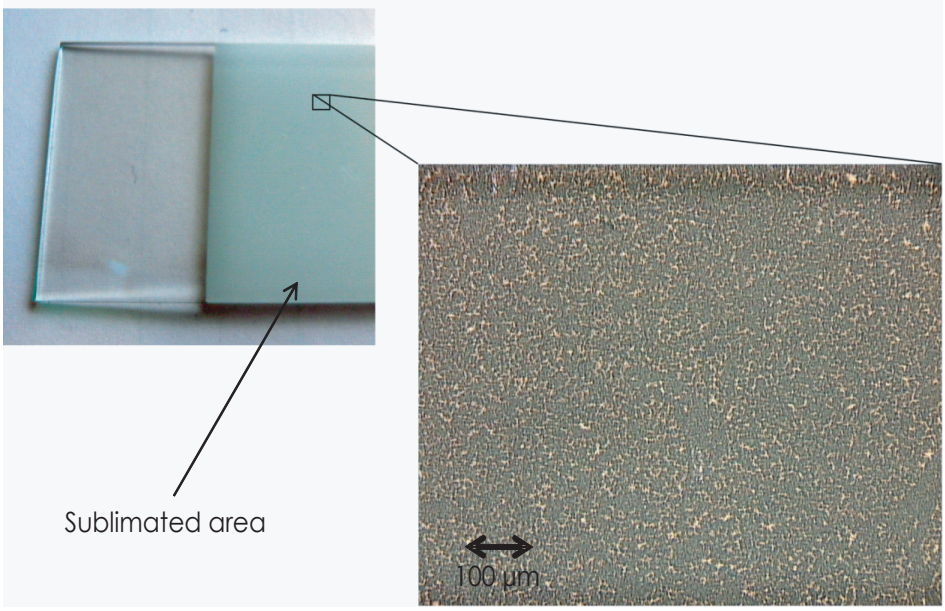

Figure 3. Right panel a photo of a sublimated ITO object glass. In the left panel a microscopic photo of the deposited matrix crystals on the ITO glass is displayed.

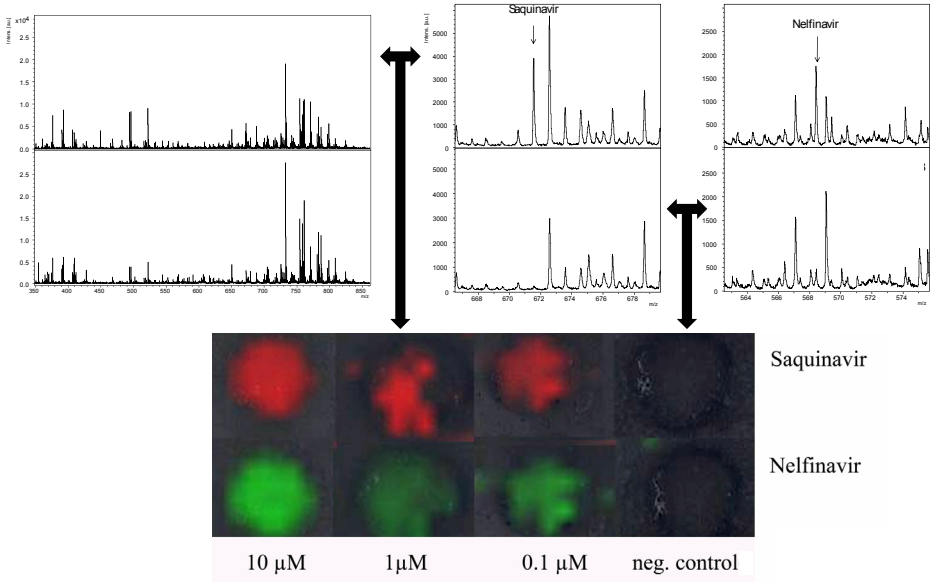

Figure 4. Left panel shows the complete mass spectra of two cytocentrifuged slides of cells cultured with 1 µM protease saquinavir and nelfinavir (upper) and of untreated cells (lower). The two right panels show close-up section of these two mass spectra for the masses of saquinavir and nelfinavir. The lower panel shows a scanned image of the cyto centrifuged cells overlayed with an intensity image of the masses of saquinavir (red) and nelfinavir (green).

as described above resulted in partial loss of the spatial information, as the signals of the analytes were observed at positions where they were not originally spotted. Recrystallization using water vapor produced by a humidifier resulted in highly increased signal intensities but without observable loss in spatial localization of the analytes as shown in Figure 4.

In a subsequent experiment, Mono Mac 6 cells were cultured in the presence of 0.1, 1 and 10 µM saquinavir and nelfinavir. These cells were cytocentrifuged onto ITO glass slides and matrix was applied using the above described protocol. MALDI–TOF MS measurements of the glass slides showed that the expected masses of both HIV protease inhibitors (*m/z* 671.4 saquinavir and *m/z* 568.3 nelfinavir) were observed at the locations were the cells were cytocentrifuged (Figure 4). No signals of saquinavir or nelfinavir were observed outside the regions were cells are present indicating co-localization of the cells and the protease inhibitors.

A difference in signal intensity was observed between the different concentrations of saquinavir and nelfinavir as indicated by the color intensity in Figure 4, showing that relative quantification is possible. Cell-specific signals were also observed in addition to the signals of the protease inhibitors (Figure 4). The signal of nelfinavir probably

overlaps with a background signal of the cells, because we also observe a peak at this mass in the negative control slide. These background signals make it almost impossible to determine whether nelfinavir is present or not in a sample. Therefore, we performed high resolution MALDI-FTICR measurements on the same slides, to confirm the presence of both protease inhibitors and to ascertain that the signal observed at *m/z* 568 in the negative control slide is indeed a background signal. As can be observed from Figure 5, the MALDI-FTICR spectra contains no chemical noise and this, in combination with the high resolution and mass accuracy of the FTICR measurements, makes it easier to interpret the results.

From the matching accurate masses for both saquinavir (*m/z* 671.3915, mass deviation 0.1 ppm) and nelfinavir (*m/z* 568.3198, mass deviation 0.9 ppm) we conclude that both compounds are present in the treated cells. In addition, the mass spectra show that the signal present in the negative control slide is indeed a background signal, because the accurate mass (*m/z* 568.3395) of the noise signal differs from the mass of nelfinavir (*m/z* 568.3198). As can be seen in Figure 5C the protease inhibitors are co-localized with the treated cells, because in the spectrum taken just outside the region where cells were cytocentrifuged no signal for any of the protease inhibitors can be observed.

The intracellular levels of nelfinavir and saquinavir were determined by MALDI-triple quadruple mass spectrometry. The intracellular concentrations in 2 x 10^5 cells were 1.5,

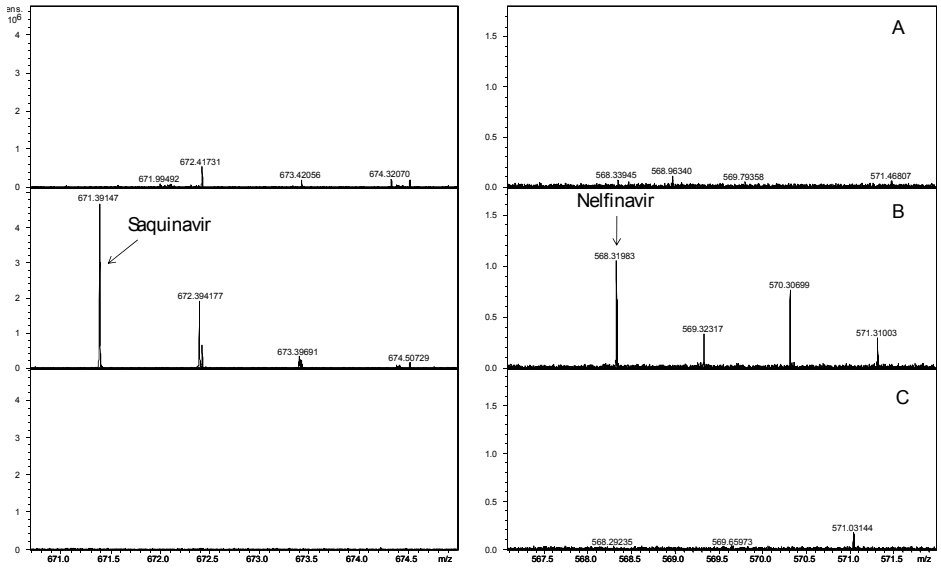

Figure 5. Zoomed in regions of high resolution MALDI-FTICR mass spectra of the cyto centrifuged slide of Mono Mac 6 cells (a) and of Mono Mac 6 cells cultured with 1 µM saquinavir and nelfinavir (b). Panel c display the spectrum of the slide with Mono Mac 6 cells treated with 1 µM saquinavir and nelfinavir this spectrum is acquired just outside the region were the cells are cytocentrifuged.

12.4 and 96 pmol for nelfinavir and 1.3, 12.4 and 82 pmol for saquinavir in the cells incubated with 0.1 µM, 1 µM and 10 µM protease inhibitor, respectively. We also measured the concentration of the HIV protease inhibitors in the final wash fluid step to ensure that the influence of remaining wash fluid is limited on the determined intracellular concentration. We estimate that 10 µL of wash fluid remained present on the cell pellet after the final wash step. In 10 µL of the wash fluid the amount of both protease inhibitors was lower than 10% of the quantity measured intracellularly. This results in a maximum contribution of 10% to the intracellular determined concentrations.

For a fair comparison of intracellular concentrations between various cell types, the concentration has to be expressed per cell volume instead of per number of cells to compensate for differences in cell size. Mono Mac 6 cells are larger (20 µm) than PBMCs (10 µm) on which most intracellular clinical assays are performed. This results in an eight times larger intracellular volume. The average volume of one PBMC cell is estimated at 0.4 pL [8] and so for a Mono Mac 6 cell this would results in a volume of approximately 3.2 pL. With our imaging assay, the lowest absolute amount per 2 x 10^5 cells that was still detectable is < 1.5 pmol for both protease inhibitors. This would imply an intracellular concentration of 2.3 nmol/mL of intracellular volume. The total concentration of most protease inhibitors in PBMC of HIV patients is in the range of 2-20 nmol [8-12] per mL of intracellular volume. This concentration range is within the sensitivity of our imaging technique showing that it is sufficiently sensitive to measure clinically relevant concentrations of these two protease inhibitors in cytocentrifuged samples. In addition, this technique can also be applied for imaging of tissue for this type of drugs. The quantitative aspect of this technique will be further investigated. The technique described can be exploited in the future to measure drugs and metabolites in specific populations of leukocytes or tissue obtained from patients treated with antiretroviral drugs.

Acknowledgements

This study was financially supported by Top Institute Pharma (project T4-212). The consortium of Project T4-212 consists of the Departments of Neurology and Virology of the Erasmus MC (Rotterdam), the Departments of Pediatrics and Clinical Pharmacy of the UMC St. Radboud (Nijmegen), TNO-Quality of Life (Zeist), and GlaxoSmithKline (Zeist) (all from The Netherlands). Antiretroviral drugs were kindly provided by Pfizer, and F. Hoffmann-La Roche. J.J.A.v.K. is supported by a grant from Aids Fonds, the Netherlands (project 2004051). The authors would like to thank A. Brouwer and co-workers from the Experimental Medical Instrumentation Department, Erasmus MC (Rotterdam) for assistance during the development process of the sublimation/deposition device and for building the device.

References

1. Reyzer ML, Caprioli RM. MALDI-MS-based imaging of small molecules and proteins in tissues. Curr Opin Chem Biol 2007;11(1):29-35.
2. McDonnell LA, Piersma SR, MaartenAltelaar AF, et al. Subcellular imaging mass spectrometry of brain tissue. J Mass Spectrom 2005;40(2):160-8.
3. Taban IM, Altelaar AF, van der Burgt YE, et al. Imaging of peptides in the rat brain using MALDI-FTICR mass spectrometry. J Am Soc Mass Spectrom 2007;18(1):145-51.
4. Hsieh Y, Chen J, Korfmacher WA. Mapping pharmaceuticals in tissues using MALDI imaging mass spectrometry. J Pharmacol Toxicol Methods 2007;55(2):193-200.
5. Hankin JA, Barkley RM, Murphy RC. Sublimation as a method of matrix application for mass spectrometric imaging. J Am Soc Mass Spectrom 2007;18(9):1646-52.
6. Kim SH, Shin CM, Yoo JS. First application of thermal vapor deposition method to matrix-assisted laser desorption ionization mass spectrometry: Determination of molecular mass of bis(p-methyl benzylidene) sorbitol. Rapid Communications in Mass Spectrometry 1998;12(11): 701 - 4.
7. Van Kampen JJ, Burgers PC, Gruters RA, et al. Rapid quantitative analysis of antiretroviral drugs in lysates of peripheral blood mononuclear cells using MALDI-triple quadrupole mass spectrometry. Anal Chem 2008 in press.
8. Crommentuyn KM, Mulder JW, Mairuhu AT, et al. The plasma and intracellular steady-state pharmacokinetics of lopinavir/ritonavir in HIV-1-infected patients. Antivir Ther 2004;9(5):779-85.
9. Ford J, Boffito M, Maitland D, et al. Influence of atazanavir 200 mg on the intracellular and plasma pharmacokinetics of saquinavir and ritonavir 1600/100 mg administered once daily in HIV-infected patients. J Antimicrob Chemother 2006;58(5):1009-16.
10. Ford J, Boffito M, Wildfire A, et al. Intracellular and plasma pharmacokinetics of saquinavir-ritonavir, administered at 1,600/100 milligrams once daily in human immunodeficiency virus-infected patients. Antimicrob Agents Chemother 2004;48(7):2388-93.
11. Ford J, Cornforth D, Hoggard PG, et al. Intracellular and plasma pharmacokinetics of nelfinavir and M8 in HIV-infected patients: relationship with P-glycoprotein expression. Antivir Ther 2004; 9(1):77-84.
12. Hennessy M, Clarke S, Spiers JP, et al. Intracellular accumulation of nelfinavir and its relationship to P-glycoprotein expression and function in HIV-infected patients. Antivir Ther 2004;9(1):115-22.

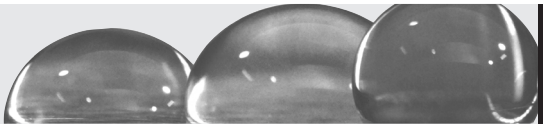

Chapter 8

Quantitative analysis of HIV-1 protease inhibitors in cell lysates using MALDI-FTICR mass spectrometry

Jeroen J.A. van Kampen, Peter C. Burgers,
Ronald de Groot, Albert D.M.E. Osterhaus, Mariska L. Reedijk,
Esther J. Verschuren, Rob A. Gruters, Theo M. Luider

Analytical Chemistry 2008, 80, 3751–3756

Abstract

In this report we explore the use of MALDI-FTICR mass spectrometry for the quantitative analysis of five HIV-1 protease inhibitors in cell lysates. 2,5-Dihydroxybenzoic acid (DHB) was used as the matrix. From a quantitative perspective, DHB is usually a poor matrix due to its poor shot-to-shot and poor spot-to-spot reproducibilities. We found that the quantitative precisions improved significantly when DMSO (dimethylsulfoxide) was added to the matrix solution. For lopinavir and ritonavir, currently the most frequently prescribed HIV-1 protease inhibitors, the signal-to-noise ratios improved significantly when potassium iodide was added to the matrix solution. The mean quantitative precisions, expressed as % relative standard deviation, were 6.4% for saquinavir, 7.3% for lopinavir, 8.5% for ritonavir, 11.1% for indinavir, and 7.2% for nelfinavir. The mean quantitative accuracies, expressed as % deviation, were 4.5% for saquinavir, 6.0% for lopinavir, 5.9% for ritonavir, 6.6% for indinavir, and 8.0% for nelfinavir. The concentrations measured for the individual quality control samples were all within 85–117% of the theoretical concentrations. The lower limits of quantification in cell lysates were 4 fmol/µL for saquinavir, 16 fmol/µL for lopinavir, 31 fmol/µL for ritonavir, and 100 fmol/µL for indinavir and nelfinavir. The mean mass accuracies for the protease inhibitors were ≤ 0.28 ppm using external calibration. Our results show that MALDI-FTICR mass spectrometry can be successfully used for precise, accurate, and selective quantitative analyses of HIV-1 protease inhibitors in cell lysates. In addition, the lower limits of quantification obtained allow clinical applications of the technique.

Introduction

Quantitative drug analysis using matrix-assisted laser desorption/ionization (MALDI) mass spectrometry is normally hampered by poor reproducibility of the signal intensities and by the presence of matrix-derived signals (leading to the so-called chemical noise) in the low mass range, i.e., below 1,000 Da. As a consequence, electrospray ionization (ESI), in particular in combination with a triple quadrupole mass analyzer, is normally preferred. When operated in the selected reaction monitoring mode (SRM), the triple quadrupole mass analyzer selectively measures unique fragments of the analyte(s) and internal standard(s). The ESI ion source can be coupled to a high pressure liquid chromatograph (HPLC), which further increases the assay's selectivity with concomitant decrease of ion suppression effects.

However, MALDI offers certain advantages over ESI for the quantitative analysis of drugs as well as for the analysis of other compounds; it is capable of a higher sample throughput [1], samples can be conveniently stored on the target plate for future reanalysis [2], and MALDI is less susceptible to ion suppression [3].

Various approaches have been developed to improve the performance of MALDI for the quantitative analysis of drugs, which aim to eliminate the disadvantages normally associated with MALDI, viz., the poor reproducibility of signal intensities and the presence of matrix-derived chemical noise [4]. Thus, high molecular weight matrices [5-9], additives [10], and matrix-less target plates [11,12] have been used to decrease and even to eliminate the matrix-derived chemical noise in the low mass range. The reproducibility can be significantly increased by using ionic liquid matrixes [13], internal standards, sophisticated sample/matrix spotting devices [14], and prestructured target plates [15], or by averaging out many spectra of a single sample. These approaches have led to the successful development of various quantitative drug assays using MALDI-TOF [8,9,16,17], MALDI-q-TOF [18,19], and MALDI-triple quadrupole [1,18,20,21] mass spectrometry.

Currently, no assays have been described which use MALDI-FTICR for the quantitative analysis of drugs. The advantage of MALDI-FTICR over other types of MALDI mass spectrometers results from its high resolving power and mass accuracy, which significantly increase the selectivity of the assay; in particular this will be the case when the molecular ions of the analyte and internal standard are used for quantitative analysis, i.e., from a full mass spectrum (MS mode).

In this study, we assess the quantitative performance of MALDI-FTICR mass spectrometry for the analysis of HIV-1 protease inhibitors in lysates of peripheral blood mononuclear cells (PBMCs).

Experimental Section

Chemicals

Lopinavir (LPV; $C_{37}H_{48}N_4O_5$; monoisotopic molecular mass 628.36247 Da) and ritonavir (RTV; $C_{37}H_{48}N_6O_5S_2$; monoisotopic molecular mass 720.31276 Da) were kindly donated by Abbott Laboratories (Illinois). Saquinavir (SQV; $C_{38}H_{50}N_6O_5$; monoisotopic molecular mass 670.38427 Da) was kindly donated by F. Hoffmann-La Roche (Basel, Switzerland). Nelfinavir (NFV; $C_{32}H_{45}N_3O_4S$; monoisotopic molecular mass 567.31308 Da) was kindly donated by Pfizer (Groton, CT), and indinavir (IDV; $C_{36}H_{47}N_5O_4$; monoisotopic molecular mass 613.36281 Da) was kindly donated by Merck (Rahway, NJ). Potassium iodide was obtained from Sigma-Aldrich. 2,5-Dihydroxybenzoic acid (DHB) was obtained from Bruker Daltonics (Germany).

Peripheral blood mononuclear cells

Peripheral blood mononuclear cells (PBMCs) were obtained from a buffy coat (Sanquin, Rotterdam, The Netherlands) using a standard Ficoll density gradient. The PBMCs were extracted overnight in methanol at 5°C. The next day, the PBMC lysates were collected, water was added to the samples until the water-to-methanol ratio was 3:1, and the PBMC lysates were loaded onto a 96-well solid-phase extraction plate (Oasis HLB µelution plate, Waters). Subsequently, the samples were washed twice with 200 µL of methanol/water (1:3 v/v). Next, the samples were eluted from the column with 100 µL of methanol. The samples were dried in a SpeedVac (Savant) and stored at -80°C until the day of analysis.

Mass spectrometry

To study the effect of various DHB preparations on the signal intensities and % CV of the analyte-to-internal standard ratios, a mixture of five pure HIV protease inhibitors was analyzed with four different DHB preparations: DHB = 10 mg/mL DHB in MeCN/water (1/1); DHB + DMSO = 10 mg/mL DHB in MeCN/water/DMSO (9/9/2); DHB + KI = 10 mg/mL DHB + 10 mM KI in MeCN/water (1/1); DHB + KI + DMSO = 10 mg/mL DHB + 10 mM KI in MeCN/water/DMSO (9/9/2). For each DHB preparation, four technical replicates, i.e., four spots on the target plate, were measured (1 µL per spot).

For quantitative analysis of HIV protease inhibitors in cell lysates, the samples were prepared by reconstituting the dried PBMC lysates in 10 µL of water/MeCN/DMSO (9/9/2, v/v/v) containing 10 mg/mL DHB, 10 mM KI, analyte at various concentrations, and 1 pmol/µL internal standard. Technical replicates of each calibrator were spotted on different positions on a 400 µm AnchorChip target plate (Bruker Daltonics, Germany) (1 µL per spot). Drying of the samples was assisted with a heat blower.

Samples were measured on an APEX IV Qe 9.4 T FTICR mass spectrometer (Bruker Daltonics) equipped with the first version of the vacuum Combisource and a 20 Hz nitrogen laser with irradiation area of ~200 µm [22]. Xmass version 7.0.8 was used to operate the

mass spectrometer, and DataAnalysis version 3.4 was used for data analysis (both from Bruker Daltonics). A multishot accumulation was used as recommended by O'Connor et al., Mize et al., and Moyer et al [23-25]. Ions produced by 10 laser shots were accumulated in the storage hexapole, transferred to the FTICR cell, and scanned for 0.78 s (TD size 512 Kb). Fifty scans were summed for each mass spectrum. The acquisition mass range was *m/z* 500-1,000. The mass spectra were subsequently apodized and zerofilled twice. An external mass calibration was applied using a quadratic equation.

Quantitative analysis of HIV protease inhibitors in cell lysates

Two data sets (A and B) were used to assess the quantitative performance of the MALDI-FTICR assay. Data set A was used to construct the calibration curve while data set B was used as quality controls and vice versa. For each sample in a data set, three spots on the target plate, i.e., three technical replicates, were measured. The quantitative precisions were obtained by calculating the % relative standard deviation of the analyte-to-internal standard ratio of the three replicate analyses of each sample. The mean analyte-to-internal standard ratios of the three replicate analyses were used to construct the calibration curve (calibrators) or to check the quantitative accuracies (quality controls). The mean analyte-to-internal standard ratios and analyte concentrations were log 10-transformed, and a linear unweighed curve was fitted through the data points.

Results and Discussion

Choice of matrix

Small molecule analysis by MALDI mass spectrometry is normally hampered by the presence of matrix-derived chemical noise in the low mass range, i.e., below 1,000 Da [26], the bane of any MALDI practitioner. The use of a high molecular weight matrix is one way to overcome this phenomenon [5]. We have recently developed a quantitative assay for HIV protease inhibitors on a MALDI-TOF mass spectrometer using the high molecular weight matrix meso-tetrakis(pentafluorophenyl)porphyrin (F20TPP) [8,9]. The molecular weight of F20TPP is 974.6 Da, and so the only matrix-derived peaks which can be observed in the low mass range result from dissociation of the matrix or from matrix impurities. Thus, using a TOF analyzer, we observed, as expected, only a few peaks in the low mass range, making F20TPP eminently suitable as a matrix in TOF analyses. We also attempted to use the F20TPP matrix on our MALDI-FTICR mass spectrometer. In contrast to our previous MALDI-TOF experiments, extensive fragmentation of the F20TPP matrix was observed in our FTICR experiments which resulted in matrix-derived interfering signals in the low mass range. Long-lived metastable decay of ions formed in the MALDI source has been extensively reported in the literature [27-34]. The metastable fragmentations in

FTICR are the result of the relatively long ion lifetime (1 s) of the ions prior to detection in FTICR, compared to the much shorter lifetimes associated with more conventional MS techniques, such as TOF (10^{-4} s), and thus they are a direct consequence of RRKM theory [35]. For example, ions with a rate constant (k) of 10^3 s^{-1} fragment on average in 10^{-3} seconds [36]. These ions formed in the MALDI process could thus easily survive the TOF time frame but would generate extensive fragmentation in FTICR [29]. In the same vein, non-covalent matrix adduct ions are expected to be metastable on the FTICR time frame, and dissociation is thus expected. This indeed appears to be the case; using our FTICR instrument, the matrix DHB hardly shows any chemical noise. Therefore, DHB was tested as a matrix for the FTICR analysis of the HIV-1 protease inhibitors.

Matrix preparation

We evaluated four different matrix solutions: DHB only, DHB with DMSO, DHB with KI, and DHB with both DMSO and KI, see Table 1. As can be seen from this table, the highest S/N ratios were obtained for the protonated forms of nelfinavir, indinavir, and saquinavir, i.e., when DHB was used without the addition of KI. In contrast, the highest S/N ratios for lopinavir and ritonavir were observed when DHB was used with the addition of KI. DHB crystallizes in an inhomogeneous way when it is spotted according to the widely used dried droplet protocol (at ambient temperature). Because of this inhomogeneous crystallization, one needs to search for so-called sweet spots in the sample/matrix crystals. In general, better quantitative precisions are obtained when the sample/matrix crystals have a homogeneous appearance. Therefore, we added DMSO to the matrix solution. With the use of DMSO, the samples dry at a much slower rate and dense homogeneous DHB crystals are formed, even when dried using a heat blower. As shown in Table 2, the quantitative precisions improved significantly when DMSO was added to the DHB solution. In addition, as shown in Table 1, the S/N of the potassiated HIV-1 protease inhibitors also improved by adding DMSO to the matrix solution.

Table 1. Mean signal-to-noise ratios for the simultaneous analysis of five HIV-1 protease inhibitors with DHB[a]

	amount (femtomole)	DHB $[analyte + H]^+$	DHB + DMSO $[analyte + H]^+$	DHB + KI $[analyte + K]^+$	DHB + KI + DMSO $[analyte + K]^+$
nelfinavir	1000	5179	2151	552	745
indinavir	1000	1363	1820	212	627
lopinavir	1000	284	149	1680	2283
saquinavir	250	5476	5924	1125	1597
ritonavir	1000	479	632	845	2933

[a] mixture of five pure HIV-1 protease inhibitors was analyzed using four different DHB preparations (see Experimental Section). The concentration per spot on the target plate was 1 pmol for nelfinavir, indinavir, lopinavir, and ritonavir and 250 fmol for saquinavir. Four technical replicates, i.e., four different spots on the target plate, were measured for each sample.

Table 2. The effect of DMSO and potassium iodide on the quantitative precisions (% CV) of five HIV protease inhibitors[a]

			Internal standard									
			nelfinavir		indinavir		lopinavir		saquinavir		ritonavir	
			DMSO–	DMSO+	DMSO–	DMSO+	DMSO–	DMSO+	DMSO–	DMSO+	DMSO–	DMSO+
analyte	NFV	K –			11.1	1.8	26.1	11.3	21.8	6.0	16.2	8.5
		K +			15.7	1.9	31.1	3.4	4.8	6.3	17.1	5.0
	IDV	K –	10.8	1.8			35.8	12.8	28.7	5.5	14.5	9.0
		K +	16.3	1.9			47.0	3.3	18.9	5.4	8.0	4.5
	LPV	K –	22.0	10.3	30.9	11.5			16.6	10.7	29.5	7.4
		K +	31.6	3.4	45.8	3.2			33.1	3.3	47.3	2.9
	SQV	K –	20.0	5.7	23.5	5.4	15.0	11.7			17.6	5.3
		K +	4.9	6.4	17.4	5.3	29.2	3.4			17.5	3.3
	RTV	K –	15.9	8.6	16.7	8.9	27.9	7.3	19.9	5.1		
		K +	18.1	5.0	7.9	4.4	49.1	2.9	20.4	3.2		

[a] A mixture of five pure HIV-1 protease inhibitors was analyzed using four different DHB preparations (see Experimental Section). One protease inhibitor was chosen as the internal standard, and the remaining four protease inhibitors served as analytes. Subsequently, the analyte-to-internal standard ratios were calculated. The signal-to-noise ratios (S/N) for the potassiated monoisotopic peaks were used when DHB was used with the addition of potassium iodide. The S/N for the protonated monoisotopic peaks were used when DHB was used without the addition of potassium iodide. This procedure was repeated until each protease inhibitor had served as the internal standard. Reported values in the tables are the % relative standard deviations (RSD) for the analyte-to-internal standard ratios. The concentration per spot on the target plate was 1 pmol for nelfinavir, indinavir, lopinavir, and ritonavir and 250 fmol for saquinavir. Four technical replicates were measured of each sample.

Quantitative analysis of HIV protease inhibitors in cell lysates

Our goal was to develop one assay for the quantitative analysis of five HIV-1 protease inhibitors. As shown above, the highest S/N values were obtained for the protonated forms of nelfinavir, indinavir, and saquinavir, while lopinavir and ritonavir were best detected as potassiated ions. Thus a trade-off was needed in the preparation of the DHB solution, i.e., preparation with or without potassium iodide. Currently, Kaletra is the most widely used HIV-1 protease inhibitor. Kaletra is a preparation of lopinavir together with ritonavir which serves as a pharmacokinetic booster. Because of the clinical importance of lopinavir and ritonavir, we added potassium iodide to the matrix solution for the quantitative analysis of HIV-1 protease inhibitors in lysates of peripheral blood mononuclear cells. In addition, DMSO was added to the matrix solution to enhance the quantitative precisions.

Stable isotope labelled internal standards would serve as the best internal standards for quantitative MALDI experiments. However, these were not commercially available for the tested HIV-1 protease inhibitors. Therefore, we chose to use nelfinavir as the internal standard for the quantitative analysis of indinavir, lopinavir, saquinavir, and ritonavir. For the quantitative analysis of nelfinavir, we used indinavir as the internal standard. Figure 1 shows the mass spectrum of lopinavir and nelfinavir (internal standard) in a lysate of 1×10^6 PBMC (125 fmol lopinavir and 1 pmol nelfinavir per spot on the target plate). It can be seen from this figure that the ionization efficiency of lopinavir is approximately a factor of 4 larger than that for nelfinavir. This factor remains constant over the entire concentration range, and accurate and precise quantitative analysis of the HIV protease inhibitors is thus possible using a chemical analogue as the internal standard.

Table 3 shows the quantitative performance of the MALDI-FTICR assay for the five HIV-1 protease inhibitors. The mean quantitative precisions, expressed as % relative standard deviation, were 6.4% for saquinavir, 7.3% for lopinavir, 8.5% for ritonavir, 11.1% for indinavir, and 7.2% for nelfinavir. The mean analyte-to-internal standard ratios of the analysis of three technical replicates were used to calculate the drug concentrations in the samples. The mean quantitative accuracies for the quality control (QC) samples, expressed as % deviation from the theoretical concentration, were 4.5% for saquinavir, 6.0% for lopinavir, 5.9% for ritonavir, 6.6% for indinavir, and 8.0% for nelfinavir. The measured drug concentrations for the individual quality control samples were all within 85–117% of the theoretical concentrations. The above shows that MALDI-FTICR can be used for accurate quantitative analysis of HIV-1 protease inhibitors in cell lysates.

Selectivity

FTICR mass spectrometry provides currently the highest mass accuracy and resolution among mass analyzers. Higher mass accuracy and resolution result in a better selectivity of the assay. We typically obtain resolutions of 100,000 (FWHM). The mean mass errors

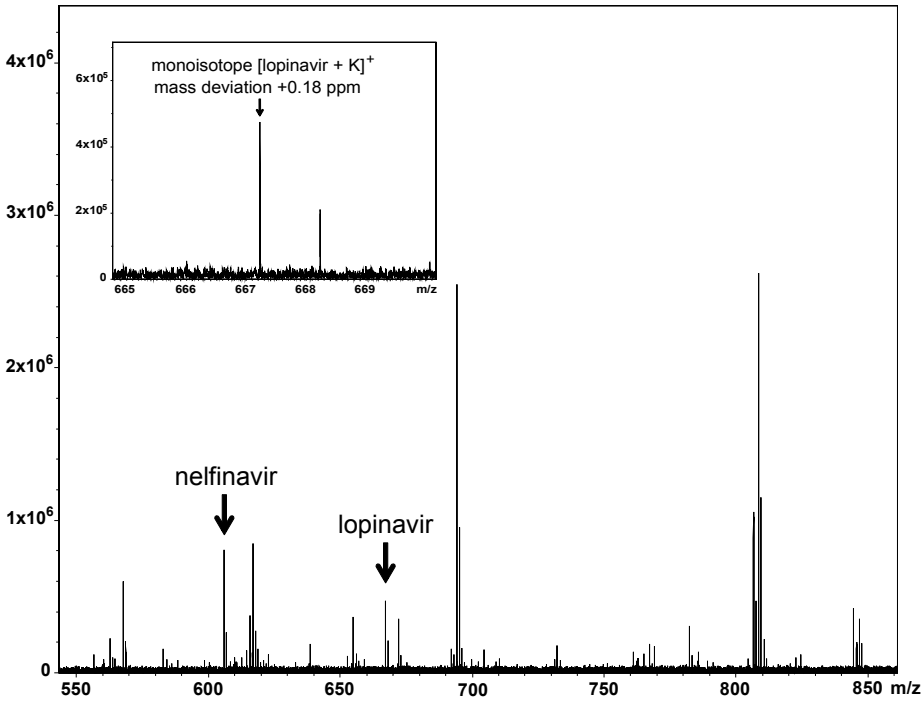

Figure 1. Analysis of lopinavir in a lysate of PBMC. Lopinavir and nelfinavir were spiked in a lysate of 1 x 10^6 PBMC. The monoisotopic peak of potassiated lopinavir had a S/N of 66 (125 fmol per spot on the target plate). The monoisotopic peak of nelfinavir had a S/N 119 (1 pmol per spot on the target plate). The inset shows a magnification of the lopinavir signal. The measured mass of the monoisotopic peak of potassiated lopinavir was 667.325 75 Da. The theoretical mass is 667.325 63 Da corresponding to a mass deviation of +0.18 ppm. An external mass calibration was used. The y-axis is in arbitrary units.

Table 3. The performance of MALDI-FTICR mass spectrometry to quantify five HIV-1 protease inhibitors in PBMC lysates[a]

	LLOQ (fmol)	ULOQ (fmol)	quantitative precision (% RSD)	quantitative accuracy (% dev)	mass deviation (ppm)
saquinavir	4	4096	6.4 (5.1)	4.5 (3.0)	- 0.05 (0.26)
lopinavir	16	2000	7.3 (4.2)	6.0 (5.2)	+ 0.11 (0.30)
ritonavir	31	2000	8.5 (3.8)	5.9 (3.6)	- 0.21 (0.46)
indinavir	100	6400	11.1 (4.7)	6.6 (4.2)	+ 0.07 (0.14)
nelfinavir	100	6400	7.2 (5.1)	8.0 (4.0)	- 0.28 (0.19)

[a] LLOQ = lower limit of quantification. ULOQ = upper limit of quantification. fmol = femtomole. % RSD = relative standard deviation of the mean analyte-to-IS ratio for each calibrator in %. % dev = mean absolute deviation of the measured concentration from the real concentration in %. ppm = mean deviation of the measured mass from the real mass in parts-per-million. The precisions and accuracies are based on three measurements of each calibrator of each sample set (total of two sample sets). The reported mass deviations are the mean mass accuracies for all measured samples of sample sets 1 and 2 combined. The mean standard deviations are reported between parentheses.

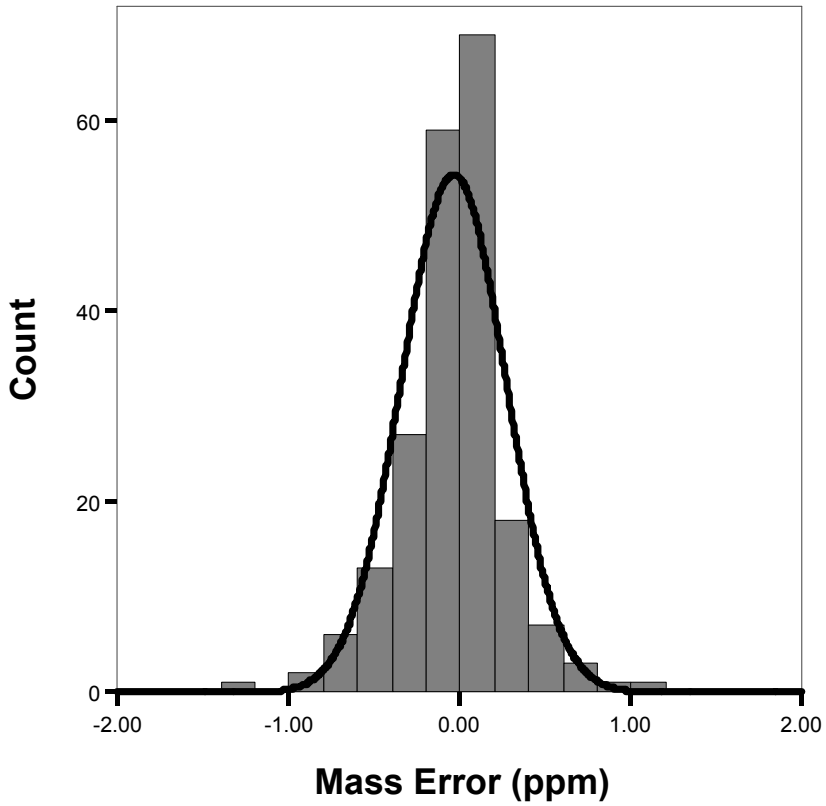

Figure 2. Histogram of mass errors. The histogram shows the mass errors in ppm for the five protease inhibitors (total of 208 measurements) using an external mass calibration. A quadratic mass calibration equation was used. The line shows the Gaussian distribution of the data.

for the HIV-1 protease inhibitors in the QC samples were -0.05 ppm for saquinavir, 0.11 ppm for lopinavir, -0.21 ppm for ritonavir, 0.07 ppm for indinavir, and -0.28 ppm for nelfinavir. Figure 2 shows the histogram of all mass errors for the HIV protease inhibitors in the QC samples. The average mass error for all measurements was -0.05 ppm, the standard deviation was 0.34 ppm, and the root-mean-square was 0.34 ppm. These mass errors were obtained using an external mass calibration. Internal calibration could result in even smaller mass errors.

Conclusions

We have shown that MALDI-FTICR can be used for precise and accurate quantitative analysis of HIV-1 protease inhibitors in PBMC lysates. This assay was developed for future studies on the intracellular pharmacokinetics of HIV protease inhibitors in PBMCs

obtained from HIV-infected adults and children receiving therapy. The lower limits of quantification needed for such studies are thus a direct consequence of the amount of material that can be obtained from these patients. One million PBMCs can be obtained from a blood sample of 1–2 mL, which is a suitable volume of blood to draw from HIV-1 infected adults and children. The lower limits of quantification (LLOQ) for HIV-1 protease inhibitors in PBMC lysates using the MALDI-FTICR assay were 4 fmol for saquinavir, 16 fmol for lopinavir, 31 fmol for ritonavir, and 100 fmol for indinavir and nelfinavir. These are however the "technical" LLOQs, i.e., the amount of drug in a single spot on the target plate. We dissolved the dried lysates of 1×10^6 PBMCs in 10 µL of solvent and subsequently deposited 1 µL of this solution on different spots on the target plate. The minimum amount of drug present in the dried lysates should thus be a factor of 10 higher in order for this assay to quantify the drugs. The "biological" LLOQs are thus 40 fmol for saquinavir, 160 fmol for lopinavir, 310 fmol for ritonavir, and 1 pmol for indinavir and nelfinavir per million PBMCs. The reported minimum intracellular concentrations (C_{min} or $C_{predose}$) of HIV-1 protease inhibitors in HIV-1 infected adults are 6.4 pmol/1×10^6 PBMCs for lopinavir [37], 850 fmol/1×10^6 PBMCs for ritonavir [37], 450 fmol/1×10^6 PBMCs for saquinavir [38], 87 fmol/1×10^6 PBMCs for indinavir [39] and 2.1 pmol/1×10^6 PBMCs for nelfinavir [40]. Except for indinavir, the MALDI-FTICR assay can thus be used for quantitative analysis of HIV-1 protease inhibitors in 1,000,000 PBMCs.

The LLOQs obtained by our MALDI-FTICR assay are comparable to those obtained using the MS-mode of a MALDI-TOF mass spectrometer [8,9]. The resolving power and mass accuracy of the MALDI-FTICR assay is superior compared to that of a MALDI-TOF. Thus, using the MS-mode, the MALDI-FTICR assay is more selective than the MALDI-TOF assay. In addition, we found that MALDI-FTICR has a larger dynamic range than MALDI-TOF [8,41]. Notari et al. used tandem mass spectrometry (MS/MS) on a MALDI-TOF/TOF for quantitative analysis of antiretroviral drugs in human plasma and obtained a LLOQ of 2.5 fmol/µL for lopinavir and ritonavir [19] To the best of our knowledge, three LC-MS/MS methods for quantitative analysis of antiretroviral drugs in PBMC have been described in detail [42-44]. Jemal et al. obtained a LLOQ of 5 fmol/1×10^6 PBMCs for atazanavir [43]. Rouzes et al. obtained a LLOQ of 3 pmol/3×10^6 PBMCs for lopinavir, 1 pmol/3×10^6 PBMCs for ritonavir, and 2 pmol/3×10^6 PBMCs for saquinavir [44]. Colombo et al. obtained LLOQ of 5 fmol for ritonavir, 6 fmol for lopinavir, 6 fmol for saquinavir, 7 fmol for indinavir, and 9 fmol for nelfinavir (minimum amount of quantifiable drug on column) [42]. Our LLOQs obtained for the HIV protease inhibitors in PBMC lysates using MALDI-FTICR are roughly comparable to those obtained by LC-MS/MS. The sample analysis time of the above-described LC-MS/MS methods range from 4 to 20 min. The measurement of one technical replicate takes 3 min using the MALDI-FTICR assay. In this study, we have measured three technical replicates of each sample; the analysis time for one sample is thus 9 min. This is much slower compared to MALDI-TOF and MALDI-QqQ measurements [1,8]. Sophisticated spot-

ting devices, such as electrospray sample deposition and inkjet printer technologies, may improve the quantitative precisions of the measurements.

Sample volumes typically used in MALDI mass spectrometry are in the order of 1 µL. The challenge for successful application of MALDI mass spectrometry for quantitative analysis of drugs is to concentrate analytes in such a small volume in a reproducible manner. In previous studies, we dissolved the dried PBMC lysates in 100 and 25 µL and subsequently spotted 1 µL [8,9]. In the present study, we dissolved the dried PBMC lysates in 10 µL of solvent. We found that dissolving the dried lysates in less than 10 µL in a reproducible way is difficult. Spotting larger volumes than 1 µL may be used to overcome this problem.

Currently, LC-ESI-MS/MS is the standard for the quantitative analysis of drugs. In this study we have developed a strategy for the quantitative assessment of drugs in biological materials by MALDI-FTICR. Our results demonstrate that MALDI-FTICR mass spectrometry can be successfully used for the precise, accurate, selective, and rapid quantitative analysis of drugs in biological materials. In particular the lower limits obtained for the quantification of HIV-1 protease inhibitors in cell lysates allow clinical application of the MALDI-FTICR technique.

Acknowledgements

We gratefully acknowledge Aids Fund, The Netherlands (Project 2004051 for J.J.A.v.K. and Project 2005038 for R.A.G.) and Top Institute Pharma (Project T4-212) for their financial support. The consortium of Project T4-212 consists of the Departments of Neurology and Virology of the Erasmus MC (Rotterdam), the Departments of Pediatrics and Clinical Pharmacy of the UMC St. Radboud (Nijmegen), TNO-Quality of Life (Zeist), and GlaxoSmithKline (Zeist) (all from The Netherlands). Antiretroviral drugs were kindly provided by Abbott Laboratories, Merck, Pfizer, and F. Hoffmann-La Roche.

References

1. Volmer DA, Sleno L, Bateman K, et al. Comparison of MALDI to ESI on a Triple Quadrupole Platform for Pharmacokinetic Analyses. Anal Chem 2007.
2. Dekker LJ, Burgers PC, Guzel C, Luider TM. FTMS and TOF/TOF mass spectrometry in concert: identifying peptides with high reliability using matrix prespotted MALDI target plates. J Chromatogr B Analyt Technol Biomed Life Sci 2007;847(1):62-4.
3. Siuzdak G. Mass Spectrometry for Biotechnology. 1st ed: Academic Press; 1996.
4. Cohen LH, Gusev AI. Small molecule analysis by MALDI mass spectrometry. Anal Bioanal Chem 2002;373(7):571-86.
5. Ayorinde FO, Hambright P, Porter TN, Keith QL, Jr. Use of meso- tetrakis(pentafluorophenyl) porphyrin as a matrix for low molecular weight alkylphenol ethoxylates in laser desorption/ionization time-of-flight mass spectrometry. Rapid Commun Mass Spectrom 1999;13(24):2474-9.
6. Chen YT, Ling YC. Detection of water-soluble vitamins by matrix-assisted laser desorption/ionization time-of-flight mass spectrometry using porphyrin matrices. J Mass Spectrom 2002;37(7):716-30.
7. Ling YC, Lin L, Chen YT. Quantitative analysis of antibiotics by matrix-assisted laser desorption/ionization time-of-flight mass spectrometry. Rapid Commun Mass Spectrom 1998;12(6):317-27.
8. van Kampen JJ, Burgers PC, de Groot R, Luider TM. Qualitative and quantitative analysis of pharmaceutical compounds by MALDI-TOF mass spectrometry. Anal Chem 2006;78(15):5403-11.
9. van Kampen JJ, Verschuren EJ, Burgers PC, et al. Validation of an HIV-1 inactivation protocol that is compatible with intracellular drug analysis by mass spectrometry. J Chromatogr B Analyt Technol Biomed Life Sci 2007;847(1):38-44.
10. Guo Z, Zhang Q, Zou H, Guo B, Ni J. A method for the analysis of low-mass molecules by MALDI-TOF mass spectrometry. Anal Chem 2002;74(7):1637-41.
11. Kang MJ, Pyun JC, Lee JC, et al. Nanowire-assisted laser desorption and ionization mass spectrometry for quantitative analysis of small molecules. Rapid Commun Mass Spectrom 2005;19:3166-70.
12. Wei J, Buriak JM, Siuzdak G. Desorption-ionization mass spectrometry on porous silicon. Nature 1999;399(6733):243-6.
13. Tholey A, Heinzle E. Ionic (liquid) matrices for matrix-assisted laser desorption/ionization mass spectrometry-applications and perspectives. Anal Bioanal Chem 2006;386(1):24-37.
14. Hensel RR, King RC, Owens KG. Electrospray sample preparation for improved quantitation in matrix-assisted laser desorption/ionization time-of-flight mass spectrometry. Rapid Commun Mass Spectrom 1997;11(16):1785-93.
15. Schuerenberg M, Luebbert C, Eickhoff H, Kalkum M, Lehrach H, Nordhoff E. Prestructured MALDI-MS sample supports. Anal Chem 2000;72(15):3436-42.
16. Duncan MW, Matanovic G, Cerpa-Poljak A. Quantitative analysis of low molecular weight compounds of biological interest by matrix-assisted laser desorption ionization. Rapid Commun Mass Spectrom 1993;7(12):1090-4.
17. Rideout D, Bustamante A, Siuzdak G. Cationic drug analysis using matrix-assisted laser desorption/ionization mass spectrometry: application to influx kinetics, multidrug resistance, and intracellular chemical change. Proc Natl Acad Sci U S A 1993;90(21):10226-9.
18. Hatsis P, Brombacher S, Corr J, Kovarik P, Volmer DA. Quantitative analysis of small pharmaceutical drugs using a high repetition rate laser matrix-assisted laser/desorption ionization source. Rapid Commun Mass Spectrom 2003;17(20):2303-9.

19. Notari S, Mancone C, Tripodi M, Narciso P, Fasano M, Ascenzi P. Determination of anti-HIV drug concentration in human plasma by MALDI-TOF/TOF. J Chromatogr B Analyt Technol Biomed Life Sci 2006;833(1):109-16.
20. Gobey J, Cole M, Janiszewski J, et al. Characterization and performance of MALDI on a triple quadrupole mass spectrometer for analysis and quantification of small molecules. Anal Chem 2005;77(17):5643-54.
21. Sleno L, Volmer DA. Toxin screening in phytoplankton: detection and quantitation using MALDI triple quadrupole mass spectrometry. Anal Chem 2005;77(5):1509-17.
22. Baykut G, Jertz R, Witt M. Matrix-assisted laser desorption/ionization fourier transform ion cyclotron resonance mass spectrometry with pulsed in-source collision gas and in-source ion accumulation. Rapid Commun Mass Spectrom 2000;14(14):1238-47.
23. Mize TH, Amster IJ. Broad-band ion accumulation with an internal source MALDI-FTICR-MS. Anal Chem 2000;72(24):5886-91.
24. Moyer SC, Budnik BA, Pittman JL, Costello CE, O'Connor PB. Attomole peptide analysis by high-pressure matrix-assisted laser desorption/ionization Fourier transform mass spectrometry. Anal Chem 2003;75(23):6449-54.
25. O'Connor PB, Costello CE. Application of multishot acquisition in Fourier transform mass spectrometry. Anal Chem 2000;72(20):5125-30.
26. Krutchinsky AN, Chait BT. On the nature of the chemical noise in MALDI mass spectra. J Am Soc Mass Spectrom 2002;13(2):129-34.
27. Cancilla MT, Wong AW, Voss LR, Lebrilla CB. Fragmentation reactions in the mass spectrometry analysis of neutral oligosaccharides. Anal Chem 1999;71(15):3206-18.
28. Ho YP, Fenselau C. Metastable decay of peptide ions on a Fourier transform mass spectrometer equipped with an external ion source. J Mass Spectrom 2000;35(2):183-8.
29. O'Connor PB, Costello CE. A high pressure matrix-assisted laser desorption/ionization Fourier transform mass spectrometry ion source for thermal stabilization of labile biomolecules. Rapid Commun Mass Spectrom 2001;15(19):1862-8.
30. Penn SG, Cancilla MT, Lebrilla CB. Collision-induced dissociation of branched oligosaccharide ions with analysis and calculation of relative dissociation thresholds. Anal Chem 1996;68(14):2331-9.
31. Stemmler EA, Buchanan MV, Hurst GB, Hettich RL. Analysis of modified oligonucleotides by matrix-assisted laser desorption/ionization Fourier transform mass spectrometry. Anal Chem 1995;67(17):2924-30.
32. Wong AW, Wang H, Lebrilla CB. Selection of anionic dopant for quantifying desialylation reactions with MALDI-FTMS. Anal Chem 2000;72(7):1419-25.
33. Cancilla MT, Penn SG, Lebrilla CB. Alkaline degradation of oligosaccharides coupled with matrix-assisted laser desorption/ionization Fourier transform mass spectrometry: a method for sequencing oligosaccharides. Anal Chem 1998;70(4):663-72.
34. Wong AW, Cancilla MT, Voss LR, Lebrilla CB. Anion dopant for oligosaccharides in matrix-assisted laser desorption/ionization mass spectrometry. Anal Chem 1999;71(1):205-11.
35. Rosenstock HM, Wallenstein MB, Wahrhaftig AL, Eyring H. Absolute rate theory for isolated systems and the mass spectra of polyatomic molecules. Proc Natl Acad Sci U S A 1952;38:667-78.
36. Gross JH. Meaning of the Rate Constant. In: Gross JH, ed. Mass Spectrometry: A Textbook. 1st ed: Springer; 2004:28-9.
37. Crommentuyn KM, Mulder JW, Mairuhu AT, et al. The plasma and intracellular steady-state pharmacokinetics of lopinavir/ritonavir in HIV-1-infected patients. Antivir Ther 2004;9(5):779-85.

38. Ford J, Boffito M, Wildfire A, et al. Intracellular and plasma pharmacokinetics of saquinavir-ritonavir, administered at 1,600/100 milligrams once daily in human immunodeficiency virus-infected patients. Antimicrob Agents Chemother 2004;48(7):2388-93.
39. Hennessy M, Clarke S, Spiers JP, et al. Intracellular indinavir pharmacokinetics in HIV-infected patients: comparison with plasma pharmacokinetics. Antivir Ther 2003;8(3):191-8.
40. Hennessy M, Clarke S, Spiers JP, et al. Intracellular accumulation of nelfinavir and its relationship to P-glycoprotein expression and function in HIV-infected patients. Antivir Ther 2004;9(1):115-22.
41. Time-of-Flight Instruments. In: Gross JH, ed. Mass spectrometry: A textbook: Springer; 2004:113-30.
42. Colombo S, Beguin A, Telenti A, et al. Intracellular measurements of anti-HIV drugs indinavir, amprenavir, saquinavir, ritonavir, nelfinavir, lopinavir, atazanavir, efavirenz and nevirapine in peripheral blood mononuclear cells by liquid chromatography coupled to tandem mass spectrometry. J Chromatogr B Analyt Technol Biomed Life Sci 2005;819(2):259-76.
43. Jemal M, Rao S, Gatz M, Whigan D. Liquid chromatography-tandem mass spectrometric quantitative determination of the HIV protease inhibitor atazanavir (BMS-232632) in human peripheral blood mononuclear cells (PBMC): practical approaches to PBMC preparation and PBMC assay design for high-throughput analysis. J Chromatogr B Analyt Technol Biomed Life Sci 2003;795(2): 273-89.
44. Rouzes A, Berthoin K, Xuereb F, et al. Simultaneous determination of the antiretroviral agents: amprenavir, lopinavir, ritonavir, saquinavir and efavirenz in human peripheral blood mononuclear cells by high-performance liquid chromatography-mass spectrometry. J Chromatogr B Analyt Technol Biomed Life Sci 2004;813(1-2):209-16.

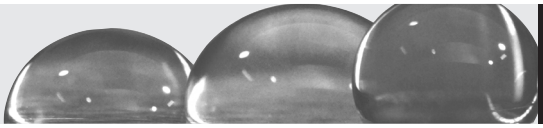

Chapter 9

Quantitative analysis of antiretroviral drugs in lysates of peripheral blood mononuclear cells using MALDI-triple quadrupole mass spectrometry

Jeroen J.A. van Kampen, Peter C. Burgers, Rob A. Gruters,
Albert D.M.E. Osterhaus, Ronald de Groot, Theo M. Luider, Dietrich A. Volmer

Analytical Chemistry 2008, 80, 4969–4975

Abstract

We report here on the use of a prototype matrix-assisted laser desorption/ionization (MALDI)-triple quadrupole mass spectrometer for quantitative analysis of six antiretroviral drugs in lysates of peripheral blood mononuclear cells (PBMCs). Of the five investigated MALDI matrixes, 2,5-dihydroxybenzoic acid (DHB) and the novel 7-hydroxy-4-(trifluoromethyl)coumarin (HFMC) showed the broadest application ranges for the antiretroviral drugs. For DHB, the mean relative errors ranged from 8.3% (ritonavir) to 4.3% (saquinavir). The mean precisions (CV) ranged from 17.3% (nevirapine) to 10.8% (saquinavir). The obtained lower limits of quantitation (LLOQ) readily allow clinical applications using just 1 million PBMCs from HIV-infected patients under therapy. The new matrix HFMC was used for quantitative analysis of the HIV protease inhibitor indinavir using a stainless steel target plate as well as a target plate with a novel, strongly hydrophobic fluoropolymer coating. Using the coated target plate, the mean relative error improved from 10.1% to 4.6%, the mean precision from 33.9% to 9.9% CV, and the LLOQ from 16 fmol to 1 fmol. In addition, the measurement time for one spot went down from 6 s to only 2.5 s.

Introduction

Matrix-assisted laser desorption/ionization (MALDI) and electrospray ionization (ESI) are extensively used as ionization techniques for mass spectrometric analysis of biological samples. For qualitative and quantitative analysis of compounds, such as pharmaceutical drugs, with molecular masses below 1,000 Da, ESI mass spectrometry is usually preferred over MALDI, because analysis of small molecules with MALDI is often hampered by matrix-derived chemical noise in the low *m/z* range. MALDI, however, does offer important advantages over ESI, namely, the much higher sample throughput and its insensitivity to ion suppression [1,2]. In addition, samples can be conveniently stored on the target plates for future (re)analysis [3].

Various approaches have been described to overcome the problem of matrix-derived chemical noise, including carefully optimized matrix-to-analyte ratios [4], the use of specialized additives [5], the use of ionic liquid matrixes [6] or inorganic matrixes [7,8] or the application of high molecular weight matrixes [9-13]. The interfering noise can also conveniently be circumvented by using tandem mass spectrometry (MS/MS). In the selected reaction monitoring mode (SRM) of a triple quadrupole mass spectrometer, interfering isobaric matrix ions are removed by monitoring only compound-specific precursor/product ion transitions [1].

Quantitative analysis of small molecules using MALDI mass spectrometry is further complicated by poor reproducibilities of ion signals from heterogeneous crystal layers. The precisions can be improved, however, by using optimized co-crystallization techniques for sample and matrix, for example, with prestructured target plates [14], fast evaporation protocols [15], and sophisticated sample spotting devices [16]. In addition, well-matched analytes and internal standards as well as a sufficient number of repeat measurements for signal averaging lead to significantly better precision values, resulting in the successful development of several quantitative drug assays using MALDI-TOF [12,13,17,18], MALDI-qTOF [19,20], MALDI-FTICR, and MALDI-triple quadrupole [19,21-27] mass spectrometry.

In this study, we have explored the feasibility of using a prototype MALDI-triple quadrupole mass spectrometer for rapid quantitative analysis of HIV protease inhibitors and a non-nucleoside reverse transcriptase inhibitor in lysates of peripheral blood mononuclear cells (PBMCs).

Experimental Section

Chemicals

7-Hydroxy-4-(trifluoromethyl)coumarin (HFMC), 2,5-dihydroxybenzoic acid (DHB), 3,5-dimethoxy-4-hydroxycinnamic acid (sinapinic acid; SA), 3-hydroxypicolinic acid (HPA), and α-cyano-4-hydroxycinnamic acid (CHCA) were obtained from Sigma-Aldrich. The investigated drug compounds were kindly donated by the following companies: lopinavir and ritonavir, Abbott Laboratories (Illinois, IL); saquinavir, F. Hoffmann-La Roche (Basel, Switzerland); nelfinavir, Pfizer (Groton, CT); indinavir, Merck (Rahway, NJ); nevirapine and tipranavir, Boehringer Ingelheim (Ingelheim am Rhein, Germany); amprenavir, GlaxoSmithKline (Middlesex, United Kingdom). Carbamazepine was purchased from Sigma-Aldrich. The proprietary PFC1601V fluoropolymer solution was obtained from Cytonix Corp. (Beltsville, MD). Eye protection and gloves should be worn when handling the fluoropolymer solution; there are no acute and chronic hazards to be expected for this product and no carcinogenic properties are known to be present (material safety data sheet, Cytonix Corp.).

Mass spectrometry

An API 3000 MALDI-triple quadrupole mass spectrometer (MDS Analytical Technologies, Concord, ON, Canada) equipped with a prototype 1000-Hz Nd:YAG laser (355 nm) (PowerChip NanoLaser, JDS Uniphase, San José, CA) MALDI source was operated in the positive ion mode. The pressure in the MALDI source was ~5 mTorr. During laser firing, the target plate was moved horizontally at a constant speed (~0.06 cm/s) and the SRM traces of the analyte(s) and internal standard(s) were recorded (dwell time, 10 ms each). Analyst software version 1.1 (MDS Analytical Technologies) was used for data acquisition.

Sample preparation

Peripheral blood mononuclear cells (PBMCs) were isolated from a buffy coat (Sanquin, Rotterdam, The Netherlands) using a standard Ficoll density gradient. PBMC pellets were lysed in 100% methanol overnight at 5°C (100 µL of MeOH per 1×10^6 PBMCs). The lysed PBMCs were spun down at 14,000 rpm for 5 min. Supernatants of 1×10^6 PBMCs were collected in 1.5-mL vials, and 400 µL of water was added to each vial. Subsequently, the supernatants were cleaned using 96-well solid-phase extraction (SPE) plates (Oasis HLB µelution plate, Waters). Methanol and water (200 µL each) were drawn through each well using a vacuum manifold according to the manufacturer's protocol. Subsequently, the samples were loaded onto the SPE plate and washed twice with methanol/water (1:4 v/v). Finally, the samples were eluted from the plate with 100 µL of methanol. Drug standards were added to the eluates and were subsequently dried using a SpeedVac (Savant).

On the day of analysis, the dried samples were reconstituted in 10 µL of matrix solution and replicates of 1 µL were spotted onto 10 × 10 stainless steel target plates (Perseptive Biosystems, Framingham, MA). For hydrophobically coated target plates, the dried samples were reconstituted in 100 µL of matrix solution and replicates of 10 µL were applied.

The following matrixes were used: 4 mg/mL CHCA, 50 mg/mL DHB, 10 mg/mL HFMC, 50 mg/mL HPA, and 4 mg/mL SA. All matrixes were dissolved in acetonitrile/water/formic acid (500:500:1; v/v/v). For the HFMC matrix in combination with the hydrophobic target plate, 1 mg/mL HFMC in acetonitrile/formic acid (200:1; v/v) was used.

Scanning electron microscope (SEM)

SEM photos were obtained on a Hitachi S-3000N SEM (Hitachi Science Systems, Hitachinaka, Japan). Various levels of magnification were used at 2.00-kV electron energy. Spot areas were determined using SimplePCI software (version 4.0.0, Compix Inc. Imaging Systems, Cranberry Township, PA).

Preparation of target plate with hydrophobic coating

The target plates were spin-coated with a hydrophobic coating using a modified centrifuge with a small hole in the top lid and a custom-fitted Teflon rotor for the MALDI plates. During spinning of the target plate at 1,000 rpm, 500 µL of PFC 1601V coating solution was slowly applied through the hole to the center of the target plate. Subsequently, the target plate was spun for 1 min to evenly distribute the coating solution. The coated plate was then heated for 20 min at ~200°C. The coating material can also be applied onto the target plate by simply using a brush, with a slight compromise in coating homogeneity.

Quantitative analysis

The following transitions were monitored for SRM: lopinavir, 630.5 → 183 (collision energy, 30 eV); ritonavir, 722 → 296 (30 eV); saquinavir, 671.5 → 570.5 (40 eV); amprenavir, 506.5 → 245.5 (30 eV); indinavir, 614.5 → 421.5 (40 eV); nelfinavir, 569 → 331 (40 eV); tipranavir, 603.5 → 411 (30 eV); nevirapine, 267 → 226 (30 eV); carbamazepine, 237 → 194 (30 eV). As internal standard, carbamazepine for nevirapine, indinavir for amprenavir, lopinavir for tipranavir, indinavir for nelfinavir, saquinavir for ritonavir, nelfinavir for indinavir, and tipranavir for lopinavir were used.

Two data sets, A and B, were measured, each containing five replicate spots per analyte. Data set A was used to construct the calibration curve while data set B served as quality control, and vice versa. For each spot, the peak area ratios of analyte to internal standard were measured. Subsequently, the average analyte/internal standard ratios for the replicate analyses were calculated, and used for the calibration curves and for

quality control purposes. Linear 1/x-weighed curves were used for calibration, unless otherwise stated.

Results and Discussion

In MALDI experiments, the nature of the matrix compound has a crucial influence on the ionization efficiencies and the signal intensities of the analytes of interest [28]. For example, DHB and CHCA are commonly used for analysis of peptides and small proteins, while SA is preferred for larger proteins. When a small molecule is used as matrix, many of the abundant peaks observed in the low-mass range of the MALDI mass spectrum arise from the matrix itself. Upon laser irradiation, matrix molecules undergo a variety of different processes such as ionization and subsequent fragmentation, photodissociation, and ion-molecule reactions, leading to matrix-derived chemical noise in the low *m/z* range. These interfering signals seriously hamper the analysis of small molecules with *m/z* values below 1,000. Various approaches have been described to overcome this limitation, for example, by carefully choosing the matrix-to-analyte ratio [4], the use of additives [5], ionic liquids [6] or inorganic matrixes [7,8]. The use of high molecular weight porphyrin matrixes can also decrease the matrix-derived chemical noise in the low *m/z* range [9-11]. We have previously shown that using the high molecular weight porphyrin matrix meso-tetrakis(pentafluorophenyl)porphyrin (F20TPP) results in a significant decrease of the matrix-related peaks in the low *m/z* range in MALDI-TOF analyses and that this matrix can be used for quantitative analysis of HIV protease inhibitors in cell lysates [12,13]. By contrast, in MALDI-FTICR mass spectrometry, the high molecular weight matrix F20TPP undergoes extensive dissociation on the time scale of the FTICR experiment (~1 s) and intense fragment ions are observed in the low mass range, which leads to interfering chemical noise. Significantly less fragmentation of such ions is observed in MALDI-TOF mass spectrometers (10^{-4} s). Thus, for the quantitative analysis of small molecules, a high molecular weight matrix was used for TOF analyses and a low molecular weight matrix for the FTICR experiments, showing that the type of mass analyzer can have a significant influence on the choice of matrix for small-molecule analysis by MALDI. Another efficient way for eliminating the chemical noise is the application of MS/MS, by monitoring only analyte-specific ion transitions. This technique is particularly useful when a triple quadrupole MS is used for MS/MS. In the SRM mode of the QqQ instrument, a nearly 100% duty cycle is obtained, and this makes it extremely efficient for small molecule target analysis. Using this technique, a wide variety of matrices, such as CHCA and DHB, have been used for small-molecule analysis. Sleno and Volmer compared CHCA, DHB, and SA for analysis of spirolide toxins, quinidine, danofloxacin, ramipril, and nadolol and found that CHCA yielded the strongest signal intensities and the best precision for these

drugs [24,25]. In addition, Gobey et al. showed that CHCA resulted in successful detection of 175 out of the 208 tested compounds [27].

Comparison of matrices

In the present study, we have compared the use of the CHCA, DHB, SA, 3-hydroxypicolinic acid (HPA), and a new matrix, 7-hydroxy-4-(trifluoromethyl)coumarin (HFMC), for the analysis of seven HIV protease inhibitors by MALDI-QqQ (Figure 1). SA and HPA yielded very poor signal intensities in comparison to CHCA, DHB, and HFMC. CHCA exhibited intense signals only for nelfinavir, indinavir, and saquinavir, but relatively weak signals for lopinavir, ritonavir, amprenavir, and tipranavir. DHB and the new matrix HFMC on the other hand generated very strong signals for all seven protease inhibitors tested. Using MALDI-TOF and MALDI-FTICR, we have previously shown that abundant signals for antiretroviral drugs can be obtained by using a cationization approach with alkali halides [12,13]. Using MS/MS on the MALDI-QqQ instrument, however, we found that the cationized drugs showed poor fragmentation efficiencies and thus low SRM sensitivities compared to the protonated precursor molecules. In general, we found that higher collision energies were needed for fragmentation of the cationized drugs as compared to the protonated forms.

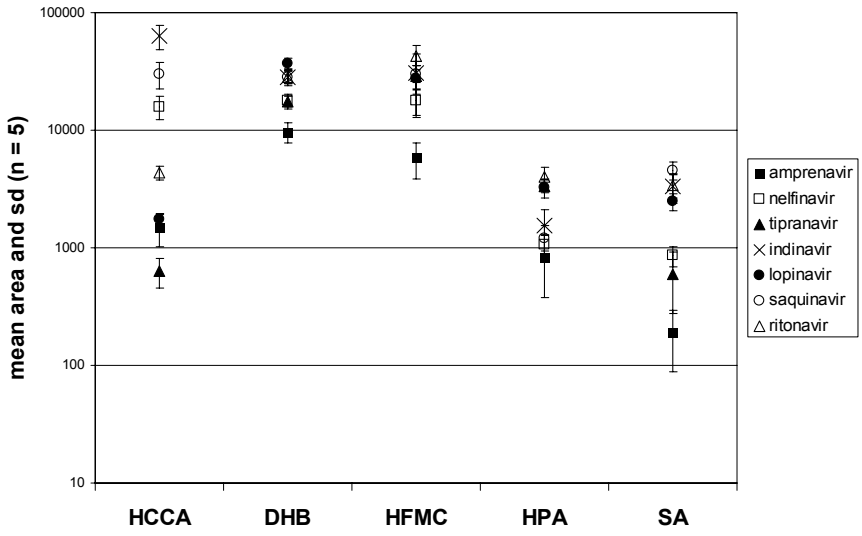

Figure 1. Comparison of signal intensities for HIV-1 protease inhibitors using various MALDI matrixes in combination with stainless steel target plates. Seven protease inhibitors were spiked in a lysate of 1 x 10^6 PBMC and analyzed using various matrixes. The amount of protease inhibitor per spot was 5 pmol. Reported are the mean areas and standard deviations of the SRM traces for a single spot (the areas for saquinavir were divided by 10).

Quantitative analysis of antiretroviral drugs in cell lysates using DHB matrix

We explored DHB as matrix for quantitative analysis of the protonated forms of the HIV protease inhibitors nelfinavir, saquinavir, indinavir, lopinavir, and ritonavir and the non-nucleoside reverse transcriptase inhibitor nevirapine in lysates of PBMCs (Table 1). The measurement precisions were relatively high compared to LC-MS/MS methods for antiretroviral drugs in PBMC lysates [29]. Sleno and Volmer showed that using CHCA resulted in significantly better precisions as compared to DHB, because of the more homogeneous crystal layers formed from CHCA solutions [25,26]. In our experiments, however, the signal intensities for antiretroviral drugs were much better for DHB as matrix as compared to CHCA (vide supra), necessitating DHB as matrix. Unfortunately, no stable isotope standards were commercially available for the analytes investigated here, to compensate for the heterogeneous crystallization. Alternatively, we used chemically similar protease inhibitors as internal standard for analysis of the protease inhibitors of interest (see Experimental Section) and carbamazepine as a chemically related internal standard for the non-nucleoside reverse transcriptase inhibitor nevirapine. Applying stable isotope standards generally results in significantly better precisions, since the chemical properties of internal standard and analyte are virtually identical. This is particularly important for MALDI, as well-matched analyte and internal standard pairs result in homogeneous co-crystallizations, as recently shown by Sleno and Volmer [24]. It was also shown in that study, however, that structural analogues of the analyte could be successfully used, as long as important solution-phase properties were appropriately matched. To compensate for the relatively high fluctuations mentioned above, we measured and averaged five replicates of each sample and used the mean analyte-to-internal standard ratio to calculate the concentration in the sample. The resulting average relative errors ranged between 5.0% for indinavir to 8.3% for ritonavir. The lower limits of quantitation,

Table 1. Quantitative analysis of antiretroviral drugs in PBMC lysate using MALDI-QqQ[a]

	LLOQ (pmol)	ULOQ (pmol)	precision (% CV)	accuracy, RE (% deviation)	r^2
nelfinavir	0.064	16	11.9 (3.2)	7.4 (4.4)	0.9998
indinavir	0.004	16	12.0 (6.8)	5.0 (3.6)	0.9999
saquinavir	0.016	4	10.8 (3.2)	4.3 (3.4)	0.9985
ritonavir	0.064	16	14.1 (8.3)	8.3 (6.2)	0.9975
lopinavir	0.064	16	12.9 (4.6)	6.7 (4.4)	0.9953
nevirapine	0.016	16	17.3 (3.8)	7.4 (4.5)	0.9999

[a] LLOQ, lower limit of quantitation in picomole per spot on the target plate. ULOQ, upper limit of quantification in picomole per spot on the target plate. Reported are the average precisions and accuracies (% relative error, RE) for data sets A and B. r^2 = regression coefficient of the 1/x weighed linear curve when data sets A and B were combined. Standard deviations are reported in parentheses. All experimental data in the table were obtained using DHB as maxtrix compound on an uncoated stainless steel target.

expressed as amount of drug per spot on the target plate, was 64 fmol for nelfinavir, 4 fmol for indinavir, 16 fmol for saquinavir, 64 fmol for lopinavir, 64 fmol for ritonavir, and 16 fmol for nevirapine. These numbers readily allow the clinical application of the technique.

Coumarin matrix and fluoropolymer-coated target plates

We also explored the use of the new matrix compound HFMC (Figure 2) for quantitative analysis of indinavir in PBMC lysates. HFMC is a photoluminescent molecule with a molecular mass of 230.02 Da. HFMC exhibits maximum light absorption at 355 nm, which ideally matches the wavelength of the frequency-tripled, solid-state Nd:YAG laser of the MALDI-QqQ system (λ = 355 nm). Upon excitation, HFMC emits fluorescent light at λ = 498 nm. In acidic solutions, HFMC is colorless, while it is bright yellow in basic solutions. When the HFMC matrix was spotted on a stainless steel target plate using the dried droplet technique, the quantitative precisions and quantitative accuracies were poor. Inspection of the SRM traces showed differential incorporation of analyte and internal standard in the HFMC crystals. A fast evaporation approach [15], i.e., spotting from 100% organic solvents, was used to obtain a more homogeneous distribution of analyte and

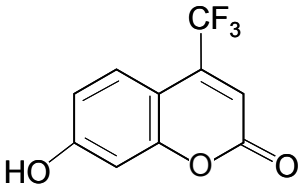

Figure 2. 7-Hydroxy-4-(trifluoromethyl)coumarin (HFMC).

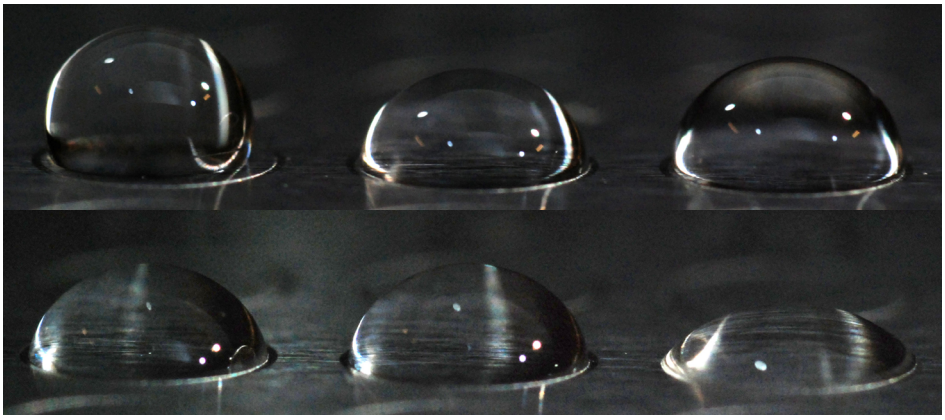

Figure 3. Droplets of 10 µL of DHB solution in various solvents spotted on a fluoropolymer-coated MALDI target. Upper row: left, DHB in water; middle, DHB in ACN/water (1:1, v/v); right, DHB in MeOH/water (1:1, v/v). Lower row: left, DHB in ACN; middle, DHB in MeOH; right, DHB in acetone.

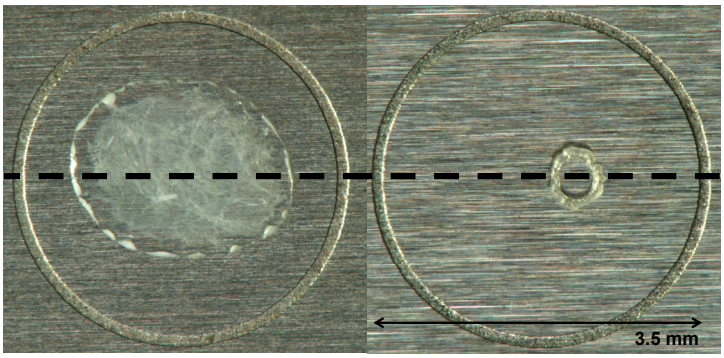

Figure 4. HFMC matrix spotted on to a stainless steel target plate and a fluoropolymer-coated target plate. Left: 1 µL of HFMC matrix spotted on to a stainless steel target plate (10 mg/mL in ACN/H_2O (1:1, v/v)). Right: 10 µL of HFMC matrix spotted on to a fluoropolymer-coated target plate (1 mg/mL in 100% acetonitrile). The dashed line represents the actual width of the laser beam (diameter, ~110 µm). The etched circle is ~3.5 mm wide.

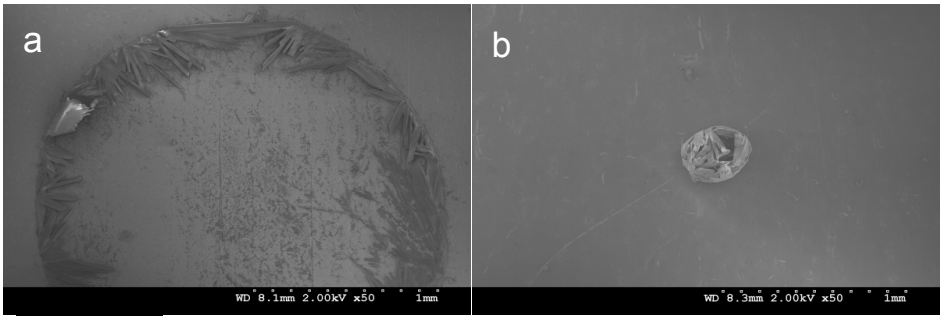

Figure 5. SEM analysis of dried sample spots. Spot size reduction for dispensed DHB solutions (25/75 acetonitrile/water): (a) 1 µL on an uncoated stainless target; (b) 1 µL on a coated plate. The diameter of the dried spot on the coated plate is ~200 µm.

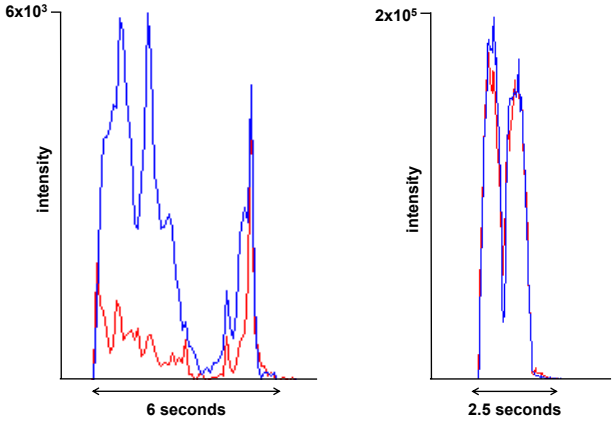

Figure 6. SRM traces of 4 pmol of indinavir (blue) and 1 pmol of saquinavir (red) in a single spot using the novel matrix HFMC on a stainless steel target plate (left) and on a fluoropolymer-coated target plate (right).

internal standard in the HFMC crystals. However, extensive spreading of the sample was observed when the fast evaporation protocol was applied in combination with stainless steel target plates. It has been previously shown that hydrophobic coatings can significantly improve crystallization behavior on MALDI plates [30-34]. In this study, we coated the target plate with an inexpensive strongly hydrophobic fluoropolymer (~0.20 US $/plate). The coated target plates allowed spotting of large volumes of sample, even for 100% organic solutions of up to 10 µL (Figure 3). Furthermore, even these large volumes of sample dried to very small crystal areas on the target plates, due to the remarkable focusing abilities of the coating material (Figure 4).

The reduction factor in the area of the crystal layers was further investigated by spotting droplets of 1-µL DHB solutions in acetonitrile/water mixtures of varying composition on coated as well as uncoated target plates (Figure 5). Using the coated target plates, the area of the dried spots reduced by a factor 18.2 (acetonitrile content of 75%), 23.3 (50% ACN), and 31.5 (25% ACN), which is significantly larger than previously reported coating materials [30-34]. Figure 6 illustrates that the coated target plates significantly improve the co-crystallization of analyte and internal standard for indinavir when HFMC is used as matrix. In addition, the measurement times for one spot were reduced from 6 s to 2.5 s. Another feature of the coating is a significant reduction in background signals from

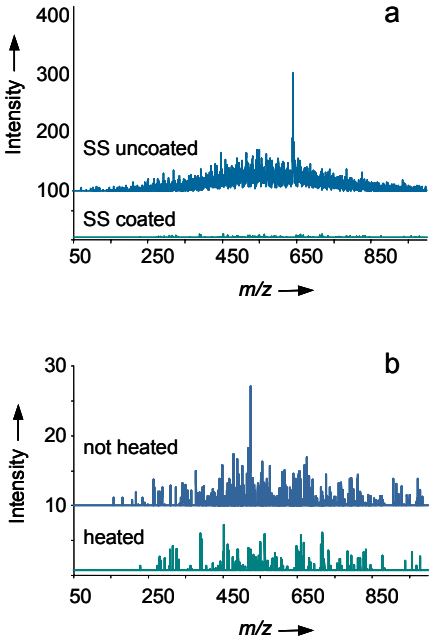

Figure 7. Comparison of background signals in the full-scan mode on uncoated and coated stainless steel (SS) plates (panel a). Panel b shows the further improvements by heat curing the coated plates for 20 min at 200°C.

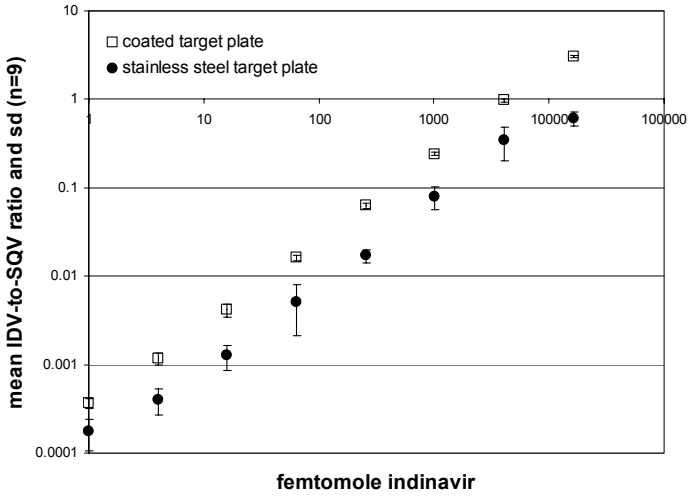

Figure 8. Quantitative analysis of indinavir in PBMC lysates using the novel matrix HFMC on a stainless steel target plate and on a fluoropolymer coated plate.

contaminants on the target plate (Figure 7). Figure 8 illustrates the improvement in the concentration-response curve for indinavir in PBMC lysates as well as improvement in precision when the fluoropolymer-coated plate was used in combination with the HFMC matrix. Using the fluoropolymer-coated plate, the average precision improved from 34% CV (sd 17.6) to 9.9% CV (sd 5.7) and the relative error went down from 10.1% (sd 4.8) to 4.6% (sd 3.6). In addition, the lower limit of quantitation improved from 16 fmol to 1 fmol per spot on the target plate using a $1/x^2$-weighed linear curve.

Conclusions

There is an increasing interest in the use of MALDI mass spectrometry for quantitative analysis of small molecules, due to its very high sample throughput capability, its insensitivity to ion suppression, and the possibility of storing samples on target plates for future use or reanalysis. Using a prototype MALDI-QqQ mass spectrometer, we have shown here that this technique can be used for accurate quantitative analysis of HIV protease inhibitors and a non-nucleoside reverse transcriptase inhibitor in lysates of 1 million peripheral blood mononuclear cells. The limits of quantitation readily allow clinical applications of the technique. In this study, we had to resort to chemical analogues as internal standards, because stable isotope internal standards were not available. Stable isotopes are often very expensive and are frequently not commercially available, and the custom synthesis of these compounds is laborious. While using chemical analogues as internal standards may not at first appear to be the best choice, it is frequently the

only practical option for quantitative analysis using LC-MS or MALDI-MS. In our study, we demonstrated that chemically similar compounds as standards and replicate analyses yielded excellent precision and accuracy. We have also shown that the optimum matrix for specific analytes can be highly compound dependent. By using a novel matrix and a fluoropolymer surface coating, we were able to achieve improved co-crystallization of analyte and internal standard, thus further improving precisions and accuracies.

Acknowledgements

Financial support was obtained from Aids Fund, The Netherlands (project 2004051 (J.J.A.v.K.), and the VIRGO consortium, an Innovative Cluster approved by The Netherlands Genomics Initiative and partially funded by the Dutch Government (BSIK 03012). Top Institute Pharma (project T4-212) and the members of project T4-212 (Erasmus MC (Rotterdam), TNO Quality of Life (Zeist), UMC St. Radboud (Nijmegen), and GlaxoSmith-Kline (Zeist)) are acknowledged for their scientific support. D.A.V. appreciates research support to his group from MDS Analytical Technologies, including the prototype MALDI-triple quadrupole instrument. Frank van der Panne (Pathology, Erasmus MC) and Jan Tuin (Thorax Center, Erasmus MC) are gratefully acknowledged for their photography skills, and Nicole Zehethofer, Andrew Leslie, Rambod Daneshfar and Felix Meier for their technical support. T.M.L. and D.A.V. contributed equally to this work.

References

1. Volmer DA, Sleno L, Bateman K, et al. Comparison of MALDI to ESI on a Triple Quadrupole Platform for Pharmacokinetic Analyses. Anal Chem 2007.
2. Yang Y, Zhang S, Howe K, et al. A comparison of nLC-ESI-MS/MS and nLC-MALDI-MS/MS for GeLC-based protein identification and iTRAQ-based shotgun quantitative proteomics. J Biomol Tech 2007;18(4):226-37.
3. Dekker LJ, Burgers PC, Guzel C, Luider TM. FTMS and TOF/TOF mass spectrometry in concert: identifying peptides with high reliability using matrix prespotted MALDI target plates. J Chromatogr B Analyt Technol Biomed Life Sci 2007;847(1):62-4.
4. McCombie G, Knochenmuss R. Small-molecule MALDI using the matrix suppression effect to reduce or eliminate matrix background interferences. Anal Chem 2004;76(17):4990-7.
5. Guo Z, Zhang Q, Zou H, Guo B, Ni J. A method for the analysis of low-mass molecules by MALDI-TOF mass spectrometry. Anal Chem 2002;74(7):1637-41.
6. Tholey A, Heinzle E. Ionic (liquid) matrices for matrix-assisted laser desorption/ionization mass spectrometry-applications and perspectives. Anal Bioanal Chem 2006;386(1):24-37.
7. Kang MJ, Pyun JC, Lee JC, et al. Nanowire-assisted laser desorption and ionization mass spectrometry for quantitative analysis of small molecules. Rapid Commun Mass Spectrom 2005;19: 3166-70.
8. Wei J, Buriak JM, Siuzdak G. Desorption-ionization mass spectrometry on porous silicon. Nature 1999;399(6733):243-6.
9. Ayorinde FO, Hambright P, Porter TN, Keith QL, Jr. Use of meso- tetrakis(pentafluorophenyl) porphyrin as a matrix for low molecular weight alkylphenol ethoxylates in laser desorption/ ionization time-of-flight mass spectrometry. Rapid Commun Mass Spectrom 1999;13(24):2474-9.
10. Chen YT, Ling YC. Detection of water-soluble vitamins by matrix-assisted laser desorption/ionization time-of-flight mass spectrometry using porphyrin matrices. J Mass Spectrom 2002;37(7): 716-30.
11. Ling YC, Lin L, Chen YT. Quantitative analysis of antibiotics by matrix-assisted laser desorption/ ionization time-of-flight mass spectrometry. Rapid Commun Mass Spectrom 1998;12(6):317-27.
12. van Kampen JJ, Burgers PC, de Groot R, Luider TM. Qualitative and quantitative analysis of pharmaceutical compounds by MALDI-TOF mass spectrometry. Anal Chem 2006;78(15):5403-11.
13. van Kampen JJ, Verschuren EJ, Burgers PC, et al. Validation of an HIV-1 inactivation protocol that is compatible with intracellular drug analysis by mass spectrometry. J Chromatogr B Analyt Technol Biomed Life Sci 2007;847(1):38-44.
14. Schuerenberg M, Luebbert C, Eickhoff H, Kalkum M, Lehrach H, Nordhoff E. Prestructured MALDI-MS sample supports. Anal Chem 2000;72(15):3436-42.
15. Vorm O, Roepstorff P, Mann M. Improved resolution and very high sensitivity in MALDI TOF of matrix surfaces made by fast evaporation. Anal Chem 1994;66(19):3281-7.
16. Hanton SD, Hyder IZ, Stets JR, et al. Investigations of electrospray sample deposition for polymer MALDI mass spectrometry. J Am Soc Mass Spectrom 2004;15(2):168-79.
17. Duncan MW, Matanovic G, Cerpa-Poljak A. Quantitative analysis of low molecular weight compounds of biological interest by matrix-assisted laser desorption ionization. Rapid Commun Mass Spectrom 1993;7(12):1090-4.
18. Rideout D, Bustamante A, Siuzdak G. Cationic drug analysis using matrix-assisted laser desorption/ionization mass spectrometry: application to influx kinetics, multidrug resistance, and intracellular chemical change. Proc Natl Acad Sci U S A 1993;90(21):10226-9.

19. Hatsis P, Brombacher S, Corr J, Kovarik P, Volmer DA. Quantitative analysis of small pharmaceutical drugs using a high repetition rate laser matrix-assisted laser/desorption ionization source. Rapid Commun Mass Spectrom 2003;17(20):2303-9.
20. Notari S, Mancone C, Tripodi M, Narciso P, Fasano M, Ascenzi P. Determination of anti-HIV drug concentration in human plasma by MALDI-TOF/TOF. J Chromatogr B Analyt Technol Biomed Life Sci 2006;833(1):109-16.
21. Corr JJ, Kovarik P, Schneider BB, Hendrikse J, Loboda A, Covey TR. Design considerations for high speed quantitative mass spectrometry with MALDI ionization. J Am Soc Mass Spectrom 2006; 17(8):1129-41.
22. Kovarik P, Grivet C, Bourgogne E, Hopfgartner G. Method development aspects for the quantitation of pharmaceutical compounds in human plasma with a matrix-assisted laser desorption/ ionization source in the multiple reaction monitoring mode. Rapid Commun Mass Spectrom 2007;21(6):911-9.
23. Signor L, Varesio E, Staack RF, Starke V, Richter WF, Hopfgartner G. Analysis of erlotinib and its metabolites in rat tissue sections by MALDI quadrupole time-of-flight mass spectrometry. J Mass Spectrom 2007;42(7):900-9.
24. Sleno L, Volmer DA. Assessing the properties of internal standards for quantitative matrix-assisted laser desorption/ionization mass spectrometry of small molecules. Rapid Commun Mass Spectrom 2006;20(10):1517-24.
25. Sleno L, Volmer DA. Some fundamental and technical aspects of the quantitative analysis of pharmaceutical drugs by matrix-assisted laser desorption/ionization mass spectrometry. Rapid Commun Mass Spectrom 2005;19(14):1928-36.
26. Sleno L, Volmer DA. Toxin screening in phytoplankton: detection and quantitation using MALDI triple quadrupole mass spectrometry. Anal Chem 2005;77(5):1509-17.
27. Gobey J, Cole M, Janiszewski J, et al. Characterization and performance of MALDI on a triple quadrupole mass spectrometer for analysis and quantification of small molecules. Anal Chem 2005;77(17):5643-54.
28. Matrix-Assisted Laser Desorption/Ionization. In: Gross JH, ed. Mass spectrometry: A textbook: Springer; 2004:411-40.
29. Colombo S, Beguin A, Telenti A, et al. Intracellular measurements of anti-HIV drugs indinavir, amprenavir, saquinavir, ritonavir, nelfinavir, lopinavir, atazanavir, efavirenz and nevirapine in peripheral blood mononuclear cells by liquid chromatography coupled to tandem mass spectrometry. J Chromatogr B Analyt Technol Biomed Life Sci 2005;819(2):259-76.
30. Owen SJ, Meier FS, Brombacher S, Volmer DA. Increasing sensitivity and decreasing spot size using an inexpensive, removable hydrophobic coating for matrix-assisted laser desorption/ ionisation plates. Rapid Commun Mass Spectrom 2003;17(21):2439-49.
31. Redeby T, Roeraade J, Emmer A. Simple fabrication of a structured matrix-assisted laser desorption/ionization target coating for increased sensitivity in mass spectrometric analysis of membrane proteins. Rapid Commun Mass Spectrom 2004;18(10):1161-6.
32. Xiong S, Ding Q, Zhao Z, Chen W, Wang G, Liu S. A new method to improve sensitivity and resolution in matrix-assisted laser desorption/ionization time of flight mass spectrometry. Proteomics 2003;3(3):265-72.
33. Konig S, Grote J. Hydrophobic targets for MALDI mass spectrometry. Biotechniques 2002;32(4): 912, 4-5.
34. Gundry RL, Edward R, Kole TP, Sutton C, Cotter RJ. Disposable hydrophobic surface on MALDI targets for enhancing MS and MS/MS data of peptides. Anal Chem 2005;77(20):6609-17.

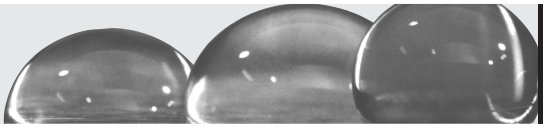

Chapter 10

Ultra-fast determination of drug concentrations in cells and in plasma

Jeroen J.A. van Kampen, Mariska L. Reedijk, Peter C. Burgers, Lennard. J.M. Dekker, Nico G. Hartwig, Ineke E. van der Ende, Ronald de Groot, Albert D.M.E. Osterhaus, David M. Burger, Theo M. Luider, Rob A. Gruters

Submitted

Abstract

Intracellular drug monitoring is important to understand pharmacotherapy. We demonstrate that the novel technique of MALDI-triple quadrupole mass spectrometry is significantly faster for quantitative analysis of drugs compared to traditional liquid chromatography (LC) based assays. In MALDI-triple quadrupole MS the LC-step is omitted resulting in sample analysis of seconds. Using HIV protease inhibitors as model compounds, we validated and applied MALDI-triple quadrupole MS assays for their quantitative analysis intracellularly and in plasma. These assays are directly applicable to pharmacokinetic studies when limited amounts of sample are available. Sample preparation is straightforward and easy to automate. Plasma is diluted in methanol and cells are processed with solid phase extraction. To show the applicability of this novel approach, assays were used to determine the plasma and intracellular concentrations of lopinavir and ritonavir in HIV infected children. This is the first time that intracellular concentrations of HIV protease inhibitors are reported for children.

Introduction

Assays to determine drug concentrations are used in many areas of life sciences, ranging from preclinical pharmacokinetic studies in drug discovery to therapeutic drug monitoring in a clinical setting. Liquid chromatography (LC) – based assays are currently the standard for such analyses, in particular assays that combine LC with UV detection or detection by electrospray ionization (ESI) mass spectrometry (MS). The LC-step, which is the most time-consuming part of the analysis, takes at least several minutes, and high throughput quantitative analysis is therefore difficult to achieve. In contrast, matrix-assisted laser desorption/ionization (MALDI) MS is a technique that is able to detect trace amounts of a compound in complex biological samples without using a LC-step, and analyses times of ≤ 5 seconds can be obtained using the recently developed MALDI-triple quadrupole mass spectrometer.[1-7]

However, interfering signals and poor precisions limit the application of MALDI-MS for quantitative analyses of small molecule drugs, i.e. drugs with molecular masses below 1,000 Da. The matrix, which is needed for efficient ionization of the analytes present in the sample, is itself a small molecule and produces a series signals that interfere with the analysis of other small molecules. Drug signals can be distinguished from these interfering matrix signals by their fragmentation pattern which is highly structure-specific. A MALDI – triple quadrupole mass spectrometer operating in the selected reaction monitoring (SRM) mode detects only the drug-specific precursor/product ion transitions, and matrix-derived interfering signals are significantly decreased or eliminated.[3] In addition, strategies that focus on homogenous crystallization of the matrix, use of an internal standard, and average multiple measurements [8-11], improve the precisions of MALDI-MS to values required for drug analysis [12].

We show that MALDI-triple quadrupole MS is a valuable tool for high throughput quantitative analysis of drugs, and compounds as diverse as methotrexate, amino acids, and antibiotics can be analyzed by this approach. HIV protease inhibitors were used as model compounds in this study and assays were developed, validated, and applied for quantitative analysis of these compounds in plasma and in cells. To show the clinical applicability of the approach, assays were used to monitor the plasma and intracellular concentrations of lopinavir and ritonavir in a cohort of HIV infected children.

Experimental Section

Chemicals and solvents

Methotrexate (Emthexate PF for parenteral administration, PharmaChemie BV, Haarlem, the Netherlands), saquinavir (donated by F. Hoffmann La-Roche, Basel, Switzerland),

indinavir (donated by Merck, Rahway, NJ, USA), nelfinavir (donated by Pfizer, Groton, CT, USA), lopinavir and ritonavir (donated by Abbott Laboratories, Illinois, IL, USA), Kaletra oral solution (80 mg/mL lopinavir and 20 mg/mL ritonavir; Abbott; obtained from dept. Pharmacy, Erasmus MC, Rotterdam, the Netherlands), nevirapine and tipranavir (donated by Boehringer Ingelheim, Ingelheim am Rhein, Germany), efavirenz (Moravek, Brea, CA, USA), metronidazole, metoprolol, piroxicam, amoxicillin, and carbamazepine (all from Sigma-Aldrich, Zwijndrecht, the Netherlands). α-cyano-4-hydroxycinnamic acid solution (Agilent Technologies; 6.2 mg/mL in methanol/acetonitrile/water 36/56/8 v/v/v, pH = 2.5). Sodium iodide (purity > 99.99%, Sigma-Aldrich, Zwijndrecht, the Netherlands). Methanol (ULC/MS grade, Biosolve, Valkenswaard, the Netherlands). Phosphate-Buffered Saline (PBS; 1x; pH = 7.4; $CaCl_2$ and $MgCl_2$; product number 10010) was obtained from Invitrogen. Red blood cell lysis buffer was obtained from Roche Diagnostics (Mannheim, Germany, Cat. No. 11814389001).

Stock solutions

All stock solutions for MALDI-triple quadrupole MS analysis were prepared in methanol by serial dilution. As internal standards we used: 20 µM nelfinavir (quantitation of lopinavir and ritonavir in plasma), 5 µM methotrexate (quantitation of saquinavir, nelfinavir, and indinavir in plasma), 2 µM nelfinavir (quantitation of lopinavir and ritonavir in 1 x 10^6 PBMCs). To investigate the effect of co-medication on the quantitation performance, the following drug mixtures were added to the quality control samples: drug mixture A: 10 µM carbamazepine, metoprolol, metronidazole, amoxicillin, piroxicam, nevirapine, saquinavir, efavirenz, indinavir, and tipranavir (quantitation of lopinavir and ritonavir in plasma). Drug mixture B: 10 µM carbamazepine, metoprolol, metronidazole, amoxicillin, piroxicam, nevirapine, lopinavir, efavirenz, ritonavir, and tipranavir (quantitation of saquinavir, indinavir, and nelfinavir in plasma).

Matrix preparation

For simultaneous quantitation of lopinavir and ritonavir, 10 µL 100 mM NaI in MeOH was added to 990 µL matrix solution. For simultaneous quantitation of saquinavir, indinavir, and nelfinavir, the matrix solution was diluted 1:1 v/v in nanopure water.

MALDI-triple quadrupole mass spectrometry

A FlashQuant Workstation equipped with a 4000 QTRAP mass analyzer (MDS Analytical Technologies, Concord, Ontario, Canada) was used for automated measurements of the samples in the selected reaction monitoring mode at unit resolution. For specific setting see Table 1. Analyst 1.4.2. and FlashQuant 1.0 software (MDS Analytical Technologies, Concord, Ontario, Canada) were used to operate the instrument and for automated data analysis. A calibration curve was constructed by plotting the analyte-to-internal stan-

Table 1. Instrument settings for quantitative analysis of HIV protease inhibitors.

compound	form	ion transition	CE (V)	CXP (V)	plate (V)	laser power (%)
lopinavir	sodiated	651.4 → 439.3	52	10	60	40
ritonavir	sodiated	743.3 → 573.3	50	10	60	40
nelfinavir	sodiated	590.4 → 338.2	50	10	60	40
saquinavir	protonated	671.4 → 570.4	44	8	65	35
indinavir	protonated	614.4 → 421.2	44	12	50	35
nelfinavir	protonated	568.4 → 330.2	45	8	50	35
methotrexate	protonated	455.2 → 308.2	30	8	50	35

The skimmer was set at 0 V, CAD gas at 6, source gas at 10. CE = collision energy. CXP = collision cell exit potential. Plate = target plate containing the samples. Dwell time for each ion transition was 10 ms.

dard area ratios against the concentrations spiked using a 1/concentration^2 weighed linear curve. Quality controls were used to check the validity of the calibration curves. The absolute lower limit of quantification was set at the mean analyte area in the zero samples + 10 times the standard deviation. Samples were spotted onto Opti-TOF 384 well stainless steel target plates (123 x 81 mm; MDS Analytical Technologies, Concord, Ontario, Canada).

Plasma sample preparation for MALDI-triple quadrupole MS

Plasma samples were prepared in 1.5 mL Eppendorf safe-lock tubes: 10 µL plasma were added to methanol, mixed using a pipette, and spiked with internal standard, analytes, and additional drugs, depending on the type of sample. Calibrators: 70 µL MeOH + 10 µL plasma + 10 µL internal standard + 10 µL analytes. Quality controls: 60 µL MeOH + 10 µL plasma + 10 µL internal standard + 10 µL analytes + 10 µL drug mixture. Unknowns: 80 µL MeOH + 10 µL plasma + 10 µL internal standard. Blank: 90 µL MeOH + 10 µL plasma. Zero: 70 µL MeOH + 10 µL plasma + 10 µL internal standard + 10 µL drug mixture. For quantitation of lopinavir and ritonavir, nelfinavir (20 µM solution) was used. For quantitation of saquinavir, indinavir, and nelfinavir, methotrexate (5 µM solution) was used. To the quality control samples for lopinavir and ritonavir quantitation, drug mixture "A" was spiked containing carbamazepine, metoprolol, metronidazole, amoxicillin, piroxicam, nevirapine, saquinavir, efavirenz, indinavir, and tipranavir (10 µM each). To the quality control samples for saquinavir, indinavir, and nelfinavir, drug mixture "B" was spiked containing carbamazepine, metoprolol, metronidazole, amoxicillin, piroxicam, nevirapine, lopinavir, efavirenz, ritonavir, and tipranavir (10 µM each). Samples were extracted for at least one hour at 5°C and were then centrifuged at 14,000 rpm at room temperature for 5 minutes. Subsequently, supernatants were mixed with matrix solution (1:2, v/v), 0.75 µL matrix/sample mixture was deposited on three positions on the target plate and was dried at room temperature. MALDI-triple quadrupole MS measurements were carried out at the dept. Neurology (Erasmus MC, Rotterdam, the Netherlands).

HPLC-UV

Lopinavir and ritonavir concentrations in plasma were determined using a validated HPLC-UV assay as described previously [13]. HPLC-UV measurements were performed at the dept. Clinical Pharmacy (UMC St. Radboud, Nijmegen, the Netherlands). For the cross-validation, the samples were prepared independently at the two sites, and analytes and internal standards were not exchanged between the laboratories.

Patients and sampling

HIV-1 infected children included were from the outpatient clinic of the Erasmus MC – Sophia, Rotterdam, the Netherlands. All children were treated with Kaletra and two nucleoside reverse transcriptase inhibitors. Venous blood was drawn at a single time point during their routine visits at the outpatient clinical. For quantitation of lopinavir and ritonavir in plasma, blood was collected in lithium-heparinised tubes. Single time point plasma concentrations of lopinavir and ritonavir were determined during each visit at our outpatient clinic, which is part of our routine clinical care (HPLC-UV assay, dept Clinical Pharmacy UMC St. Radboud). Samples used for cross validation were obtained from an HIV-1 infected child who was admitted to our pediatric ward for determination of lopinavir and ritonavir plasma concentrations over a 12 hour time interval after observed intake of Kaletra. For quantitation of lopinavir and ritonavir in PBMC, venous blood was collected in one or two Vacutainer CPT tubes (BD, NJ, USA). The Vacutainer CPT tubes were transported to the laboratory immediately after drawing of the blood sample.

Isolation of PBMC from HIV infected patients

The Vacutainer CPT tubes were processed immediately upon arrival in the laboratory. Tubes were centrifuged at 1,750 x *g*, brake 5, at room temperature for 15 minutes. The plasma layer containing the PBMCs was transferred to 15 mL polypropylene tubes (Falcon conical tubes; BD, NJ, USA) and ice-cold PBS was added until a volume of 12 mL was reached. Samples were centrifuged at 350 x *g* with brake 9, at 4 °C for 6 minutes. The supernatant was discarded and the cell pellet was loosened by gently ticking against the tube. Two mL of red blood cell lysis buffer (room temperature) was added, and cells were incubated for 1 – 2 minutes while gently swirling the cells. Ice-cold PBS was added until a volume of 12 mL was reached. For part of the samples, the red blood cell lysis buffer was not used. In that case, ice-cold PBS was directly added after loosening of the cell pellet. Samples were centrifuged at 350 x *g* with brake 9, at 4°C for 6 minutes. The supernatant was discarded and ice-cold PBS was added until a volume of 12 mL was reached. Samples were centrifuged at 350 x *g*, brake 9, at 4°C for 6 minutes. For part of the samples, 1 mL of supernatant was collected to investigate the amount of drugs present in the final wash step, and the remaining supernatants were discarded.

We estimated that ~ 20 µL washing fluid remained on top of the cell pellet after discarding the supernatant. Cells were then suspended in a small volume of ice-cold PBS, typically 200 – 400 µL depending on the estimated amount of cells isolated. Nucleated cells were counted by trypan blue dye exclusion and/or Türks using a Burker-Türk counting chamber and a light microscope. Cell viability was over 95%. Subsequently, ice-cold PBS was added until a concentration was reached of one million PBMCs per 100 µL PBS. Cell suspensions were aliquoted as one million nucleated cells, i.e. PBMCs, in 100 µL per 1.5 mL polypropylene tube, and were stored at –80°C.

Isolation of PBMC from buffy coat

For preparation of the calibrators, quality controls, blanks, and zeros, PBMCs were isolated from a buffy coat (Sanquin, Rotterdam, the Netherlands) using a standard Ficoll density gradient. Nucleated cells were counted by trypan blue dye exclusion using a Burker-Türk cell chamber and a light microscope. Cell viability was over 95%. PBMCs were aliquoted in 1.5 mL polypropylene tubes at a concentration of 10 million cells in 500 µL PBS, and were subsequently stored at –80°C.

Preparation of PBMC from HIV infected patients

PBMC samples were thawed to room temperature. Subsequently, 300 µL MeOH was added and 20 µL internal standard (2 µM nelfinavir in MeOH). Samples were extracted for at least one hour at 5°C. Samples were then sonicated at 70% amplitude at -7°C for 10 seconds (Branson Digital Sonifier), and then further extracted at 5°C overnight. The next day, samples were centrifuged at 14,000 rpm at room temperature for 5 minutes, supernatants were collected and transferred to a 96-wells polypropylene plate. Nanopure water (800 µL) was added to each sample and the samples were processed using a 96-wells solid phase extraction (SPE) plate (Oasis HLB µelution plate, Waters Corporation, Milford, Massachusetts, USA). SPE wells were conditioned with 200 µL MeOH, and equilibrated with 200 µL nanopure water. Subsequently, the samples were loaded on to the SPE wells (600 µL twice). The wells were washed twice with 600 µL MeOH/nanopure water (1:3, v/v), and the samples were eluted from SPE wells with 50 µL MeOH twice. The eluates were collected in a polypropylene microtiter plate, and dried using a SpeedVac (~ 1 hour using a heated mantle at 45°C). Samples were then reconstituted in 10 µL matrix solution, 0.75 µL matrix/sample mixture was deposited on three positions on the target plate and dried at room temperature.

Preparation of PBMC obtained from buffy coat

PBMC samples (10 million PBMC in 500 µL PBS per vial) were thawed to room temperature, and 500 µL MeOH was added to each vial. Subsequently, samples were spiked with 20 µL internal standard (20 µM nelfinavir) and 20 µL analytes (Kaletra oral solution

diluted in MeOH). Samples were then sonicated at 70% amplitude at -7°C for 10 seconds (Branson Digital Sonifier). The equivalent of one million PBMC (104 µL) was transferred to a clean 1.5 mL polypropylene vial and 300 µL MeOH/PBS (5/1, v/v) was added. Samples were extracted at 5°C overnight and further processed as described above for the PBMC samples of HIV infected patients.

Safety statement

Blood samples of HIV infected patients were transported in closed containers and were processed in a biosafety level 2 laboratory. Extraction of the plasma and PBMC samples in methanol for one hour inactivated infectious HIV as reported previously [14,15]. Further sample preparation steps and measurements were performed under less stringent safety conditions.

Results

Plasma

First we tested the MALDI-triple quadrupole MS approach on plasma samples, which is currently the standard sample type for drug monitoring. A protein precipitation with methanol was used to prepare the plasma samples prior to MALDI-triple quadrupole MS analysis: Ten µL of plasma were diluted in 90 µL methanol. After mixing of the supernatants with matrix solution (α-cyano-hydroxycinnamic acid; CHCA; 1:2 v/v), samples were spotted in triplicate on to a 384-wells stainless steel target plate (0.75 µL per spot). The spots were measured in the selected reaction monitoring mode by moving the target plate in a straight horizontal line at a speed of 1 mm per second while firing of the laser at 1,000 Hz, which corresponds to an analysis time of 4.5 seconds per spot. Simultaneous quantification of lopinavir and ritonavir was achieved using nelfinavir as internal standard, and SRMs were performed on the sodium adducts of these drugs. For these analyses, sodium iodide (NaI) was added to the matrix solution to increase the intensity of the sodium adducts of the drugs. For the simultaneous quantification of saquinavir, indinavir, and nelfinavir, we used methotrexate as internal standard and SRMs were performed on the protonated forms of the drugs (for instrument settings see Table 1). The lower limits of quantification (LLOQ) obtained in plasma were 167 nM for lopinavir, 14.5 nM for ritonavir, 16 nM for nelfinavir, 16 nM for indinavir, and 3.2 nM for saquinavir, and the precisions and accuracies were within the criteria set by the FDA for bioanalysis [12]. Co-medication did not affect the performance of the assays, as shown by spiking of the quality control samples with an additional ten drugs at a plasma concentration of 10 µM each (see Table 2). The MALDI-triple quadrupole MS assay was used to determine a pharmacokinetic curve of lopinavir and ritonavir in an HIV-1 infected

Table 2. Quantitative analysis of HIV protease inhibitors in plasma.

			calibrators	quality controls
compound	**µM in plasma**	**fmol per spot**	**% deviation (%CV)**	**% deviation (%CV)**
lopinavir	40.71	1017.8	1.1 (1.3)	4.6 (1.0)
lopinavir	16.28	407	1.2 (2.3)	-1.1 (2.2)
lopinavir	6.51	162.8	-1.7 (2.8)	-0.5 (1.8)
lopinavir	2.61	65.3	-2.2 (1.9)	0.0 (2.7)
lopinavir	1.04	26	2.0 (5.2)	3.9 (3.4)
lopinavir	0.417	10.4	-0.4 (9.2)	6.0 (6.9)
lopinavir	0.167	4.2	0.0 (9.0)	-4.3 (8.6)
ritonavir	8.88	222	-0.2 (2.2)	5.7 (1.3)
ritonavir	3.55	88.8	2.0 (2.1)	0.2 (1.6)
ritonavir	1.42	35.5	-0.6 (1.7)	0.5 (1.5)
ritonavir	0.568	14.2	-1.3 (2.4)	1.3 (3.0)
ritonavir	0.227	5.7	-0.3 (3.4)	5.9 (4.5)
ritonavir	0.0909	2.3	1.6 (2.5)	4.6 (3.1)
ritonavir	0.0364	0.91	-1.7 (8.1)	5.2 (8.0)
ritonavir	0.0145	0.36	0.5 (12.2)	7.3 (11.0)
nelfinavir	10	250	-6.8 (4.3)	-13.3 (2.7)
nelfinavir	2	50	-4.4 (2.5)	-7.9 (2.6)
nelfinavir	0.4	10	4.8 (4.1)	-4.7 (2.4)
nelfinavir	0.08	2	8.1 (4.2)	-3.1 (4.1)
nelfinavir	0.016	0.4	-1.8 (4.4)	-10.1 (11.0)
indinavir	10	250	-4.4 (3.7)	-6.9 (2.4)
indinavir	2	50	-2.2 (1.8)	-5.0 (2.6)
indinavir	0.4	10	2.6 (3.6)	-2.4 (3.8)
indinavir	0.08	2	5.2 (4.7)	2.1 (4.2)
indinavir	0.016	0.4	-1.1 (7.4)	-1.9 (12.0)
saquinavir	10	250	-5.2 (5.1)	-9.9 (3.9)
saquinavir	2	50	-5.3 (2.1)	-8.8 (2.8)
saquinavir	0.4	10	1.2 (2.8)	-6.3 (2.4)
saquinavir	0.08	2	5.2 (3.7)	-6.9 (3.3)
saquinavir	0.016	0.4	5.5 (7.4)	2.4 (6.2)
saquinavir	0.0032	0.08	-1.3 (10.5)	-8.8 (14.9)

The first column shows the specific drug and the second column shows the concentration of the drug spiked in plasma in µM. The third column shows the actual amount of drug in femtomoles (fmol) in a single spot on the target plate. The fourth column shows the accuracies, expressed as % deviation, for samples used to construct the calibration curve (calibrators), and the fifth column show the accuracies for samples used to test the validity of the calibration curve (quality controls). Precisions, expressed as %CV, are reported between brackets (n= 9 spots on the target plate). For the analysis of lopinavir and ritonavir, quality controls were spiked with carbamazepine, metoprolol, metronidazol, amoxicillin, piroxicam, nevirapine, saquinavir, efavirenz, indinavir, and tipranavir at a plasma concentration of 10 µM each. For analysis of nelfinavir, saquinavir, and indinavir, quality controls were spiked with efavirenz, tipranavir, lopinavir, ritonavir, carbamazepine, metoprolol, metronidazol, amoxicillin, prioxicam, and nevirapine at a plasma concentration of 10 µM each. These drugs were not added to the calibrators. The calibrators were prepared in plasma from a different healthy donor than the quality controls were.

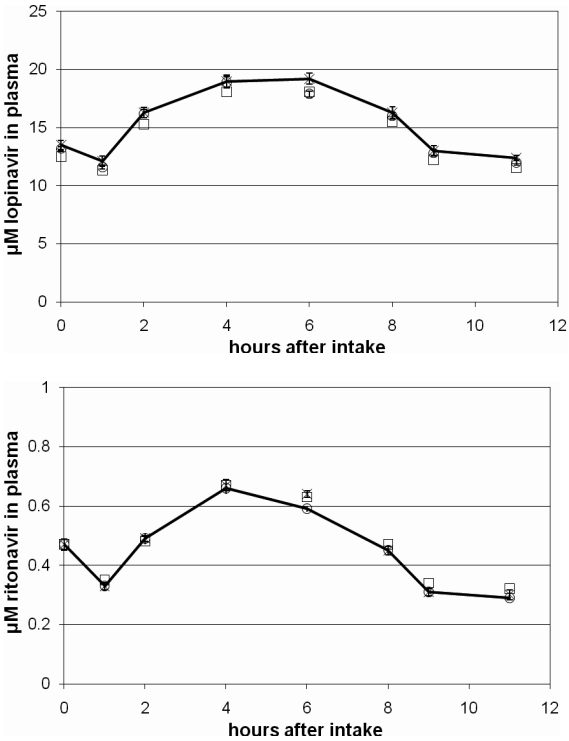

Figure 1. Lopinavir and ritonavir concentrations in an HIV infected child determined by HPLC-UV and by MALDI-triple quadrupole MS. Pharmacokinetic curve of lopinavir (above) and ritonavir (below) in one HIV infected child determined by HPLC-UV (squares), MALDI-triple quadrupole MS (circles), and MALDI-triple quadrupole MS when ten additional drugs (10 µM per drug) were spiked to the patient's samples (crosses).

child receiving Kaletra and two nucleoside reverse transcriptase inhibitors (NRTI) twice daily per os. Samples were also measured using a validated HPLC-UV assay (International Quality Control Program for Therapeutic Drug Monitoring in HIV infection, Department of Clinical Pharmacy, University Medical Center Nijmegen, the Netherlands) [13]. The two assays yielded similar results. For the MALDI-triple quadrupole MS assay, spiking of the patient's samples with an additional ten drugs (10 µM each) did not affect the results (see Figure 1 and Table 3).

PBMCs

We developed a MALDI-triple quadrupole MS assay for simultaneous quantification of lopinavir and ritonavir in one million peripheral blood mononuclear cells (PBMC). Internal standard (nelfinavir), matrix (CHCA), cationization agent (NaI), and instrument settings were the same as for the plasma analysis of these drugs. Following a methanol extraction of one million PBMC, samples were processed using solid phase extraction.

Table 3. Lopinavir and ritonavir concentrations in plasma in an HIV-1 infected child.

			no drugs added	drugs added	no drugs added	drugs added
time (h)	**compound**	**HPLC-UV**	**MALDI (%CV)**	**MALDI (%CV)**	**% deviation**	**% deviation**
0	lopinavir	12.5	13.2 (1.5)	13.5 (2.7)	5.7	8.4
	ritonavir	0.47	0.47 (3.2)	0.47 (4.1)	-1.1	0.2
1	lopinavir	11.3	11.6 (1.4)	12.1 (3.8)	3.0	6.8
	ritonavir	0.35	0.33 (2.2)	0.33 (3.6)	-6.6	-5.1
2	lopinavir	15.3	16.2 (2.2)	16.3 (2.7)	5.8	6.8
	ritonavir	0.48	0.49 (3.7)	0.49 (2.1)	1.6	2.6
4	lopinavir	18.1	18.9 (2.6)	19.0 (2.7)	4.3	5.2
	ritonavir	0.67	0.66 (2.9)	0.67 (2.9)	-1.0	-0.4
6	lopinavir	18.1	17.9 (1.4)	19.2 (2.5)	-1.2	6.2
	ritonavir	0.63	0.59 (1.7)	0.64 (1.8)	-6.6	1.4
8	lopinavir	15.5	16.0 (1.8)	16.3 (3.1)	3.3	5.0
	ritonavir	0.47	0.45 (2.3)	0.45 (3.2)	-3.4	-4.1
9	lopinavir	12.2	12.8 (2.0)	13.0 (3.3)	5.2	6.8
	ritonavir	0.34	0.31 (2.0)	0.31 (4.0)	-7.6	-7.5
11	lopinavir	11.5	12.0 (1.7)	12.4 (1.8)	4.2	8.2
	ritonavir	0.32	0.29 (2.5)	0.30 (5.4)	-10.1	-5.8

The first column shows the time points in hours at which blood samples were collected from one HIV-1 infected child after observed intake of Kaletra. The second column shows the components of Kaletra, i.e. lopinavir and ritonavir. The third column shows the concentration of the compounds in µM determined by HPLC-UV. The fourth and fifth columns show the concentration of the compounds in µM determined by MALDI-triple quadrupole MS. Three technical replicates were measured for each sample, i.e. three spots on the target plate. The precisions (%CV) are reported between brackets. The sixth and seventh columns show the deviations in percentage between the concentration of the compounds determined by MALDI-triple quadrupole MS and by HPLC-UV. For the MALDI-triple quadrupole MS analyses, one set of samples was spiked with an additional ten drugs ("drugs added") and one set was not ("no drugs added"). The additional ten drugs spiked were carbamazepine, metoprolol, metronidazol, amoxicillin, piroxicam, nevirapine, saquinavir, efavirenz, indinavir, and tipranavir at a plasma concentration of 10 µM each.

After drying, the samples were reconstituted in 10 µL matrix solution and were spotted in triplicate on to a 384-wells target plate (0.75 µL per spot). The LLOQ was 834 nM for lopinavir and 73 nM for ritonavir, and the precisions and accuracies were within the criteria set by the FDA for bioanalysis (see Table 4). Storage of the sample on the target plate in a closed container at ambient conditions for up to one month analyzed did not affect the precisions, accuracies, or LLOQs (data not shown).

The intracellular concentrations were determined by taking into account that one PBMC corresponds to an intracellular volume of 4×10^{-13} L. To assess the effect of solid phase extraction on the precisions and accuracies, we processed one set of plasma samples that were used for cross-validation with HPLC-UV using the solid phase extraction protocol for PBMCs, and we found that this step did not affect the precisions or

Table 4. Quantitative analysis of lopinavir and ritonavir in 1x10^6 PBMC.

				calibrators (n=3)	quality controls (n=33)
compound	**µM in PBMC**	**pmol 1x10^6 PBMC**	**fmol per spot**	**% deviation (%CV)**	**% deviation (%CV)**
lopinavir	203.5	81.4	6105	- 4.7 (4.0)	- 7.3 (7.2)
lopinavir	81.4	32.6	2442	- 1.1 (0.9)	- 0.9 (7.3)
lopinavir	32.6	13.0	977	- 1.0 (1.2)	2.1 (8.1)
lopinavir	13.0	5.2	391	5.4 (2.7)	2.4 (8.1)
lopinavir	5.2	2.1	156	0.8 (2.4)	1.2 (6.9)
lopinavir	2.1	0.834	63	1.6 (2.4)	- 2.4 (11.5)
lopinavir	0.834	0.334	25	- 1.1 (9.6)	- 2.5 (17.5)
ritonavir	44.4	17.8	1335	- 6.6 (4.2)	- 8.4 (6.8)
ritonavir	17.8	7.1	534	- 1.1 (0.2)	- 2.3 (5.6)
ritonavir	7.1	2.8	214	- 0.8 (1.4)	1.1 (5.8)
ritonavir	2.8	1.1	85	2.9 (1.7)	2.0 (4.9)
ritonavir	1.1	0.455	34	0.3 (1.2)	1.1 (5.3)
ritonavir	0.455	0.182	14	5.2 (2.7)	0.6 (7.4)
ritonavir	0.182	0.073	5.5	1.5 (2.2)	- 2.1 (7.2)
ritonavir	0.073	0.029	2.2	- 1.5 (6.2)	- 13.4 (13.7)

The regression coefficient were > 0.998

Table 5. Repeat analysis of PBMC aliquots obtained from HIV-1 infected children.

		aliquot 1			**aliquot 2**			**aliquot 3**			**mean**	**%CV**
patient	drug	spot 1	spot 2	spot 3	spot 1	spot 2	spot 3	spot 1	spot 2	spot 3		
1	LPV	2.61	2.70	2.70	2.71	2.84	2.73	2.80	3.14	2.90	2.79	5.6
2	LPV	4.66	5.34	5.01	3.97	4.22	4.01	4.48	4.00	4.88	4.51	11.1
3	LPV	2.11	2.05	2.08	2.43	2.48	2.47	2.13	2.24	2.65	2.29	9.5
1	RTV	0.299	0.279	0.322	0.290	0.278	0.277	0.340	0.313	0.309	0.301	7.3
2	RTV	0.495	0.478	0.469	0.401	0.427	0.396	0.427	0.443	0.459	0.444	7.7
3	RTV	0.336	0.351	0.346	0.336	0.347	0.359	0.375	0.354	0.369	0.352	3.8

For three HIV-1 infected children receiving Kaletra once daily, three aliquots of one million PBMC each were processed as described in the text (solid phase extraction followed by methanol extraction, and spotting in triplicate) to determine the overall precisions (%CV) of PBMC processing and sample measurements. Shown are the concentrations of lopinavir (LPV) and ritonavir (RTV) in µM as determined in a single spot on the target plate.

the accuracies for lopinavir and ritonavir (data not shown). Shown in Table 5 are the precisions for biological replicates, i.e. analysis of multiple PBMC aliquots from HIV infected children (three aliquots per child). The protocol for isolation of PBMCs is shown in Figure 2.

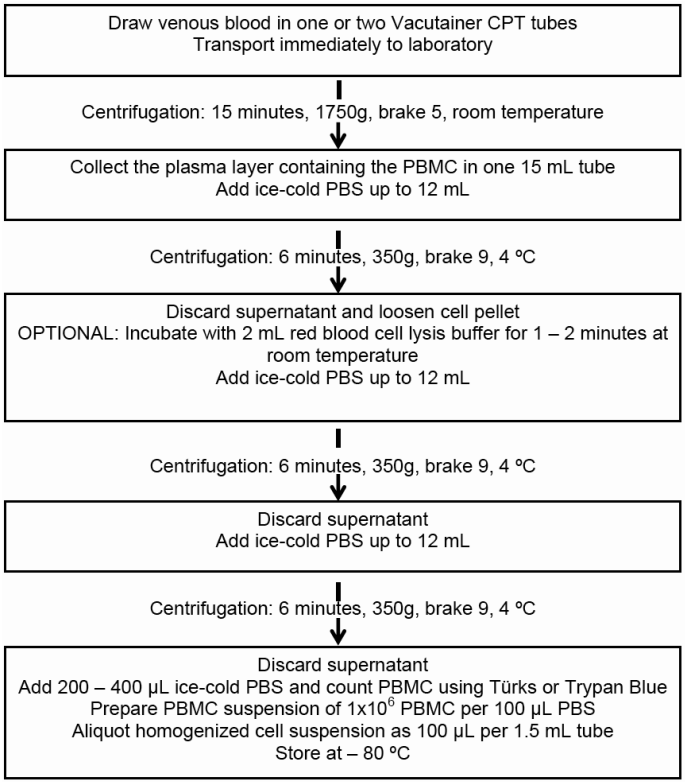

Figure 2. PBMC isolation protocol.

Assessment of the purity of the cells aliquoted showed that 4.6 x 10^5 erythrocytes (sd 3.4 x 10^5, n=5) were present per aliquot of 1 x 10^6 PBMCs. Treatment of the cells isolated with red blood cell lysis buffer (2 minutes, room temperature) during the washing procedure resulted in > 2 Log reduction in the number of erythrocytes per million PBMCs (mean 3.8 x 10^3 erythrocytes, sd 5.9 x 10^3, n=5). For eight HIV-1 infected children receiving Kaletra and 2 NRTIs once daily, we determined the concentrations of lopinavir and ritonavir in the final wash step and found that these constitute less than 4.5% (lopinavir) and less than 8.7% (ritonavir) of the amount measured in one aliquot of one million PBMCs.

Application

The MALDI-triple quadrupole MS assay was used to determine the intracellular concentrations of lopinavir and ritonavir in PBMC obtained from HIV-1 infected children receiving Kaletra (lopinavir + ritonavir) and two NRTIs once daily. Part of the samples was processed with red blood cell lysis buffer and part without to further investigate the effect of using this buffer on the concentrations determined. Plasma concentrations of lopinavir and ritonavir were determined by HPLC-UV, which is part of the routine clinical

Table 6. Plasma and intracellular concentrations of lopinavir and ritonavir in HIV-1 infected children.

	RBCLB+ (n=17)	RBCLB- (n=8)	p-value
µM lopinavir plasma	16.1 (9.8 – 21.2)	15.7 (10.3 – 19.7)	0.930
µM lopinavir PBMC	4.4 (2.8 – 6.0)	3.3 (3.0 – 7.1)	0.975
PBMC / plasma ratio lopinavir	0.34 (0.19 – 0.39)	0.26 (0.18 – 0.36)	0.634
µM ritonavir plasma	0.62 (0.36 – 1.17)	0.72 (0.42 – 0.90)	0.884
µM ritonavir PBMC	0.32 (0.28 – 0.35)	0.89 (0.49 – 1.23)	0.001
PBMC / plasma ratio ritonavir	0.46 (0.31 – 0.70)	1.53 (0.85 – 2.36)	0.004
Hours after intake	16.0 (14.8 – 17.3)	14.5 (13.3 – 16.5)	0.243
Age	10.5 (8.6 – 13.7)	10.5 (8.9 – 13.0)	0.861
PBMC processing time (minutes)	80 (75 – 90)	78 (72 – 83)	0.188

Values between brackets are expressed as medians (25^{th} percentile – 75^{th} percentile). P values were determined using a Mann Whitney U test. All patients administered Kaletra (lopinavir + ritonavir) + 2 NRTIs once daily. RBCLB+ = PBMCs treated with red blood cell lysis buffer. RBCLB- = PBMCs not treated with red blood cell lysis buffer. The RBCLB+ group consisted of 16 HIV-1 infected children. For one child, concentrations were determined during two separate visits at the outpatient clinic. RBCLB- group consisted of 8 HIV-1 infected children. Three children were included in both the RBCLB+ group and RBCLB- group as for these patients samples were processed with and without RBCLB. Plasma concentrations were determined by HPLC-UV and intracellular concentrations by MALDI-triple quadrupole MS. For one patient in the RBCLB- group, intracellular concentration of lopinavir was below the LLOQ while the intracellular concentration of ritonavir was above the LLOQ. Hours after intake = time difference in hours between medication intake and drawing of the blood sample. PBMC processing time = time difference between drawing of the blood sample and aliquoting of the PBMC.

Table 7. Correlations between plasma and intracellular levels, and correlations between the concentrations of the two drugs in HIV-1 infected children.

	RBCLB+ (n=17)	RBCLB- (n=8)
lopinavir and ritonavir in plasma	0.973 (0.01)	0.952 (0.01)
lopinavir and ritonavir in PBMC	0.613 (0.01)	0.757 (0.05)
lopinavir in plasma and in PBMC	0.475 (NS)	0.613 (NS)
Ritonavir in plasma and in PBMC	0.510 (0.05)	0.500 (NS)
PBMC/plasma ratio lopinavir and PBMC/ plasma ratio ritonavir	0.604 (0.05)	0.464 (NS)
lopinavir in plasma and in PBMC	0.531 (0.01) (RBCLB+ and RBCLB- combined)	
lopinavir and ritonavir in plasma	0.965 (0.01) (RBCLB+ and RBCLB- combined)	

Correlations were calculated using a Spearman correlation. Significance levels are reported between brackets. NS = not significant.

care in our setting. Blood samples were drawn at a single time point after medication intake. Plasma and intracellular concentrations of lopinavir and ritonavir are shown in Table 6, and the correlations are shown in Table 7. Scatter plots are shown in Figure 3.

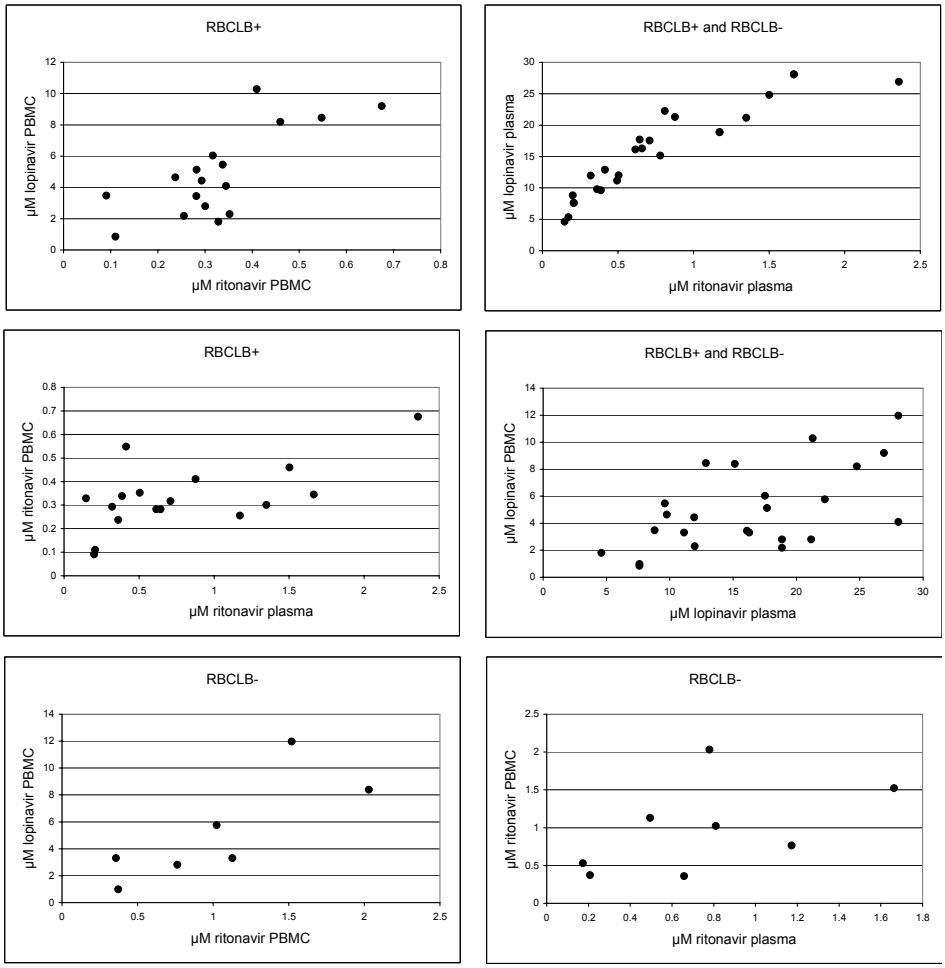

Figure 3. Scatter plots of lopinavir and ritonavir concentrations in plasma and in PBMC obtained from HIV-1 infected children.

Discussion

In this paper, we show a MALDI-triple quadrupole MS approach for ultra-fast determination of plasma and intracellular concentrations of drugs. This approach offers several advantages over the traditionally used LC-based assays such as HPLC-UV and LC-MS/MS. Most importantly, the analysis time is considerably shorter; in this case samples were measured at a speed of 13.5 seconds per sample (triplicate analysis). For the traditional approach, typical analysis times for HIV protease inhibitors, the model compounds used in this study, are 23 minutes when HPLC-UV is used, and 6 minutes (plasma) or 20 minutes (PBMCs) when LC-MS/MS is used [13,16,17]. Furthermore, the sample preparation

techniques used prior to MALDI-triple quadrupole MS analysis allow for fast and automated processing of large numbers of samples, e.g. in 96-wells plate format. Normally, these sample preparation techniques are also used for subsequent analysis by LC-based assays. Plasma and cells were extracted in methanol, which simultaneously inactivates infectious HIV [14,15]. For plasma, no further sample preparation steps were needed, i.e. the lysates were mixed with matrix solution and deposited on a target plate. Drying of the plasma lysates after protein precipitation and subsequent reconstitution in a small volume of matrix solution resulted in poor crystallization of the samples and severe loss in sensitivity, which is in agreement with two previous reports [2,17]. In our approach, the plasma samples are simply diluted 30 times, which results in good crystallization and highly sensitive measurements. In this study we used HIV protease inhibitors as model compounds, but the approach is also applicable to other drugs. For example, we were able to quantify methotrexate down to 5 nM in plasma (data not shown).

The MALDI-triple quadrupole MS approach allows for multi-target quantitation using a chemical analogue as internal standard. Although chemical analogue internal standards are considered to be inferior compared to stable isotope labelled internal standards, accuracies and precisions were within the criteria of the FDA for bioanalysis, and co-medication did not affect the performance of the assays.

Only a small amount of material was needed for analyses, 10 µL plasma or one million cells, which allowed application of the MALDI-triple quadrupole MS assay for clinical pharmacokinetic research in children. The amount of sample consumed in MALDI-MS is very low; at the LLOQ for saquinavir, a total amount of only 80 attomoles is present in each spot. It should be noted that only 2% - 4% of a spot is consumed during the measurement procedure [4]. Furthermore, samples co-crystallized with matrix are stable at ambient conditions for up to a month. Thus, samples can be stored and measured multiple times with the same or a different type of MALDI mass spectrometer.

The MALDI-triple quadrupole MS assay was used to investigate the intracellular concentrations of lopinavir and ritonavir in relation to their plasma concentrations in HIV-1 infected children receiving Kaletra, a co-formulation of the HIV protease inhibitors lopinavir and ritonavir (4:1, w/w), once daily. Both drugs are metabolized in the liver by CYP3A4 isoenzymes. Ritonavir inhibits the CYP3A4-mediated metabolism, thereby enhancing the pharmacokinetic properties of lopinavir [18]. This is in agreement with the strong correlation ($r = 0.97$, $p = 0.01$) that we found between the plasma concentrations of lopinavir and the plasma concentrations of ritonavir in HIV-1 infected children. Ribera et al. also found a correlation between the plasma AUC of lopinavir and ritonavir in HIV-1 infected adults, although this correlation was less pronounced ($r = 0.63$, $p < 0.001$) [19].

Whether lopinavir and ritonavir enter the cellular compartment in blood by passive diffusion, active transport, or a combination of both, is currently unknown. Passive

diffusion is likely to occur as lopinavir and ritonavir are both lipophilic drugs with an octanol/saline partition coefficient of 214 and 22.2, respectively, and are thus able to cross the plasma membrane and enter the cells. Active transport into cells has not been reported yet. On the other hand, lopinavir and ritonavir are substrates for drug efflux pumps, although there is no correlation between drug efflux pumps and intracellular concentrations of HIV protease inhibitors in HIV infected patients [20,21]. It should be noted that only free, unbound, and non-ionized drugs can cross the cell membrane by passive diffusion. *In vivo*, the unbound concentrations of lopinavir and ritonavir are only 1 – 2% of the total amount in plasma. *In vitro* studies have already shown that this significantly affects the accumulation of protease inhibitors [22,23]. It is expected that lopinavir and ritonavir are also highly bound to proteins within cells. To which proteins and to what extent is currently unknown.

Disposition studies of lopinavir and ritonavir in rats showed that both HIV protease inhibitors penetrate poorly into the cellular fraction of blood. Literature indicates a whole blood / plasma ratio of 0.5 for lopinavir and a whole blood / plasma ratio of 0.26 to 0.68 for ritonavir [24,25]. Koal et al. also reported lower concentrations of HIV protease inhibitors in whole blood compared to plasma in HIV infected patients [26]. For one HIV-1 infected child, we found that the analyte-to-internal standard ratio were ~ 20% lower in whole blood compared to plasma. This shows that lopinavir and ritonavir penetrate poorly into the cellular fraction of blood. It should be noted that the cellular fraction of whole blood consists for > 99% of erythrocytes, and that differences may exist between penetration in erythrocytes and in PBMC.

Accumulation of lopinavir [27,28] and ritonavir [28] in PBMC has been reported in HIV-1 infected adults receiving Kaletra BID: Breilh et al. reported a PBMC / plasma ratio of lopinavir of 3.2 (month 1) and 2.4 (month 6) in patients who responded to therapy, and 2.3 (month 1) and 1.4 (month 6) in patients who failed on therapy [27]. Ritonavir concentrations were not determined in this study. Crommentuyn et al. reported a PBMC / plasma ratio of 1.18 for lopinavir and 4.59 for ritonavir in HIV-1 infected adults receiving Kaletra BID [28]. Ritonavir accumulation was also reported by Khoo et al. They observed a PBMC / plasma ratio of 1 when ritonavir is administered as sole protease inhibitor, 1.25 using ritonavir-boosted saquinavir, and 1.8 using ritonavir-boosted indinavir [29]. On the other hand, Colombo et al. reported a PBMC / plasma ratio of 0.55 for lopinavir in HIV infected adults [16,30]. Ehrhardt et al. showed in one healthy volunteer that, after a single dose of Kaletra, lopinavir concentrations were lower in PBMCs than in plasma, but ritonavir concentrations were higher in PBMCs than in plasma [31].

In this study, we found lower lopinavir concentrations in PBMCs than in plasma in HIV-1 infected children receiving Kaletra once daily. For ritonavir, accumulation in PBMCs was highly dependent on the sample preparation used. When erythrocytes were removed by RBCLB no accumulation was found, while accumulation was found when not using

RBCLB. This shows that sample preparation can have a major influence on the concentrations measured. This step was included in the sample preparation protocol because of the erythrocytes present in cell suspensions after Ficoll density gradient centrifugation and subsequent thorough washing of the cells. Although cells were incubated for only two minutes in this buffer, we cannot exclude efflux of ritonavir because this incubation occurred at room temperature. However, this does not explain the lower PBMC concentrations compared to plasma for lopinavir as there were no significant differences in the PBMC / plasma ratio when PBMC were prepared with RBCLB or without RBCLB.

In our opinion, the higher PBMC / plasma ratios when RBCLB is not used is not due to high intracellular concentrations of ritonavir in erythrocytes. Previous studies have already shown poor penetration of this drug in blood cells (see above). In addition, when RBCLB was not used, the erythrocyte / PBMC ratio in the cell preparation was ~ 1:2 (count/count), and the intracellular volume of an erythrocyte is lower (~ 80 fL) compared to that of an average PBMC (~ 400 fL). An explanation might be that, due to erythrocyte lysis, proteins are released into the lysis buffer and that ritonavir bound to proteins on the outside of the plasma membrane now bind to the erythrocyte-derived proteins in the buffer. Ritonavir but also lopinavir are highly bound in plasma to albumin and α1-acid glycoprotein [18]. *In vitro* studies have already shown that higher protein concentrations in cell cultures result in significantly lower intracellular concentrations [22,23].

We found a correlation between the intracellular concentrations of lopinavir and the intracellular concentrations of ritonavir ($r = 0.61$, $p = 0.01$ and $r = 0.76$, $p = 0.05$; RBCLB+ and RBCLB-, respectively). This is in agreement with previous reports on ritonavir-boosted saquinavir and ritonavir-boosted indinavir [20,29,32]. To our best knowledge this is the first time such correlation is shown for Kaletra. We found that the correlation between the plasma concentrations and intracellular concentrations of lopinavir ($r = 0.53$, $p = 0.01$) or ritonavir ($r = 0.51$, $p = 0.05$ and $r = 0.5$, NS; RBCLB+ and RBCLB- respectively) were less pronounced. Breilh et al. showed for HIV-1 infected adults receiving Kaletra BID that the plasma concentrations of lopinavir correlated with the intracellular concentrations of lopinavir after one month of treatment ($r^2 = 0.72$, $p < 10^{-6}$). Yet, this correlation was not found after six months of treatment ($r^2=0.17$, $p = 0.3$) [27]. For ritonavir, this correlation was not assessed. For ritonavir-boosted saquinavir, the plasma concentrations of ritonavir correlated poorly to the intracellular concentrations: $r^2 = 0.33$; $p = 0.053$ and $r^2 = 0.31$, $p = 0.06$) [20,32]. Above shows that lopinavir levels and ritonavir levels correlate to each other within the same compartment, i.e. plasma or PBMC, but also that for each drug the correlation between these compartments is poor.

In conclusion, we have developed a novel assay for the fast and sensitive quantification of compounds that can be applied to monitor drugs in plasma and intracellularly in treatment of various illnesses including antiviral treatment.

Acknowledgements

This work was supported by a grant from Top Institute Pharma (project T4-212). The consortium of project T4-212 consists of the departments of Neurology and Virology of the Erasmus MC (Rotterdam, the Netherlands), the departments of Pediatrics and Clinical Pharmacy of the UMC St. Radboud (Nijmegen, the Netherlands), TNO Quality-of-Life (Zeist, the Netherlands), and GlaxoSmithKline (Zeist, the Netherlands). Jeroen van Kampen is supported by a grant from Aids Fonds, the Netherlands (project 2004051), and Rob Gruters is supported by VIRGO. HIV protease inhibitors were kindly donated by F. Hoffmann La-Roche (saquinavir), Pfizer (nelfinavir), Abbott Laboratories (lopinavir and ritonavir), Boehringer Ingelheim (nevirapine and tipranavir), and Merck (indinavir). We would like to thank the patients for participation in this study.

References

1. Corr JJ, Kovarik P, Schneider BB, Hendrikse J, Loboda A, Covey TR. Design considerations for high speed quantitative mass spectrometry with MALDI ionization. J Am Soc Mass Spectrom 2006; 17(8):1129-41.
2. Gobey J, Cole M, Janiszewski J, et al. Characterization and performance of MALDI on a triple quadrupole mass spectrometer for analysis and quantification of small molecules. Anal Chem 2005;77(17):5643-54.
3. Hatsis P, Brombacher S, Corr J, Kovarik P, Volmer DA. Quantitative analysis of small pharmaceutical drugs using a high repetition rate laser matrix-assisted laser/desorption ionization source. Rapid Commun Mass Spectrom 2003;17(20):2303-9.
4. Sleno L, Volmer DA. Some fundamental and technical aspects of the quantitative analysis of pharmaceutical drugs by matrix-assisted laser desorption/ionization mass spectrometry. Rapid Commun Mass Spectrom 2005;19(14):1928-36.
5. Sleno L, Volmer DA. Toxin screening in phytoplankton: detection and quantitation using MALDI triple quadrupole mass spectrometry. Anal Chem 2005;77(5):1509-17.
6. van Kampen JJ, Burgers PC, Gruters RA, et al. Quantitative analysis of antiretroviral drugs in lysates of peripheral blood mononuclear cells using MALDI-triple quadrupole mass spectrometry. Anal Chem 2008;80(13):4969-75.
7. Volmer DA, Sleno L, Bateman K, et al. Comparison of MALDI to ESI on a Triple Quadrupole Platform for Pharmacokinetic Analyses. Anal Chem 2007.
8. Onnerfjord P, Ekstrom S, Bergquist J, Nilsson J, Laurell T, Marko-Varga G. Homogeneous sample preparation for automated high throughput analysis with matrix-assisted laser desorption/ ionisation time-of-flight mass spectrometry. Rapid Commun Mass Spectrom 1999;13(5):315-22.
9. Sleno L, Volmer DA. Assessing the properties of internal standards for quantitative matrix-assisted laser desorption/ionization mass spectrometry of small molecules. Rapid Commun Mass Spectrom 2006;20(10):1517-24.
10. van Kampen JJ, Burgers PC, de Groot R, Luider TM. Qualitative and quantitative analysis of pharmaceutical compounds by MALDI-TOF mass spectrometry. Anal Chem 2006;78(15):5403-11.
11. Vorm O, Roepstorff P, Mann M. Improved resolution and very high sensitivity in MALDI TOF of matrix surfaces made by fast evaporation. Anal Chem 1994;66(19):3281-7.
12. Guidance for industry: bioanalytical method validation. FDA 2001 available at http://www.fda.gov/cder/guidance/4252fnl.pdf.
13. Droste JA, Verweij-Van Wissen CP, Burger DM. Simultaneous determination of the HIV drugs indinavir, amprenavir, saquinavir, ritonavir, lopinavir, nelfinavir, the nelfinavir hydroxymetabolite M8, and nevirapine in human plasma by reversed-phase high-performance liquid chromatography. Ther Drug Monit 2003;25(3):393-9.
14. van Bueren J, Larkin DP, Simpson RA. Inactivation of human immunodeficiency virus type 1 by alcohols. J Hosp Infect 1994;28(2):137-48.
15. van Kampen JJ, Verschuren EJ, Burgers PC, et al. Validation of an HIV-1 inactivation protocol that is compatible with intracellular drug analysis by mass spectrometry. J Chromatogr B Analyt Technol Biomed Life Sci 2007;847(1):38-44.
16. Colombo S, Beguin A, Telenti A, et al. Intracellular measurements of anti-HIV drugs indinavir, amprenavir, saquinavir, ritonavir, nelfinavir, lopinavir, atazanavir, efavirenz and nevirapine in peripheral blood mononuclear cells by liquid chromatography coupled to tandem mass spectrometry. J Chromatogr B Analyt Technol Biomed Life Sci 2005;819(2):259-76.

17. Wagner M, Varesio E, Hopfgartner G. Ultra-fast quantitation of saquinavir in human plasma by matrix-assisted laser desorption/ionization and selected reaction monitoring mode detection. J Chromatogr B Analyt Technol Biomed Life Sci 2008;872(1-2):68-76.
18. Cvetkovic RS, Goa KL. Lopinavir/ritonavir: a review of its use in the management of HIV infection. Drugs 2003;63(8):769-802.
19. Ribera E, Lopez RM, Diaz M, et al. Steady-state pharmacokinetics of a double-boosting regimen of saquinavir soft gel plus lopinavir plus minidose ritonavir in human immunodeficiency virus-infected adults. Antimicrob Agents Chemother 2004;48(11):4256-62.
20. Ford J, Boffito M, Wildfire A, et al. Intracellular and plasma pharmacokinetics of saquinavir-ritonavir, administered at 1,600/100 milligrams once daily in human immunodeficiency virus-infected patients. Antimicrob Agents Chemother 2004;48(7):2388-93.
21. Hoggard PG, Owen A. The mechanisms that control intracellular penetration of the HIV protease inhibitors. J Antimicrob Chemother 2003;51(3):493-6.
22. Bilello JA, Bilello PA, Stellrecht K, et al. Human serum alpha 1 acid glycoprotein reduces uptake, intracellular concentration, and antiviral activity of A-80987, an inhibitor of the human immunodeficiency virus type 1 protease. Antimicrob Agents Chemother 1996;40(6):1491-7.
23. Jones K, Hoggard PG, Khoo S, Maher B, Back DJ. Effect of alpha1-acid glycoprotein on the intracellular accumulation of the HIV protease inhibitors saquinavir, ritonavir and indinavir in vitro. Br J Clin Pharmacol 2001;51(1):99-102.
24. Denissen JF, Grabowski BA, Johnson MK, et al. Metabolism and disposition of the HIV-1 protease inhibitor ritonavir (ABT-538) in rats, dogs, and humans. Drug Metab Dispos 1997;25(4):489-501.
25. Kumar GN, Jayanti VK, Johnson MK, et al. Metabolism and disposition of the HIV-1 protease inhibitor lopinavir (ABT-378) given in combination with ritonavir in rats, dogs, and humans. Pharm Res 2004;21(9):1622-30.
26. Koal T, Burhenne H, Romling R, Svoboda M, Resch K, Kaever V. Quantification of antiretroviral drugs in dried blood spot samples by means of liquid chromatography/tandem mass spectrometry. Rapid Commun Mass Spectrom 2005;19(21):2995-3001.
27. Breilh D, Pellegrin I, Rouzes A, et al. Virological, intracellular and plasma pharmacological parameters predicting response to lopinavir/ritonavir (KALEPHAR study). Aids 2004;18(9):1305-10.
28. Crommentuyn KM, Mulder JW, Mairuhu AT, et al. The plasma and intracellular steady-state pharmacokinetics of lopinavir/ritonavir in HIV-1-infected patients. Antivir Ther 2004;9(5):779-85.
29. Khoo SH, Hoggard PG, Williams I, et al. Intracellular accumulation of human immunodeficiency virus protease inhibitors. Antimicrob Agents Chemother 2002;46(10):3228-35.
30. Colombo S, Telenti A, Buclin T, et al. Are plasma levels valid surrogates for cellular concentrations of antiretroviral drugs in HIV-infected patients? Ther Drug Monit 2006;28(3):332-8.
31. Ehrhardt M, Mock M, Haefeli WE, Mikus G, Burhenne J. Monitoring of lopinavir and ritonavir in peripheral blood mononuclear cells, plasma, and ultrafiltrate using a selective and highly sensitive LC/MS/MS assay. J Chromatogr B Analyt Technol Biomed Life Sci 2007;850(1-2):249-58.
32. Ford J, Boffito M, Maitland D, et al. Influence of atazanavir 200 mg on the intracellular and plasma pharmacokinetics of saquinavir and ritonavir 1600/100 mg administered once daily in HIV-infected patients. J Antimicrob Chemother 2006;58(5):1009-16.

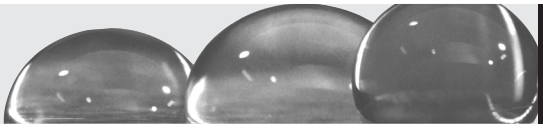

Chapter 11

Biomedical application of MALDI mass spectrometry for small-molecule analysis

Jeroen J.A. van Kampen, Peter C. Burgers,
Ronald de Groot, Rob A. Gruters, Theo M. Luider

Mass Spectrometry Reviews 2009, in press

Abstract

Matrix-assisted laser desorption/ionization (MALDI) mass spectrometry is an emerging analytical tool for the analysis of molecules with molar masses below 1,000 Daltons; i.e., small molecules. This technique offers rapid analysis, high sensitivity, low sample consumption, a relative high tolerance towards salts and buffers, and the possibility to store samples on the target plate. The successful application of the technique is, however, hampered by low molecular weight (LMW) matrix-derived interference signals and by poor reproducibility of signal intensities during quantitative analyses. In this review, we focus on the biomedical application of MALDI mass spectrometry for the analysis of small molecules, and discuss its favorable properties and its challenges as well as strategies to improve the performance of the technique. Furthermore, practical aspects and applications are presented.

I. Introduction

MALDI mass spectrometry (MS) has gained a prominent role in the analysis of biopolymers such as proteins, peptides, oligonucleotides, and oligosaccharides. Yet, this technique is not commonly applied to the analysis of molecules with molar masses below 1,000 Da, which are called small molecules or LMW molecules. For this application, MALDI-MS has found strong competition from the combination of liquid chromatography (LC) with atmospheric pressure ionization MS (LC-MS), in particular from the combination of LC and electrospray ionization (ESI) MS. Unambiguous annotation of MALDI mass spectra of LMW compounds can be complicated due to the presence of matrix-derived peaks in the low mass range; i.e., below *m/z* 1,000. The poor reproducibilities of signal intensities that have frequently been reported for MALDI-MS hampered its application to quantitative analysis.

Notwithstanding the above, MALDI-MS has some intrinsic properties that favor its use for the analysis of LMW molecules such as its high tolerance towards salts and buffers, rapid analyses, its high absolute sensitivity, the small amount of sample consumed during analysis, and the possibility to store samples on a target plate for longer periods of time. These intrinsic properties of MALDI-MS have inspired scientists to find ways to improve the performance of this technique for the analysis of LMW compounds. A variety of approaches have been described to decrease or circumvent matrix-related peaks, such as the use of high molecular weight matrices, alternative sample preparation procedures, and application of tandem mass spectrometry. Reproducibility of signal intensities can be improved, for example, with internal standards, and by procedures to enhance homogeneous crystallization of matrix and sample. Recently, a MALDI-triple quadrupole mass spectrometer has been introduced, which is the first MALDI mass spectrometer developed specifically for the quantitative analysis of LMW compounds. Although MALDI-MS is gaining acceptance as an analytical tool for the analysis of LMW compounds, application of the technique to this field is still limited.

In this review, we discuss the biomedical application of MALDI-MS to the analysis of LMW compounds. The review published in 2002 also deals with the analysis of small molecules by MALDI-MS, and serves as an excellent background to the present report [1]. We first discuss the properties of MALDI-MS that favor its application to the analysis of LMW molecules, which are the high-throughput analysis, its relative insensitivity for ion suppression in complex and clinical samples, the high absolute sensitivity, the low sample consumption, and the storage of samples on target plates. The two main challenges of MALDI-MS for small molecule analysis are discussed, which are the interfering signals derived from the MALDI matrix and the poor reproducibility of signal intensities. Strategies are presented to overcome these challenges. Practical aspects of small-molecule analysis are discussed, which are cationization agents, MS and MS/MS

strategies, and preparation of biological samples. We focus on the application of MALDI-MS to the quantitative analysis of drugs, metabolomics, and monitoring of enzymatic conversion of small molecules. Finally, we present our thoughts on the future directions of MALDI-MS to the analysis of LMW compounds.

II. Choice of MALDI for Small-molecule Analysis

A. High-throughput analysis

For MALDI-MS, offline sample preparation techniques such as solid-phase extraction (SPE), liquid-liquid extraction (LLE), and protein precipitation (PP) provide sufficiently clean extracts of biological samples for direct analysis. These sample preparation techniques are performed offline (i.e., sample preparation and MALDI measurements are completely decoupled), and are highly suited for the simultaneous preparation of relatively large sets of samples. To increase the throughput of sample preparation prior to MALDI-MS, these relatively easy sample extraction methods as well as spotting of samples onto target plates can readily be automated with 96- or 384-well formats. MALDI-MS is less susceptible to ion suppression compared to ESI-MS [2], and a LC step is normally not needed to prepare samples of biological origin.

The major contributor to the total analysis time in LC-MS is the LC step. For quantitative analysis of pharmaceutical compounds in biological samples, the LC step still takes several minutes, even with new LC developments such as monolithic columns and ultra-pressure liquid chromatography. In MALDI-MS, however, the sample analysis time is primarily determined by the number of laser shots needed to generate an average mass spectrum of high quality and the repetition rate of the laser used. Dwell time of the ions does not contribute significantly to the analysis time, although the detection time of ions can take second(s) per scan in Fourier-transform ion cyclotron resonance (FTICR) MS and Orbitrap MS. With a high repetition rate laser that fires at 1,000 – 2,000 Hz, an averaged mass spectrum of high quality can be obtained in a few seconds with MALDI-TOF MS or MALDI-triple quadrupole MS [3-6]. For quantitative analysis of, for instance, HIV protease inhibitors, analysis times for a single spot on the target plate have been reported of ~ 3 minutes for MALDI-FTICR MS (20-Hz laser), ~ 30 seconds for MALDI-TOF MS (50-Hz laser), and ~ 5 seconds for MALDI-triple quadrupole MS (1,000-Hz laser) [7-10]. Recently, an analysis time of 1.75 minutes for an entire 384-well target plate was reported for an assay to screen for small-molecule inhibitors of enzymes with MALDI-triple quadrupole MS [6]. When the time required for vacuum pump down was included, the total analysis time for a single target plate was still just under 3.5 minutes.

B. Ion suppression

In MALDI-MS, strong signals can be obtained for analytes that are present in complex biological samples and in samples that contain salts and buffers that are frequently used in biomedical research. Various studies report in detail on the effect of various buffers and salts on the MALDI MS analysis of biopolymers such as proteins, peptides, and DNA [11-16]. Such studies have not yet been performed for pharmaceutical compounds. Some general statements on contaminants and tolerance limits can be made: (1) Contaminants can affect analyte signals by inducing extensive, concentration-dependent adduct formation such as salts. Also, crystallization of the sample might be impaired when contaminants such as Tris and urea are present [15]. (2) The tolerance limits for a contaminant can depend on the type of analyte under investigation. For example, the tolerance limit for alkali metal salt impurities in protein and peptide analysis is ~ 1 M, whereas it is 10^{-2} M for DNA [15]. On the other hand, the tolerance limit for the buffer Tris is comparable for proteins, peptides, and DNA (~ 0.5 M) [13,15,16]. (3) The tolerance limit depends on the type of contaminant. In particular, phosphate buffers are known to quench analyte signals [13,14]. (4) The effect of buffers on the sample crystallization is matrix-dependent. For example, Kallweit et al., showed that crystallization of 2,5-dihydroxybenzoic acid (2,5-DHB) and in particular of 2,6-dihydroxyacetophenone is more affected by commonly used buffers compared to sinapinic acid (SA) [13]. (5) Sample preparation might influence tolerance limits. For example, buffer tolerances are increased significantly when higher matrix-to-analyte ratios are used [16], and additives such as diammoniumhydrogencitrate (DAHC) can improve the tolerance of the matrices against the buffers and salt adduct formation [13]. Recently, a comprehensive database has been compiled of known interferences and background-ions in modern mass spectrometry [17].

C. Sample consumption and sensitivity

Sample volumes used for bioanalysis are lower for MALDI-MS than for LC-MS. Typically, 0.5 – 1 µL of sample/matrix mixture is deposited on a target plate for MALDI-MS analysis. For LC-MS, sample volumes of typically 25 – 50 µL are injected into the LC, which separates and concentrates the compounds before ionization. Thus, in LC-MS, larger sample volumes can be used and the whole sample is consumed during analysis. In MALDI-MS, only a small portion of the spotted sample is consumed during analysis. Approximately 4% of a sample is ablated during MALDI-triple quadrupole MS analysis with a 1,000-Hz laser that fires 3,000 – 4,000 shots per sample [18]. However, the smaller sample volumes that can be used in MALDI-MS, and the low sample consumption during measurements, are compensated for by the high sensitivity of MALDI-MS. Sleno and Volmer calculated that, at the limit of detection of ramipril (0.5 nM), an average of 6.5 zeptomole of this compound was ablated per laser shot [18]. Direct comparison of analyte signal in relation to sample consumption between MALDI-triple quadrupole MS and LC-ESI-triple

quadrupole MS showed that MALDI-MS is approximately 100-times more efficient than ESI-MS [19]. Thus, in MALDI-MS, smaller volumes of samples can be used for analysis, smaller amounts of the samples are consumed during analysis, but higher efficiencies are obtained. Application of MALDI-triple quadrupole MS has shown that the intrinsic differences between MALDI-MS and LC-MS described above approximately cancel, and in practice therefore, the limits of quantification obtained by MALDI-MS and ESI-MS are approximately comparable [20].

D. Storage of samples on target plates

The low sample consumption during MALDI-MS measurements allows storage and reanalysis of the samples. Reanalysis of a tryptic digest after one month storage on a target plate in a closed container showed that peak intensities were not affected [21]. For HIV protease inhibitors, we have shown that neither precision, accuracy, nor the limit of quantification (LOQ) were affected when calibrators and quality control samples for HIV protease inhibitors in plasma were stored in a closed container for a month under ambient conditions [10]. Target plates that contain the co-crystallized sample/matrix mixtures should be stored in the dark, because MALDI matrices are photoactive. Furthermore, storage under an inert gas can prevent sample degradation over time; for example, oxidation of the analyte might occur under ambient conditions. Sample storage on a target plate also allows researchers to obtain mass spectra of the same sample with different types of MALDI mass spectrometers. Dekker et al. showed that protein identification of a tryptic digest improved when accurate mass measurements of the precursor ions obtained by MALDI-FTICR were combined with the MS/MS data obtained by MALDI-TOF [21].

III. Challenges of MALDI-MS for small-molecule analysis: chemical noise

A. Origin of chemical noise in MALDI

MALDI-MS spectra are characterized by various strong signals that derive from the matrix such as signals from the protonated matrix ($[matrix + H]^+$ for positive ion MALDI), fragment ions (e.g., $[matrix - H_2O + H]^+$, and clusters thereof (e.g., $[matrix_n - H]^+$, $[matrix_n - alkali]^+$, and $[matrix_n - H_2O_n + H]^+$). For example, 2,5-DHB ($C_7H_6O_4$) produces, after laser irradiation, the series of $(C_7H_5O_4Na)_nNa^+$ ions in admixture with other adducts, even in the absence of extraneous sodium ions [22]. Typically, these intense matrix signals are observed up to *m/z* 500. At higher *m/z* values, the number of these matrix signals, as well as their intensity, is generally less. In addition to the various intense matrix signals, a "bumpy" baseline is observed over the entire *m/z* range. Krutchinsky and Chait further investigated the nature of this baseline by performing MALDI-ion trap MS/MS experiments and found that essentially every *m/z* value of the baseline is derived from matrix

ions [23]; see Figure 1. Furthermore, they found that these matrix ions have lower activation energies for fragmentation than the analyte ions. Thus, by performing broadband collisional activation below the threshold for analyte fragmentation, the chemical noise levels were decreased to thereby improve the signal-to-noise ratio (S/N) of the analyte signal. An important consequence of the lower activation energies for matrix-derived signals is that they will have decomposed after very long ion life-times. This important property, which is a direct consequence of RRKM theory, can be exploited in vacuum

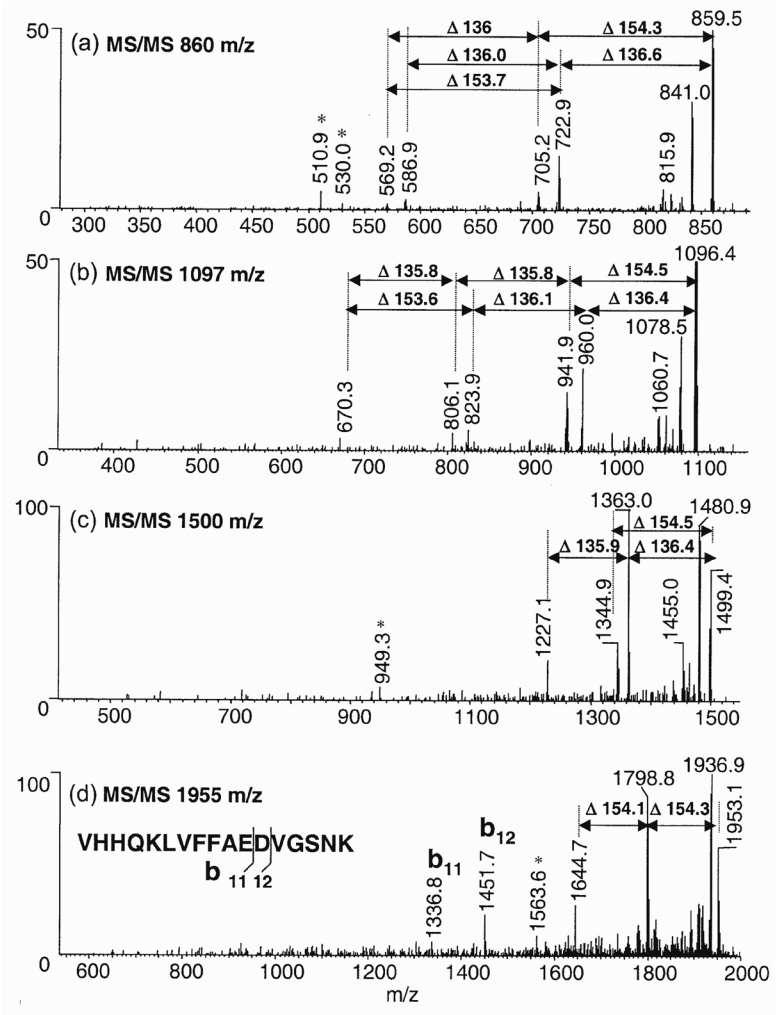

Figure 1. Origin of chemical noise in MALDI. MALDI-MS/MS mass spectra obtained from a selection of *m/z* values where no analyte signals are expected (a-c), as well as one *m/z* value (1955) where a peptide signal is expected (d). Characteristic losses of intact molecules of DHB (154 Da) and molecules of DHB with eliminated water (136 Da) from the precursor are indicated. The asterisk indicates unexplained ion peaks. Reprinted with permission from Krutchinsky and Chait (2002), copyright 2002 Elsevier Science B.V.

MALDI-FTICR, where matrix-derived signals are correspondingly absent, or greatly reduced (see section III C).

B. High molecular weight matrices

One way to avoid the interfering matrix signals in the low *m/z* range is to choose a matrix whose molar mass exceeds that of the analyte. In this way, the matrix-derived peaks in the low mass range result only from dissociation of the matrix or from matrix impurities, but not from the molecular ion of the matrix, matrix adducts, and matrix clusters. Srinivasan et al. reported that some porphyrins could act as auto-matrices [24], and various porphyrins have been tested as matrix in MALDI-MS [25,26]. In particular, meso-tetrakis(pentafluorophenyl)porphyrin (F20TPP; MW 974) appears to be a useful matrix for the analysis of small molecules with MALDI-TOF mass spectrometry [7,27-33]. Ayorinde compared the use of α-cyano-hydroxycinnamic acid (CHCA) and F20TPP for analysis of alkylphenol ethoxylates, and found that F20TPP generated spectra with significantly less matrix interference in the low mass range [29]; see Figure 2. Further studies showed that F20TPP is a suitable matrix for determination and quantification of fatty acids [28,30,33],

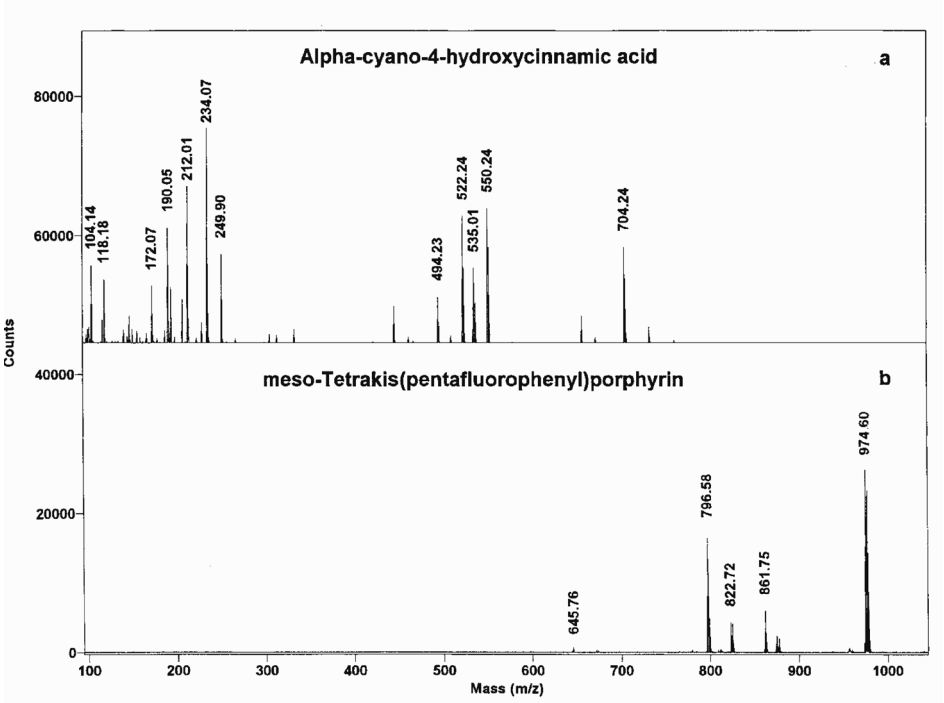

Figure 2. High molecular weight porphyrin matrix. MALDI-TOF mass spectra of the matrix α-cyano-hydroxycinnamic acid (a) and the matrix meso-tetrakis(pentafluorophenyl)porphyrin (b) without the addition of analytes. Reprinted with permission from Ayorinde, Hambright, Porter, Keith jr. (1999), copyright 2009 John Wiley & Sons, Ltd.

and to determine the constituents of non-alcoholic beverages such as sugars, ascorbic acid, and citric acid [27]. F20TPP is also a useful matrix for MALDI-TOF analysis of several pharmaceutical compounds such as HIV protease inhibitors, reverse transcriptase inhibitors, and antibiotics [7]. In addition, the matrix can be used for the quantitative analysis of lopinavir and ritonavir in cell lysates [7,32]. Limits of quantification were 25 femtomole for lopinavir and 16 femtomole for ritonavir, and precisions and accuracies were within the ± 20/15% FDA criteria (i.e., precision and accuracy below 20% CV and 20% deviation, respectively, at the LOQ, and below 15% CV and 15% deviation, respectively, at higher concentrations). F20TPP has also been used for the quantitative analysis of doping agents in urine with a MALDI-ion trap mass spectrometer [31]. Testosterone, nandrolone, betametasone, boldenone, and trenbolone were quantified down to 0.1 ng/mL. Precisions and accuracies fulfilled the ± 20/15% criteria. The light-absorbing, electrically conductive polymer polythiophene has been used as a high molecular weight matrix for negative ion MALDI-MS [34]. Buckminsterfullerene (C_{60}; MW 720) has also been used as a high molecular weight matrix for the analysis of small molecules. This approach was used to screen for diuretics in urine [35], and detection limits of 0.1 – 1 µg/mL were obtained. C_{60} is insoluble in many solvents, including water, and this property might complicate sample preparation. Derivatives of fullerene such as hexa(sulfonbutyl)fullerene are water-soluble, and can be used to selectively precipitate analytes in aqueous solutions, which are then analyzed with MALDI-MS without the addition of a matrix [36].

C. MALDI-FTICR

When MALDI-FTICR is used for small-molecule analysis, a LMW matrix might be preferred over a high molecular weight matrix [8]. Attempts to use the high molecular weight matrix F20TPP for MALDI-FTICR analysis showed extensive fragmentation of F20TPP, which resulted in matrix-derived peaks in the low mass range. In contrast, the use of 2,5-DHB for MALDI-FTICR analysis gives spectra that are relatively free of matrix adducts. The opposite is observed when these matrices are used for MALDI-TOF analysis. These seemingly contrasting results can be explained by the quasi-equilibrium theory, which is a model to describe the unimolecular decomposition of ions. In this model, the rate constant for dissociation of ions is a function of excess energy [37]. The rate constants have the dimension of s^{-1}; i.e., the process can happen that often per second. For example, if we postulate a rate constant of 10^3 s^{-1} for F20TPP, then F20TPP ions dissociate on average in 10^{-3} seconds. The time between ionization and detection of ions varies among mass analyzers. Typically, it takes 10^{-4} seconds to detect ions in a TOF or a quadrupole, and 1 second in FTICR. Thus, with the postulated rate constant, the F20TPP ions formed in the MALDI process easily survive the TOF and quadrupole time scale, but not the FTICR time scale. In the same vein, noncovalent matrix adducts of a LMW matrix such as 2,5-DHB have lower activation energies for dissociation compared to analyte ions [23], therefore

these matrix-derived ions dissociate on the FTICR time scale to produce a mass spectrum free of interfering matrix peaks even in the low mass range.

D. Matrix-free approaches

Matrix-free laser desorption/ionization (LDI) is an approach in which a sample is placed on a photoactive but non-desorbable support, and analyzed without any matrix. For the purpose of this review, we consider this approach as a form of MALDI-MS, although no matrix is used and some differences exist in the mechanism of ion formation. The main advantage of this approach is that little or no signals from the modified surfaces are observed in the mass spectrum. In addition, sample preparation is simplified because the analyte does not need to be mixed and/or co-crystallized with a matrix. The first matrix-free MALDI method was introduced by Wei et al., who used porous silicon surfaces (desorption ionization on porous silicon; DIOS) [38]. The porous silicon surfaces are easily oxidized to allow for chemical modification of the surfaces. Silylation of oxidized porous silicon has been shown to improve sensitivity, shelf-life, ease of modification, and analyte specificity [39]. Furthermore, these modified surfaces can be used to selectively capture analytes from a complex mixture [40]. Silicon nanowires have also been used for matrix-free LDI [41]. Chemical modification of silicon nanowires can also improve performance. Other types of nanostructures such as carbon nanotubes and mesoporous tungsten titanium oxide surfaces have been used for matrix-free LDI. Reviews of matrix-free MALDI approaches can be found in the literature [40,42,43].

E. Additives

Additives such as the cationic surfactant cetyltrimethylammonium bromide (CTAB) can significantly decrease, or even eliminate, matrix-derived signals of CHCA [44]. High-quality spectra were obtained with a CHCA-to-CTAB molar ratio of 1,000:1. However, detection limits of the analytes were approximately one order of magnitude worse. Su et al. used the CHCA/CTAB matrix to screen for the drugs amphetamine, metamphetamine, 3,4-methylenedioxyamphetamine, 3,4-methylenedioxymethamphetamine, caffeine, ketamine, and tramadol in clandestine tablets [45]. Limits of detection ranged from 2 ng/mL to 10 ng/mL. Results were comparable to GC-MS. GC-MS, however, required derivatization of the analytes and additional sample handling. For MALDI-TOF MS, tablet powder was simply dissolved in methanol and directly used for analysis. Grant et al. showed that CTAB can also be used to suppress matrix-derived signals of 2,4,6-trihydroxyacetophenone (THAP), 2,5-DHB, SA, and dithranol [46]. The THAP/CTAB matrix was used to analyze flavonoids in berry extracts [46], and the CHCA/CTAB matrix was used to analyze vitamins and caffeine in energy drinks [47]. In addition to suppression of matrix-derived signals, CTAB also improved the resolution and the quantitative performance; i.e., the %CV decreased and the linearity improved. Other surfactants can also be used to decrease the

number of matrix-derived signals of CHCA [48]; various cationic surfactants were tested, and CTAB showed in general the best performance in terms of strong analyte signals and suppressed matrix signals. The anionic surfactant sodium dodecyl sulphate was useful to analyze small peptides, and the neutral surfactant Brij 30 was useful to analyze caffeine. Cyclodextrin has been used to suppress alkali metal ion adducts, cluster formation, and fragmentation of matrix and analyte [49]. Washing CHCA crystallized samples with ammonium-containing buffers eliminated the alkali-metal matrix cluster signals and improved intensities of peptides. Ammonium salts can also be used as an additive in the matrix solution, although a weaker effect is observed [50].

Suppression of matrix-related peaks can also be achieved by mixing two conventional MALDI matrices [51]. A mixture of the acidic matrix CHCA and the basic matrix 9-aminoacridine (9-AA) resulted predominantly in the formation of $[CHCA - H]^-$ and $[9\text{-}AA + H]^+$, and an overall reduction in matrix clusters. The binary matrix improved the S/N of the analytes; however, this improvement was only observed when the pKa values of the analytes were substantially different than those of the matrices; analyte protonation was not affected by 9-AA when compounds were tested with more basic pKa values than 9-AA. In that case, 9-AA reduced the amount of CHCA-related peaks to thereby improve the S/N of the analytes. For the negative-ion mode, the reverse was observed; analyte deprotonation was not affected when compounds were used that were better proton donors than CHCA.

F. Matrix-suppression effect

The matrix-suppression effect (MSE) is attributed to a depletion of primary matrix ions by neutral analytes via a secondary ion-molecule reaction in the plume; i.e., suppression of matrix peaks is observed when sufficient analyte is present to react with all matrix ions. The MSE is observed for the disappearance of all types of matrix ions; e.g., $[M + H]^+$ and $[M + Na]^+$ [52-54]. McCombie and Knochenmuss tested the utility of MSE for routine MALDI analysis of small molecules [55]. The most important and easy adjustable factors in MSE were the molar ratio of analyte and matrix in the sample, and the laser intensity [52,53]. The highest MSE was achieved at low laser intensities and high analyte concentrations. Analyte/matrix ratios of 1:10 or less were needed to induce MSE for small-molecule analysis. The extent of MSE was related to the type of analyte under investigation. For proton transfer to the analyte, the MSE was greater for analytes with higher gas-phase basicity than for analytes with lower gas-phase basicity. The utility of MSE has been investigated for metabolome analysis by MALDI-MS [56]. MSE was obtained for a cocktail of 30 metabolites that included amino acids, organic acids, and other metabolites. Furthermore, it was possible to detect the metabolites spiked in a microbial extract. However, suppression of analytes was also observed when the concentration of the analyte was increased in relation to the other metabolites.

G. Tandem mass spectrometry

An elegant way to circumvent the problem of the intense matrix-related peaks as well as the noisy baseline is to perform tandem mass spectrometry (MS/MS). In this way, commonly employed matrices such as CHCA and 2,5-DHB can be used without further sample preparation adaptations to decrease matrix-related noise. Tandem mass spectrometry is widely used for bioanalysis with LC-MS/MS, and triple quadrupoles are regarded as the cornerstone mass analyzer for targeted quantitative analysis of small molecules. Recently, a MALDI-triple quadrupole mass spectrometer was developed [3,57]. In the selected reaction monitoring (SRM) mode of a triple quadrupole instrument, isobaric matrix ion interferences can be removed by monitoring only compound-specific precursor/product ion transitions. Other mass analyzers such as ion traps and quadrupole TOFs (QqTOFs) have been used for tandem mass spectrometry of small molecules. A triple quadrupole instrument, however, reaches a higher duty cycle of almost 100%, which results in highly sensitive measurements. Direct comparison of MALDI-QqTOF and MALDI- triple quadrupole showed indeed that MALDI- triple quadrupole offers ~ 10-fold better detection limits than MALDI-QqTOF [3]. Furthermore, the dynamic ranges of the calibration curves obtained with MALDI- triple quadrupole were ~ 1 order of magnitude larger than those obtained with MALDI-QqTOF. This improvement in dynamic range was attributed to the higher sensitivity of the triple quadrupole that thereby extended the linearity of the calibration curves at the low end.

IV. Reproducibility in MALDI

A. Origin of poor precision in MALDI

Quantitative analysis of small molecules with MALDI-MS is complicated by the poor reproducibility of the absolute intensities of the analyte signals. Reproducibility of the signal intensities depends to a large extent on the type of matrix used [18], and on the sample preparation [8,9]. For example, when the widely applied dried droplet protocol is used, CHCA forms small round crystals that are relatively evenly deposited throughout the spot, whereas 2,5-DHB tends to forms different types of crystals with large needle-like crystals in the outer rim and smaller denser crystals in the center of the spot. As a rule of thumb, better reproducibilities are obtained when sample/matrix crystals have a homogeneous appearance and when they evenly cover the spot. The reproducibilities of the absolute signal intensities of quinidine and danofloxacin were compared with the three commonly employed matrices CHCA, 2,5-DHB, and SA that were spotted according to the dried-droplet protocol [18]. The use of CHCA resulted in acceptable precisions of 15% CV and less, whereas the precisions ranged between 23% - 41% CV for SA and from 42% – 90% for 2,5-DHB. Better precisions were obtained when higher matrix concentra-

tions were used, because of a better coverage of the spot with crystals. It has also been noted that strong analyte signals are observed in certain locations of the crystals (the so-called sweet spots), whereas less-intense or even no signals are obtained in other parts of the crystals. The commonly held notion to explain this phenomenon is that the analyte is inhomogeneously distributed in the crystals [58]. Matrix and analytes tend to partition during slow crystallization of the sample when solubilities of the components in the sample are not matched [59]. Segregation is of particular concern when solvent mixtures are used, and one of the solvent components evaporates more easily than the other [60,61]. The use of azeotropic mixtures can avoid fractional precipitation of the analytes during sample evaporation [61]. The sweet spot phenomenon has also been attributed to a different ionization state of the analyte in different parts of the crystals [58], and to a heterogeneous orientation of the crystals relative to the mass spectrometer axis [58]. Matching analyte and matrix in terms of relative polarity is also important for homogenous incorporation of the analyte in the matrix crystals [62].

B. Increasing homogeneous sample / matrix crystallization

Practice has shown that precision can be improved by forcing a homogeneous distribution of the analytes in the crystals, and/or by forcing homogeneous sample/matrix crystals that are evenly distributed throughout the spot. Improved homogeneity of matrix crystals can be obtained when matrix surfaces are prepared by fast evaporation [63]. First, a thin matrix layer of microcrystals is obtained by spotting a matrix solution that contains a high percentage of volatile organic solvent; e.g., acetone. Samples dissolved in any solution that does not redissolve the matrix are deposited on top of the thin layer. This approach is widely used for cinnamic acid-derived matrices such a CHCA and SA, which do not dissolve or poorly dissolve in solutions with a high water content. For water-soluble matrices such as 2,5-DHB, this approach is complicated. Mixtures of analyte and matrix in a solution that contains a high percentage of volatile organic solvent can also be used to create sample/matrix crystals with a more homogeneous appearance that are more evenly distributed throughout the spot.

In the seed-layer approach [64,65], a diluted matrix solution that contains a high percentage of organic solvent is spotted on the target plate, and is allowed to dry. An aqueous solution of sample and matrix is deposited on the dried matrix crystals, which acts as seeds for crystallization, to produce homogeneous sample surfaces.

In the crushed-crystal method [66,67], matrix solution is allowed to crystallize on the target plate in a standard dried-droplet protocol; crystals are crushed, and the sample/matrix mixture is spotted onto the crushed crystals.

We have shown an improved precision for analysis of HIV protease inhibitors with 2,5-DHB as matrix by adding a small amount of dimethylsulfoxide to the sample/matrix mixture [8]. Although the deposited sample/matrix solutions dry at a much slower rate,

homogeneous sample surfaces are obtained. Additives such as fucose [68] also improve the homogeneity of the crystal structures.

Hydrophobic target plates can also be used to improve the homogeneous sample/matrix crystallization as well as to achieve a concentration of the sample/matrix crystals onto a smaller area [9,69,70]. In the AnchorChip technology [70], hydrophilic anchors of 200 – 800 µm in diameter are placed onto a hydrophobic surface to allow more control over the size of the area onto which the sample/matrix crystals are deposited compared to hydrophobic target plates without anchors. Hydrophobic target plates can be prepared relatively easily by applying hydrophobic coating such as Scotch Gard [69] or fluoropolymers [9] onto normal stainless steel target plates. For the novel matrix 7-hydroxy-4-(trifluoromethyl)coumarin (HFMC), we have shown that precision improves when sample/matrix mixtures with a high percentage organic solvent are deposited onto a target plate that is coated with a strongly hydrophobic fluoropolymer [9]. Furthermore, improved LOQs and accuracies were obtained, and the sample/matrix crystals were concentrated onto a small area, even with sample volumes ≤ 10 µL.

Homogeneous thin microcrystal layers can be obtained by a thermal vapor deposition of matrix [71-73]. Dekker et al. use an in-house built sublimation/deposition device to deposit 2,5-DHB onto cytocentrifuged cells that were cultured in the presence of HIV

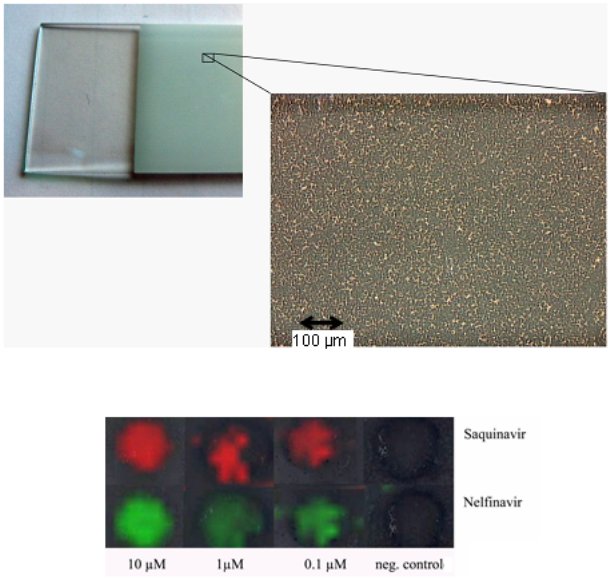

Figure 3. Sublimation deposition of matrix. The picture above shows the sublimation / deposition of 2,5-DHB onto a glass slide. The picture below shows the application of this technique to the analysis of cytocentrifuged Mono Mac 6 cells that were cultured in the presence of the HIV protease inhibitors saquinavir and nelfinavir. Color intensities represent the signal intensities of saquinavir (red) and nelfinavir (green) in the cytocentrifuged cells. Reprinted with permission from Dekker, van Kampen, Reedijk, Burgers, Gruters, Osterhaus, Luider (2009), copyright 2009 John Wiley & Sons, Ltd.

protease inhibitors [71]; see Figure 3. Prespotted target plates that contain, e.g., CHCA spots, can also be prepared in this way.

Sophisticated spotting devices such as electrospray deposition instruments [59,74,75] or piezo-electric droplet dispensers [76-78] can be used to obtain a highly homogeneous layer of co-crystallized sample and matrix to thereby improve the precisions compared to dried-droplet sample preparation. These sophisticated spotting devices might be particularly useful when matrices are used that are known for their heterogeneous crystallization behavior such as 2,5-DHB. Furthermore, these spotting devices might be used to force homogeneous co-crystallization of analyte and internal standard even when segregation occurs under dried-droplet sample preparation conditions [79].

C. Ionic liquid matrices

Armstrong et al. showed that some room-temperature ionic liquids (RTIL) can be used as effective matrices in UV-MALDI [80]. The RTIL that possess matrix properties are often called ionic liquid matrices (ILM), although ionic matrices or class II RTIL are also used to describe these matrices. RTIL are a class of compounds that consist of ions, have melting points < 100°C and are often liquid at room temperature, and have negligible vapor pressure [81]. Most ILM form smooth viscous films on the target plate, and retain this property under vacuum. ILM can be obtained by mixing a commonly used crystalline MALDI matrix such 2,5-DHB, CHCA, or SA with an equimolar amount of organic base such as tributylamine, pyridine or 1-methylimidazole [82]. As a rule of thumb, the preference of the crystalline matrix for a certain class of analytes is retained when these matrices are converted into ILM. An interesting property of several ILM for analysis of small molecules is that the amount and intensity of matrix-derived peaks is decreased [83]. The greatest advantage of ILM is that these matrices allow for homogeneous sample preparation, which significantly improves the reproducibility of MALDI. ILM have been tested for the analysis of various small molecules [82], metabolome analysis [56], oligodeoxynucleotides [84], oligosaccharides [85], peptides and proteins [84,85], and even for tissue imaging [86]. Zabet Moghaddam et al. reported that peak intensities of small molecules in solid matrices varied by more than 60%, whereas variations of less than 10% were observed for their ionic liquid forms [82]. The correlation coefficients for the calibration curves also improved when an ILM was used. Other properties of ILM compared to their solid counterparts are that slightly increased laser fluences are needed for ionization, and that ILM favor formation of sodium and potassium adducts [82,85]; those properties can be exploited for analytes with poor protonation [7,8,10,22]. For further information on ILM, see the review of Tholey and Heinzle [83].

D. Internal standards

The use of an internal standard is indispensable for the robust and reproducible quantitative analysis of small molecules with MALDI mass spectrometry. Ideally, the internal standard compensates for all variations in analyte recovery during the sample preparation process, and yields identical mass spectrometric behavior as the analyte. In MALDI mass spectrometry, the internal standard should compensate for crystallization irregularities and for desorption and gas-phase effects. In particular, the crystallization irregularities might present a problem in quantitative MALDI mass spectrometry. Matrix, analyte, and internal standard tend to partition during the crystallization process [59-62, 79]. In mixed solvents such as acetonitrile/water and methanol/water where one component evaporates faster than another, such segregation effects might be of particular concern. The use of azeotropic mixtures avoids segregation of components during crystallization. The stable isotope-labeled version of an analyte is regarded as the ideal internal standard, because solvent, desorption, and gas-phase properties are nearly identical to that of the analyte [87,88]. The stable isotope-labeled internal standard and analyte are incorporated into the matrix crystals in the same extent and in the same locations, and therefore heterogeneous sample / matrix crystallization might not cause a detrimental effect on precision and accuracy. However, such stable isotope-labeled internal standards are expensive, and might not be commercially available, and, in practice, other pharmaceutical compounds are frequently used as internal standards. Precise and accurate quantification can be obtained using "look-alike" pharmaceutical compounds as internal standards. Sleno and Volmer investigated the influence of solution-phase ionization equilibria and hydrophobicity on the relative response of analyte and internal standard [79]. The predicted apparent octanol/water partition coefficient D was a good parameter to search for an appropriate internal standard; precise and accurate quantitation was obtained only when analyte and internal standard had a similar log D; see Figure 4. Furthermore, when analyte and internal standard had matching log Ds and thus a good co-crystallization, precise and accurate quantification could be obtained even when the analyte and internal standard were not homogeneously distributed throughout the whole crystallized sample.

E. Averaging

A common method to improve reproducibility is to average a large number of individual data points. In this respect, firing the laser at a higher frequency is advantageous to obtain a good precision without compromising sample analysis times. Comparison between laser firing at 20-Hz and 1,000-Hz for analysis of clonazepam and nordiazepam showed that the higher laser frequency improved the within spot and spot-to-spot precisions by at least a factor of five [3].

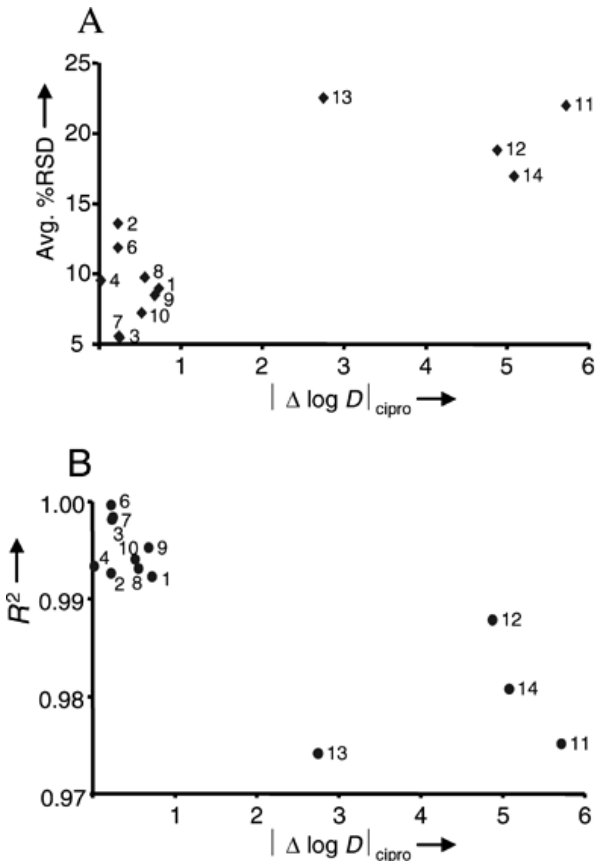

Figure 4. Octanol/water partition coefficients of analyte and internal standards. Quantitation of ciprofloxacin with thirteen different 4-quinolones as internal standard. The y-axis shows %RSD or r^2 for quantitation of ciprofloxacin. The x-axis shows the difference in log D between ciprofloxacin and the internal standard. CHCA dissolved in acetonitrile / water (1:1; v/v) and 0.2% TFA was used as matrix. Log D values were predicted for pH = 2.0. Reprinted with permission from Sleno and Volmer (2006), copyright 2009 John Wiley & Sons, Ltd.

F. Algorithms for data collection and analysis

Nicola et al. developed a correlative analysis algorithm for automated data collection to improve the quality of the average mass spectrum by compensating for shifts along the mass axis of the single-shot MALDI-TOF spectra [89]. This method resulted in an improved mass resolution (3x), better reproducibility of signal intensities (4x), and better quantitative accuracy (1.3x). Horak et al. compared data acquisition at constant laser power with data acquisition at constant ion abundance for quantitative analysis of chlormequat [90]. Data acquisition at constant ion abundance resulted in a better sample-to-sample reproducibility compared to data acquisition at a constant laser power. We tested the effect of baseline subtraction, peak parameter (intensity, S/N or area), and analyte signal (monoisotope versus all isotopes) on the precision of lopinavir and ritonavir analysed by

MALDI-TOF, and found that the best %CVs were obtained when the monoisotopic peak area without baseline subtraction was used [7].

V. Practical aspects of small-molecule analysis with MALDI

A. Protonation versus cationization

For biopolymers such as proteins, peptides, and nucleic acids, a (de)protonation strategy is usually pursued, and the formation of salt adducts is regarded as disadvantageous. It is well-known that additives can significantly decrease these salt adduct formations. We have used DAHC as an additive in the binary matrix nicotinic acid / anthranilic acid (55 mM / 45 mM / 45 mM, respectively) to decrease the amount of salt adducts for analysis of (deoxy)nucleotide-triphosphates and the triphosphorylated form of the nucleoside reverse transcriptase inhibitor zidovudine in negative ion MALDI-TOF experiments [91]. An advantageous additional effect of DAHC and other additives is that they result in a more homogeneous crystallization of matrix and analyte to thereby improve the precision.

Cationization strategies are, however, preferred for analytes that lack basic sites such as oligosaccharides and synthetic polymers. We have successfully pursued a cationization strategy to quantify drugs with MALDI-TOF [7,32], MALDI-FTICTR [8], and MALDI-triple quadrupole MS [9,10]. For the high molecular weight porphyrin matrix F20TPP, we tested which alkali metal, i.e. Li, Na, K, Rb or Cs, produced the strongest signal for cationized drugs [7], and we found that analytes were most efficiently ionized by Li^+ attachment. This result was surprising, because analysis of mixtures of the F20TPP matrix with equimolar amounts of LiI, NaI, KI, RbI, and CsI revealed that hardly any free Li^+ is detected. The intensities of the free alkali-metal ions showed the distribution of Li^+ (=0) < Na^+ < K^+ < Rb^+ < Cs^+, that result can be explained by the inverse relationship of the alkali iodide lattice energies and size of the alkali metal. Thus, with the same halide as counter ion, the larger alkali metal the lower the lattice energy, to liberate more alkali metal ions during the desorption/ionization process. This distribution is also observed when 2,5-DHB is used as matrix. On the other hand, studies with LMW poly(ethyleneglycols) (PEG) showed that the intrinsic affinity of analyte for the alkali metal ions follows the order of Li^+ > Na^+ > K^+ > Rb^+ > Cs^+. Thus, the intrinsic metal ion affinity appears to be governed primarily by the charge density of the cation. In practice, the quantitative distribution of PEG ionized with alkali metals can be rationalized on the basis of a trade-off between these two opposing effects; namely, the gas-phase availability of the alkali cation (Li^+ < Na^+ < K^+ < Rb^+ < Cs^+) and the intrinsic alkali affinity of PEG (Li^+ > Na^+ > K^+ > Rb^+ > Cs^+) leading to an observed optimum affinity for K^+ [8,92]. The optimum affinity for K^+ is indeed the case when 2,5-DHB is used as matrix. With F20TPP, the most abundant signals are observed for PEG cationized by Li^+, followed by Na^+, hardly any kaliated signals are

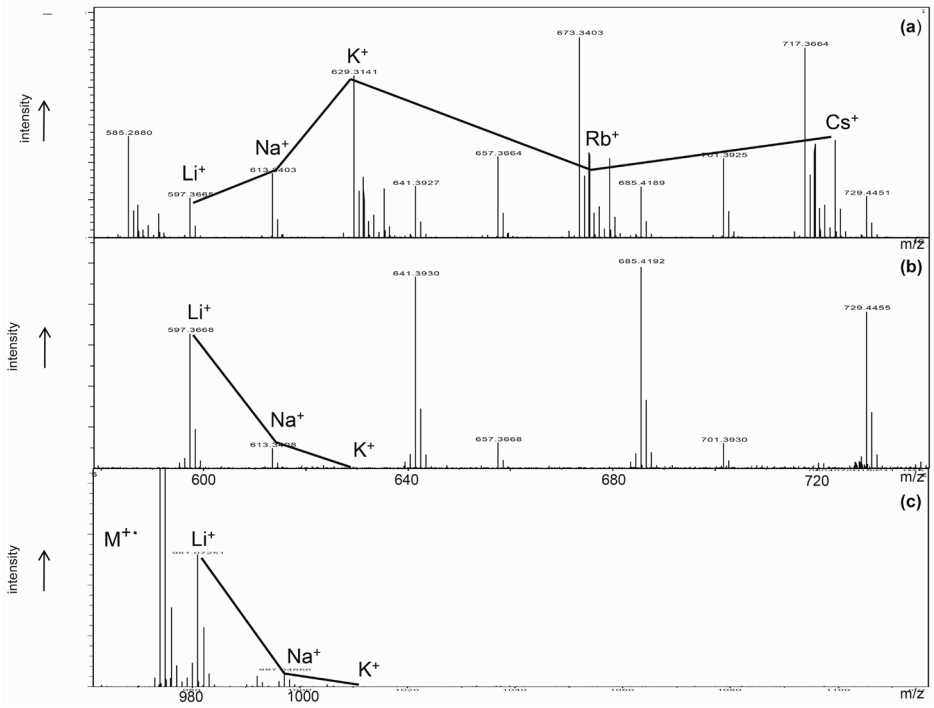

Figure 5. Porphyrin matrix and alkali cation distribution of analyte. Alkali-metal distribution of PEG with an equimolar mixture of LiI, NaI, KI, RbI, and CsI in combination with the matrix 2,5-DHB (a) and F20TPP (b). Alkali metal of the matrix F20TPP itself (c). Reprinted with permission from van Kampen, Luider, Ruttink, Burgers (2009), copyright 2009 John Wiley & Sons, Ltd.

observed, and virtually no adducts are formed with rubidium or cesium (see Figure 5). Furthermore, the binding efficiencies of Li^+ towards LMW PEGs strongly depend on the number of sites where the Li^+ ion can interact [92,93]. The intensity order of F20TPP itself cationized by various alkali metals is very similar to that of the LMW PEGs; i.e., $Li^+ > Na^+ > K^+ > Rb^+ > Cs^+$. We propose that, for porphyrins, the cationized matrix might well be the cation donator to the analytes, whereas analyte cationization with other matrices seems to occur predominantly through attachment of free cations in the gas-phase [94]. *Ab initio* calculations showed that Li^+ is attached to the porphyrin cavity and not to the F atoms of the C_6F_5 groups. Equilibrium structures for porphyrin + Li^+ showed that the Li^+ is situated on, but not in, the porphyrin cavity, and that the whole porphyrin chain becomes bent. The observation that the lithium ion is not in, but outside, the cavity means that the lithium ion is exposed and is therefore accessible for transfer to analyte molecules. The larger the cation, the more exposed the cation is (and the lesser the porphyrin skeleton will be bent); however, at the same time, the cation affinities become less; see Figure 6. Our experiments showed that only lithium ions produce intense signals for attachment to F20TPP, and that such F20TPP + Li^+ ions might act as

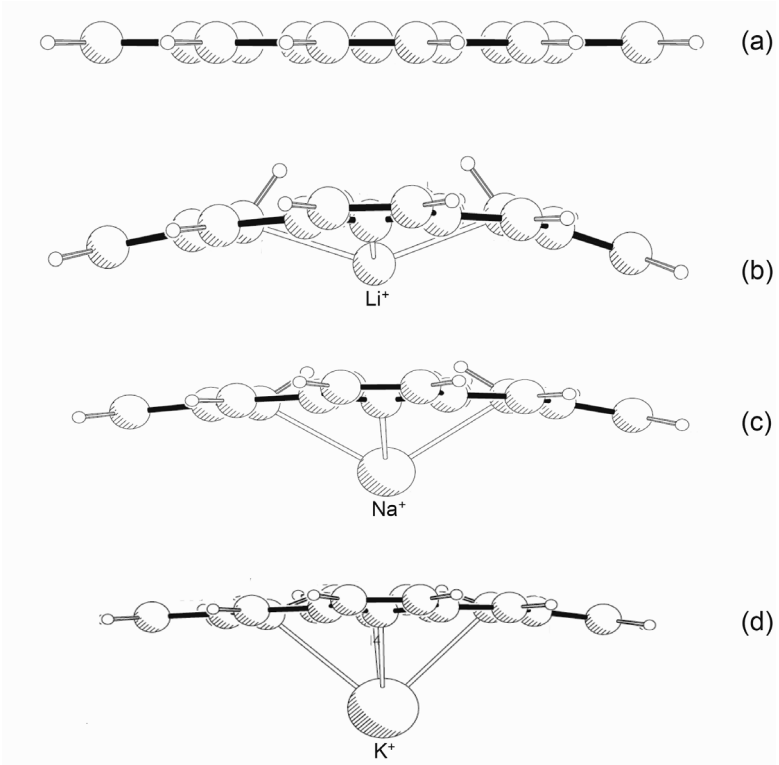

Figure 6. Interaction of porphyrin with alkali metals. Side views of porphyrin + H^+ (a), porphyrin + Li^+ (b), porphyrin + Na^+ (c), and porphyrin + K^+ (d). Reprinted with permission from van Kampen, Luider, Ruttink, Burgers (2009), copyright 2009 John Wiley & Sons, Ltd.

cation donator. The preference for Li^+ attachment to matrix and analyte was also found for other porphyrin matrices.

Hoberg et al. showed that, when an alkali metal cationization strategy is pursued with alkali halide salts, a halide counter anion should be chosen that results in the lowest lattice energy of the alkali halide salt [95]. For example, when cationization with sodium is pursued, more abundant sodiated signals for the analyte are observed when sodium iodide is used as cationizing agent compared to sodium chloride. The proton affinity of porphyrin is large (245 kcal/mol), and thus many analytes cannot be charged by protonation with this matrix. Indeed, for various drugs we found no protonated molecules with F20TPP. We have, however, found evidence for protonated fragments of protease inhibitors (van Kampen, unpublished experiments), and it might be that, for protonation, F20TPP should be regarded as a hot matrix that can result in prompt in-source fragmentation of protonated analytes. On the other hand, Kosanam et al. successfully applied the F20TPP matrix for the quantitative analysis of doping agents in urine with MS/MS on the protonated analytes in MALDI-ion trap experiments [31].

Preference for certain cations also depends on the nature of the analyte. For example, Burgers and co-workers showed that tryptic peptides that contain the calcium-binding domain of calcium-binding proteins retain their preference for calcium in MALDI experiments, and that intense signals are observed for the calciated peptides [96]. SRM experiments on a MALDI-triple quadrupole MS showed that protonated precursor molecules produce product ions of higher intensity than cationized precursor ions [9]. Furthermore, for analytes cationized with the larger alkali cations (K^+, Rb^+, Cs^+), MS/MS results in loss of the analyte as a neutral. This fragmentation pattern is due to the low affinity of the larger cation towards the analyte [97]. With CHCA as matrix to quantify five HIV protease inhibitors on a MALDI-triple quadrupole MS, we found weak signals for the protonated molecules of lopinavir and ritonavir; SRMs on the sodiated forms of lopinavir and ritonavir, however, resulted in sensitive, precise, and accurate quantification [10]. An interesting matrix for cationization of various small molecules is lead pencil. Black et al. showed that pencil lead, which contains graphite, clay, and "gliding" agents such as wax, acts as a matrix for MALDI-MS [98, 99]. With this matrix, the success rate (S/N > 5; ~ 10 ng spotted) was 88% for a library of 50 small molecules that contained tripeptides, steroids, drugs, herbicides, dyes, and polyethylene glycols (PEGs). Examples of drugs included in the library are haloperidol, carbamazepine, tamoxifen and 4-hydroxytamoxifen, erythromycin, cefuroxime, and mebendazole. In particular, intense signals for the sodiated or kaliated analytes were observed. Indeed, with lead pencil as matrix to analyze the HIV protease inhibitor saquinavir in MALDI-TOF and MALDI-FTICR experiments, strong signals were found for the sodium and potassium adducts, but not for protonated saquinavir (van Kampen, unpublished experiments). Those data contrast sharply with matrices such as 2,5-DHB and CHCA, which yield intense signals for the protonated molecule [10, 74]. Adding either a sodium salt or a potassium salt to the sample enhances analyte cationization, and thereby improves the sensitivity (van Kampen, unpublished experiments). Charcoal behaves in a similar way as pencil lead, although this matrix needs to be applied on to a target plate with a rough surface; e.g., a groundsteel target plate (Burgers, unpublished experiments).

B. MS versus MS/MS

For quantitative analysis of drugs in the MS mode, high resolution and high mass accuracy are advantageous because higher mass accuracy results in a higher certainty that the peak in the mass spectrum is actually the drug of interest, and high resolution increases the selectivity to discriminate between the analyte and isobaric matrix interferences. An additional advantage of high mass accuracy MS measurements over a targeted MS/MS approach for quantitative analysis of drugs is that the accurate masses of other peaks than the drug itself present in the mass spectrum could be used to establish whether these peaks are (unexpected) drug metabolites or not. We propose that MALDI instruments

such as TOF, Orbitrap, and FTICR are suitable for discovery-type applications. Neutral-loss scans and precursor-ion scans on a triple quadrupole instrument can also be used to search for drug metabolites. For targeted quantitative analysis of drugs, we propose an MS/MS approach. Using this approach, conventional small-molecule matrices can be used without any problems that are associated with matrix-derived interfering signals. Furthermore, MS/MS approaches normally result in higher sensitivities. In this respect, the triple quadrupole mass spectrometer would be the instrument of choice because such an instrument allows for SRM with a nearly 100% duty cycle.

C. Preparation of biological samples

Relatively simple, fast, and easy-to-automate procedures that allow batch preparation of biological samples are needed to truly benefit from the high-throughput measurements of MALDI mass spectrometry. Sample-preparation procedures in 96-well plates or 384-well plates are highly suited for MALDI, because these formats are widely used for MALDI target plates, and allow a relatively easy spotting of the processed samples with a pipetting robot [10, 74, 100].

Preparation of samples with SPE, LLE, and PP have been tested for quantitative analysis of small molecules by MALDI mass spectrometry. The processed samples are normally dried after these procedures, and are reconstituted in a smaller volume of an appropriate solvent or matrix solution. This drying-step is frequently needed to maintain the required sensitivity because sample volumes of only 0.5 – 1 µL are deposited onto the target plate for measurement. We have shown that SPE-processed samples can be reconstituted in volumes as low as 10 µL for sensitive, precise, and accurate quantitation of HIV protease inhibitors in cell lysates [8, 9]. Gobey et al. showed that the drying-step can be omitted for SPE-processed plasma by eluting the samples from the SPE columns with 25 µL matrix solution [19]. Wagner et al. used LLE to process plasma samples from HIV-infected patients who were treated with the protease inhibitor saquinavir [74]. When protein precipitation is used, however, the drying-step has a detrimental effect on the crystallization of the sample with a concordant severe loss of sensitivity [19, 74, 101]. For quantitative analysis of HIV protease inhibitors in plasma of HIV-infected children, we found that good crystallization and high sensitivity can be obtained for protein-precipitated samples when the drying-step is omitted [10]. Ten µL of plasma was "diluted" in 90 µL methanol that contained the internal standard, the supernatant was diluted in matrix solution (1:2, v/v), and 0.75 µL matrix/sample solution was deposited onto a target plate; i.e., the plasma sample was diluted 30-times in an organic solvent. Detrimental effects on crystallization were observed only when the solvent that was used for the protein precipitation consisted of a high percentage of water, or when lower dilution was used.

Analytes can also be captured from biological samples with target plates with functionalized surfaces [40]. Functionalized magnetic nanoparticles and water-soluble fuller-

ene derivatives, which serve also as a MALDI matrix, have been used to capture analytes from complex biological samples [36, 102].

VI. Biomedical applications of MALDI

A. Quantitative analysis of drugs

Although many studies have shown promising results for MALDI-MS quantitative analysis of small molecules, real-life applications of MALDI-MS for analysis of drugs in biological samples are still limited. Below, we discuss some of the studies that have shown successful application for MALDI-MS for quantitative analysis of drugs.

MALDI-triple quadrupole MS has been used for analysis of several spirolide toxins in phytoplankton [103]. Samples were extracted in methanol, and LC-fractionated. For some samples, an additional SPE procedure was used. Cross-validation showed good agreement for the quantitation obtained with MALDI-MS and ESI-MS. Furthermore, MALDI-MS precursor-ion scans and neutral-loss scans were successfully applied to discover unknown spirolide analogues in the phytoplankton samples.

Gobey et al. have applied MALDI-triple quadrupole mass spectrometry to the rapid analysis of human liver microsome half-lives of 53 pharmaceutical compounds [19]. Comparison with ESI-MS showed good agreement among the assays.

Rideout applied MALDI-TOF MS for quantitative analysis of the cationic drug tetraphenylphosphonium (TPP) in carcinoma cell lines [104]. Methyltriphenylphosphonium was used as the internal standard. The cells incubated with the drug were prepared by simple lysis with a freeze-thaw cycle. Subpicomole amounts of the drug were quantified, and scintillation counting showed good agreement with the MALDI-TOF assay. Furthermore, the assay was used to monitor the formation of hydrazones from aldehydes and hydrazine derivates inside cells. MALDI-TOF mass spectrometry has also been used to study the uptake of TPP and other phosphonium cations in cell lines [105] and the uptake of cell-penetrating peptides [106].

We used MALDI-TOF and MALDI-FTICR mass spectrometry to image HIV protease inhibitors in Mono Mac 6 cells cultured in the presence of 0.1 – 10 µM saquinavir and nelfinavir [71]. Cells (2×10^5) were cytocentrifuged on electrically conductive glass-slides, and matrix was applied with an in-house build sublimation/deposition device. To obtain good sensitivities, the deposited matrix was recrystallized with water vapor; this recrystallization procedure did not result in loss of spatial information.

Volmer et al. compared MALDI-triple quadrupole mass spectrometry and LC-MS for the plasma pharmacokinetic analysis of two drug candidates that were administered to rats [20]. Chemical analogues were used as internal standards, and plasma samples (125 µL) were prepared with SPE. The LOQs were 536 nM (osteoporosis candidate drug) and

426 nM (asthma candidate drug) for the LC-MS assay and the MALDI-MS assay. There was excellent agreement between the pharmacokinetic parameters obtained with MALDI-MS and with LC-MS.

Muddiman et al. applied MALDI-TOF and SIMS-TOF to quantify cyclosporine A in the whole blood of transplant patients [107]. Cyclosporin D was used as internal standard, and whole blood samples were prepared with LLE. The LOQ was 19 nM for SIMS-TOF and 33 nM for MALDI-TOF. It was also demonstrated that these techniques can provide information on cyclosporine metabolites. Wu et al. used an automated MALDI-TOF platform to quantify this drug [100]. Tacrolimus and its hepatic metabolites were quantified with MALDI-TOF and SIMS-TOF mass spectrometry [108].

Wagner et al. used MALDI-triple quadrupole mass spectrometry to quantify the HIV protease inhibitor saquinavir in plasma from HIV-infected patients [74]. LLE was used to prepare the plasma samples (250 µL), and deuterated saquinavir was used as internal standard. The LOQ was 7.5 nM. Cross-validation between MALDI-MS and LC-MS of clinical samples showed an excellent agreement between the assays. To investigate the effect of co-medication, which is frequently encountered in clinical applications, on the performance of the assay, eight antiretroviral drugs were spiked to human plasma that contained saquinavir. Selectivity and accuracy were not compromised by the presence of these other antiretroviral drugs. Further experiments showed that reserpine could also be used as an appropriate internal standard.

Notari et al. used MALDI-TOF/TOF MS to quantify the antiretroviral drugs abacavir, stavudine, didanosine, efavirenz, nevirapine, and amprenavir in the plasma of HIV-infected patients [109]. 4-Hydroxybenzoic acid was used as matrix. A plasma sample (600 µL) was used, and sample preparation consisted of a SPE. The limits of quantification were 10 nM. Cross-validation between MALDI-TOF/TOF and high-pressure liquid chromatography with UV detection (HPLC-UV) showed an excellent agreement.

Antiretroviral drugs have been quantified with MALDI-TOF [7,32], MALDI-FTICR [8], and MALDI-triple quadrupole MS [9,10]. A MALDI-triple quadrupole yielded the best applicability for clinical studies, and was used to investigate the plasma and intracellular pharmacokinetics of the HIV protease inhibitors lopinavir and ritonavir in HIV-infected children. Plasma samples were processed with protein precipitation with methanol, and cell samples were processed with a methanol extraction followed by SPE. The methanol-extraction step simultaneously inactivated HIV, and further sample handling after this step can be performed under less-stringent biosafety conditions [32]. The assays were specifically developed for application in children and care was taken that quantification could be performed on a small amount of patient sample. Accurate and precise quantification was obtained from only 10 µL plasma or one million peripheral blood mononuclear cells (PBMCs; ~ 0.4 µL intracellular volume). Furthermore, an assay was developed for multiplexed quantitative analysis of saquinavir, nelfinavir, and indinavir with

methotrexate as internal standard. Nelfinavir was used as internal standard to quantify lopinavir and ritonavir in plasma and in cells. The LOQs obtained in plasma were 167 nM (lopinavir), 16 nM (indinavir, nelfinavir), 15 nM (ritonavir), and 3.2 nM (saquinavir). The LOQs in PBMCs were 834 nM for lopinavir and 73 nM for ritonavir. To investigate the effect of co-medication on the assays, a mixture of ten drugs was added to plasma samples from an HIV-infected child treated with Kaletra (lopinavir/ritonavir). The added drugs did not affect precision or accuracy for lopinavir and ritonavir as shown by an analysis of the same samples without the drug mixture, and a cross-validation with HPLC-UV.

B. Metabolomics

The suitability of MALDI mass spectrometry for metabolome analysis has been investigated [110,111]. These studies aimed to simultaneously identify and quantify a cocktail of metabolites with a few internal standards. It was shown that MALDI mass spectrometry can be used for the simultaneous analysis of a cocktail of metabolites. However, analyte suppression was observed for some metabolites when the relative portion of one analyte dominated the others in the mixture. Furthermore, the isomeric interferences encountered in metabolomics applications show the need for tandem mass spectrometry and / or appropriate sample-preparation procedures. For example, ATP and dGTP have the same elemental composition, but can be separated from each other in MALDI post-source decay experiments [91]. Offline spotting of LC fractions on target plates is frequently used for MALDI in proteomics to increase the number of identified peptides. Such approaches might also proof useful for MALDI-MS metabolomics. LC-MALDI and LC-ESI of the same set of samples showed that only one-third of all identified peptides were found by both techniques, and that the techniques can thus be regarded as complementary [112,113]. Nordström et al. showed that a multiple ionization strategy consisting of ESI, atmospheric pressure chemical ionization, and DIOS mass spectrometry significantly increased the number of ions detected in metabolome analysis [114]. Another approach to increase the success rate in metabolome analysis, which is also suitable for pharmaceutical compounds, is charge-derivatization of small molecules or derivatization of analyte molecules with a matrix [115,116].

C. Monitoring the conversion of small molecule substrates by enzymes

An interesting application of MALDI mass spectrometry is to monitor enzymatic reactions with small-molecule substrates. In this approach, substrate and product are simultaneously detected, and the substrate-to-product ratio is calculated to quantitatively monitor the enzymatic reactions without an internal standard [6,117-120]. For example, MALDI-triple quadrupole MS was also used to screen for kinase inhibitors of cyclic AMP-dependent protein kinase [6]. The substrate in this assay was the peptide kemptide (Leu-Arg-Arg-Ala-Ser-Leu-Gly), which is phosphorylated by the protein kinase.

VII. Future directions

Currently, there is still no comprehensive model that accurately predicts the MALDI mass spectra in a qualitative and quantitative way given a certain sample, matrix, sample preparation, and instrument, even though much progress has been made in this area [58, 121, 122]. We propose that a better mechanistic understanding of the relative response of analyte and internal standard in biological samples greatly benefits the application of MALDI for targeted quantitation of small molecules, and for metabolomics applications. Such an understanding could be used to correct for differential suppression effects (i.e., unequal suppression of analyte and internal standard), and improves MALDI quantification and reliability. The apparent octanol / water partition coefficients have already been shown to be useful to predict which internal standard should be used for precise and accurate quantitation [79]. A better understanding of the MALDI mechanism can also be used to discover or even synthesize new matrices for MALDI. Sometimes, we test for matrix properties of molecules when they have favorable UV-light absorption profiles; that process led to the discovery of the novel matrix HFMC [9]. *Ab initio* calculations were used to create new hypotheses of how matrices act in MALDI such as in the case of porphyrin matrices [92]. A breakthrough in finding matrices for MALDI was the rational design of the new matrix 4-chloro-α-cyanocinnamic acid [123]. This matrix showed a much more uniform response to analytes of different basicities than the commonly used CHCA. This approach might also be used to produce new matrices for improved analysis of small molecule, or to produce matrices that work particularly well for a certain interesting class of molecules. The position of MALDI as an analytical tool for small-molecule analysis will be strengthened by further improvements of matrix-free approaches [40, 42, 43].

Real-life applications of MALDI for small molecule analysis in biomedical research, diagnostics, and clinical medicine are still limited. We expect that MALDI will be applied in particular when large numbers of samples must be measured (e.g., in epidemiological studies), or when fast results are needed, such as in diagnosis of infectious diseases. Small-molecule markers and conversions of small molecules by enzymes are routinely used to diagnose pathogens in medical microbiology laboratories, and we expect that MALDI mass spectrometry can play an important role in this area. For some drugs, therapeutic drug monitoring is routinely applied in a clinical setting; MALDI can also play a significant role in this area. We propose that MALDI should not be seen as an analytical tool that makes tested-and-proven methods such as LC-MS/MS or HPLC-UV obsolete, but that MALDI should be regarded as an addition to the analytical armory. For example, one MALDI mass spectrometer can be used as a work-horse in the setting of university medical center to answer many research questions in a relatively short time. Other analytical tools can be used to translate the positive results to a clinical setting; e.g., the finding that the concentration of a certain drug correlates with clinical outcome.

We propose that, at this moment, MALDI is not yet ready for routine use in clinical laboratories, and, first, long-term head-to-head comparison with proven analytical assays must be performed and standard operating procedures must be developed that deal specifically with the nature of MALDI; e.g., life-time of the laser.

Currently, the use of different types of MALDI mass spectrometers is not fully exploited; not the least, concerted measurements are often hampered by practical problems such as variations in the dimensions of the target plates used by different mass spectrometry vendors. Studies have shown that samples can be stored on target plates in their matrix co-crystallized form, and that sample consumption during measurements is low. The low sample consumption and storage of samples on target plates allow researchers to combine the specific strengths of mass analyzers like FTICR, TOF, Orbitrap, and triple quadrupole to obtain answers to the research questions. For example, the high resolution and high mass accuracy of MALDI-FTICR can be used to search for (unexpected) drug metabolites in a selected group of samples; a MALDI-triple quadrupole can be used for a fast, relatively quantitative analysis of the drug metabolites in a large number of samples. Storage of samples on a target plate also allows researchers to send samples to other laboratories that have a particular expertise or a particular type of MALDI mass spectrometer that is not present in the original laboratory.

We expect further improvements in the biomedical application of MALDI mass spectrometry for small-molecule analysis by the specific development of techniques for clinical samples that range from biofluids, lysates of tissues, and frozen-tissue sections that can be screened with MALDI-MS for specific small molecules.

VIII. Concluding remarks

MALDI-MS offers some intrinsic properties that favor its use for small-molecule analysis such as its high tolerance towards salts and buffers, the rapid analyses, its high absolute sensitivity, the small amount of sample consumed during analysis, and the possibility to store samples on a target plate. For this application, however, approaches should be used that are specifically developed for this application to overcome or circumvent matrix-related noise in the low-mass range and the poor reproducibilities of signal intensities. A variety of such approaches have been developed and allow unambiguous qualitative annotation of small molecules as well as precise and accurate quantitation. These approaches are now ready to be tested in a clinical environment.

IX. Acknowledgements

This review was supported by a grant from Top Institute Pharma (project T4-212). The consortium of project T4-212 consists of the departments of Neurology and Virology of the Erasmus MC (Rotterdam, the Netherlands), the departments of Pediatrics and Clinical Pharmacy of the UMC St. Radboud (Nijmegen, the Netherlands), TNO Quality-of-Life (Zeist, the Netherlands), and GlaxoSmithKline (Zeist, the Netherlands). Jeroen van Kampen is supported by a grant from Aids Fonds, the Netherlands (project 2004051), and Rob Gruters is supported by VIRGO.

X. References

1. Cohen LH, Gusev AI. Small molecule analysis by MALDI mass spectrometry. Anal Bioanal Chem 2002;373(7):571-86.
2. Yang Y, Zhang S, Howe K, et al. A comparison of nLC-ESI-MS/MS and nLC-MALDI-MS/MS for GeLC-based protein identification and iTRAQ-based shotgun quantitative proteomics. J Biomol Tech 2007;18(4):226-37.
3. Hatsis P, Brombacher S, Corr J, Kovarik P, Volmer DA. Quantitative analysis of small pharmaceutical drugs using a high repetition rate laser matrix-assisted laser/desorption ionization source. Rapid Commun Mass Spectrom 2003;17(20):2303-9.
4. McLean JA, Russell WK, Russell DH. A high repetition rate (1 kHz) microcrystal laser for high throughput atmospheric pressure MALDI-quadrupole-time-of-flight mass spectrometry. Anal Chem 2003;75(3):648-54.
5. Moskovets E, Preisler J, Chen HS, Rejtar T, Andreev V, Karger BL. High-throughput axial MALDI-TOF MS using a 2-kHz repetition rate laser. Anal Chem 2006;78(3):912-9.
6. Rathore R, Corr J, Scott G, Vollmerhaus P, Greis KD. Development of an inhibitor screening platform via mass spectrometry. J Biomol Screen 2008;13(10):1007-13.
7. van Kampen JJ, Burgers PC, de Groot R, Luider TM. Qualitative and quantitative analysis of pharmaceutical compounds by MALDI-TOF mass spectrometry. Anal Chem 2006;78(15):5403-11.
8. van Kampen JJ, Burgers PC, de Groot R, et al. Quantitative analysis of HIV-1 protease inhibitors in cell lysates using MALDI-FTICR mass spectrometry. Anal Chem 2008;80(10):3751-6.
9. van Kampen JJ, Burgers PC, Gruters RA, et al. Quantitative analysis of antiretroviral drugs in lysates of peripheral blood mononuclear cells using MALDI-triple quadrupole mass spectrometry. Anal Chem 2008;80(13):4969-75.
10. van Kampen JJA, Reedijk ML, Burgers PC, et al. Ultra-fast determination of drug concentrations in plasma and in cells. Submitted 2009.
11. Amini A, Dormady SJ, Riggs L, Regnier FE. The impact of buffers and surfactants from micellar electrokinetic chromatography on matrix-assisted laser desorption ionization (MALDI) mass spectrometry of peptides. Effect of buffer type and concentration on mass determination by MALDI-time-of-flight mass spectrometry. J Chromatogr A 2000;894(1-2):345-55.
12. Bajuk A, Gluch K, Michalak L. Effect of impurities on the matrix-assisted laser desorption/ionization mass spectra of insulin. Rapid Commun Mass Spectrom 2001;15(24):2383-6.
13. Kallweit U, Börnsen KO, Kresbach GM, Widmer HM. Matrix compatible buffers for analysis of proteins with matrix-assisted laser desorption/ionization mass spectrometry. Rapid Commun Mass Spectrom 1996;10:845-9.
14. Mock KK, Sutton CW, Cottrell JS. Sample immobilization protocols for matrix-asssisted laser-desorption mass spectrometry. Rapid Commun Mass Spectrom 1992;6(4):233 - 8.
15. Shaler TA, Wickham JN, Sannes KA, Wu KJ, Becker CH. Effect of impurities on the matrix-assisted laser desorption mass spectra of single-stranded oligodeoxynucleotides. Anal Chem 1996;68(3): 576-9.
16. Yao J, Scott JR, Young MK, Wilkins CL. Importance of matrix:analyte ratio for buffer tolerance using 2,5-dihydroxybenzoic acid as a matrix in matrix-assisted laser desorption/ionization-Fourier transform mass spectrometry and matrix-assisted laser desorption/ionization-time of flight. J Am Soc Mass Spectrom 1998;9(8):805-13.
17. Keller BO, Sui J, Young AB, Whittal RM. Interferences and contaminants encountered in modern mass spectrometry. Anal Chim Acta 2008;627(1):71-81.

18. Sleno L, Volmer DA. Some fundamental and technical aspects of the quantitative analysis of pharmaceutical drugs by matrix-assisted laser desorption/ionization mass spectrometry. Rapid Commun Mass Spectrom 2005;19(14):1928-36.
19. Gobey J, Cole M, Janiszewski J, et al. Characterization and performance of MALDI on a triple quadrupole mass spectrometer for analysis and quantification of small molecules. Anal Chem 2005;77(17):5643-54.
20. Volmer DA, Sleno L, Bateman K, et al. Comparison of MALDI to ESI on a Triple Quadrupole Platform for Pharmacokinetic Analyses. Anal Chem 2007.
21. Dekker LJ, Burgers PC, Guzel C, Luider TM. FTMS and TOF/TOF mass spectrometry in concert: identifying peptides with high reliability using matrix prespotted MALDI target plates. J Chromatogr B Analyt Technol Biomed Life Sci 2007;847(1):62-4.
22. Gouw JW, Burgers PC, Trikoupis MA, Terlouw JK. Derivatization of small oligosaccharides prior to analysis by matrix-assisted laser desorption/ionization using glycidyltrimethylammonium chloride and Girard's reagent T. Rapid Commun Mass Spectrom 2002;16(10):905-12.
23. Krutchinsky AN, Chait BT. On the nature of the chemical noise in MALDI mass spectra. J Am Soc Mass Spectrom 2002;13(2):129-34.
24. Srinivasan N, Haney CA, Lindsey JS, Zhang W, Chait BT. Investigation of MALDI-TOF mass spectrometry of diverse synthetic metalloporphyrins, phthalocyanines and multiporphyrin arrays. Journal of Porphyrins and Phthalocyanines 1999;3(4):283 - 91.
25. Chen YT, Ling YC. Detection of water-soluble vitamins by matrix-assisted laser desorption/ionization time-of-flight mass spectrometry using porphyrin matrices. J Mass Spectrom 2002;37(7): 716-30.
26. Jones RM, Lamb JH, Lim CK. 5,10,15,20-meso-tetra(hydroxyphenyl)chlorin as a matrix for the analysis of low molecular weights compounds by matrix-assisted laser desorption/ionization time-of-flight mass spectrometry. Rapid Communications in Mass Spectrometry 1995;9(10):968 - 9.
27. Ayorinde FO, Bezabeh DZ, Delves IG. Preliminary investigation of the simultaneous detection of sugars, ascorbic acid, citric acid, and sodium benzoate in non-alcoholic beverages by matrix-assisted laser desorption/ionization time-of-flight mass spectrometry. Rapid Commun Mass Spectrom 2003;17(15):1735-42.
28. Ayorinde FO, Garvin K, Saeed K. Determination of the fatty acid composition of saponified vegetable oils using matrix-assisted laser desorption/ionization time-of-flight mass spectrometry. Rapid Commun Mass Spectrom 2000;14(7):608-15.
29. Ayorinde FO, Hambright P, Porter TN, Keith QL, Jr. Use of meso- tetrakis(pentafluorophenyl) porphyrin as a matrix for low molecular weight alkylphenol ethoxylates in laser desorption/ ionization time-of-flight mass spectrometry. Rapid Commun Mass Spectrom 1999;13(24):2474-9.
30. Hlongwane C, Delves IG, Wan LW, Ayorinde FO. Comparative quantitative fatty acid analysis of triacylglycerols using matrix-assisted laser desorption/ionization time-of-flight mass spectrometry and gas chromatography. Rapid Commun Mass Spectrom 2001;15(21):2027-34.
31. Kosanam H, Prakash PK, Yates CR, Miller DD, Ramagiri S. Rapid screening of doping agents in human urine by vacuum MALDI-linear ion trap mass spectrometry. Anal Chem 2007;79(15):6020-6.
32. van Kampen JJ, Verschuren EJ, Burgers PC, et al. Validation of an HIV-1 inactivation protocol that is compatible with intracellular drug analysis by mass spectrometry. J Chromatogr B Analyt Technol Biomed Life Sci 2007;847(1):38-44.

33. Yu H, Lopez E, Young SW, Luo J, Tian H, Cao P. Quantitative analysis of free fatty acids in rat plasma using matrix-assisted laser desorption/ionization time-of-flight mass spectrometry with meso-tetrakis porphyrin as matrix. Anal Biochem 2006;354(2):182-91.
34. Soltzberg LJ, Patel P. Small molecule matrix-assisted laser desorption/ionization time-of-flight mass spectrometry using a polymer matrix. Rapid Commun Mass Spectrom 2004;18(13):1455-8.
35. Huang JP, Yuan CH, Shiea J, Chen YC. Rapid screening for diuretic doping agents in urine by C60-assisted laser-desorption-ionization-time-of-flight mass spectrometry. J Anal Toxicol 1999;23(5): 337-42.
36. Shiea J, Huang JP, Teng CF, Jeng J, Wang LY, Chiang LY. Use of a water-soluble fullerene derivative as precipitating reagent and matrix-assisted laser desorption/ionization matrix to selectively detect charged species in aqueous solutions. Anal Chem 2003;75(14):3587-95.
37. Gross JH. Meaning of the Rate Constant. In: Gross JH, ed. Mass Spectrometry: A Textbook. 1st ed: Springer; 2004:28-9.
38. Wei J, Buriak JM, Siuzdak G. Desorption-ionization mass spectrometry on porous silicon. Nature 1999;399(6733):243-6.
39. Trauger SA, Go EP, Shen Z, et al. High sensitivity and analyte capture with desorption/ionization mass spectrometry on silylated porous silicon. Anal Chem 2004;76(15):4484-9.
40. Cohen LH, Go EP, Siuzdak G. Small Molecule Desorption/Ionization Mass Analysis. In: Hillenkamp F, Peter-Katalinic J, eds. MALDI MS: A Practical Guide to Instrumentation, Methods and Applications. Weinheim: Wiley-VCH; 2007.
41. Kang MJ, Pyun JC, Lee JC, et al. Nanowire-assisted laser desorption and ionization mass spectrometry for quantitative analysis of small molecules. Rapid Commun Mass Spectrom 2005;19: 3166-70.
42. Najam-ul-Haq M, Rainer M, Szabo Z, Vallant R, Huck CW, Bonn GK. Role of carbon nano-materials in the analysis of biological materials by laser desorption/ionization-mass spectrometry. J Biochem Biophys Methods 2007;70(2):319-28.
43. Petterson DS. Matrix-free methods for laser desorption/ionization mass spectrometry. Mass spectrometry reviews 2007;26(1):19-34.
44. Guo Z, Zhang Q, Zou H, Guo B, Ni J. A method for the analysis of low-mass molecules by MALDI-TOF mass spectrometry. Anal Chem 2002;74(7):1637-41.
45. Su AK, Liu JT, Lin CH. Rapid drug-screening of clandestine tablets by MALDI-TOF mass spectrometry. Talanta 2005;67(4):718-24.
46. Grant DC, Helleur RJ. Rapid screening of anthocyanins in berry samples by surfactant-mediated matrix-assisted laser desorption/ionization time-of-flight mass spectrometry. Rapid Commun Mass Spectrom 2008;22(2):156-64.
47. Grant DC, Helleur RJ. Simultaneous analysis of vitamins and caffeine in energy drinks by surfactant-mediated matrix-assisted laser desorption/ionization. Anal Bioanal Chem 2008;391(8): 2811-8.
48. Grant DC, Helleur RJ. Surfactant-mediated matrix-assisted laser desorption/ionization time-of-flight mass spectrometry of small molecules. Rapid Commun Mass Spectrom 2007;21(6):837-45.
49. Yamaguchi S, Fujita T, Fujino T, Korenaga T. Suppression of matrix-related ions using cyclodextrin in MALDI mass spectrometry. Anal Sci 2008;24(11):1497-500.
50. Smirnov IP, Zhu X, Taylor T, et al. Suppression of alpha-cyano-4-hydroxycinnamic acid matrix clusters and reduction of chemical noise in MALDI-TOF mass spectrometry. Anal Chem 2004;76(10): 2958-65.

51. Guo Z, He L. A binary matrix for background suppression in MALDI-MS of small molecules. Analytical and Bioanalytical Chemistry 2007;387(5):1939-44.
52. Knochenmuss R, Dubois F, Dale MJ, Zenobi R. The Matrix Suppression Effect and Ionization Mechanisms in Matrix-assisted Laser Desorption/Ionization. Rapid Communications in Mass Spectrometry 1996;10(8):871 - 7.
53. Knochenmuss R, Karbach V, Wiesli W, Breuker K, Zenobi R. The matrix suppression effect in matrix-assisted laser desorption/ionization: Application to negative ions and further characteristics. Rapid Communications in Mass Spectrometry 1998;12(9): 529 - 34.
54. Knochenmuss R, Stortelder A, Breuker K, Zenobi R. Secondary ion-molecule reactions in matrix-assisted laser desorption/ionization. J Mass Spectrom 2000;35(11):1237-45.
55. McCombie G, Knochenmuss R. Small-molecule MALDI using the matrix suppression effect to reduce or eliminate matrix background interferences. Anal Chem 2004;76(17):4990-7.
56. Vaidyanathan S, Gaskell S, Goodacre R. Matrix-suppressed laser desorption/ionisation mass spectrometry and its suitability for metabolome analyses. Rapid Commun Mass Spectrom 2006; 20(8):1192-8.
57. Corr JJ, Kovarik P, Schneider BB, Hendrikse J, Loboda A, Covey TR. Design considerations for high speed quantitative mass spectrometry with MALDI ionization. J Am Soc Mass Spectrom 2006; 17(8):1129-41.
58. Hillenkamp F, Karas M. The MALDI Process and Method. In: Hillenkamp F, Peter-Katalinic J, eds. MALDI MS: A Practical Guide to Instrumentation, Methods and Applications. Weinheim: Wiley-VCH; 2007.
59. Hensel RR, King RC, Owens KG. Electrospray sample preparation for improved quantitation in matrix-assisted laser desorption/ionization time-of-flight mass spectrometry. Rapid Commun Mass Spectrom 1997;11(16):1785-93.
60. Chen H, Guo B. Use of binary solvent systems in the MALDI-TOF analysis of poly(methyl methacrylate). Anal Chem 1997;69(21):4399-404.
61. Hoteling AJ, Mourey TH, Owens KG. Importance of solubility in the sample preparation of poly(ethylene terephthalate) for MALDI TOFMS. Anal Chem 2005;77(3):750-6.
62. Hoteling AJ, Erb WJ, Tyson RJ, Owens KG. Exploring the importance of the relative solubility of matrix and analyte in MALDI sample preparation using HPLC. Anal Chem 2004;76(17):5157-64.
63. Vorm O, Roepstorff P, Mann M. Improved resolution and very high sensitivity in MALDI TOF of matrix surfaces made by fast evaporation. Anal Chem 1994;66(19):3281-7.
64. Onnerfjord P, Ekstrom S, Bergquist J, Nilsson J, Laurell T, Marko-Varga G. Homogeneous sample preparation for automated high throughput analysis with matrix-assisted laser desorption/ ionisation time-of-flight mass spectrometry. Rapid Commun Mass Spectrom 1999;13(5):315-22.
65. Westman A, Nilsson CL, Ekman R. Matrix-assisted laser desorption/ionization time-of-flight mass spectrometry analysis of proteins in human cerebrospinal fluid. Rapid Commun Mass Spectrom 1998;12(16):1092-8.
66. Westman A, Demirev P, Huth-Fehre T, Bielawski J, Sundqvist BUR. Sample exposure effects in matrix-assisted laser desorption—ionization mass spectrometry of large biomolecules International Journal of Mass Spectrometry and Ion Processes 1994;130(1-2):107-15
67. Xiang F, Beavis RC, Ens W. A method to increase contaminant tolerance in protein matrix-assisted laser desorption/ionization by the fabrication of thin protein-doped polycrystalline films. Rapid Communications in Mass Spectrometry 1994;8(2): 199 - 204.
68. Gusev AI, Wilkinson WR, Proctor A, Hercules DM. Improvement of signal reproducibility and matrix/comatrix effects in MALDI analysis. Anal Chem 1995;67(6):1034–41.

69. Owen SJ, Meier FS, Brombacher S, Volmer DA. Increasing sensitivity and decreasing spot size using an inexpensive, removable hydrophobic coating for matrix-assisted laser desorption/ionisation plates. Rapid Commun Mass Spectrom 2003;17(21):2439-49.
70. Schuerenberg M, Luebbert C, Eickhoff H, Kalkum M, Lehrach H, Nordhoff E. Prestructured MALDI-MS sample supports. Anal Chem 2000;72(15):3436-42.
71. Dekker LJ, van Kampen JJ, Reedijk ML, et al. A mass spectrometry based imaging method developed for the intracellular detection of HIV protease inhibitors. Rapid Commun Mass Spectrom 2009;23(8):1183-8.
72. Hankin JA, Barkley RM, Murphy RC. Sublimation as a method of matrix application for mass spectrometric imaging. J Am Soc Mass Spectrom 2007;18(9):1646-52.
73. Kim SH, Shin CM, Yoo JS. First application of thermal vapor deposition method to matrix-assisted laser desorption ionization mass spectrometry: Determination of molecular mass of bis(p-methyl benzylidene) sorbitol. Rapid Communications in Mass Spectrometry 1998;12(11): 701 - 4.
74. Wagner M, Varesio E, Hopfgartner G. Ultra-fast quantitation of saquinavir in human plasma by matrix-assisted laser desorption/ionization and selected reaction monitoring mode detection. J Chromatogr B Analyt Technol Biomed Life Sci 2008;872(1-2):68-76.
75. Wei H, Nolkrantz K, Powell DH, Woods JH, Ko MC, Kennedy RT. Electrospray sample deposition for matrix-assisted laser desorption/ionization (MALDI) and atmospheric pressure MALDI mass spectrometry with attomole detection limits. Rapid Commun Mass Spectrom 2004;18(11):1193-200.
76. Allmaier G. Picoliter to nanoliter deposition of peptide and protein solutions for matrix-assisted laser desorption/ionization mass spectrometry. Rapid Communications in Mass Spectrometry 1998;11(14):1567 - 9.
77. Little DP, Cornish TJ, O'Donnell MO, Braun A, Cotter RJ, Kolster H. MALDI on a Chip: Analysis of Arrays of Low-Femtomole to Subfemtomole Quantities of Synthetic Oligonucleotides and DNA Diagnostic Products Dispensed by a Piezoelectric Pipet. Anal Chem 1997;69(22):4540-6.
78. Onnerfjord P, Nilsson J, Wallman L, Laurell T, Marko-Varga G. Picoliter sample preparation in MALDI-TOF MS using a micromachined silicon flow-through dispenser. Anal Chem 1998;70(22): 4755-60.
79. Sleno L, Volmer DA. Assessing the properties of internal standards for quantitative matrix-assisted laser desorption/ionization mass spectrometry of small molecules. Rapid Commun Mass Spectrom 2006;20(10):1517-24.
80. Armstrong DW, Zhang LK, He L, Gross ML. Ionic liquids as matrixes for matrix-assisted laser desorption/ionization mass spectrometry. Anal Chem 2001;73(15):3679-86.
81. Wasserscheid P, Keim W. Ionic Liquids-New "Solutions" for Transition Metal Catalysis. Angew Chem Int Ed Engl 2000;39(21):3772-89.
82. Zabet-Moghaddam M, Heinzle E, Tholey A. Qualitative and quantitative analysis of low molecular weight compounds by ultraviolet matrix-assisted laser desorption/ionization mass spectrometry using ionic liquid matrices. Rapid Commun Mass Spectrom 2004;18(2):141-8.
83. Tholey A, Heinzle E. Ionic (liquid) matrices for matrix-assisted laser desorption/ionization mass spectrometry-applications and perspectives. Anal Bioanal Chem 2006;386(1):24-37.
84. Li YL, Gross ML. Ionic-liquid matrices for quantitative analysis by MALDI-TOF mass spectrometry Journal of the American Society for Mass Spectrometry 2004;15(12):1833-7.
85. Mank M, Stahl B, Boehm G. 2,5-Dihydroxybenzoic acid butylamine and other ionic liquid matrixes for enhanced MALDI-MS analysis of biomolecules. Anal Chem 2004;76(10):2938-50.

86. Lemaire R, Tabet JC, Ducoroy P, Hendra JB, Salzet M, Fournier I. Solid ionic matrixes for direct tissue analysis and MALDI imaging. Anal Chem 2006;78(3):809-19.
87. Kang MJ, Tholey A, Heinzle E. Application of automated matrix-assisted laser desorption/ionization time-of-flight mass spectrometry for the measurement of enzyme activities. Rapid Commun Mass Spectrom 2001;15(15):1327-33.
88. Wilkinson WR, Gusev AI, Proctor A, Houalla M, Hercules DM. Selection of internal standards for quantitative analysis by matrix-assisted laser desorption-ionization (MALDI) time-of-flight mass spectrometry Analytical and Bioanalytical Chemistry 1997;357(3):241-8.
89. Nicola AJ, Gusev AI, Proctor A, Hercules DM. Automation of data collection for matrix-assisted laser desorption/ionization mass spectrometry using a correlative analysis algorithm. Anal Chem 1998;70(15):3213-9.
90. Horak J, Werther W, Schmid ER. Optimisation of the quantitative determination of chlormequat by matrix-assisted laser desorption/ionisation mass spectrometry. Rapid Commun Mass Spectrom 2001;15(4):241-8.
91. van Kampen JJ, Fraaij PL, Hira V, et al. A new method for analysis of AZT-triphosphate and nucleotide-triphosphates. Biochem Biophys Res Commun 2004;315(1):151-9.
92. van Kampen JJA, Luider TM, Ruttink PJA, Burgers PC. Metal ion attachment to the matrix meso-tetrakis(pentafluorophenyl)porphyrin, related matrices and analytes: an experimental and theoretical study. J Mass Spectrom 2009: In Press.
93. Bogan MJ, Agnes GR. Poly(ethylene glycol) doubly and singly cationized by different alkali metal ions: Relative cation affinities and cation-dependent resolution in a quadrupole ion trap mass spectrometer. Journal of the American Society for Mass Spectrometry 2002;13(2):177-86
94. Zhang J, Zenobi R. Matrix-dependent cationization in MALDI mass spectrometry. J Mass Spectrom 2004;39(7):808-16.
95. Hoberg AM, Haddleton DM, Derrick PJ, Jackon AT, Scrivens JH. The effect of counter ions in matrix-assisted laser desorption/ionization of poly(methyl methacrylate). Eur Mass Spectrom 1998;4: 435-40.
96. Jobst KJ, Terlouw JK, Luider TM, Burgers PC. On the interaction of peptides with calcium ions as studied by matrix-assisted laser desorption/ionization Fourier transform mass spectrometry: towards peptide fishing using metal ion baits. Anal Chim Acta 2008;627(1):136-47.
97. Francis GJ, Forbes M, Volmer DA, Bohme DK. Periodicity in collision-induced and remote-bond activation of alkali metal ions attached to polyether ionophores. Analyst 2005;130(4):508-13.
98. Black C, Poile C, Langley J, Herniman J. The use of pencil lead as a matrix and calibrant for matrix-assisted laser desorption/ionisation. Rapid Commun Mass Spectrom 2006;20(7):1053-60.
99. Langley GJ, Herniman JM, Townell MS. 2B or not 2B, that is the question: further investigations into the use of pencil as a matrix for matrix-assisted laser desorption/ionisation. Rapid Commun Mass Spectrom 2007;21(2):180-90.
100. Wu J, Chatman K, Harris K, Siuzdak G. An automated MALDI mass spectrometry approach for optimizing cyclosporin extraction and quantitation. Anal Chem 1997;69(18):3767-71.
101. Kovarik P, Grivet C, Bourgogne E, Hopfgartner G. Method development aspects for the quantitation of pharmaceutical compounds in human plasma with a matrix-assisted laser desorption/ionization source in the multiple reaction monitoring mode. Rapid Commun Mass Spectrom 2007;21(6):911-9.
102. Lin PC, Tseng MC, Su AK, Chen YJ, Lin CC. Functionalized magnetic nanoparticles for small-molecule isolation, identification, and quantification. Anal Chem 2007;79(9):3401-8.

103. Sleno L, Volmer DA. Toxin screening in phytoplankton: detection and quantitation using MALDI triple quadrupole mass spectrometry. Anal Chem 2005;77(5):1509-17.
104. Rideout D, Bustamante A, Siuzdak G. Cationic drug analysis using matrix-assisted laser desorption/ionization mass spectrometry: application to influx kinetics, multidrug resistance, and intracellular chemical change. Proc Natl Acad Sci U S A 1993;90(21):10226-9.
105. Cheng Z, Winant RC, Gambhir SS. A new strategy to screen molecular imaging probe uptake in cell culture without radiolabeling using matrix-assisted laser desorption/ionization time-of-flight mass spectrometry. J Nucl Med 2005;46(5):878-86.
106. Burlina F, Sagan S, Bolbach G, Chassaing G. Quantification of the cellular uptake of cell-penetrating peptides by MALDI-TOF mass spectrometry. Angew Chem Int Ed Engl 2005;44(27):4244-7.
107. Muddiman DC, Gusev AI, Proctor A, Hercules DM, Venkataramanan R, Diven W. Quantitative measurement of cyclosporin A in blood by time-of-flight mass spectrometry. Anal Chem 1994; 66(14):2362-8.
108. Gusev AI, Muddiman DC, Proctor A, et al. A quantitative study of in vitro hepatic metabolism of tacrolimus (FK506) using secondary ion and matrix-assisted laser desorption/ionization mass spectrometry. Rapid Commun Mass Spectrom 1996;10(10):1215-8.
109. Notari S, Mancone C, Alonzi T, Tripodi M, Narciso P, Ascenzi P. Determination of abacavir, amprenavir, didanosine, efavirenz, nevirapine, and stavudine concentration in human plasma by MALDI-TOF/TOF. J Chromatogr B Analyt Technol Biomed Life Sci 2008;863(2):249-57.
110. Vaidyanathan S, Goodacre R. Quantitative detection of metabolites using matrix-assisted laser desorption/ionization mass spectrometry with 9-aminoacridine as the matrix. Rapid Commun Mass Spectrom 2007;21(13):2072-8.
111. Vaidyanathan S, Jones D, Ellis J, et al. Laser desorption/ionization mass spectrometry on porous silicon for metabolome analyses: influence of surface oxidation. Rapid Commun Mass Spectrom 2007;21(13):2157-66.
112. Rompp A, Dekker L, Taban I, et al. Identification of leptomeningeal metastasis-related proteins in cerebrospinal fluid of patients with breast cancer by a combination of MALDI-TOF, MALDI-FTICR and nanoLC-FTICR MS. Proteomics 2007;7(3):474-81.
113. Stoop MP, Lamers RJ, Burgers PC, Sillevis Smitt PA, Hintzen RQ, Luider TM. The rate of false positive sequence matches of peptides profiled by MALDI MS and identified by MS/MS. J Proteome Res 2008;7(11):4841-7.
114. Nordstrom A, Want E, Northen T, Lehtio J, Siuzdak G. Multiple ionization mass spectrometry strategy used to reveal the complexity of metabolomics. Anal Chem 2008;80(2):421-9.
115. Brombacher S, Owen SJ, Volmer DA. Automated coupling of capillary-HPLC to matrix-assisted laser desorption/ionization mass spectrometry for the analysis of small molecules utilizing a reactive matrix. Anal Bioanal Chem 2003;376(6):773-9.
116. Lee PJ, Chen W, Gebler JC. Qualitative and Quantitative Analysis of Small Amine Molecules by MALDI-TOF Mass Spectrometry through Charge Derivatization. Anal Chem 2004;76(16):4888–93.
117. Kang MJ, Tholey A, Heinzle E. Quantitation of low molecular mass substrates and products of enzyme catalyzed reactions using matrix-assisted laser desorption/ionization time-of-flight mass spectrometry. Rapid Commun Mass Spectrom 2000;14(21):1972-8.
118. Shen Z, Go EP, Gamez A, et al. A mass spectrometry plate reader: monitoring enzyme activity and inhibition with a Desorption/Ionization on Silicon (DIOS) platform. Chembiochem 2004;5(7): 921-7.

119. Tholey A, Zabet-Moghaddam M, Heinzle E. Quantification of peptides for the monitoring of protease-catalyzed reactions by matrix-assisted laser desorption/ionization mass spectrometry using ionic liquid matrixes. Anal Chem 2006;78(1):291-7.
120. Whittal RM, Palcic MM, Hindsgaul O, Li L. Direct analysis of enzymatic reactions of oligosaccharides in human serum using matrix-assisted laser desorption ionization mass spectrometry. Anal Chem 1995;67(19):3509-14.
121. Knochenmuss R. Ion formation mechanisms in UV-MALDI. Analyst 2006;131(9):966-86.
122. Knochenmuss R. A quantitative model of ultraviolet matrix-assisted laser desorption/ionization including analyte ion generation. Anal Chem 2003;75(10):2199-207.
123. Jaskolla TW, Lehmann WD, Karas M. 4-Chloro-alpha-cyanocinnamic acid is an advanced, rationally designed MALDI matrix. Proc Natl Acad Sci U S A 2008;105(34):12200-5.

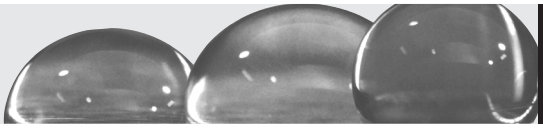

Chapter 12

Summary & discussion

Summary & discussion

In this thesis we show various approaches to determine clinically relevant intracellular concentrations of antiretroviral drugs. The assays were developed to study the intracellular pharmacokinetics of antiretroviral drugs in HIV infected children, and therefore we set the criterion that the measurements could be performed using 1 x 10^6 PBMCs which corresponds to a blood sample of 1-2 mL. We mainly explored the applicability of MALDI mass spectrometry for this purpose. By MALDI mass spectrometry, (sub)femtomole amounts of compounds can be detected, which should allow one to determine antiretroviral drug concentrations in 1 x 10^6 PBMCs. Furthermore, in MALDI mass spectrometry, measurements can be performed in a high throughput manner, which is highly desirable when analysis of relative large numbers of samples is foreseen. The assays should also fulfil the ± 20/15% criteria for precision and accuracy. In this respect, MALDI mass spectrometry is normally not the first choice of mass spectrometric techniques. Poor reproducibilities of signal intensities have frequently been reported for MALDI mass spectrometry. The heterogeneous crystallization of matrix and sample as well as position-dependent variations in the amount of compound incorporated in the crystals, result in poor shot-to-shot reproducibility and poor spot-to-spot reproducibility. An additional drawback of MALDI for measurements of small molecules (< 1,000 Da) such as drugs is that commonly employed matrices produce interfering signals in the low mass range. Yet, when strategies are employed that focus on reproducible analysis of small molecules, precise and accurate quantitative analysis of drugs can be obtained within the set ± 20/15% criteria, and matrix-derived interfering signals can be eliminated or circumvented.

We have tested three forms of MALDI mass spectrometry for the quantitative analysis of NNRTIs and HIV protease inhibitors; MALDI time-of-flight (TOF), MALDI Fourier-transform ion cyclotron resonance (FTICR), and MALDI triple quadrupole (QqQ).

The high molecular weigh matrix meso-tetrakis(pentafluorophenyl)porphyrin (F20TPP; MW 974) was used for the analyses of various pharmaceutical compounds by MALDI-TOF mass spectrometry. Because the molecular mass of this matrix is in excess of that of the compounds investigated, the only matrix-derived interfering signals that are observed in the low mass range originate from matrix impurities or matrix dissociation, but not from matrix adduct formation. This matrix results in mass spectra that are virtually free of matrix-derived interfering peaks in the low mass range. We could however not detect protonated forms of the drugs tested when F20TPP was used as matrix. Due to the relative high proton affinity of 245 kcal/mol for F20TPP many compounds may not be protonated by this matrix. Another possibility is that the analytes show prompt in-source fragmentation when F20TPP does transfer a proton to the analyte. Strong signals were however observed for the drugs ionized by alkali metal ions. Surprisingly,

compounds were most efficiently cationized by Li^+ attachment instead of K^+ which is found with commonly employed matrices such as 2,5-dihydroxybenzoic acid (DHB). This feature was exploited by adding lithium iodide to the matrix solution. To improve the reproducibility of the measurements, the matrix solution was applied on prestructured target plates using a brushing spotting technique, which resulted in a homogeneous crystal layer. Samples dissolved in methanol/water (1:1) were deposited on to the homogeneous crystal layer without perturbing the crystal homogeneity, because F20TPP does not dissolve in this solution. To further improve precisions, an internal standard was employed, many laser shots were used to obtain an averaged mass spectrum, and multiple spots were measured. This combination resulted in accurate, precise, and sensitive quantitative analysis of lopinavir spiked in extracts of 1×10^6 PBMCs. The combination of internal standard, averaging out, and focussing on homogeneous crystallization of sample and matrix showed to be the key for precise and accurate quantitative analysis of small molecules by the various forms of MALDI mass spectrometry tested. The preference for lithium cationization of F20TPP and other porphyrin matrices was investigated. *Ab initio* calculations showed that lithium is attached to the cavity of porphyrin. Li^+ is situated on but not in the porphyrin cavity and the whole porphyrin molecule becomes bent. The lithium ion is thus still exposed and therefore accessible for transfer to the analyte. Other alkali metal ions such as sodium and potassium are also situated on the porphyrin and are more exposed than Li^+ but at the same time the cation affinity becomes less. Experimental data showed that only lithium ions produce intense signals for attachment to F20TPP, and, since model analytes show the same quantitative distribution of alkali metal attachment as the F20TPP matrix, we propose that such F20TPP + Li^+ ions are the cation donators to the analytes.

Attempts to use F20TPP as matrix in MALDI-FTICR mass spectrometry showed extensive matrix-derived fragment ions in the low mass range in contrast to the MALDI-TOF experiments. This is due to the relatively long time needed before ions are detected (~ 1 s) in FTICR compared to TOF (~ 10^{-4} s). When the time needed for detection is longer than the averaged life-time of the matrix ions, intense matrix fragmentation will be observed, which seems to be the case for F20TPP. In the same vein, it is expected that matrix clusters of small molecules matrices such as DHB (MW 154) also dissociate on the FTICR time scale resulting mass spectra with little or no matrix-derived signals. This appeared to be the case when DHB was used for analysis of antiretroviral drugs. The HIV protease inhibitors indinavir, nelfinavir and saquinavir showed strong signals for their protonated forms. However, for lopinavir and ritonavir such signals were weak. Again a cationization approach with alkali metals resulted in signals of good intensity for all HIV protease inhibitors tested. To improve the precisions, dimethylsulfoxide (DMSO) was added to the matrix solutions and samples were spotted on to prestructered target plates. Using this

approach, clinically relevant amounts of antiretroviral drugs were determined in lysates of 1 x 10^6 PBMCs in a precise and accurate manner.

Isobaric matrix interferences, i.e. ions with the same nominal mass as the analyte, are expected to show product ions of different masses upon fragmentation. Thus, by performing tandem mass spectrometry measurements, one is able to distinguish matrix from analyte. For this approach, we used the MALDI-QqQ mass spectrometer. This apparatus is equipped with a high repetition rate laser (1,000 Hz) and a sample can be measured within seconds. In the selected reaction monitoring (SRM) mode of the QqQ instrument, only compound specific precursor/product ion transition are monitored and interfering matrix ions are removed, which means that commonly employed small molecule matrices can be used in this approach. DHB showed to be a good matrix for protonation of antiretroviral drugs although this matrix resulted in relatively high %CVs. The novel matrix 7-hydroxy-4-(trifluoromethyl)coumarin (HFMC) also proved to be a good matrix for protonation of antiretroviral drugs. To improve the sensitivity, accuracy, and precisions when using HFMC, samples were spotted on target plates that were coated with a strongly hydrophobic fluoropolymer. The matrix α-cyano-4-hydroxycinnamic acid (CHCA) showed the best precisions and was therefore used for the MALDI-QqQ assay that was applied to determine the intracellular concentrations of lopinavir and ritonavir in HIV infected children. Again, for lopinavir and ritonavir a cationization strategy with alkali metals was pursued, while other antiretroviral drugs were best detected in their protonated forms.

Of the three forms of MALDI mass spectrometry tested, we found that MALDI-QqQ has the best applicability for quantitative analysis of small molecule drugs. Precisions, accuracies, dynamic range and sensitivity are superior to that obtained by FTICR or TOF, and there is no restriction in the type of matrix used. Furthermore, sample analysis time is only a few seconds and measurements and data analysis are performed in an automated way. This holds true when MALDI-QqQ is used in the SRM mode, i.e. in this mode you only find what you are looking for, and this approach should thus be used for targeted quantification. What may then be the role of MALDI-TOF and MALDI-FTICR in small molecule analysis? We used MALDI-TOF and MALDI-FTICR in the MS-mode, i.e. a broadband mass spectrum is recorded, and, besides the compounds of interest, other analytes are detected which may include endogenous components or drug metabolites. We propose that these techniques should be used for discovery type applications, for example when quantitative analysis of compounds as well as finding drug metabolites is pursued. For such applications, MALDI-FTICR would be the first choice of MALDI mass spectrometer due to its superior resolution and mass accuracy.

NRTI-triphosphates proved to be a more difficult class of compounds to quantify using MALDI mass spectrometry due to isomeric interferences. ATP, dGTP, and zidovudine-triphosphate have the same composition in elements, i.e. they are isomeric, and can not

be distinguished on mass alone. We used MALDI-TOF post-source decay experiments, a form of tandem mass spectrometry, to distinguish zidovudine-triphosphate from ATP and dGTP. Sensitivity obtained on that particular instrument may not be enough for clinical application. Therefore, we investigated the use of LC-MS for this purpose. We used ion-pair LC-MS for proper separation of NRTIs, endogenous (deoxy)nucleosides and mono-, di-, and triphosphate forms thereof. Sensitivity, precision, and accuracies allow for clinical application of this assay. Sample analysis time with this assay is much longer compared to the use of MALDI mass spectrometry. On the other hand, many compounds are quantified in a single run.

For our MALDI assays, we used 96-well solid phase extraction plates to clean and to concentrate lysates of 1 x 10^6 PBMCs. An entire SPE plate can be processed in ~ 30 minutes which is desirable when large numbers of samples need to be measured. We also succeeded in the semi-quantitative analysis of HIV protease inhibitors in cytocentrifuged cells *in vitro*. In this approach, the SPE step is omitted. For quantitative analysis of HIV protease inhibitors in plasma, we showed that a simple protein precipitation with methanol is sufficient to prepare samples prior to MALDI analysis. Safety issues are a concern when working with HIV infected samples. We therefore validated a protocol for inactivation of infectious HIV. Incubation of HIV infected cells for one hour in solutions containing ≥ 40% methanol or ethanol resulted in reduction of infectious titers of more than 6 log. Solutions containing ≥ 40% methanol or ethanol are also used to extract antiretroviral drugs from cells. Thus, a dual purpose protocol was developed.

Application of the assays in HIV infected children treated with Kaletra (lopinavir/ritonavir) and two NRTIs showed a poor correlation between plasma and intracellular concentrations of lopinavir as well as for ritonavir. Furthermore, we found lower concentrations of lopinavir in PBMCs than in plasma. For ritonavir, this was dependent on the isolation procedure of the PBMCs. Further research in this area at a larger scale is however limited by the PBMC isolation protocol, which is laborious and time-consuming, and requires extensive planning between clinic and laboratory. The challenge is now to develop a straight forward and simple cell isolation protocol. One approach would be to isolate $CD4^+$ T-cells and $CD14^+$ monocytes directly from whole blood using magnetic beads labelled with the appropriate antibodies. An additional advantage would be that the intracellular concentrations are now measured in the for HIV relevant subsets of PBMCs. We have shown that MALDI mass spectrometry can be used for semi-quantitative analysis of antiretroviral drugs in cytocentrifuged cells in vitro. Further optimization of this approach may allow one to determine drug concentrations in patients' samples in a more easy way. Notwithstanding the above, our studies show that MALDI mass spectrometry is excellent tool for fast, sensitive, and reproducible analysis of small molecules such as antiretroviral drugs in clinical samples.

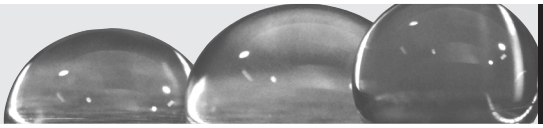

Appendices

Samenvatting

Dankwoord

PhD Portfolio

Samenvatting

In dit proefschrift beschrijven wij verschillende methoden om klinisch relevante concentraties van antiretrovirale geneesmiddelen te meten in plasma en in cellen. De meeste antiretrovirale geneesmiddelen zoals nucleoside reverse transcriptase remmers (NRTIs), non-NRTIs en protease remmers zijn werkzaam in bepaalde witte bloedcellen die geïnfecteerd kunnen worden door HIV. Het feit dat antiretrovirale medicatie bij sommige patiënten HIV niet optimaal onderdrukt, zou verklaard kunnen worden door afwijkende intracellulaire concentraties van deze geneesmiddelen. We hebben ervoor gekozen om de intracellulaire concentraties te bepalen in mononucleaire cellen uit perifeer bloed (PBMCs), omdat een deel van deze cellen - namelijk de $CD4^+$ T-cellen en monocyten - geïnfecteerd kan worden door HIV. Eén van de criteria voor ontwikkeling van de nieuwe meetmethoden is dat de methoden toegepast kunnen worden om de intracellulaire farmacokinetiek van antiretrovirale geneesmiddelen bij HIV-1 geïnfecteerde kinderen te bepalen. We hebben daarom gesteld dat de metingen verricht kunnen worden met een bloedmonster van twee mL. Uit twee mL bloed kan ongeveer 1×10^6 PBMCs worden geïsoleerd. Het intracellulaire volume van 1×10^6 PBMCs is ongeveer 0,4 µL. Om de intracellulaire concentraties van antiretrovirale geneesmiddelen te kunnen meten is dus een zeer gevoelige methode nodig. Daartoe hebben we massaspectrometrie gebruikt voor de nieuw ontwikkelde meetmethoden, met name matrix-assisted laser desorption/ionization (MALDI) massaspectrometrie. MALDI massaspectrometrie wordt echter weinig toegepast voor het meten van geneesmiddelen, omdat deze techniek geassocieerd wordt met een slechte reproduceerbaarheid van de intensiteit van signalen en omdat de matrix die gebruikt wordt bij MALDI massaspectrometrie vaak achtergrondsignalen geeft hetgeen de analyse van geneesmiddelen bemoeilijkt. MALDI massaspectrometrie is echter wel een zeer gevoelige, specifieke en snelle methode om stoffen te analyseren. Het verbeteren van de reproduceerbaarheid en het onderdrukken van de matrixsignalen bij het gebruik van MALDI massaspectrometrie is de rode draad in dit proefschrift. Daarnaast is vloeistofchromatografie, gekoppeld aan een electrospray ionization massaspectrometer (LC-MS), gebruikt voor één van de methoden.

In **Hoofdstuk 2** beschrijven we een methode om met MALDI-time-of-flight (TOF) massaspectrometrie NRTI-trifosfaten en endogene (deoxy)nucleotide-trifosfaten te meten. Adenosine-trifosfaat (ATP), deoxyguanosine-trifosfaat (dGTP) en zidovudine-trifosfaat (AZT-TP) zijn echter isomeren en kunnen dus niet op basis van massa van elkaar onder-

scheiden worden. Door deze isomeren te fragmenteren met MALDI-post-source decay (PSD) is het echter wel mogelijk om AZT-TP van ATP en dGTP te onderscheiden. Echter, de gevoeligheid van MALDI-PSD bleek niet toereikend om klinisch relevante concentraties van NRTI-trifosfaten te bepalen in 1 x 10^6 PBMCs. In **Hoofdstuk 3** beschrijven wij een LC-MS methode om NRTIs, (deoxy)nucleosiden en de gefosforyleerde vormen te bepalen in één enkele meting. Met deze methode is het mogelijk om klinisch relevante concentraties van de gefosforyleerde NRTIs en endogene (deoxy)nucleosiden gevoelig en reproduceerbaar te bepalen in 1 x 10^6 PBMCs.

In **Hoofdstuk 4** beschrijven wij dat MALDI-TOF massaspectrometrie een snelle en gevoelige manier is om geneesmiddelen aan te tonen en de concentraties daarvan te bepalen. Wij gebruikten hiervoor de matrix meso-tetrakis(pentafluorofenyl)porfyrine (F20TPP; MW 974 Da). F20TPP heeft een hogere moleculaire massa dan de meeste geneesmiddelen en matrixadducten interfereren daarom niet met de analyse van het geneesmiddel. Dit in tegenstelling tot de veel toegepaste matrices 2,5-dihydroxybenzoëzuur (2,5-DHB) en α-cyano-4-hydroxykaneelzuur (CHCA) die veelal een lagere moleculaire massa hebben dan geneesmiddelen. We vonden echter geen signaal voor de geprotoneerde vormen van geneesmiddelen wanneer F20TPP werd gebruikt, maar wel intensieve signalen voor de zoutadducten van de geneesmiddelen. Verschillende alkalizouten werden daarom toegevoegd aan de F20TPP-matrix en het lithiumadduct van de geneesmiddelen bleek het meest intensieve signaal te geven. Wij brachten de F20TPP-matrix aan met de "brushing-spotting"-methode om zo de concentratie van de geneesmiddelen nauwkeuriger te kunnen bepalen. Daarnaast gebruikten wij een "look-alike" interne standaard en werden de massaspectra van meerdere laserschoten uitgemiddeld. De snelheid van de meetmethode is 2 minuten en 20 seconden per monster en klinisch relevante concentraties van lopinavir en ritonavir (**Hoofdstuk 6**) kunnen reproduceerbaar bepaald worden in 1 x 10^6 PBMCs.

In **Hoofdstuk 5** onderzoeken wij waarom F20TPP en andere porfyrinematrices een sterker signaal geven voor de lithiumadducten van geneesmiddelen vergeleken met andere alkali-adducten. Bij kationisatie met de veel gebruikte matrices 2,5-DHB en CHCA geeft het kaliumadduct van een geneesmiddel normaliter het meest intensieve signaal. Uit de literatuur blijkt dat bij gebruik van die matrices de geneesmiddelen geïoniseerd worden met de alkali-ionen die vrijkomen in de gasfase. Hierbij spelen twee processen een rol: (1) De intrinsieke affiniteit van geneesmiddelen voor alkali-ionen: $Li^+ > Na^+ > K^+ > Rb^+ > Cs^+$. (2) De hoeveelheid alkali-ionen die voorkomen in de gasfase: $Cs^+ > Rb^+ > K^+ > Na^+ > Li^+$. Deze twee tegen elkaar inwerkende processen leiden ertoe dat het kaliumadduct van een geneesmiddel het meest intensieve signaal geeft. Onze experimenten laten ook zien dat geen vrij Li^+ detecteerbaar is met MALDI massaspectrometrie. Dit verklaart waarom de intensiteit van lithiumadducten van geneesmiddelen zo laag is bij gebruik van de frequent toegepaste matrices 2,5-DHB en CHCA. Geneesmiddelen

die gekationiseerd worden met een porfyrinematrix laten echter een andere distributie in intensiteit zien, namelijk $Li^+ > Na^+ > K^+ > Rb^+ > Cs^+$. De porfyrinematrix wordt zelf ook gekationiseerd en laat dezelfde kwantitatieve distributie zien van de alkali-adducten. Voor porfyrine matrices stellen wij daarom voor dat kationisatie van geneesmiddelen niet plaatsvindt door binding met vrije alkali-ionen in de gasfase, maar door het alkali-adduct van de porfyrine zelf dat in overmaat aanwezig is. *Ab initio* berekeningen laten zien dat een porfyrinematrix zich om het Li^+ heenbuigt en dat Li^+ niet geheel in de porfineholte past, maar er boven op ligt. Het Li^+ is dus nog steeds toegankelijk om overgedragen te worden aan het geneesmiddel. Andere alkali-ionen zoals Na^+ en K^+ zijn nog meer blootgesteld, maar de affiniteit van deze ionen voor het geneesmiddel en voor de porfyrine is daarentegen minder. Dit heeft als gevolg dat bij gebruik van een porfyrinematrix, lithium het meest intensieve signaal geeft voor de alkali-adducten van een geneesmiddel.

In **Hoofdstuk 7** beschrijven wij dat F20TPP fragmenteert als MALDI-Fourier-transform ion cyclotron resonance (FTICR) massaspectrometrie wordt gebruikt en daarom minder geschikt is als matrix voor metingen van HIV protease remmers bij dit type massaspectrometer. Het gebruik van de matrix 2,5-DHB, dat juist een lagere moleculaire massa heeft dan de HIV protease remmers, leidde tot massaspectra met vrijwel geen interfererende signalen van de matrixadducten. Dit kan worden verklaard door de langere levensduur van de ionen bij MALDI-FTICR massaspectrometrie (~1 s) in vergelijking met MALDI-TOF massaspectrometrie (~10^{-4} s). Voor een matrix met een hoge moleculaire massa zoals F20TPP, leidt dit tot fragmentatie van F20TPP zelf en resulteert dit in interferentie in het lage massagebied bij MALDI-FTICR. Voor matrices met lage moleculaire massa's zoals 2,5-DHB, resulteert de langere levensduur van de ionen in vrijwel volledige dissociatie van de ongewenste matrixclusters en is er dus nu juist geen interferentie. Het toevoegen van een kaliumzout aan de matrix 2,5-DHB resulteerde in gevoeligere metingen van lopinavir en ritonavir en het gebruik van dimethylsulfoxide verbeterde de kristallisatie van de matrix hetgeen leidde tot nauwkeurigere bepalingen van concentraties van de HIV protease remmers. Ook bij deze meetmethode maakten we gebruik van een "look-alike" interne standaard en werden de massaspectra van meerdere laserschoten uitgemiddeld. De snelheid van de meetmethode is 9 minuten per monster en klinisch relevante concentraties van HIV protease remmers kunnen bepaald worden in 1 x 10^6 PBMCs.

In **Hoofdstuk 9 en 10** beschrijven we het gebruik van MALDI-triple quadrupole massaspectrometrie om de concentraties van geneesmiddelen te bepalen in plasma en in cellen. Dit type apparaat is zeer geschikt om isobare matrixionen te scheiden van de geneesmiddelionen door middel van specifieke fragmentatie. Hierdoor kunnen de veel gebruikte matrices 2,5-DHB en CHCA goed worden toegepast. Ook beschrijven we een nieuwe matrix, namelijk 7-hydroxy-4-(trifluoromethyl)coumarine (HFMC). Met MALDI-triple quadrupole massaspectrometrie is het mogelijk om de concentraties van HIV

protease remmers zeer gevoelig en reproduceerbaar te bepalen in 1 x 10^6 PBMCs of 10 µL plasma met een snelheid van 13.5 seconde per monster. Ook bij deze methode maakten we gebruik van een "look-alike" interne standaard en werden de massaspectra van meerdere laserschoten uitgemiddeld. We hebben de MALDI-triple quadrupole methode gebruikt om de concentraties van de HIV protease remmers lopinavir en ritonavir te bepalen in plasma en in PBMCs van HIV-1 geïnfecteerde kinderen. De bloedmonsters werden direct na afname getransporteerd naar het laboratorium en opgewerkt. We wasten de geïsoleerde PBMCs met gekoelde fosfaatbuffer om zo het overgebleven plasma met daarin de geneesmiddelen te verwijderen, maar ook om te voorkomen dat de PBMCs de HIV protease remmers de cel uitpompen. Bij een deel van de PBMC monsters werden de overgebleven rode bloedcellen verwijderd met een lysis buffer. De antiretrovirale geneesmiddelen werden geëxtraheerd uit de PBMCs en tegelijkertijd werd HIV geïnactiveerd volgens het protocol beschreven in **Hoofdstuk 6**. De extractie van PBMCs met ≥ 40% methanol of ethanol gedurende 1 uur is voldoende om de infectiviteit van HIV met meer dan 6 log te reduceren. Verdere verwerking van de monsters en de metingen kunnen hierdoor plaats vinden in laboratoria met minder strenge veiligheidseisen. PBMCs werden vervolgens opgewerkt met een solid-phase extractie. Voor plasma bleek een extractie met methanol voldoende om de monsters op te werken. Onze metingen bij HIV-1 geïnfecteerde kinderen lieten zien dat er een slechte correlatie is tussen de plasmaspiegels van lopinavir en ritonavir en de intracellulaire spiegels van deze twee geneesmiddelen. Verder vonden we dat de intracellulaire spiegels van lopinavir lager waren dan die in plasma. Voor ritonavir was dit echter afhankelijk van het gebruik van de buffer om rode bloedcellen te lyseren. Ook vonden we een goede correlatie tussen de plasmaspiegels van lopinavir en die van ritonavir en vonden we een correlatie tussen de intracellulaire spiegels van lopinavir en die van ritonavir.

Uit dit proefschrift blijkt dat MALDI massaspectrometrie een geschikte methode is om snel, reproduceerbaar en gevoelig de concentratie van geneesmiddelen te bepalen in kleine hoeveelheden plasma en cellen. De ontwikkeling van eenvoudige manieren om PBMCs en andere relevante cellen te isoleren uit bloed zal de toepassing op grotere schaal bevorderen en zal de methoden toegankelijk maken voor klinisch-chemische toepassingen. In **Hoofdstuk 7** laten we zien dat het afdraaien van cellen op objectglaasjes wellicht een eenvoudige manier is van opwerking om intracellulaire geneesmiddelconcentraties te bepalen. Andere methoden kunnen wellicht ook het opwerken van de monsters vereenvoudigen, bijvoorbeeld door $CD4^+$ T-cellen en monocyten direct uit bloed te isoleren met magnetische beads die zijn gecoat met antilichamen. Naast antiretrovirale geneesmiddelen hebben we laten zien dat ook andere geneesmiddelen en metabolieten snel, gevoelig en reproduceerbaar gemeten kunnen worden met MALDI massaspectrometrie. MALDI massaspectrometrie is daarom breed toepasbaar voor de bepaling van concentraties van geneesmiddelen en metabolieten.

Dankwoord

Zo, mijn proefschrift is af. Promoveren doe je echter niet alleen. Daarom wil ik iedereen van de laboratoria voor neuro-oncologie en clinical & cancer proteomics, de subafdeling infectieziekten/immunologie en de afdeling virologie bedanken voor de prettige en inspirerende werkomgeving waarbinnen dit promotieonderzoek heeft plaatsgevonden. Uiteraard wil ik een aantal personen bij naam noemen, omdat zij in het bijzonder hebben bijgedragen aan dit proefschrift.

Beste Theo, ik wil je bedanken voor de fantastische begeleiding. Ongeveer tien jaar geleden kwam ik samen met Pieter bij je langs, omdat we een massaspectrometer nodig hadden. Ik had geen flauw idee wat voor een ding dat nu precies was. Op de vierde verdieping van het JNI stond ergens in een kamertje zonder ramen..... de MALDI-TOF. Ja, daar was chemie, zeker tussen ons. We deden samen onderzoek tijdens mijn afstudeerperiode, mijn co-schappen en uiteraard tijdens mijn promotieperiode. Je zorgde er bovendien voor dat ik een aanstelling kreeg bij de afdeling neurologie. Ik vind het mooi om te zien hoe jij gedurende al die jaren een grote, volwaardige massaspectrometriegroep hebt weten op te bouwen, die innovatief en hoogstaand onderzoek verricht. Theo, je bent een rasoptimist en dat heeft me op sommige momenten staande gehouden. Ik wil je bovenal bedanken voor de fijne samenwerking en hoop dat we de komende jaren nog veel onderzoek gaan doen.

Beste Ronald, jij inspireert de jonge generatie. Ook mij toen ik als afstudeerstudent begon in het Sophia Kinderziekenhuis. Jouw stimulans heeft uiteindelijk geleid tot dit proefschrift. Ik wil je bedanken voor alle hulp die je hebt geboden en ik kijk met heel veel plezier terug op onze samenwerking.

Beste Peter (Sillevis Smitt), ik wil je hartelijk bedanken voor de prettige samenwerking. Ik waardeer het ontzettend dat je me hebt aangesteld bij de afdeling neurologie, ondanks dat mijn onderzoek niet veel hiermee te maken had. Je bleek toch precies te weten waar ik mee bezig was, wat duidelijk werd bij mijn jaarlijks terugkomende voordrachten bij de neuro-oncologie. Je gaf me dan goede adviezen mee, wat ik zeer heb gewaardeerd.

Beste Peter (Burgers), jij hebt me enorm geholpen gedurende mijn gehele promotietraject. Ik heb veel van jou geleerd over de hardcore massaspectrometrie en zelfs iets over de relativiteitstheorie. Met jouw uitzonderlijke kennis over MALDI massaspectro-

metrie heb je een belangrijke bijdrage geleverd aan dit proefschrift. In het laboratorium hebben we ook veel lol beleefd. Ik kijk dan ook met heel veel plezier terug op onze fijne en creatieve samenwerking en hoop dat er nog vele jaren volgen. Beste Peter, stelling tien draag ik op aan jou.

Beste Rob, ook jij hebt me enorm geholpen gedurende mijn promotietraject. Daarvoor wil ik je hartelijk bedanken, maar uiteraard ook voor de leuke tijd die we hebben gehad. Vanaf het moment dat ik langs kwam voor een HIV-inactivatieprotocol heb je veel tijd besteed aan mijn onderzoek. Onze vele gesprekken hebben er mede toe geleid dat ik me wil gaan specialiseren in de richting virologie. Ik hoop daarom dat we onze samenwerking kunnen voortzetten.

Beste Ab, je stond voor me klaar op belangrijke momenten. Zo mocht ik op jouw afdeling een HIV-inactivatieprotocol ontwikkelen, ondanks dat je me een slome duikelaar vond. Ik heb veel tijd doorgebracht op de afdeling virologie en voelde me daar altijd welkom. Ik wil je hartelijk bedanken voor de leerzame en inspirerende samenwerking.

Beste Nico, je was van het begin af aan al betrokken bij dit promotietraject en tot het einde toe heb je me bijgestaan met raad en daad. Daar wil ik je hartelijk voor bedanken.

Dear Dietrich, I would like to thank you for the nice time Hee Jin and I had in Halifax. It was a pleasure to collaborate with you.

Beste Marleen en Esther, ik wil jullie bedanken voor de bijdrage die jullie hebben geleverd aan dit proefschrift. Esther, je hebt me wegwijs gemaakt in het BSL-3 lab en veel hulp geboden bij het ontwikkelen van het HIV-inactivatieprotocol. Marleen, door jou hebben we nu een mooie collectie van PBMC- monsters die op de juiste manier zijn opgewerkt. Ik kijk met veel plezier terug op de samenwerking met jullie. Daarnaast wil ik ook Patrick, Jeanette, Monique, Anna en Carel bedanken voor de gezellige tijd en goede hulp die jullie hebben geboden.

Beste Conne, dank voor je hulp gedurende al die jaren. Annemarie wil ik bedanken voor de prettige begeleiding tijdens mijn afstuderen. Ik wil Linda, Petronette, Michiel, Gert-Jan en Ineke bedanken voor de prettige samenwerking en goede afstemming tussen kliniek en laboratorium. De patiënten wil ik hartelijk bedanken voor hun deelname aan de studies. Paul bedank ik voor de *ab initio* berekeningen aan porfine. David, bedankt voor de prettige samenwerking en voor de discussies over de intracellulaire farmacokinetiek van antiretrovirale geneesmiddelen. Leon, Henk, William en Lars wil ik bedanken voor de fijne samenwerking en voor de ontwikkeling van de LC-MS methode. Ook wil ik Vishal, Gijs, Oanh en Rachel bedanken voor hun inzet.

Beste Lennard, ik wil je bedanken voor de lol die we hebben gehad en de mooie paper die we hebben gepubliceerd. Marcel en Coskun, ik vond het erg leuk om jullie kamergenoot te zijn. Ook wil ik Arzu, Halima en Linda bedanken voor de gezellige werksfeer.

Beste Pieter en Marco, ik kan me geen betere paranimfen voorstellen. Pieter, we zijn ooit samen dit massaspec-avontuur begonnen en wil je bedanken voor de samenwerking, begeleiding en de leuke tijd.

Lieve ma, pa, Eléa, Daphne, Nanda, Philip, Eelco, Gwen, Megan, Danique, Ria, Ton, Emil, Onno en Patsy, ik wil jullie bedanken voor jullie steun en interesse gedurende mijn promotietraject. Jullie hebben de afgelopen jaren weinig van me gezien, maar dat wil niet zeggen dat ik jullie ben vergeten. Pa, ik vond het erg leuk dat je met me filosofeerde over mijn onderzoek en dat je me af en toe wat chemicaliën uit de schuur meegaf die ik vervolgens testte als matrix. Ma, ook jij heel erg bedankt voor je steun en begrip. Ton en Ria, jullie bedankt voor de leuke gesprekken over de wetenschap en voor de trouwe support.

Lieve Hee Jin, bedankt voor al jouw liefde en steun. Ik hou van jou.

PhD Portfolio

Name PhD student:	Jeroen Jacob Alexander van Kampen
Erasmus MC department:	Neurology
PhD period:	2004 - 2008
Research school:	Erasmus Postgraduate school Molecular Medicine
Promotores:	prof.dr. P.A.E. Sillevis Smitt
	prof.dr. R. de Groot
Co-promotor:	dr. T.M. Luider

In-depth courses

- Principles and Applications of Fourier Transform Mass Spectrometry, 55th Conference of the American Society for Mass Spectrometry, 2007.
- Molecular Immunology, Erasmus Postgraduate school Molecular Medicine, 2007.
- Drug Discovery Using Mass Spectrometry, 54th Conference of the American Society for Mass Spectrometry, 2006.
- Biomedical English Writing and Communication, Erasmus MC, 2005.
- Quantitative Mass Spectrometry, 53rd Conference of the American Society for Mass Spectrometry, 2005.
- MALDI-TOF-MS Analysis with the Bruker Daltonik Ultraflex MALDI-TOF/TOF, Bruker Daltonik, 2004.

Poster and oral presentations

JJA van Kampen, PC Burgers, NG Hartwig, R de Groot, ML Reedijk, ADME Osterhaus, RA Gruters, TM Luider. Development and application of a mass spectrometry based platform to study the intracellular pharmacokinetics of antiretroviral drugs. Poster presentation, 26th annual meeting of the European Society for Paediatric Infectious Diseases, Graz, Austria, 2008.

JJA van Kampen, PC Burgers, NG Hartwig, R de Groot, ML Reedijk, ADME Osterhaus, RA Gruters, TM Luider. Development and application of a mass spectrometry based platform to study the intracellular pharmacokinetics of antiretroviral drugs. Oral presentation, 12th Molecular Medicine Day of the Erasmus Postgraduate school Molecular Medicine, Rotterdam, 2008.

JJA van Kampen, PC Burgers, R de Groot, ADME Osterhaus, EJ Verschuren, RA Gruters, TM Luider. Quantitative analysis of five HIV-1 protease inhibitors in cell lysates by MALDI-FTICR mass spectrometry. Oral presentation, 55th Conference of the American Society for Mass Spectrometry, Indianapolis, IN, USA, 2007.

JJA van Kampen, PC Burgers (*presenting author*), R de Groot, AMDE Osterhaus, EJ Verschuren, RA Gruters, TM Luider. Quantitative analysis of five HIV-1 protease inhibitors in cell lysates by MALDI-FTICR mass spectrometry. Oral presentation, 25th Informal Meeting on Mass Spectrometry, Nyiregyhaza, Hungary, 2007.

JJA van Kampen, PC Burgers, R de Groot, TM Luider. Quantitative analysis of HIV-1 protease inhibitors in biological matrices using MALDI-TOF mass spectrometry. Poster presentation, 54th Conference of the American Society for Mass Spectrometry, Seattle, WA, USA, 2006.

PC Burgers (*presenting author*), **JJA van Kampen**, R de Groot, TM Luider, PJA Ruttink. Quantitative analysis of pharmaceutical compounds by MALDI-TOF MS: mechanism for alkali ion attachment. Oral presentation, 24th Informal Meeting on Mass Spectrometry, Ustron, Poland, 2006.

JJA van Kampen, EJ Verschuren, PC Burgers, TM Luider, R de Groot, ADME Osterhaus, RA Gruters. Validation of an HIV-1 inactivation protocol that is compatible with intracellular drug analysis by mass spectrometry. Poster presentation, Biomarker Discovery by Mass Spectrometry, Amsterdam, 2006.

JJA van Kampen, PC Burgers, R de Groot, TM Luider. Quantitative analysis of antiretroviral drugs by MALDI-TOF mass spectrometry. Poster presentation, 53rd Conference of the American Society for Mass Spectrometry, San Antonio, TX, USA, 2005.

JJA van Kampen, PLA Fraaij, V Hira, AMC van Rossum, NG Hartwig, R de Groot, TM Luider. MALDI-TOF mass spectrometry of nucleotide-triphosphates. Poster presentation, Biomarker Discovery by Mass Spectrometry, Rotterdam, 2004.

JJA van Kampen, PLA Fraaij, V Hira, AMC van Rossum, NG Hartwig, R de Groot, TM Luider. MALDI-TOF mass spectrometry of nucleotide-triphosphates. Poster" presentation, Voorjaarsbijeenkomst van de Nederlandse Vereniging voor Massaspectrometrie (NVMS), Tilburg, 2004.

JJA van Kampen. Development of a method for NRTI treatment monitoring in HIV-1 infected children. Oral presentation, Sectiedag Kinderinfectieziekten van de Nederlandse Vereniging voor Kindergeneeskunde (NVK), Amsterdam, 2004.

JJA van Kampen, PLA Fraaij, TM Luider, R de Groot. Measurement of zidovudine-triphosphate (AZT-TP) with Matrix-Assisted Laser Desorption / Ionization (MALDI) mass

spectrometry. Poster presentation, 19th annual meeting of the European Society for Paediatric Infectious Diseases, Istanbul, Turkey, 2001.

Publications

JJA van Kampen, PC Burgers, R de Groot, RA Gruters, TM Luider. Biomedical application of MALDI mass spectrometry for small-molecule analysis. Mass Spectrometry Reviews, 2009, in press.

JJA van Kampen, TM Luider, PJA Ruttink, PC Burgers. Metal ion attachment to the matrix meso-tetrakis(pentafluorophenyl)porphyrin, related matrices and analytes: an experimental and theoretical study. Journal of Mass Spectrometry, 2009, in press.

LJM Dekker, **JJA van Kampen**, ML Reedijk, PC Burgers, RA Gruters, AMDE Osterhaus, TM Luider. A mass spectrometry based imaging method developed for the intracellular detection of HIV protease inhibitors. Rapid Communications in Mass Spectrometry, 2009, 23(8), 1183-1188.

L Coulier, **JJA van Kampen**, R de Groot, HW Gerritsen, RC Bas, WD van Dongen, LP Brüll, TM Luider. Simultaneous determination of endogenous deoxynucleotides and phosphorylated nucleoside reverse transcriptase inhibitors in peripheral blood mononuclear cells using ion-pair liquid chromatography coupled to mass spectrometry. Proteomics Clinical Applications, 2008, 2(10-11), 1557–1562.

JJA van Kampen, PC Burgers, RA Gruters, ADME Osterhaus, R de Groot, TM Luider, DA Volmer. Quantitative analysis of antiretroviral drugs in lysates of peripheral blood mononuclear cells using MALDI-triple quadrupole mass spectrometry. Analytical Chemistry, 2008, 80(13), 4969-4975.

JJA van Kampen, PC Burgers, R de Groot, ADME Osterhaus, ML Reedijk, EJ Verschuren, RA Gruters, TM Luider. Quantitative analysis of HIV-1 protease inhibitors in cell lysates using MALDI-FTICR mass spectrometry. Analytical Chemistry, 2008, 80(10), 3751-3756.

JJA van Kampen, EJ Verschuren, PC Burgers, TM Luider, R de Groot, ADME Osterhaus, RA Gruters. Validation of an HIV-1 inactivation protocol that is compatible with intracellular drug analysis by mass spectrometry. Journal of Chromatography B, 2007, 847(1), 38-44.

JJA van Kampen, PC Burgers, R de Groot, TM Luider. Qualitative and quantitative analysis of pharmaceutical compounds by MALDI-TOF mass spectrometry. Analytical Chemistry, 2006, 78(15), 5403-5411.

PLA Fraaij, **JJA van Kampen**, DM Burger, R de Groot. Pharmacokinetics of antiretroviral therapy in HIV-1-infected children. Clinical Pharmacokinetics, 2005, 44(9), 935-956.

JJA van Kampen, PLA Fraaij, V Hira, AMC van Rossum, NG Hartwig, R de Groot, TM Luider. A new method for analysis of AZT-triphosphate and nucleotide-triphosphates.

Biochemical and Biophysical Research Communications, 2004, 315(1), 151-159. Erratum in 2004, 316(3), 967.

Research experience abroad

- Institute for Marine Biosciences, National Research Council Canada, Halifax, Nova Scotia, Canada. Quantitative analysis of antiretroviral drugs using a prototype MALDI-triple quadrupole mass spectrometer. Supervision: dr. D.A. Volmer. October – November 2006.

Other activities

- PhD / Post-doc committee of the Erasmus Postgraduate school Molecular Medicine, 2004 – 2006.
- Organizing committee of the 10th Molecular Medicine Day of the Erasmus Postgraduate school Molecular Medicine, 2006.
- Organizing committee of the 9th Molecular Medicine Day of the Erasmus Postgraduate school Molecular Medicine, 2005.

Awards

- Award for best oral presentation on the 12th Molecular Medicine Day of the Erasmus Postgraduate school Molecular Medicine, February 6th 2008, Rotterdam.
- Jan C Molenaar Award for best defence of a grant proposal, 2003.

Grants

ADME Osterhaus (*principal investigator*), RA Gruters, TM Luider, **JJA van Kampen**, WA van Dongen, L Brüll, R de Groot, DM Burger, JA Raaijmakers, RJ Remorie, KG van Schagen, BB Roosjen. A multidisciplinary approach to monitor and select effective therapy in HIV infection. Top Institute Pharma, the Netherlands. Project T4-212.
JJA van Kampen, R de Groot (*principal investigator*), TM Luider, F Miedema, ME van der Ende, ADME Osterhaus. Development and application of a sensitive high throughput method for quantification of intracellular NRTI-triphosphates. Aids Fonds, the Netherlands. Project 2004051.